



## City Research Online

### City, University of London Institutional Repository

---

**Citation:** Cole, V. A. (1997). Aspects of the pupil light response and colour vision using pupillometric and psychophysical tests. (Unpublished Doctoral thesis, City, University of London)

This is the accepted version of the paper.

This version of the publication may differ from the final published version.

---

**Permanent repository link:** <https://openaccess.city.ac.uk/id/eprint/30755/>

**Link to published version:**

**Copyright:** City Research Online aims to make research outputs of City, University of London available to a wider audience. Copyright and Moral Rights remain with the author(s) and/or copyright holders. URLs from City Research Online may be freely distributed and linked to.

**Reuse:** Copies of full items can be used for personal research or study, educational, or not-for-profit purposes without prior permission or charge. Provided that the authors, title and full bibliographic details are credited, a hyperlink and/or URL is given for the original metadata page and the content is not changed in any way.

---

---

---

City Research Online:

<http://openaccess.city.ac.uk/>

[publications@city.ac.uk](mailto:publications@city.ac.uk)

---

**ASPECTS OF THE PUPIL LIGHT RESPONSE AND  
COLOUR VISION USING PUPILLOMETRIC AND  
PSYCHOPHYSICAL TESTS**

by

**VICTORIA ANNE COLE**

Thesis submitted for the Degree of  
Doctor of Philosophy

to

City University  
Department of Optometry and Visual Science

**OCTOBER 1997**

## TABLE OF CONTENTS

<b>TABLE OF CONTENTS</b> .....	iii
<b>LIST OF TABLES</b> .....	v
<b>LIST OF ILLUSTRATIONS</b> .....	vii
<b>ACKNOWLEDGMENTS</b> .....	xi
<b>DECLARATION</b> .....	xiii
<b>ABSTRACT</b> .....	xv
<b>CHAPTER 1 INTRODUCTION</b> .....	1
1.1 <b>Anatomy and physiology of the visual system</b> .....	1
1.1.1 Introduction .....	1
1.1.2 The eye .....	1
1.1.3 The retina .....	2
1.1.4 Optic nerve, chiasm and tract .....	9
1.1.5 Lateral geniculate nucleus .....	10
1.1.6 Primary visual cortex .....	12
1.1.7 Prestriate cortex .....	14
1.1.8 Higher visual areas .....	16
1.1.9 Parallel pathways .....	16
1.1.10 Midbrain and diencephalic structures and projections .....	18
1.2 <b>The pupil</b> .....	22
1.2.1 Introduction .....	22
1.2.2 Anatomy and physiology of the pupillary pathways .....	22
1.2.3 Methods for studying pupillary behaviour .....	25
1.2.4 Steady-state pupil size .....	27
1.2.5 Dynamic pupil responses .....	28
1.2.6 Abnormal pupil responses .....	34
1.3 <b>Visual function in subjects with cortical lesions</b> .....	37
1.3.1 Introduction .....	37
1.3.2 Visual abilities that have been described in the absence of striate cortex .....	37
1.3.3 The neurobiology of blindsight .....	44
1.3.4 Could blindsight be mediated by scattered light or spared cortex? .....	46
1.3.5 Effects of non-striate cortical lesions .....	47
1.4 <b>Colour vision</b> .....	50
1.4.1 Introduction .....	50
1.4.2 Physiology of colour vision .....	50
1.4.3 Colour matching and chromaticity diagrams .....	52

1.4.4	Congenital and acquired colour vision deficiencies .....	53
1.4.5	Colour vision testing .....	57
<b>CHAPTER 2 EQUIPMENT AND EXPERIMENTAL METHODS .....</b>		<b>60</b>
2.1	Introduction .....	60
2.2	Measurement of pupil responses .....	60
2.3	Stimuli used in pupillometry experiments .....	62
2.4	Equipment and stimuli used in colour vision measurement .....	64
2.5	Experimental room conditions .....	65
2.6	<del>Definition of contrast</del> .....	<del>65</del>
<b>CHAPTER 3 A STUDY OF PUPIL LIGHT REFLEX COMPONENTS IN HUMAN VISION .....</b>		<b>66</b>
3.1	Introduction .....	66
3.2	Initial experiments - RLM <sub>s</sub> alone .....	66
3.3	Introduction of RLM <sub>t</sub> .....	69
3.4	Repeatability of readings .....	70
3.5	Further investigation of the effects of RLM <sub>s</sub> on the pupil light reflex ..	72
3.6	The effect of stimulus contrast on the pupil light reflex .....	74
3.7	The effect of stimulus area on the pupil light reflex .....	76
3.8	Two proposed components of the pupil light reflex .....	79
3.9	Summary .....	83
<b>CHAPTER 4 INVESTIGATION OF THE PUPIL COLOUR RESPONSE ..</b>		<b>86</b>
4.1	Introduction .....	86
4.2	Pupil colour responses in normal subjects .....	88
4.3	Pupil colour responses in dichromats .....	90
4.4	Pupil colour responses in subjects with cortical damage .....	92
4.5	Summary .....	98
<b>CHAPTER 5 COLOUR VISION IN SUBJECTS WITH DAMAGE AFFECTING THE EARLY-STAGE VISUAL PATHWAYS .....</b>		<b>100</b>
5.1	Introduction .....	100
5.2	Chromatic discrimination ability in normal subjects .....	102
5.3	Colour vision in subjects with acquired selective colour vision loss ....	105
5.4	Colour vision in subjects who have had optic neuritis .....	111
5.5	Summary .....	116
<b>CHAPTER 6 CONCLUDING REMARKS .....</b>		<b>118</b>
<b>REFERENCES .....</b>		<b>123</b>

## LIST OF TABLES

Table		Page
1.1	Retinal layers and their components.....	Following 2
1.2	Characteristics of retinal ganglion cells in cat.....	Following 8
1.3	Cell types in monkey lateral geniculate nucleus.....	Following 12
1.4	Physiological differences of the magnocellular and parvocellular geniculate divisions.....	Following 12
1.5	Layers of the primate striate cortex.....	Following 14
1.6	Summary of the major subdivisions and connections of the primate geniculocortical visual system.....	Following 18
1.7	Summary of some aspects of the experiments carried out by Pasik and Pasik (1982).....	39
1.8	Features of congenital colour vision deficiencies.....	Following 54
1.9	Comparison of congenital and acquired colour vision deficiencies.....	55
1.10	Examples of acquired colour vision deficiencies.....	57
2.1	Typical staircase parameters for CVTEST.....	65
3.1	Summary of amplitudes and variances measured for 6 identical consecutive runs, subject JB.....	Following 72
3.2	One-way analysis of variance of results in Table 3.1.....	Following 72
3.3	Summary of amplitudes and variances measured for 6 identical consecutive runs, subject GY.....	Following 72
3.4	One-way analysis of variance of results in Table 3.3.....	Following 72
3.5	Summary of the two PLR components described in Chapter 3.....	83
4.1	Details of normal trichromatic subjects participating in PCR experiments.....	Following 88
4.2	Details of dichromats participating in PCR experiments..	Following 88
4.3	Angles of chromatic displacement used for SA (protanope) and significance of results obtained.....	Following 90
4.4	Angles of chromatic displacement used for PE (protanope) and significance of results obtained.....	Following 90
4.5	Angles of chromatic displacement used for RV (deutanope) and significance of results obtained.....	Following 90
4.6	Angles of chromatic displacement used for JF (tritanope) and significance of results obtained.....	Following 90

Table	Page
5.1	Directions of chromatic displacement tested for subjects GW and DM, and TM (congenital protanope)..... 108
5.2	Details of subjects who have had optic neuritis..... 113
5.3	Comparison of results obtained for left and right eyes of optic neuritis patients for pattern and colour tests, t-test for paired samples..... 113
5.4	Comparison of performance of optic neuritis patients at the pattern and colour tests for affected and unaffected eyes, t-test for paired samples..... 114

## LIST OF ILLUSTRATIONS

Figure	Following page
1.1	A horizontal section of the right human eye.....2
1.2	Drawing of the major cell types found in the primate retina.. 2
1.3	Schematic diagram of rods and cones.....4
1.4	Graph showing cone and rod photoreceptor density.....4
1.5	Spectral sensitivity of the photoresponse of cones and rods... 4
1.6	Idealised responses and receptive field maps for ganglion cells.....8
1.7	The connections from the retina to the cerebral hemispheres. ....10
1.8	The layers of the lateral geniculate nucleus.....10
1.9	Lateral and medial views of the cerebral cortex.....12
1.10	Diagram showing location of primary visual cortex.....12
1.11	Golgi and Nissl-stained section of striate area of macaque.... 14
1.12	Diagram showing connections made by striate cortex cells... 14
1.13	A model of the macaque primary visual cortex.....14
1.14	Lateral view of the brain stem.....18
1.15	Structure of the iris.....24
1.16	Afferent and parasympathetic efferent pathways of the pupillary light reflexes.....24
1.17	The known pathways from the eye into the brain.....44
1.18	Colour matching functions of the CIE 1931 standard colorimetric observer.....52
1.19	(r,g) chromaticity diagram of the CIE 1931 standard colorimetric observer.....52
1.20	(x,y) chromaticity diagram of the CIE 1931 standard colorimetric observer.....54
1.21	(x,y) and (u',v') chromaticity diagrams compared.....54
1.22	Colour confusion lines for dichromats.....54
1.23	Luminous efficiency functions for dichromats.....56
2.1	Schematic drawing of the P_SCAN 100 system.....60
2.2	Diagram to illustrate appearance of pupil and scan lines.....60
2.3	A typical averaged trace showing the pupil response to a given stimulus.....62
2.4	Spectral radiance of the screen phosphors.....62
2.5	Diagram showing luminance profiles for individual frames of spatial random luminance modulation.....64
2.6	Luminance profiles for spatial and temporal random luminance modulation.....64

3.1	Stimulus configuration for initial pupil light reflex responses .....	68
3.2	Pupil responses using different RLM <sub>s</sub> contrasts, subject JB... ..	68
3.3	Effect of increasing RLM <sub>s</sub> contrast on pupil response amplitude, subject JB.....	68
3.4	Pupil responses with and without RLM <sub>s</sub> , subject GY.....	68
3.5	Pupil responses using different RLM <sub>t</sub> contrasts, subject JB... ..	70
3.6	Effect of increasing RLM <sub>t</sub> contrast on pupil response amplitude, subject JB.....	70
3.7	Summary of pupil traces obtained, subject JB.....	70
3.8	Pupil traces obtained, subject GY, blind hemifield.....	70
3.9	Pupil traces obtained, subject GY, sighted hemifield.....	70
3.10	Stimulus configuration for further investigation of effect of RLM <sub>s</sub> contrast, subject JB.....	72
3.11	Stimulus configuration for further investigation of effect of RLM <sub>s</sub> contrast, subject GY.....	72
3.12	Effect of RLM <sub>s</sub> contrast on pupil response amplitudes for stimuli of different contrasts, subject JB.....	74
3.13	Effect of RLM <sub>s</sub> contrast on pupil response amplitudes for stimuli of different contrasts, subject GY.....	74
3.14	Effect of increasing stimulus contrast, no RLM <sub>s</sub> , subject JB.. ..	74
3.15	Effect of increasing stimulus contrast, no RLM <sub>s</sub> , subject GY. ....	74
3.16	Pupil responses to stimuli of different contrasts, subject GY. ....	76
3.17	Pupil responses to stimuli of different contrasts, subject FS... ..	76
3.18	Pupil responses to stimuli of different areas, stimulus contrast=30%, subject JB.....	78
3.19	Pupil responses to stimuli of different areas, stimulus contrast=90%, subject JB.....	78
3.20	Pupil responses to stimuli of different areas, subject GY.....	78
3.21	Pupil responses as a function of log stimulus area, stimulus contrast=30%, subject JB.....	78
3.22	Pupil responses as a function of log stimulus area, stimulus contrast=90%, subject JB.....	78
3.23	Pupil responses as a function of log stimulus area, subject GY.....	78
3.24	Pupil responses for foveal stimulus presentation, subject JB.. ..	80
3.25	Pupil responses with static RLM <sub>s</sub> , subject JB.....	80
3.26	Pupil responses with monocular and binocular viewing, subject AB.....	82
3.27	Pupil responses with and without RLM <sub>s</sub> , subject AB.....	82
4.1	Stimulus configuration for measuring PCRs in normal subjects and dichromats.....	88

4.2	Pupil responses, normal subject MH.....	90
4.3	Pupil response amplitudes, normal subject MH.....	90
4.4	Pupil response amplitudes, normal subject RT.....	90
4.5	Pupil response amplitudes, normal subject JB.....	90
4.6	Chromatic discrimination ellipse, tritanope JF.....	90
4.7	Pupil responses, protanope SA.....	92
4.8	Pupil response amplitudes, protanope SA.....	92
4.9	Pupil response amplitudes, protanope PE.....	92
4.10	Pupil response amplitudes, deuteranope RV.....	92
4.11	Pupil response amplitudes, tritanope JF.....	92
4.12	Pupil response amplitudes, subject GY, foveal presentation..	92
4.13	Pupil response amplitudes, subject GY, blind and sighted hemifields.....	92
4.14	Pupil response amplitudes, subject CAG.....	94
4.15	Chromatic discrimination thresholds, subject LR.....	94
4.16	Contrast sensitivity functions, subject LR.....	94
4.17	Pupil responses to large coloured stimuli, subject JB.....	96
4.18	Pupil responses to large coloured stimuli, subject GY, sighted hemifield.....	96
4.19	Pupil responses to large coloured stimuli, subject GY, blind hemifield.....	96
4.20	Pupil responses to large coloured stimuli, subject LR, unaffected visual field.....	96
4.21	Pupil responses to large coloured stimuli, subject LR, affected visual field.....	96
5.1	MacAdam ellipses plotted on the (x,y) chromaticity diagram .....	100
5.2	Stimulus configurations used for the 'pattern' and 'colour' tests.....	104
5.3	Chromatic discrimination thresholds for normal observers, pattern test.....	104
5.4	Chromatic discrimination thresholds for normal observers, colour test.....	104
5.5	Chromatic discrimination thresholds for normal observers, comparison of results from this and previous studies.....	106
5.6	Results of F-M 100-hue test, subject GW.....	106
5.7	Humphrey visual field plots, subject DM.....	108
5.8	Contrast sensitivity functions, subject DM.....	108
5.9	Chromatic discrimination ellipses, pattern test, subject GW..	108
5.10	Chromatic discrimination ellipses, colour test, subject GW...	108

5.11	Chromatic discrimination ellipses, pattern and colour tests, subject TM (congenital protanope).....	108
5.12	Chromatic discrimination ellipses, pattern test, subject DM..	108
5.13	Chromatic discrimination ellipses, colour test, subject DM...	108
5.14	Chromatic discrimination ellipses, colour and pattern tests, subjects RH and PL.....	114
5.15	Chromatic discrimination ellipses, colour and pattern tests, subjects POL and RA.....	114
5.16	Chromatic discrimination ellipses, colour and pattern tests, subjects CH and AM.....	114
5.17	Major axis dimensions for ellipses fitted to data for affected eyes of optic neuritis patients.....	116
5.18	Major axis dimensions for ellipses fitted to data for unaffected eyes of optic neuritis patients.....	116

## ACKNOWLEDGMENTS

This thesis could not have been written without the help, support and encouragement of many people. In particular, I would like to thank:

Professor John Barbur, for his enthusiastic and wise supervision and endless patience

Ali Harlow and Stuart Brundritt, for patient help with even basic computing

Alf Goodbody, for technical assistance and help with experiments

Dr Gordon Plant and Mr Ivor Levy, for referring some of the patients

The subjects and patients who willingly gave up hours of time to participate in the experiments. GY in particular spent many days taking part in pupillometry experiments and I am grateful for his patience

The College of Optometrists, for awarding me a Research Scholarship

Janet and Peter Wolf, for providing me with a home in London and plenty of moral support and the odd glass of wine

Jim and Laure Barwood, for looking after my other home and being marvellous friends and neighbours

Steve Ladd, for being a marvellous boss and for lending me his printer

Eyetech Practice Systems and Michael Plant for help with the production of this thesis

My parents, for moral support and encouragement at all times

My husband Alan, who is a tower of strength - thank you for putting up with it all

## **DECLARATION**

I grant powers of discretion to the University Librarian to allow this thesis to be copied in whole or in part without further reference to me. This permission covers only single copies made for study purposes, subject to normal conditions of acknowledgment.

## ABSTRACT

The pupil light reflex response (PLR) has been used as an indicator of visual function in neuro-ophthalmology but its usefulness is limited by the use of large light sources and gross measurement techniques. In this study, sophisticated recording equipment (the P\_SCAN 100 system) and computer-generated stimuli have been used to study certain aspects of the PLR. Luminance masking techniques have been developed which affect the PLR in different ways. In normal observers, local luminance masking eliminates some but not all of the PLR, while light flux changes over a larger area completely eliminate the PLR. Two components of the PLR have been proposed, based on experiments involving normal observers and subjects with cortical damage and optic nerve damage. The first component appears to involve cortical mechanisms as it is absent in subjects with cortical damage. This component has a high contrast gain, but saturates at contrasts above about 30%. The second component may equate with the classical subcortical pupil pathway. It has a lower contrast gain and exhibits extensive spatial summation, and may be involved with the control of steady state pupil size.

The pupil has also been shown to respond to spectral changes. This study measures the pupil colour response (PCR) using the P\_SCAN 100 system and computer-generated stimuli. Luminance masking techniques were again used to ensure that the pupil was responding only to colour change, and not to any increase in light flux when the stimulus was presented. Significant PCRs were measured for a range of colours in normal subjects, but were not present in dichromats when the stimuli were chosen to fall in the same isochromatic zone as the background for each class of dichromat. PCRs were also investigated in subjects with damage to V1 and V4. Small but significant responses were measured when large saturated stimuli were used. It is proposed that these responses may involve subcortical mechanisms.

A psychophysical colour vision test has been used to investigate the processing of chromatic signals in normal subjects and patients with damage to the early-stage visual pathways. Two stimulus configurations were used - the first involves the detection of vertical bars defined only by chromatic signals (the 'pattern' test), and the second involves the detection of a colour change of a large target already defined by luminance contrast (the 'colour' test). In normal subjects, there is no difference between the chromatic discrimination thresholds found for the two types of test. In this study, two subjects were investigated who performed worse on the pattern test than the colour test. A group of patients who had previously suffered optic neuritis was also investigated to see if the same pattern of results was obtained, but this group showed a great variation in performance. It was proposed that performance at the two tests, indicating the use of chromatic signals, is mediated by two separable neural substrates. These two neural mechanisms can be affected differently but not specifically in optic neuritis. Type I colour-opponent centre-surround cells could be responsible for performance at the pattern test, while Type II colour-opponent spatially co-extensive cells could mediate colour detection when larger targets are used.

## **CHAPTER 1 INTRODUCTION**

### 1.1 Anatomy and physiology of the visual system

#### 1.1.1 Introduction

In order for any visual function to take place, light from the outside world must reach the retina and be converted into a message which can be sent to the brain. This section describes how this takes place by outlining the anatomy and physiology of the retina and visual pathway from eye to brain. The retino-geniculo-striate pathway will be described, and then higher areas of the brain. The concept of parallel pathways will be considered. Subcortical structures will also be described, including those involved in pupillary responses and perhaps blindsight, which will be considered in sections 1.2 and 1.3.

#### 1.1.2 The eye

The eye or eyeball is an almost spherical globe of about 25 mm diameter, which is formed of three coats (Figure 1.1). The outermost coat is formed from avascular connective tissue and has two regions; the dense white sclera and anteriorly the transparent cornea. The middle coat or uvea is vascular and consists of the choroid, ciliary body and iris. The inner coat is the retina, which contains the light sensitive elements necessary to initiate vision. This will be considered in detail in the next section. The optic disc interrupts the retina where the optic nerve leaves the eye, causing a "blind spot". It is about 2 mm by 1.5 mm in size, and therefore the blind spot projects about 7° by 5° into space. About 17° temporal to the disc is a special region of the retina called the fovea which is about 1.5 mm in diameter.

The eyeball is filled with aqueous humour and vitreous humour which are transparent and are separated by a crystalline lens. This lens is a transparent flexible structure which can change shape according to the tension exerted on it by the suspensory ligaments which encircle it. These ligaments are attached to the ciliary body, and exert maximum tension on the lens when the ciliary muscles are relaxed. If the ciliary muscles contract, tension on the lens is reduced, allowing it to take up a more curved shape, and therefore ~~an~~ increase in power. The ability to increase lens power is called accommodation, and a child of ten may have as much as 14 dioptres of accommodation (Bennett and Rabbetts,

1984). As the elasticity of the lens decreases, so does the amplitude of accommodation, leading eventually to the frustrating inability to see close objects clearly (presbyopia).

The first step in the perception of an object is the formation of an image of that object on the retina. The main refractive element of the eye is the cornea, which in the average eye contributes some 43 dioptres of power, and further refraction is provided by the crystalline lens, which contributes another 21 dioptres (Bennett and Rabbetts, 1984). In an ideal situation light from a distant object is perfectly focused on the retina with relaxed ciliary muscles. Refractive errors occur when the cornea and lens focus the image of a distant object in front of or behind the retina (myopia and hyperopia, respectively). In hyperopia, the image can be placed on the retina if there is sufficient accommodation available, but otherwise spectacle or contact lenses can be used to achieve a focused image.

Image degradation can also occur if any of the ocular media (ie, cornea, aqueous humour, lens and vitreous humour) are not transparent. The commonest opacities to be found are cataracts, age-related changes in which the lens undergoes varying degrees of opacification. Corneal scarring or dystrophies and vitreous floaters or haemorrhages can also interfere with the formation of a clear retinal image, either by blocking the light from the retina, or by scattering light which degrades the final retinal image.

When light reaches the retina the physiological processes leading to perception begin.

### 1.1.3 The retina

The retina is a complicated ten-layered structure (Figure 1.2). A summary of its layers and components are given in Table 1.1.

The outermost layer is the retinal pigment epithelium, and this is formed of a single layer of tightly packed pigment epithelial cells which are tightly joined to the choroid. This layer serves the photoreceptors by transporting their metabolites away into the choroidal circulation, phagocytosing their used outer segment discs and providing them with a means of attachment. The pigment in the cells also absorbs light that reaches this layer,

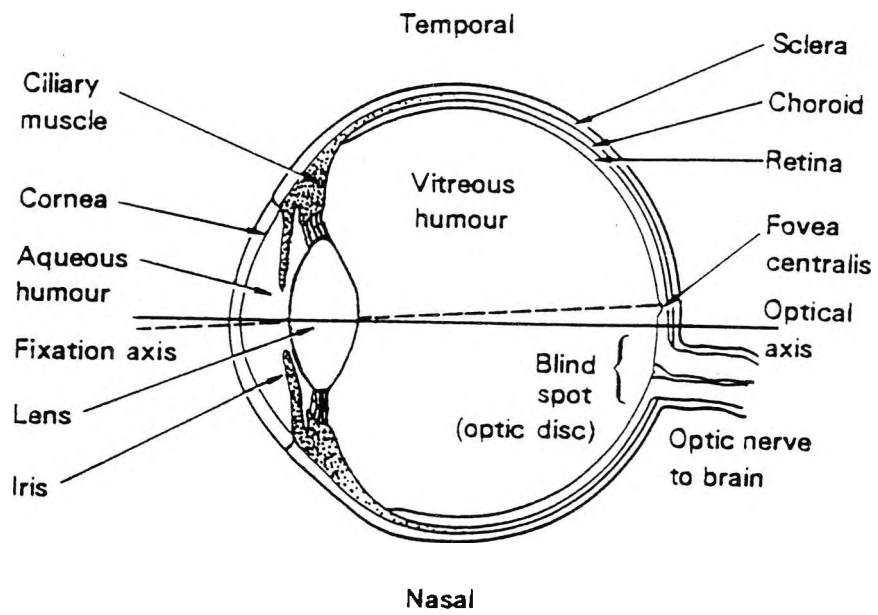


Figure 1.1 A horizontal section of the right human eye (Padgham and Saunders, 1975)

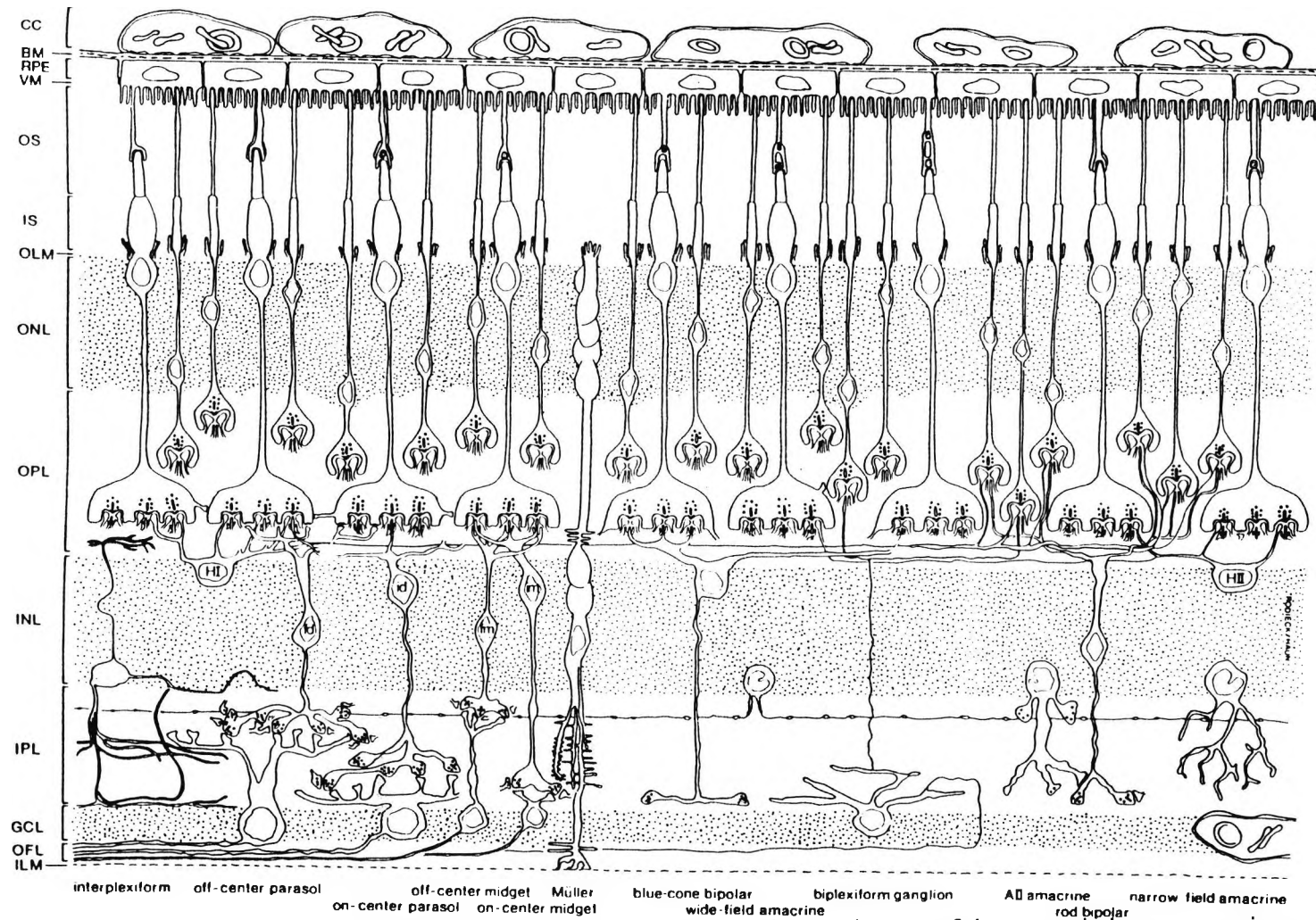


Figure 1.2 Drawing of the major cell types found in the primate retina, and some of the synaptic interconnections among them. (CC=choriocapillaris, BM=Bruch's membrane, RPE=retinal pigment epithelium, VM=Verhoeff's membrane, OS=outer segments of photoreceptors, IS=inner segments of photoreceptors, OLM=outer limiting membrane, ONL=outer nuclear layer, OPL=outer plexiform layer, INL=inner nuclear layer, IPL=inner plexiform layer, GCL=ganglion cell layer, OFL=optic fibre layer, ILM=inner limiting membrane) From Rodieck (1988)

Layer	Name	Components of layer
1	Retinal pigment epithelium	Single layer of pigment epithelial cells
2	Photoreceptor layer	Inner and outer segments of photoreceptors
3	Outer limiting membrane	Intermediate junctions between receptors and Muller cells all at level of photoreceptor inner segments
4	Outer nuclear layer	Cell bodies of photoreceptors
5	Outer plexiform layer	Synapses between photoreceptors, bipolar and horizontal cells
6	Inner nuclear layer	Cell bodies of bipolar, horizontal and amacrine cells
7	Inner plexiform layer	Synapses between bipolar, ganglion and amacrine cells
8	Ganglion cell layer	Cell bodies of ganglion cells
9	Nerve fibre layer	Axons of ganglion cells, thickest near optic nerve head, thinnest at periphery
10	Inner limiting membrane	Inner surface of the retina, bordering vitreous humour

Table 1.1 Retinal layers and their components (Ruskell (1988), Kolb (1991))

having failed to bleach the photoreceptor pigments, preventing it from scattering back into the eye (Ruskell, 1988).

The other nine layers form the neural retina, and are made up of five types of nerve cells, interspersed with glial cells. Because the retinal pigment epithelium and neural retina originate from different embryological layers, they are only loosely attached, except at the optic nerve head and ora serrata. Elsewhere, it is relatively easy for the neural retina to become separated from the pigment epithelium, giving rise to the clinical condition of retinal detachment.

The first stage in the processing of vision is to convert the light falling on the retina into electrical signals (that is, transduction), and this process is carried out by photoreceptors. To reach the photoreceptors light must pass through the other layers of the retina, so these must be transparent.

In the normal human retina, there are two types of receptors, rods and cones, so named because of their shapes (Figure 1.3). The inner and outer segments of rods are thin cylindrical structures approximately 1.4  $\mu\text{m}$  in diameter, while the outer segments of cones taper from their base to their tips, being approximately 5  $\mu\text{m}$  at their widest point. At the fovea however, cones are cylindrical and are approximately 1.5  $\mu\text{m}$  in diameter (Kolb, 1991).

Osterberg (1935) estimated that there are between 110 million and 125 million rods in the retina, and 6.4 million cones. The photoreceptors are not distributed evenly throughout the retina (Figure 1.4). The greatest density of cones is found at the fovea, but the density of cones drops off sharply away from the fovea, giving greatest spatial resolution at the fovea. There are no rods at the fovea, then an increasing density of rods which reaches a maximum at about 20° from the fovea before decreasing towards the periphery.

The transduction process takes place in the outer segments of the photoreceptors. These consist of a stack of disc-like structures formed of double membranes. In cones the discs are continuous with the outer segment membrane, while in rods the discs are separate from this membrane and from each other. In the disc membranes are the visual

pigments, which are the source of the retina's sensitivity to light. They contain complexes of retinal bound to proteins called opsins. The retinal is in the 11-*cis* isomer form when it is in the dark, but when a quantum of light energy is absorbed a series of chemical changes is triggered, ending with the retinal changed to its all-*trans* isomer form and detached from the opsin. This process is called bleaching because it results in loss of colour from the molecules. The net effect of this change is to prevent the entry of sodium ions into the receptor, causing the cell to hyperpolarise. Graded potentials are then transmitted from the photoreceptors to bipolar cells.

The visual pigment in rods (rhodopsin) absorbs light most efficiently at wavelengths of about 500 nm (Figure 1.5a). Rods are extremely sensitive to light, and may respond even to single photons. Scotopic vision (in light levels from about  $10^{-6}$  to about  $10^{-3}$  cd/m<sup>2</sup>) is thus mediated by rods. They have relatively poor spatial and temporal resolution. Rod-mediated vision is monochromatic.

There are three different types of cone, with visual pigments absorbing light maximally of wavelengths of about 565 nm, 530 nm and 450 nm (Smith and Pokorny, 1975) as shown in Figure 1.5b. These are sometimes referred to as red, green and blue cones respectively, or long-wavelength-sensitive (L), middle-wavelength-sensitive (M) or short-wavelength-sensitive (S) cones. Cones are not as sensitive as rods - a cone must absorb forty times as many photons to produce the same current as a rod (Falk, 1991). The spectral sensitivity curves of the different classes of cone are predicted from psychophysical experiments, and confirmed by microspectrophotometry and retinal densitometry techniques.

It is thought that in monkeys and humans between 10% and 18% of retinal cones are blue cones (Wassle and Boycott, 1991). They have been distinguished by histochemical techniques (Marc and Sperling, 1977), dye uptake studies (de Monasterio et al, 1981) and morphological investigation (Ahnelt et al, 1987). Few blue cones are found at the fovea (Marc and Sperling, 1977; Ahnelt et al, 1987) which accounts for the phenomenon of small field tritanopia.

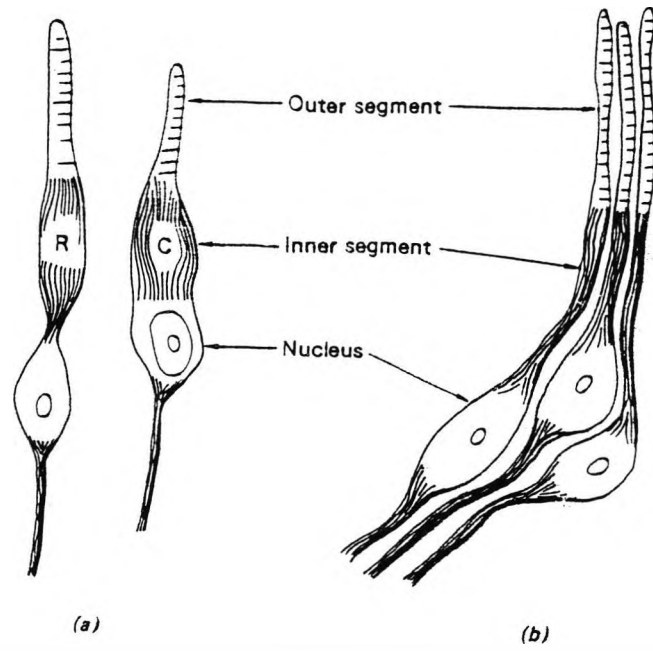


Figure 1.3 Schematic diagram of (a) peripheral rods (R) and cones (C) and (b) foveal cones (Padgham and Saunders, 1975)

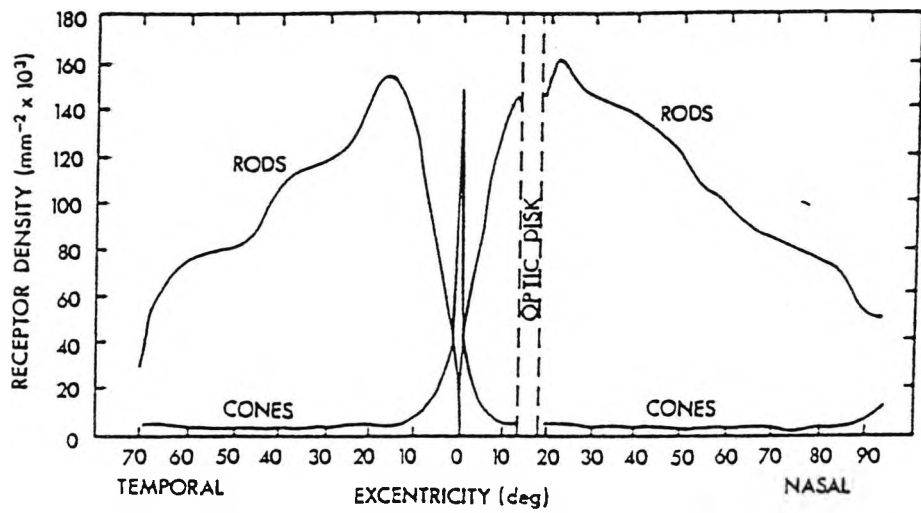


Figure 1.4 Graph showing the cone and rod photoreceptor density along the horizontal meridian of the human retina (Osterberg, 1935)

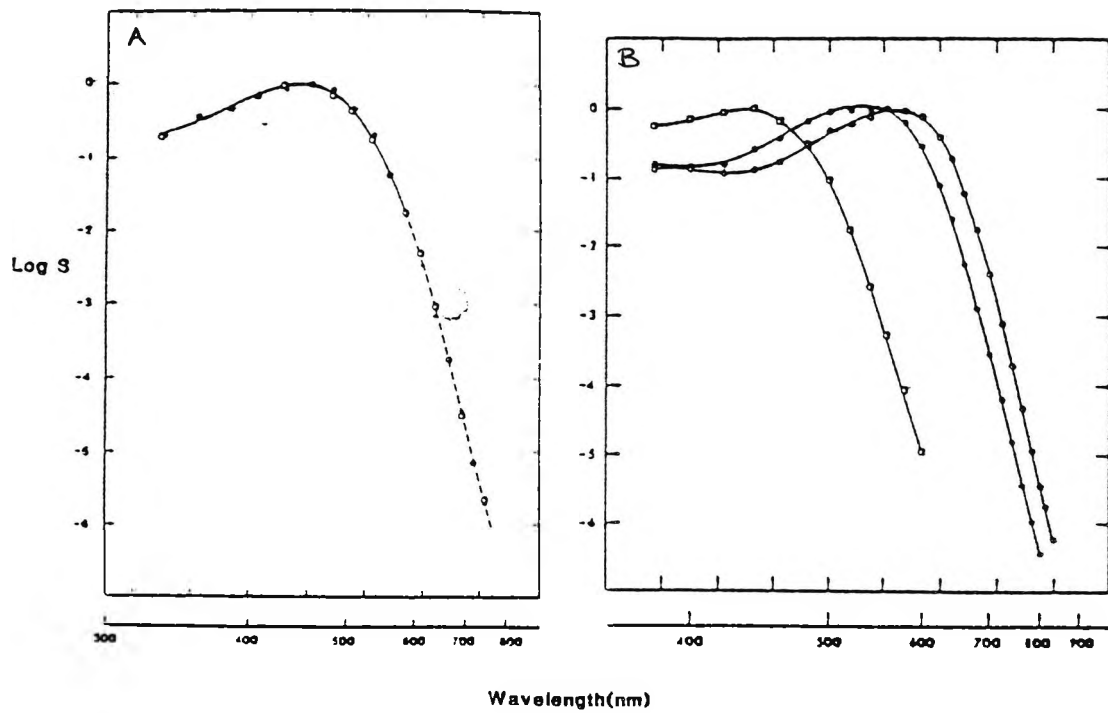


Figure 1.5 Spectral sensitivity (S) of the photoreponse of individual cones and rods of the monkey retina. The cones (shown on the right) have their peak sensitivity at about 565 nm, 530 nm and 450 nm. Open circles in the graph on the left represent the averaged spectral sensitivity of individual rods, while the closed circles show the human scotopic spectral sensitivity. (Falk, 1991)

It has not yet proved possible to distinguish between red and green cones, and there are conflicting reports of their relative frequencies. Marc and Sperling (1977) suggest that in the baboon there are twice as many green cones as red cones, while the psychophysical experiments of Cicerone and Nerger (1989) suggest that there are about two red cones for every green cone. Calkins et al. (1995) found that the 'non-blue' cones could be divided into two roughly equal groups according to the number of synapses subsequently made between bipolar and ganglion cells, and they hypothesise that these two groups correspond to red and green cones.

Photoreceptors synapse on to bipolar cells in the outer plexiform layer of the retina. Bipolar cells receive input from either rods or cones, and send outputs to amacrine or ganglion cells. A rod bipolar cell may be in contact with between 15 and 40 rod terminals in primates (Wassle and Boycott, 1991; Kolb, 1991). Several different types of cone bipolar are present, and may be classified as invaginating or flat according to the type of synapse they form with the cones. They may also be divided into the diffuse type, which collect information from several cones, and midget type, which are only in contact with one cone and are found at the fovea. There is also a cone bipolar which is specific for blue cones only, having several strong connections with one cone and a few weaker connections with other blue cones (Mariani, 1984; Kolb, 1991). Bipolar cells have antagonistic centre-surround receptive fields and a further distinction may be made between ON- and OFF-cells which are depolarised and hyperpolarised respectively by light falling on their receptive field centres.

Also in the outer plexiform layer are horizontal cells which are laterally interconnected neurons which have been divided into three morphologically distinct groups, HI, HII and HIII by Kolb (1991) and colleagues. She suggests that HI cells primarily contact red and green cones, with a few contacts to any blue cones within the dendritic spread, while their axons contact rod spherules. The dendrites of HII cells mainly contact blue cones, with a few contacts to red and green cones, while their axons contact blue cones. HIII cell dendrites only contact red and green cones. Wassle and Boycott (1991) have divided horizontal cells into two classes and suggest that both types connect all cones within their dendritic fields. Recent intracellular recordings by Dacey et al (1996) showed that all horizontal cells receive combined excitatory input from red and green

cells ie, no red-green opponency. They found that HI cells make no connections with blue cones and are unaffected by selective stimulation of blue cones. Selective stimulation of blue cones causes HII cell responses of the same sign and similar amplitude to the red or green cone stimuli, meaning that these cells are not blue-yellow opponent.

From the many lateral connections they form, horizontal cells contribute to the inhibitory receptive field surrounds of bipolar and ganglion cells, although not ganglion cell centre-surround chromatic opponency (Dacey et al, 1996).

Interplexiform cells should be mentioned here, as they synapse on to bipolar cells and horizontal cells in the outer plexiform layer (Dowling, 1990). Their input however occurs in the inner plexiform layer. The function of these cells is unclear, but they appear to be dopaminergic, and may therefore decrease the responsiveness of horizontal cells to light and decrease the electrical coupling between horizontal cells.

Synaptic contacts between bipolar cells, ganglion cells and amacrine cells are found in the inner plexiform layer. There are at least 25 different types of amacrine cell in the human retina, and these can be classified in terms of stratification of their dendrites in the inner plexiform layer, size, branching characteristics (Kolb, 1991) and neurotransmitters (Boycott and Wässle, 1991). They make contact with bipolar cells, other amacrine cells and the cell bodies and dendrites of ganglion cells.

Rod bipolar cells synapse with three types of amacrine cell, and not directly with ganglion cells. Kolb (1991) summarises the connections involved in the rod circuitry. The amacrine cells pass on input from rod bipolars to ganglion cells, and also link this information to cone pathways. Wide-field amacrine cells (A17 cells) link about 1000 rod bipolar cells each, and these cells may be integrating units involved in setting sensitivity levels over a large field. Convergence in the rod system therefore takes place at this level as well as at the rod-bipolar synapse. This gives a wide area over which quanta of light may be absorbed in order to initiate a ganglion cell response, and accounts for the high sensitivity to light of the rod system, but also its poor resolution.

Cone bipolars make direct synapses on to ganglion cells, with much less convergence than in the rod system. Amacrine cells probably contribute to the centres and surrounds of ganglion cells in the cone system. In the foveal region midget bipolars (which receive input from only one cone type) have a one-to-one connection with midget ganglion cells, thus preserving the potential for high spatial resolution at the fovea.

Retinal ganglion cells are neurons with cell bodies in the retina and axons forming the optic nerve, and it is estimated that there are about 1.2 million ganglion cells in the human retina. They fire spike or 'all-or-none' discharges, and fire a steady stream of impulses when no stimulus is presented. Most ganglion cells in the human retina have antagonistic centre-surround receptive fields, and they can be classified into on-centre and off-centre cells depending on whether a light increment on the centre of the receptive field causes an increase or decrease in firing rate (Figure 1.6). There are also on-off ganglion cells, which respond with a burst of impulses at stimulus onset and offset, and some of these are direction-sensitive (Dowling, 1987). These are far less common than on-centre and off-centre cells in the human and primate retina, but form a high proportion of the ganglion cells of lower vertebrates.

Various types of ganglion cells have been described and different classifications developed (Stone, 1983). Enroth-Cugell and Robson (1966) found two classes of ganglion cell which they described as X and Y, according to the responses of the cells to a sinusoidal grating drifting across their receptive fields. On-centre X-cells discharged maximally when a light bar crossed the centre of the receptive field, and off-centre X-cells gave the greatest response to a dark bar on the centre of the receptive field. For both types of X-cell there was a position of the grating for which no response was obtained. In this case the changes in luminance over one half of the receptive field were the exact inverse of the changes over the other half, suggesting that the cells were exhibiting approximately linear summation over the receptive field. For Y-cells no such 'null' position could be found, and the cells responded to the onset and the offset of the grating whatever its phase.

Gouras (1969) classified monkey ganglion cells as tonic cells which fire all the time the stimulus is on, and phasic cells which only fire at stimulus onset. Phasic cells generally

have faster axonal conduction than tonic cells. Similarly, in the cat, Cleland et al (1971) described sustained and transient ganglion cells, transient cells having faster-conducting axons. Sustained cells appear to receive most of their input from bipolar cells which give sustained responses, while transient cells receive more input from amacrine cells, many of which respond with transient potentials (Dowling, 1987).

'Other' cat cells were later classified as W-cells (Stone, 1983), and this group includes cells with different morphological and physiological characteristics (Rowe, 1991) although they are all slow-conducting. Rowe and Cox (1993) investigated the spatial receptive field structure of W-cells in cat and found that tonic and most ON-centre and OFF-centre phasic cells showed centre-surround mechanisms additively combining the centre and surround signals like X-cells. ON-OFF and directionally sensitive W-cells show nonlinearity like Y-cells. Many phasic W-cells have a large (20°) suppressive field surrounding the local receptive fields, which is effective for moving patterns (Rowe and Palmer, 1995).

Boycott and Wässle (1974) classified cat retinal ganglion cells anatomically into alpha, beta and gamma cells and suggested that they may correlate with Y-, X- and W-cells respectively. Delta and epsilon cells have since been specified (Wässle and Boycott, 1991). Table 1.2 summarises the characteristics of the chief groups of cat retinal ganglion cells.

In the macaque, Perry et al (1984) describe P-alpha and P-beta cells (P for primate) which project to magnocellular and parvocellular layers of the dorsal lateral geniculate nucleus (LGN) respectively. Because of their target sites in the LGN they are sometimes called M and P cells. 80% of all retinal ganglion cells are P-beta cells, while P-alpha cells are 10% of retinal ganglion cells. Perry and Cowey (1984) describe P-delta and P-epsilon cells which project to the midbrain, and which together make up the remaining 10% of ganglion cells.

The functional properties of ganglion cells in the rhesus monkey retina were investigated by de Monasterio and Gouras (1975). They found a class of cells with sustained, colour-opponent responses and mostly concentrically organised centre-surround

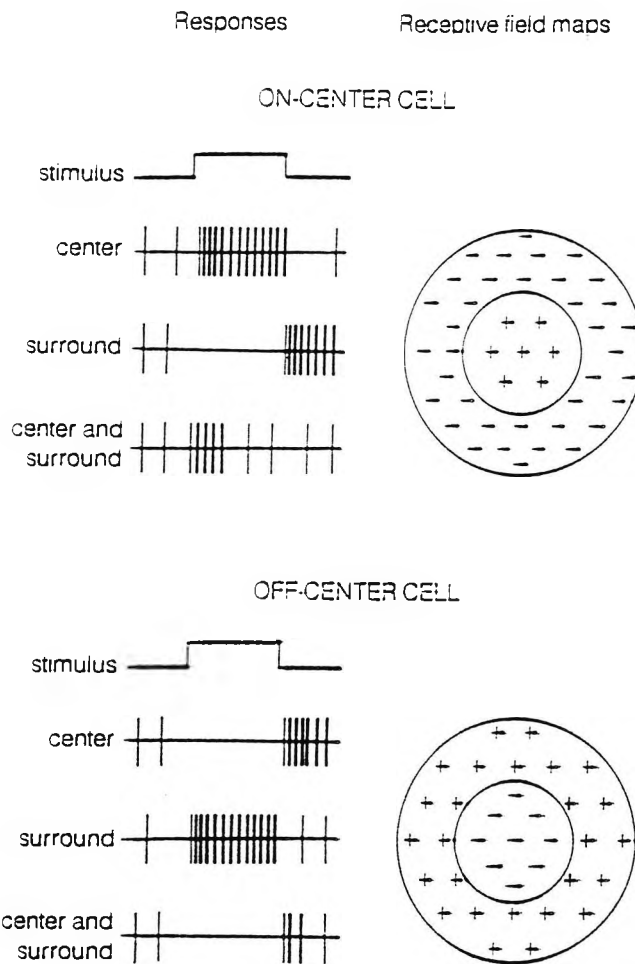


Figure 1.6 Idealised responses and receptive field maps for on-centre (top) and off-centre (bottom) contrast-sensitive ganglion cells. The drawings on the left represent hypothetical responses to a spot of light presented in the centre of the receptive field, in the surround of the receptive field, or in both the centre and surround regions of the receptive field. A + symbol on the receptive field map indicates an increase in the firing rate of the cell, that is, excitation; a - symbol indicates a decrease in the firing rate, that is, inhibition. (Dowling, 1987)

PROPERTIES	CHIEF GROUPS OF CAT RETINAL GANGLION CELLS		
Anatomical classification	Alpha	Beta	Gamma
Physiological classification	Y	X	W
Response characteristics	Brisk Transient	Brisk Sustained	Sluggish Sustained
Type of discharges	Phasic	Tonic	Phasic and tonic
Axon diameter	Thick	Medium	Thin
Conduction velocity	Relatively fast	Slower	Slowest
Proportions	4%	55%	41%
Distribution in the retina	Densest at parafovea, less dense in centre and periphery	Densest in central area, less dense in periphery	Densest in central area, less dense in periphery
Cell diameter ( $\mu\text{m}$ )	24-28	12-25*	5-15
Dendritic spread ( $\mu\text{m}$ )	300-600	25-250*	Wide
Receptive field size	Large	Small	Large
Spatial summation	Non-linear	Linear	Linear
On/off-centre	Both	Both	Both
Projections	LGN, SC	LGN (collateral branches to tectum and pretectum)	LGN, SC, PT, AOS
Possible function	Movement detection	Visual resolution	Pupillary reflexes

\*Diameter and dendritic spread increase with eccentricity

Table 1.2 Characteristics of retinal ganglion cells in cat (after Boycott and Wassle, 1974, and Ruskell, 1988). LGN=lateral geniculate nucleus, SC=superior colliculus, PT=pretectum, AOS=accessory optic system.

receptive fields, although a few cells of this class had co-extensive receptive field organisation. These correspond to P-beta or parvocellular cells. A second class had transient broadband responses and concentrically organised receptive fields, and correspond to P-alpha or magnocellular cells. A third class of cells did not have concentrically organised receptive fields. This class was not homogeneous and comprised cells with phasic ON-, OFF- and ON-OFF responses, and cells responsive only to moving stimuli.

Kaplan and Shapley (1986) investigated the contrast sensitivity of macaque retinal ganglion cells and found that M cells are much more sensitive to luminance contrast than P cells. Purpura et al (1988) show that the contrast gain of M cells is higher than that of P cells even at low levels of retinal illumination. They suggest that scotopic vision is mediated by M cells, which must therefore indicate a high rod input into the M system.

Lee et al (1990) found that M cells are more sensitive to luminance modulation, while P cells are more sensitive to chromatic modulation under most conditions. Under isoluminant conditions then, it would be expected that M cells would have a minimum response. Experiments have shown that this is the case for two different techniques for finding isoluminance between two colours. Using heterochromatic flicker photometry, minimum flicker is seen between two colours at the same ratio as M cells have their minimum response (Lee et al, 1988). Kaiser et al (1990) found that phasic (M cells) show a minimum response near equal luminance as defined by the minimally distinct border technique.

There are therefore functional differences between M and P cells in the retina, and these differences are maintained along parallel pathways which extend from the retina deeper into the visual system.

#### 1.1.4 Optic nerve, chiasm and tract

Axons of retinal ganglion cells turn into the plane of the retina and head towards the optic disc, through which they exit from the eye to form the optic nerve. They travel about 50 mm to reach the optic chiasm which is a midline structure <sup>below</sup> of the hypothalamus

of the brain. Fibres from temporal retinal ganglion cells pass through the chiasm laterally and continue into the ipsilateral optic tracts. Nasal fibres cross at the chiasm to join the contralateral optic tracts. This is known as semi-decussation, and the result is that information from the left visual hemifield is sent to the right side of the brain and vice versa (Figure 1.7).

90% of the fibres then travel along the optic tracts to terminate in the lateral geniculate nuclei, but a few leave the optic chiasm to enter the bilateral suprachiasmatic nuclei. A larger minority leave each of the optic tracts just before the lateral geniculate nucleus in the superior brachium, and these fibres head for the pregeniculate nucleus, the pretectal nuclei, the superior colliculus, the pulvinar and the accessory optic nuclei (Ruskell, 1988).

#### 1.1.5 Lateral geniculate nucleus

The dorsal lateral geniculate nucleus (LGN) is situated in the ventrolateral part of the dorsal thalamus, separated from the rest of the thalamus by the optic tract. It has six layers of neurons which curve round the hilum (Figure 1.8). The two layers nearest to the hilum (numbered 1 and 2) have large cells, and are called the magnocellular layers, and the other four layers have smaller cells and are called the parvocellular layers (numbered 3-6). The magnocellular layers receive input from P-alpha cells, while P-beta cells project to the parvocellular layers (Perry et al, 1984). Layers 1, 4 and 6 receive crossed fibres from ganglion cells in the contralateral nasal retina and layers 2, 3 and 5 receive fibres from the ipsilateral temporal retina. At the level of the LGN therefore input from the two eyes is not integrated.

Parvocellular and magnocellular cells are not the only LGN neurons. It is thought that about 20% of LGN neurons are interneurons (Garey et al, 1991) which make connections within but not between layers. In primate LGN there is a superficial or S-layer of small koniocellular neurons which appear to receive input from W-like cells (Garey et al, 1991).

The magnocellular and parvocellular layers have been shown to contain functionally different cells. Wiesel and Hubel (1966) categorised rhesus monkey LGN cells into four

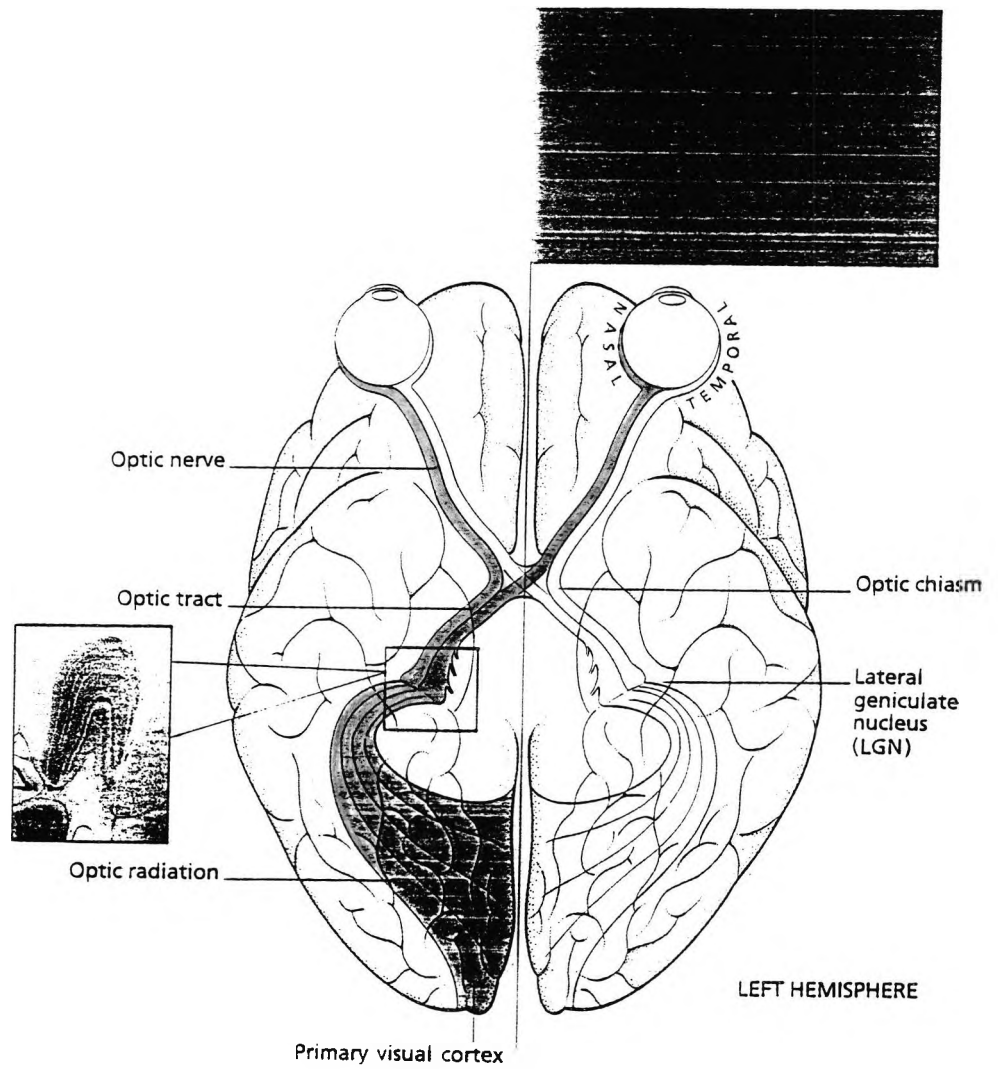


Figure 1.7 The connections from the retina to the cerebral hemispheres. The primary visual cortex receives information from the contralateral hemifield, as indicated by the shaded pathway. (Zeki, 1993)



Figure 1.8 The layers of the lateral geniculate nucleus (LGN). The lower two layers (1 and 2) have large cells and are called the magnocellular layers, receiving input from P-alpha cells. The upper four layers (3,4,5 and 6) have small cells and are thus termed parvocellular layers, and their input is from P-beta cells. Layers 1,4 and 6 receive crossed fibres from the contralateral nasal retina and layers 2,3 and 5 receive fibres from the ipsilateral temporal retina. There is precise retinal mapping within the LGN, for example, cells along the line shown receive inputs from homologous points in the two retinas and therefore all register identical points in visual space. (Zeki, 1993)

types. In the parvocellular layers they describe three types of cell: Type I cells which have centre-surround fields, the centre and surround having different spectral sensitivities, Type II cells with two spatially coextensive but spectrally different systems and Type III cells with opponent centre-surround systems having the same spectral sensitivity, ie, not colour-opponent. Schiller and Malpeli (1978) found that layers 5 and 6 of the rhesus monkey contain predominantly ON-centre Type I cells, while layers 3 and 4 contain predominantly OFF-centre Type I cells. Wiesel and Hubel (1966) also found Type III cells in the magnocellular layers, together with cells classified as Type IV cells. These had a centre-surround field in which the centre responded to most wavelengths while the inhibition of the surround was dominant but only for wavelengths above 580 nm.

This classification has been revised to suggest that Type I and Type III cells are similar except that Type I cells have strong chromatic opponency and Type III cells have weak chromatic opponency (Derrington et al, 1984). Derrington and Lennie (1984) conclude that parvocellular cells can be divided into two types: the Type I/Type III group which has a spatially and chromatically opponent receptive field which is driven only by red and green cones, and another type which receives blue cone input opposed to some combination of red and green cone input, with more nearly spatially co-extensive mechanisms. In the magnocellular layers Derrington et al (1984) found that most cells have chromatically opponent receptive fields, with spatially segregated antagonistic mechanisms.

LGN cells can be also classified as X-like or Y-like cells depending on their spatial summation properties similarly to retinal ganglion cells (Enroth-Cugell and Robson, 1966). 99% of parvocellular cells in macaque are X-like (Shapley et al, 1981; Kaplan and Shapley, 1982), while 75% of magnocellular cells are X-like, and the rest are Y-like. Parvocellular X-like cells have different properties from magnocellular ones (Kaplan and Shapley, 1982, Table 1.3).

The functional differences between the parvocellular and magnocellular systems have already been touched upon in section 1.1.3, and are summarised in Table 1.4.

In primates, the bulk of LGN cell axons project via the optic radiations to the primary visual cortex, V1, although direct projections from LGN to prestriate cortex have been found (Yukie and Iwai, 1981; Bullier and Kennedy, 1983).

#### 1.1.6 Primary visual cortex, V1

Primary visual cortex, or V1, is equivalent to Brodmann's area 17 (Brodmann, 1909; Figure 1.9), and is distinguishable from the rest of the cortex by a band of medullated nerve fibres parallel to its surface. Hence it is often referred to as the striate cortex. It lies in the occipital lobe mainly on the medial aspect of each hemisphere hidden in the calcarine sulcus (Figure 1.10) and is also sometimes called the calcarine cortex. The rest of the occipital lobe is taken up by areas 18 and 19, which are described as prestriate cortex, and will be described in section 1.1.7.

V1 contains a precise topographic map of the retina. This means that the patch of retina receiving input from a particular area of the visual field is always connected to a particular part of V1 and that adjacent retinal areas (stimulated by light from neighbouring parts of the visual field) are found to project to adjacent areas of V1. The central part of the visual field is represented at the occipital pole of V1, while the inferior field and superior field are represented in the upper and lower calcarine cortex respectively. A greater proportion of the cells in V1 is involved in processing information from the central part of the field than from peripheral areas. This has been described in terms of 'magnification factor', that is, the amount of cortex, in square millimetres, devoted to every degree of visual space.

If a lesion occurs in V1 its whereabouts can be predicted fairly accurately from the position of the resulting scotoma in the visual field. Complete damage to V1 on one side of the brain results in a homonymous hemianopia or a loss of vision in the contralateral field of view. This field loss may be associated with 'macular sparing', where the central 5° of visual field is spared. This may be explained by the dual blood supply to the pole of the occipital cortex rendering it less liable to damage, or by the fact that some of the neurons representing the central field close to the vertical midline cross at the optic chiasm while others carry information to the ipsilateral side of the brain.

Subject GY who took part in the experiments described in Chapters 3 and 4 has a right

	Parvo-X	Magno-X	Magno-Y
Spatial summation	Linear	Linear	Non-linear
Chiasm latency	Long	Short	Short
Spatial resolution (Fundamental)	High	Medium to high	Low
Spatial resolution (2nd harmonic)	–	–	Medium to high
Colour	Opponent Concealed opponent	Non-opponent Type IV	Non-opponent
Contrast sensitivity	Low	High	High

Table 1.3. Cell types in monkey lateral geniculate nucleus (from Kaplan and Shapley, 1982)

Property	Parvocellular	Magnocellular
Colour	Yes (colour-opponent)	No (broadband)
Contrast sensitivity	Low (threshold > 10%)	High (threshold < 2%)
Spatial resolution	High	Low
Temporal resolution	Slow (sustained responses, low conduction velocity)	Fast (transient responses, high conduction velocity)

Table 1.4 Physiological differences of the magnocellular and parvocellular geniculate divisions (from Livingstone and Hubel, 1987)

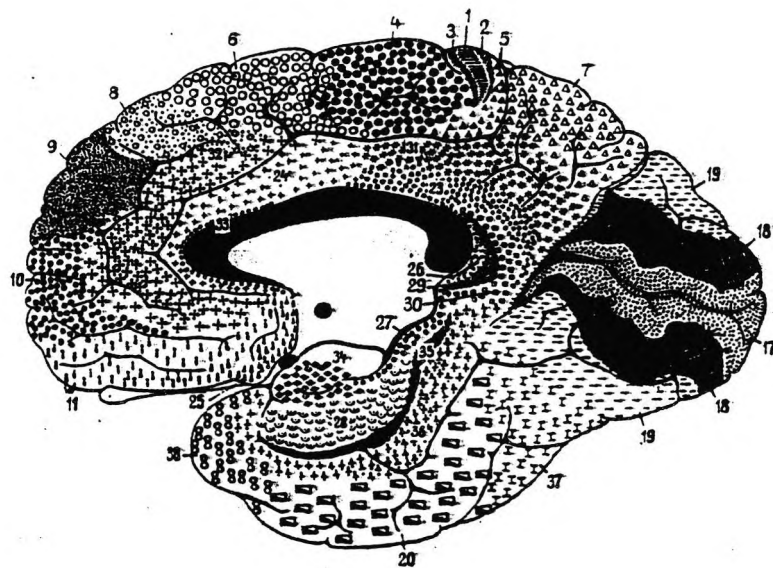
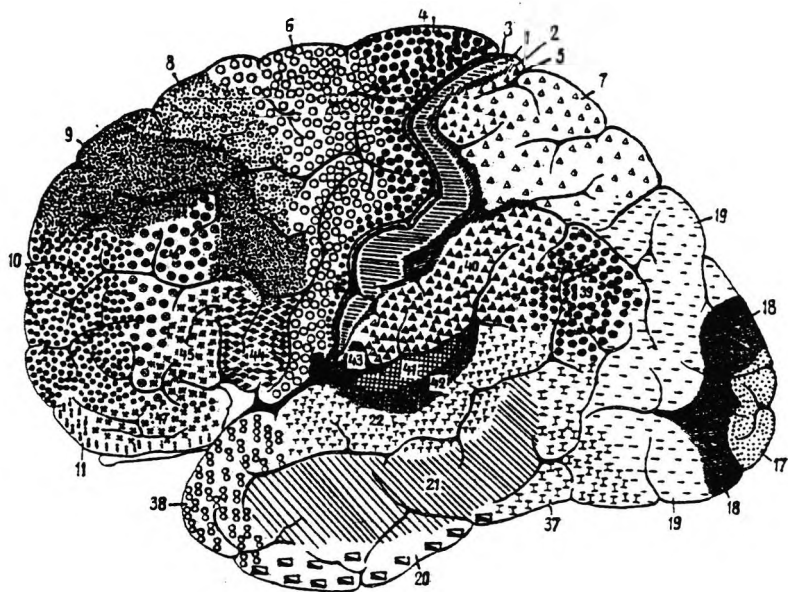


Figure 1.9 Lateral (upper diagram) and medial (lower diagram) views of the cerebral cortex showing different areas classified by Brodmann (1909)

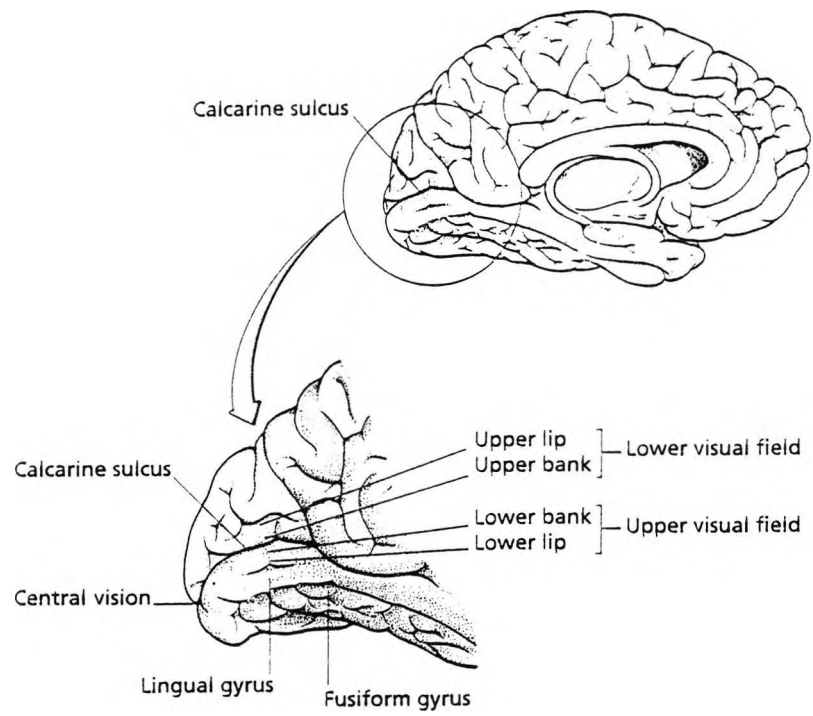


Figure 1.10 Diagram showing location of primary visual cortex (V1), and the relationship between areas of V1 and the field of view (Zeki, 1993)

homonymous hemianopia with macular sparing, following a traumatic injury to the left occipital cortex.

The primary visual cortex has a laminar structure (Figure 1.11), whose layers were named by Brodmann and later Lund as shown in Table 1.5. Some of the between-layer connections of striate cortex cells are summarised in Figure 1.12. It is extremely complex! One important feature of these connections is that the parvocellular and magnocellular neurons project to different layers (parvo→IVA and IVC $\beta$  and magno→IVC $\alpha$ ) and so segregation of these two pathways is maintained.

As well as the laminar structure described above, cells in the visual cortex may be classified according to receptive field properties, ocular dominance and histochemical staining. Hubel and Wiesel classified cat striate cortex cells into simple, complex and hypercomplex or end-stopped cells (Hubel, 1988). Simple cells respond best to slits of light along a particular orientation and in a particular position in their receptive field. Complex cells will respond to an appropriately orientated line anywhere in the receptive field, and most vigorously if the line is moved across the receptive field. Many complex cells respond better to one direction of movement across the receptive field than the opposite, and therefore show direction selectivity. End-stopped cells respond best to slits of particular orientation and length. In monkey, Hubel and Wiesel found that cells in layer IVC $\beta$ , which receives parvocellular input, were of centre-surround organisation without orientation selectivity. Layer IVC $\alpha$  which receives magnocellular input contains both cells with centre-surround fields and simple cells. In the other layers most cells are complex, although there are different types of complex cells in different layers. For example, in cells in layers II and III are end-stopped, while in layer V short slits and long slits seem to be equally effective stimuli, and cells in layer VI prefer long stimuli (Hubel, 1988). In the rhesus monkey, Schiller et al (1976) found S-type cells (similar to simple cells) and CX-type cells (similar to complex cells), but suggested that hypercomplex cells were not a distinct category in their own right.

Figure 1.13 shows a model of the cortex in terms of ocular dominance columns, orientation columns and blobs and interblobs. Although binocularly driven neurons are seen for the first time in the striate cortex, many of the cells respond preferentially to stimuli presented to a particular eye, and are said to exhibit ocular dominance. Ocular

dominance columns are approximately 0.5 mm wide 'slabs' of cells all with the same ocular preference to a greater or lesser extent. In layer IV the columns are clearly defined, while in the other layers the boundaries are not as sharp.

Orientation columns arise from cells vertically above one another having the same orientation preference. In a transverse penetration through the striate cortex (ie, parallel to the surface) the orientation preference gradually alters from cell to cell in an organised manner (Figure 1.13). The columnar organisation of orientation selectivity does not appear to be related to that of ocular dominance.

The 'blobs' shown in Figure 1.13, are oval pillar-like columns of about 150 x 200  $\mu\text{m}$  which show up with a stain for cytochrome oxidase (Livingstone and Hubel, 1984a). They are seen most conspicuously in layers II and III, faintly in layers IVB, V and VI, and not at all in layers IVA and IVC. They are centred along ocular dominance columns. The areas between blobs are known as interblobs. Livingstone and Hubel (1984a) found that cells in the blobs did not show orientation selectivity, while interblob cells were highly orientation specific and responded well to coloured slits if the orientation was right. Blob cells had concentrically organised receptive fields of three types: broad-band, and red-green and blue-yellow double opponent cells, which gave maximum response to one colour surrounded by its complementary. They did not find double opponent cells in layer IVC $\beta$ , although Michael (1989) found that approximately half of the cells he investigated in this layer were double opponent. Ts'o and Gilbert (1988) found blob cells corresponding to the Type I and Type II cells of the LGN (Wiesel and Hubel, 1966), but no double opponent cells. Livingstone and Hubel (1984b) found that blob cells connected blob cells, and interblob cells connected with interblob cells, ie that the two systems remain segregated from each other. Ts'o and Gilbert (1988) also found lateral interactions between blob cells in the same and adjacent blobs which had the same receptive field type, colour opponency and ocular dominance. Interblob cells sharing orientation and eye preferences were also connected. The segregation between blobs and interblobs is continued into the prestriate cortex.

### 1.1.7 Prestriate cortex

The non-striate cortex in the occipital lobe of the brain (Brodmann's areas 18 and 19; Figure 1.9) lie anterior to the striate cortex, and have been divided into different areas

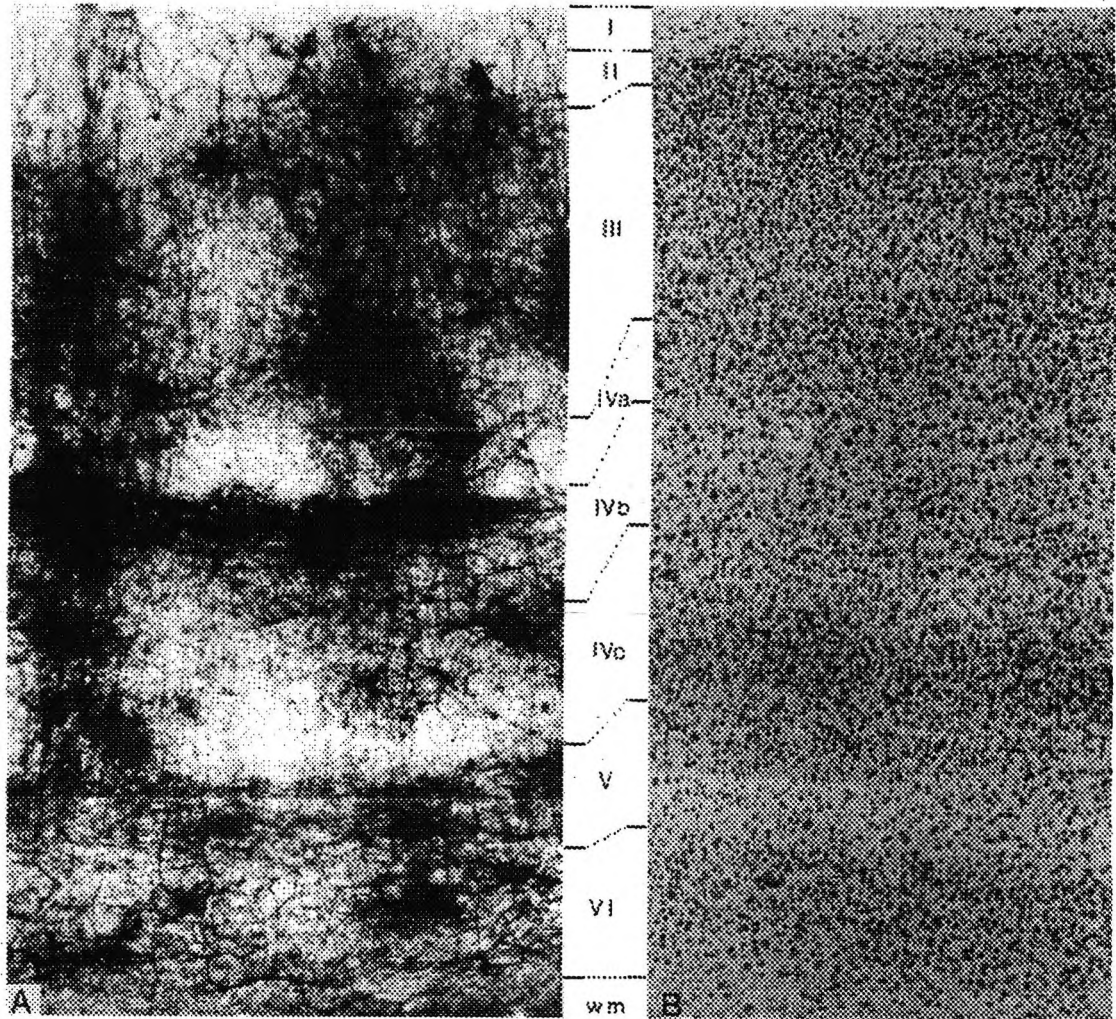


Figure 1.11 (A) Golgi section of the striate area of *Macaca mulatta*  
(B) Nissl-stained section of the same region in another monkey. (Valverde, 1985)

Layer I			Lamina zonalis
Layer II			Lamina granularis externa
Layer III			Lamina pyramidalis
Layer IV	Layer IVa		Lamina granularis interna superficialis
	Layer IVb		Lamina (granularis interna) intermedia
	Layer IVc	Layer IVc-alpha	Lamina granularis interna profunda
		Layer IVc-beta	
Layer V			Lamina ganglionaris
Layer VI	Layer VIa	Lamina triangularis	Lamina multiformis
	Layer VIb	Lamina fusiformis	

Table 1.5. Layers of the primate striate cortex (Valverde, 1985)

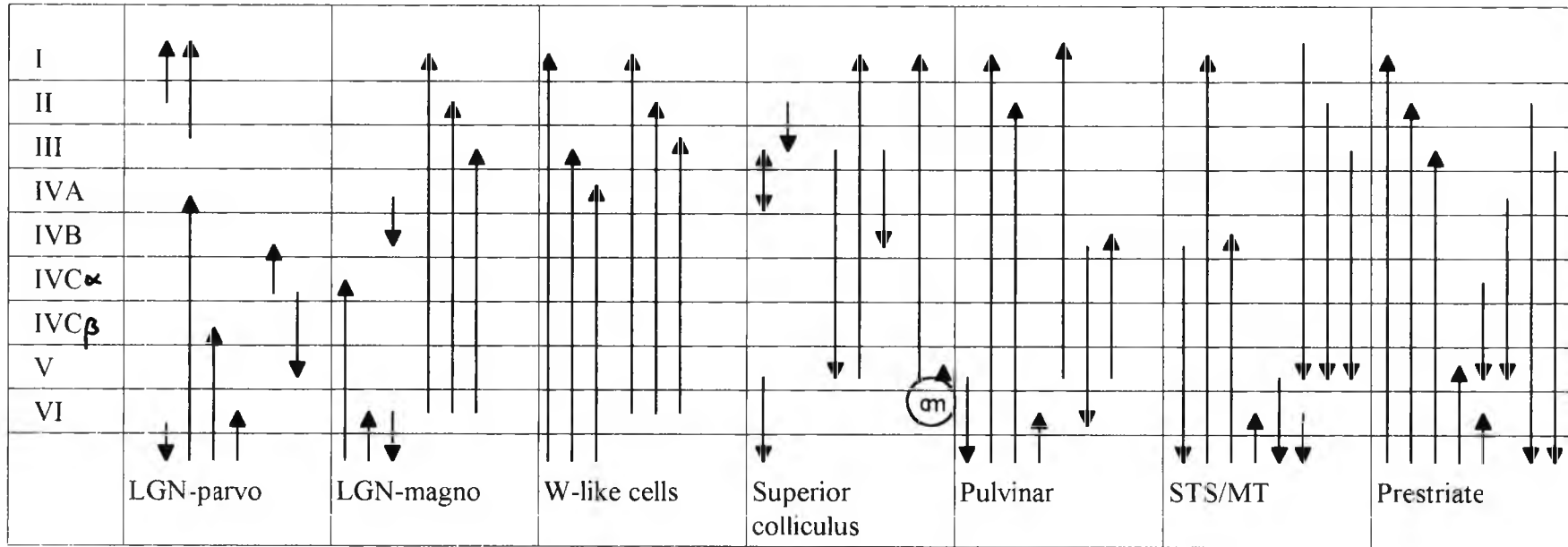


Figure 1.12. Diagram showing connections made by striate cortex cells (from Valverde, 1985, 1991) LGN=lateral geniculate nucleus; STS=superior temporal sulcus; MT=middle temporal area; cm=solitary cell of Meynert.

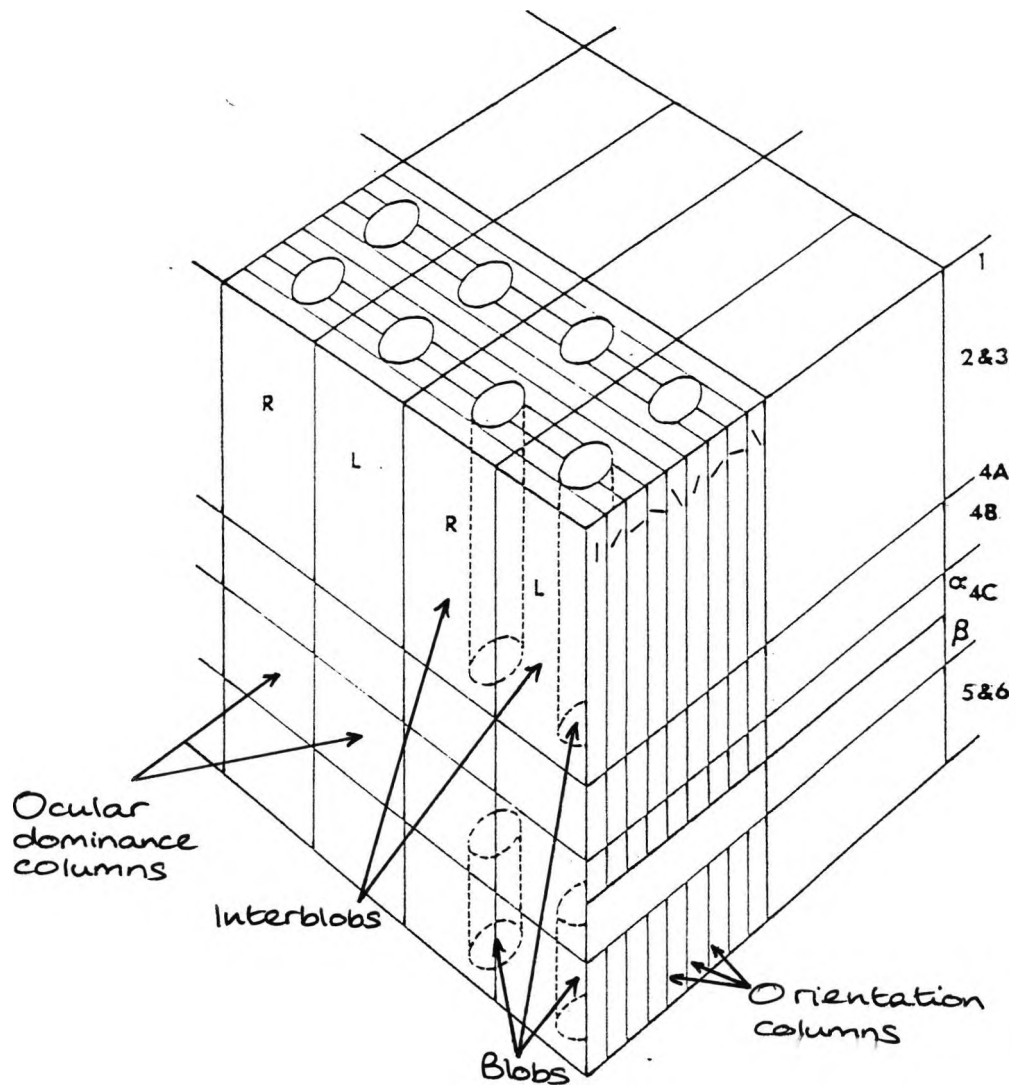


Figure 1.13 A model of the macaque primary visual cortex in terms of ocular dominance columns, orientation columns and blobs and interblobs (Livingstone and Hubel, 1984a)

according to functional specialisation, namely V2, V3, V3A, V4 and V5 (Zeki, 1993). Together these areas are known as prestriate cortex.

V2 surrounds area V1 and is distinguished from the rest of the prestriate cortex by the distinctive pattern produced by staining for cytochrome oxidase. A pattern of alternating wide and narrow densely staining stripes is separated by paler interstripes (Livingstone and Hubel, 1984a). In the macaque monkey, the cycle of thick stripe, interstripe, thin stripe, interstripe covers 4.5-5 mm (Zeki, 1993). Using horseradish peroxidase labelling, Livingstone and Hubel (1984a) showed that cells in the blobs of V1 project to the thin stripes of V2 with reciprocal connections between V2 thin stripes and V1 blobs, and that interblob cells of V1 project to the interstripes of V2 and vice versa. They also found stripe-to-stripe and interstripe-to-interstripe connections within V2. Cells in V2 have been found which respond to specific binocular disparities, and also to wavelength, orientation, direction and illusory contours (Van Essen, 1985; Hubel and Livingstone, 1987).

Next to V2 and receiving point-to-point input from V1, lies V3, which contains cells mostly responsive to lines of specific orientation. V3A receives input from V3, but not from V1, and contains cells similar to those of V3.

V3A is bordered anteriorly by V4, which is situated on the lateral side of the brain. V4 receives some input from the part of V1 which receives information from the fovea via the LGN, but its main input is from V2. V4 is concerned with colour vision (see section 1.4.2).

V5 or MT is again on the lateral side of the brain, anterior to V4. It receives input from V1 and the thick stripes of V2, and contains cells which are selective for direction of motion.

The above is a great simplification of the prestriate cortical areas - for example, there are further areas associated with V4 and V5, and there are many reciprocal connections between areas, described in Felleman and Van Essen (1991).

### 1.1.8 Higher visual areas

This section will briefly describe some higher visual and polysensory areas. For a review of all visual areas and their connections, see Felleman and Van Essen (1991).

MST (medial superior temporal area) occupies a narrow strip of cortex medial to MT or V5, and receives input from V5. In this area, cells have been found which are selective for rotatory motion and changing size (Maunsell and Newsome, 1987). MST projects to Area 7a in the parietal lobe, which may be concerned with motion towards or away from the centre of gaze, ie optical flow, and STP, the superior temporal polysensory area in the temporal lobe, which contains cells responsive to visual, auditory and somatosensory stimuli. V5 cells also project to VIP (ventral intraparietal area) which lies along the intraparietal sulcus, but little is known about cells in this area.

PIT and AIT are the posterior and anterior inferotemporal areas respectively. PIT receives input from V4, and AIT receives input from PIT. The inferotemporal cortex contributes to later stages of form analysis (Maunsell and Newsome, 1987), for example, cells are found which respond preferentially to particular objects such as hands and faces. Even more specific preferences have been found, for example, hands carrying out specific actions, or faces viewed at a specific angle (Perrett et al, 1990).

Area 8, in the frontal lobe, is called the frontal eye field, and receives visual inputs from areas V4 and MST. It is thought to be involved in eye movements. In the parietal lobe, LIP (lateral intraparietal area) receives visual and somatosensory inputs.

### 1.1.9 Parallel pathways

In the preceding sections some aspects of the anatomy and physiology of the visual system have been discussed. It is clear that there are functional differences between the 'parvo' and 'magno' systems (see Table 1.4), and for this reason the visual system has often been described in terms of parallel pathways, summarised below (from Livingstone and Hubel, 1987):

1. The magno pathway - P- $\alpha$  retinal ganglion cells  $\rightarrow$  magnocellular layers of the LGN  $\rightarrow$  4C $\alpha$   $\rightarrow$  4B  $\rightarrow$  MT (directly and via the thick stripes of V2)

2. The parvo-interblob pathway - P- $\beta$  retinal ganglion cells  $\rightarrow$  parvocellular layers of the LGN  $\rightarrow$  4C $\beta$   $\rightarrow$  interblobs  $\rightarrow$  interstripes of V2  $\rightarrow$  V4

3. The blob pathway - magnocellular, parvocellular LGN cells (?) and koniocellular LGN cells (?, Casagrande, 1994)  $\rightarrow$  4C $\beta$ (?)  $\rightarrow$  blobs  $\rightarrow$  thin stripes of V2  $\rightarrow$  V4

Table 1.6 summarises the above pathways and properties of these pathways. From the functional properties of the cells involved, it seems likely that the magno pathway would be involved in movement perception, depth perception and linking properties, the parvo-interblob pathway would be involved in shape discrimination and the blob pathway would be involved with colour perception. Psychophysical experiments carried out by Livingstone and Hubel (1987) provide some support for this scheme.

Others have demonstrated parallel pathways by lesion studies. Schiller et al (1990) showed that the colour-opponent channel (parvo) is essential for the processing of colour, texture, fine pattern and fine stereopsis, while the broad-band channel (magno) is involved with perception of motion and fast flicker. Merigan (1991) found that the P (parvo) pathway transmits information about high spatial and lower temporal frequencies and colour, while the M (magno) pathway transmits the higher temporal and lower spatial frequencies.

However, the distinction between parvo and magno pathways is not as clear cut as suggested above. Merigan (1991) suggests that certain modalities of vision, for example, stereopsis, could be mediated by either pathway depending on the spatiotemporal characteristics of the stimulus. Merigan and Maunsell (1993) describe interactions between the two pathways, for example that there is magno input to the V1 blobs, and more recently it has been found that there is also magno input to the interblobs (see Shipp, 1995). Shipp concludes that 'there is no such thing as a pure P pathway in the brain, because there is no part of the cortex, outside V1, where the P system maintains exclusive access'. As well as parvo and magno input, blobs also receive input from the so-called koniocellular layers of the LGN (Casagrande, 1994).

Thus it is probably an oversimplification to think of the visual system in terms of strictly segregated parallel pathways.

### 1.1.10 Midbrain and diencephalic structures and projections

Midbrain structures and projections will be described, as they are involved in pupil control (see section 1.2) and have also been implicated in blindsight and residual vision (see section 1.3).

The midbrain is the top portion of the brainstem, lying beneath the thalamus and above the pons. The ventral aspect has pillar-like bulges called the cerebral peduncles, and the dorsal aspect has four protrusions of white matter, the superior and inferior colliculi, collectively called the corpora quadrigemina. The cerebral aqueduct runs down the centre of the midbrain and is surrounded by grey matter containing several nuclei, such as the substantia nigra, red nucleus and oculomotor nucleus (figure 1.14).

The superior colliculi are involved in vision and eye movements. Schiller and Koerner (1971) found that superficial cells in the rhesus monkey superior colliculi responded almost exclusively to visual stimuli, regardless of stimulus shape, orientation, wavelength or direction of movement. These cells were however differentially sensitive to stimulus size. Some cells only responded to jerky stimulus movements, while others responded to smoothly moving and stationary flashing stimuli. Deeper cells fired prior to saccadic eye movements. Schiller and Koerner (1971) suggested that the superior colliculi play an important role in foveal acquisition and maintenance of visual targets. A slightly later study by Goldberg and Wurtz (1972) also found that collicular cells had receptive fields favouring stimuli of a particular size, but they found no 'jerk detectors' and they did find some cells (about 10%) showing directional selectivity. In squirrel monkey, nearly half the superficial superior colliculus cells studied by Kadoya et al (1971) were found to have wavelength-specific responses, almost all 'red on' responses. In macaque monkey, Marrocco and Li (1977) found that 68% of superficial colliculus cells tested were preferentially excited by light of 570 nm, with the rest preferring light of either 600 nm or 500 nm. Neither of these studies found the spectrally-opponent receptive fields present in the geniculostriate pathway.

Input from retinal ganglion cells comes via the optic nerve and optic tract via the brachium of the superior colliculus, and most fibres are from the ~~from the~~ retina of the contralateral eye (Carpenter and Sutin, 1983). Perry and Cowey (1984) found that not

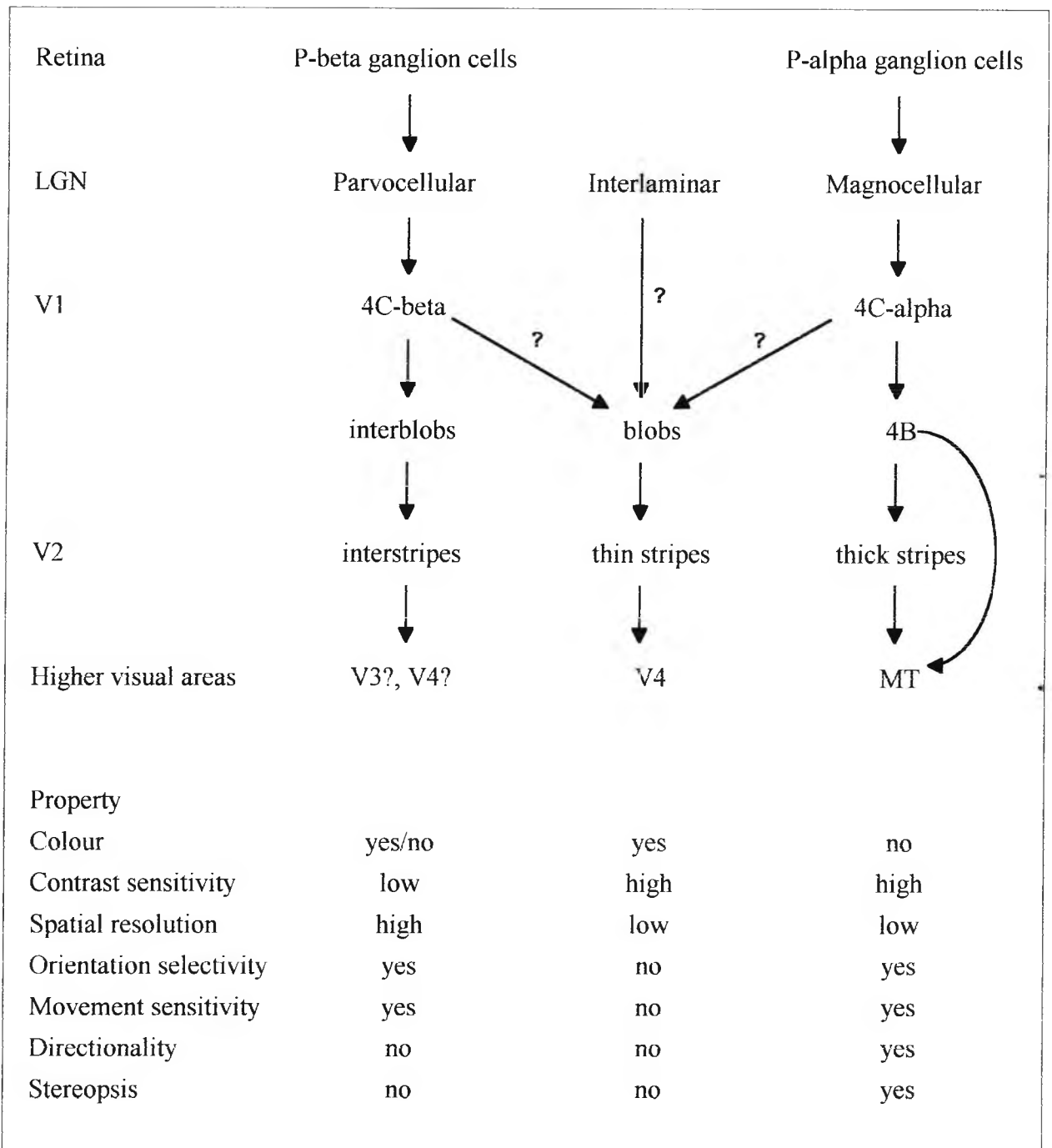


Table 1.6 Summary of the major subdivisions and connections of the primate geniculocortical visual system (from Livingstone and Hubel, 1987)

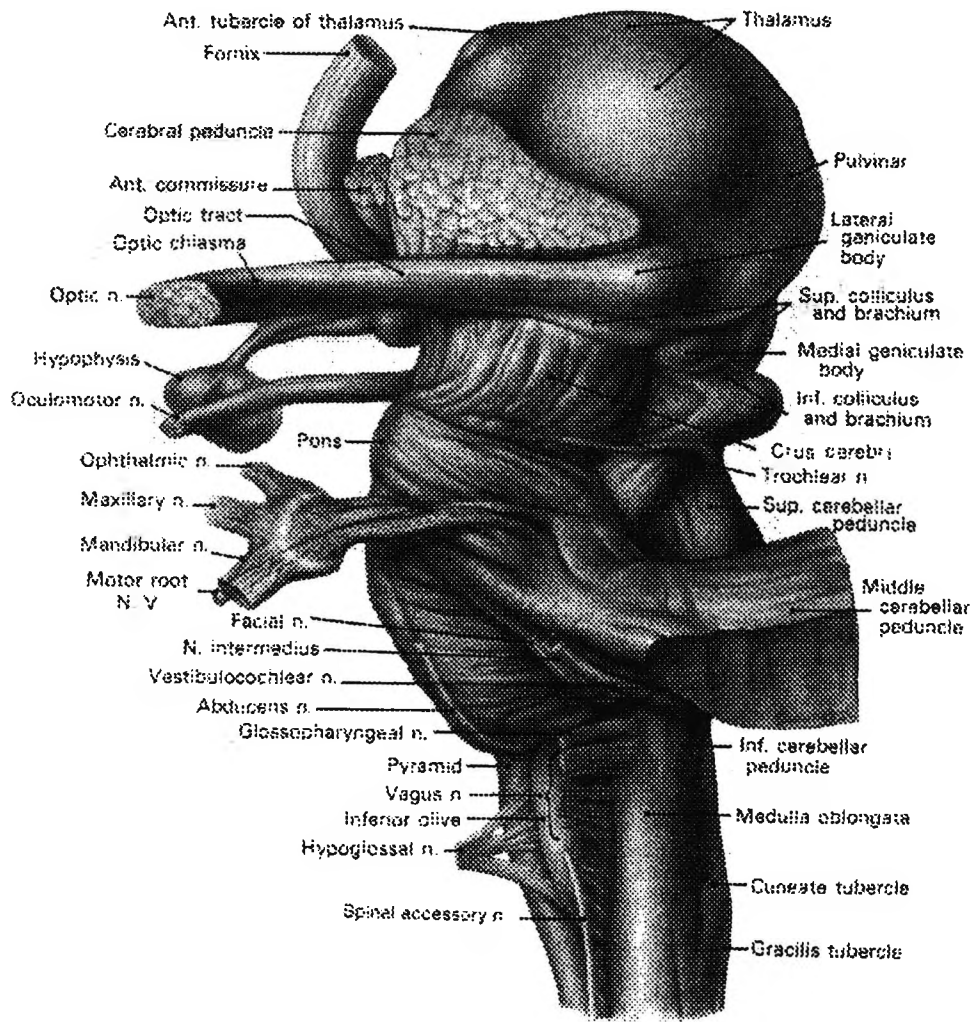


Figure 1.14 Lateral view of the brain stem, with the cerebellum removed, showing the sites of emergence and entrance of the cranial nerves (Carpenter and Sutin, 1983)

more than 10% of all retinal ganglion cells project to the superior colliculus in the macaque. Of these cells, none were P-beta cells, only a few were P-alpha cells, and most were small to medium sized cells which they called P-gamma and P-epsilon. Rodieck and Watanabe (1993) found almost no parasol cells (equivalent to P-alpha cells), and divided the other cells into three groups: M cells, which were monostратified, without overlap of their dendritic fields; S cells, which had sparse and sometimes bistratified dendritic fields and T cells which had dense and usually bistratified dendritic fields.

There is also cortical input to the superior colliculus. The most substantial projection comes from the visual cortex, which is magnocellular in origin (Schiller et al, 1979). There are also projections from the frontal eye field (area 8) which terminate in the middle layers of the superior colliculus, and from the auditory cortex, terminating in the deep layers (Carpenter and Sutin, 1983). Within the brain stem, the superior colliculus receives input from the inferior colliculus and parabigeminal and auditory relay nuclei.

Fibres from the superior colliculus terminate in the pulvinar, intralaminar regions of the LGN, pons, inferior colliculus, reticular formation and accessory oculomotor and olivary nuclei.

The accessory optic system (AOS) is situated in the anterior midbrain (Simpson, 1984), and in primates consists of a group of fibres called the inferior fasciculus of the accessory optic tract, a dorsal terminal nucleus and a comparatively substantial lateral terminal nucleus. In lower animals, the AOS also includes a superior fasciculus and a medial terminal nucleus. There is direct retinal input to the AOS, in cats from the 'gamma' class of ganglion cells. Nonretinal input includes projections from the nucleus of the optic tract, ventral lateral geniculate nucleus, ipsilateral visual cortex and part of the midbrain reticular formation. Efferents from the AOS include those towards the inferior olivary nucleus, nucleus of the optic tract and the interstitial nucleus of Cajal (which plays a role in vertical and rotatory eye movements (Carpenter and Sutin, 1983)). Simpson (1984) reviews visual response properties of AOS neurons, from which it is suggested that this system is specialised for detecting movement in the vertical plane and may therefore be concerned with changes in eye position relative to

the horizon. In the rabbit, AOS neurons respond well to large slowly moving textured patterns, which could correspond to the slip of the visual world over the retina during the movement of the animal. This suggests that the AOS may be involved in stabilising the eyes and head in space.

The pretectal region lies immediately rostral to the superior colliculus, includes several nuclei (Carpenter and Sutin, 1983): the nucleus of the optic tract; the sublentiform nucleus; the nucleus of the pretectal area; the pretectal olivary nucleus and the principal pretectal nucleus. Benevento and Standage (1983) found retinal input via the optic tract and brachium of the superior colliculus to these areas except the nucleus of the pretectal area. There is also input from the lateral geniculate body, the cortex, AOS and thalamic nuclei (Carpenter and Sutin, 1983). The pretectal olivary nucleus projects to the Edinger-Westphal nucleus and hence the pretectum is the principal midbrain centre involved in the pupillary light reflex, which will be considered in section 1.2. There are also pretectal projections to the lateral and inferior pulvinar (Benevento and Standage, 1983) and the LGN, and hence information from the superior colliculus reaches the cortex through the pulvinar (Petersen et al, 1985).

The pulvinar is the most caudal part of the thalamus and is a large nuclear mass overhanging the geniculate bodies and the dorsolateral surface of the midbrain (Carpenter and Sutin, 1983). It has been divided into four regions: the oral, inferior, medial and lateral nuclei. Petersen et al (1985) studied the visual responses of pulvinar cells, and found cells sensitive to stimulus orientation and direction of stimulus movement. Most cells respond to stimulus onset, with many of these also responding at stimulus offset. Felsten et al (1983) found some neurons in the pulvinar to have colour-opponent properties.

The pulvinar receives direct input from the retina and superior colliculus, and makes reciprocal connections with striate, prestriate and inferior temporal cortex. Pulvinar cells are sensitive to stimulus orientation, while cells of the superior colliculus are not, which suggests that the visual properties of the pulvinar are related to cortical input rather than collicular input. Lesions of the primate superior colliculus (Bender, 1988) had little effect on the pulvinar while striate cortex lesions dramatically reduced visual

responsiveness. Following cortical lesions, some pulvinar cells regained visual sensitivity after about three weeks but ended up with response properties similar to those of the superior colliculus. Further lesion experiments by Bender (1988) showed that collicular lesions affected spatial localisation, colour discrimination, visual search and ~~tachistopic~~<sup>tachistoscopic</sup> discrimination, while pulvinar lesions had little effect unless corticotectal fibres were also damaged.

As a relay between retina and extrastriate cortex, the pulvinar has been implicated in residual vision in patients with striate damage (for example, Cowey and Stoerig, 1991a,b), which will be considered further in section 1.3.

## 1.2 The pupil

### 1.2.1 Introduction

The entrance pupil of the eye is regulated by the iris, which acts as a diaphragm or aperture stop. The size of the pupil is determined by the action of radial and circular muscles within the iris, which are innervated by the autonomic nervous system.

Lowenstein and Loewenfeld (1969) therefore describe the pupil as 'an ideal indicator for studies on the physiology of the autonomic nervous system and, clinically, for the detection of lesions within the centers and pathways of pupillary control'.

In man, the pupillary diameter can vary between 1.5-2.0 mm and 7.5-8.0 mm (Alexandridis, 1985) which means that the pupil can vary the amount of light entering the eye by a factor of approximately 20. This extends the range of external luminance levels over which the eye can function, although in practice the pupil's contribution is small compared with the dark adaptation mechanism of the retina which allows visual function over a range of about 7 log units. Reducing the size of the pupil increases the depth of focus of the eye and reduces spherical aberration and also the effects of chromatic aberrations.

This section will describe the anatomy and innervation of the iris, methods of studying the pupil, and some aspects of pupillary behaviour in normal and abnormal subjects.

### 1.2.2 Anatomy and physiology of the pupillary pathways

#### Anatomy of the iris

The outer edge of the iris is attached to the trabecular meshwork at the anterior chamber angle of the eye, and has a diameter of about 12 mm (Lowenstein and Loewenfeld, 1969). The inner edge forms the border of the pupil, and its diameter can vary between 1.5 mm and 8.0 mm. The iris is thinnest near the attachment to the trabeculae and at the pupil margin. About 1.5 mm from the pupil margin, the iris becomes thicker at a region called the collarette. The anterior surface of the iris is irregular and shows pit-like depressions called the crypts of Fuchs. Concentric lines or contraction furrows may also be seen, particularly during dilation of the pupil. The posterior iris surface normally rests on the anterior surface of the crystalline lens and is lined with pigment epithelium.

The pigment cells are melanocytes, and the amount of pigment present determines the iris colour. In albino eyes with no pigment, the iris may appear pink *due to the absence of shielding of the fundus reflex*. The iris is a highly vascular structure, with the major and minor iridic circles at the ciliary body and collarette respectively. The capillary arcades near the pupil margins are connected by radial vessels.

The pupil size is determined by the net action of the iris muscles, namely, the circular sphincter pupillae and radial dilator pupillae.

The sphincter pupillae is 0.5-1.0 mm wide and consists of bundles of smooth muscle fibres forming a circular band. It is situated close to the pupillary margin in the posterior stroma of the iris. It is predominantly innervated by parasympathetic fibres, but there is also some sympathetic innervation. It is tightly attached to its surrounding structures by connective tissue fibres and blood vessels, and if part of the sphincter is damaged, for example, by surgery or trauma, the remaining muscle continues to function (Zinn, 1972). When the sphincter pupillae contracts, the pupil constricts.

The dilator pupillae is a myoepithelial layer, about 2  $\mu\text{m}$  thick, which extends radially between the sphincter pupillae and ciliary margin. It is situated immediately anterior to the pigment epithelium, and when it contracts, the pupil dilates. It is predominantly innervated by the sympathetic nervous system.

The structure of the iris is shown in Figure 1.15.

#### The afferent pupillary pathway

In some lower vertebrates, the iris itself is sensitive to light, so that the pupil can constrict even if the optic nerve has been cut (Lowenstein and Loewenfeld, 1969; Alpern et al, 1974). However in mammals the detection of light takes place in the retina, and it is here that the afferent pupillary pathway begins. Signals are passed from the photoreceptors via bipolar cells to the retinal ganglion cells. The bulk of pupillary afferent information is mediated by W-cells, but there may also be pupillary input from collaterals of Y and X cells (Loewenfeld, 1993). Initially axons of these ganglion cells follow the same course as for the transmission of visual information from the retina to

the visual cortex. At the posterior third of each optic tract, pupillary afferent fibres branch off into the brachium of the superior colliculus and terminate in the pretectal olivary nucleus (Gamlin and Clarke, 1995). Warwick (1953) described the oculomotor nuclear complex, which is a collection of cell columns and nuclei situated in the midbrain at the level of the superior colliculi, and which includes the Edinger-Westphal nucleus. Neurons project from the pretectal olivary nucleus to the Edinger-Westphal nucleus, and it has been suggested that there may be both contralateral and ipsilateral projections (Lowenstein and Loewenfeld, 1969; Zinn, 1972; Carpenter and Sutin, 1983) which would readily explain the existence of consensual pupil responses. The results of Gamlin and Clarke (1995) strongly suggest however that the projection is almost entirely contralateral. They suggest that consensual pupil responses could be mediated indirectly by neurons connecting the two pretectal olivary nuclei. The afferent pathways are shown in Figure 1.16.

The parasympathetic efferent pathway to the sphincter pupillae

Axons of the Edinger-Westphal nucleus exit from the brain stem with the oculomotor nerve and travel with this nerve until the superior orbital fissure. The pupillomotor fibres then follow the inferior division of the oculomotor nerve towards the inferior oblique muscle, before leaving the nerve to synapse in the motor root of the ciliary ganglion. The postganglionic fibres travel via the short ciliary nerves to terminate on the sphincter pupillae (to cause pupil constriction) and the ciliary body (to cause accommodation). Only 3% of these fibres are thought to supply the sphincter pupillae (Carpenter and Sutin, 1983). The parasympathetic pathway is illustrated in Figure 1.16.

The Edinger-Westphal nucleus has an inherent rhythmic discharge which maintains tone on the sphincter pupillae. There is also a supranuclear inhibitory influence on the Edinger-Westphal nucleus when a state of consciousness exists (Zinn, 1972) which originates from the hypothalamus. The output activity of this nucleus is therefore the net effect of the inherent discharge, the hypothalamic inhibition and any other excitatory or inhibitory inputs. The effects on the pupil will be considered further in Sections 1.2.4 and 1.2.5.

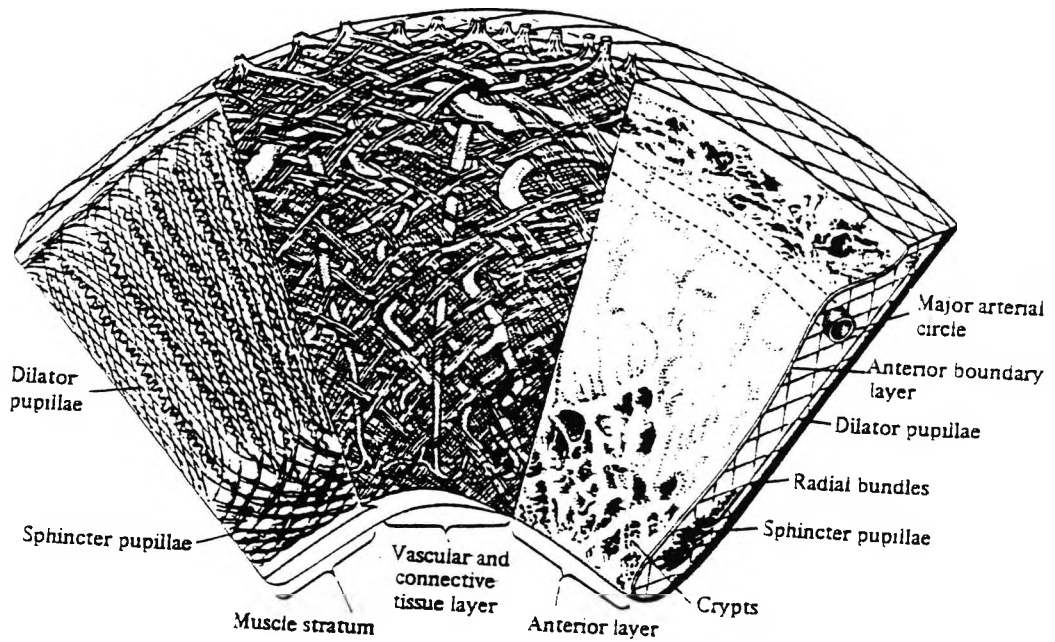


Figure 1.15 Structure of the iris (Alexandridis, 1985)

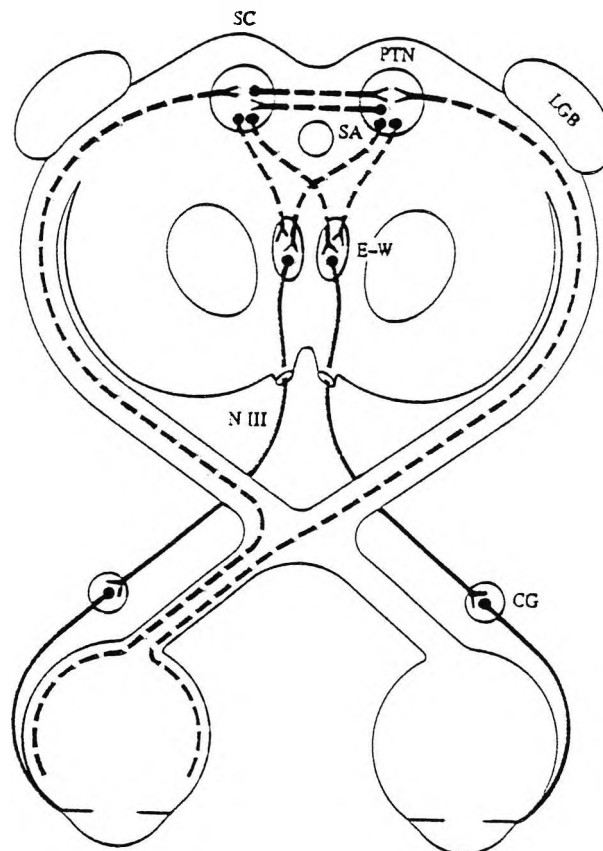


Figure 1.16 Afferent and parasympathetic efferent pathway of the pupillary light reflexes (Alexandridis, 1985). SC=superior colliculus, PTN=pretectal nucleus, LGB=lateral geniculate body, SA=sylvian aqueduct, E-W=Edinger-Westphal nucleus, CG=ciliary ganglion

The sympathetic efferent pathway to the dilator pupillae

The first neuron in the sympathetic efferent pupillary pathway descends from the posterior and lateral regions of the hypothalamus to the ciliospinal centre of Budge, which is situated in the grey matter of the spinal cord. The second (preganglionic) neuron passes into the paravertebral sympathetic chain, and travels through the stellate ganglion and on to the superior cervical ganglion. Most of these fibres pass past the apex of the lung and the subclavian artery. The superior cervical ganglion is situated at the base of the skull between the internal carotid artery and the jugular vein. The third (postganglionic) neuron has a more complicated path. It leaves the superior cervical ganglion to form a plexus round the common carotid artery and internal carotid artery. Some of the fibres branch off to the middle ear before rejoining the internal carotid artery plexus which then enters the cavernous sinus. The fibres arborise to form the cavernous sinus plexus, and from this plexus, the pupillomotor fibres join the ophthalmic division of the trigeminal nerve. They follow the nasociliary branch to enter the globe as the long ciliary nerves which innervate the dilator pupillae.

### 1.2.3 Methods for studying pupillary behaviour

The earliest methods of pupil examination involved direct observation, and such methods are in common clinical use today. For example, pupil size can be measured directly with a scale or by comparison with charts showing different sized circles (for example, the Haab scale, or the circles printed on some direct ophthalmoscopes). The swinging flashlight test is used to detect a relative afferent pupillary defect (Levatin, 1959). These are useful clinically for gross abnormalities but do not give any information on dynamic pupil responses, and cannot be carried out in low light levels.

Photographic methods using infra-red film allow the pupil to be assessed in very low light levels. Sequential photographs or the technique of kymography can show how the pupil reacts over time (Alexandridis, 1985).

As technology has developed, more accurate methods for measurement of the pupil have evolved. At present, the two main principles of pupillography are infrared reflex photometry and video-image processing (Alexandridis et al, 1991). An example of infrared reflex pupillography is the Heidelberg Pupillograph (described in Alexandridis et

al, 1991). With this instrument, a small infrared beam is shone on to the eye through a circular hole in a photoelectric cell held in a headmount about 3 cm from the eye. Considerably more infrared is reflected back from the iris than from the fundus, and so changes in the photoelectric current measured indicate changes in iris area, from which changes in pupil size can be inferred. This method has good temporal resolution but cannot determine the absolute pupil size.

Infrared video-image processing was first used by Lowenstein and Loewenfeld in 1958. The eye is illuminated by an infrared source and filmed using infrared cameras. The image is then produced by scanning the image on a screen. Luminance levels in the image correspond to voltage levels. Little of the infrared reflected from the fundus reaches the cameras in comparison with the infrared reflected from the iris, so the pupil in the image is dark compared with the iris and sclera. Threshold voltage levels can be set so that the processing system can identify the pupil in each frame. A system is described by Leendertz in Alexandridis et al (1991) in which the processing system identifies the widest part of a single scan line that has a below-threshold voltage as the pupil diameter for that frame.

The P\_SCAN 100 system developed at City University (Barbur et al, 1987; Alexandridis et al, 1991) also uses infrared video-image processing. In this system, the processing system identifies the pupil by using a threshold voltage level and fits a circle to the pupil margin. The diameter of this circle for each frame is taken to be the diameter of the pupil. This system can also measure two-dimensional eye movements by plotting the position of the centre of the best-fit circle for successive frames. This system will be described in detail in Chapter 2.

The temporal resolution of the video-processing techniques is limited by the frame rate of the television system. In practice, a sampling rate of 50 Hz gives sufficiently good resolution to record dynamic pupil responses accurately. For accurate latency measurements however, this may become a problem. Barbur et al (1987) describe an alternative method using two orthogonal arrays of light sensitive elements, which can give a sampling rate of 500 Hz. However this assumes that the pupil being measured is perfectly circular and this is not always the case.

#### 1.2.4 Steady-state pupil size

The normal pupil is never truly steady as it is subject to physiological pupillary unrest causing continual small pupil diameter changes. When these periodic changes are larger, with diameter changes of 2 to 3 mm, the unrest is called hippus. It is seen in neurological disorders, for example, multiple sclerosis, meningitis and epilepsy, but may also be seen in normal subjects, especially younger people.

Steady-state pupil size therefore refers to the mean pupil diameter over a time during which no external factors are changed. It will depend on the balance between the actions of the sphincter pupillae and dilator pupillae, as described above. This balance in turn depends on the neuronal input to the muscles which includes factors such as retinal illuminance, state of consciousness or arousal, or accommodation or pain (see section 1.2.5).

Winn et al (1994) investigated the effects of age, gender, refractive error and iris colour on light-adapted human observers. They found that pupil size decreased linearly as a function of age for the group of 91 subjects that were studied, although there was considerable variation in pupil size between subjects of the same age. Pupil size was found to be independent of gender, refractive error and iris colour.

The pupil size largely depends on retinal illuminance. Schweitzer (1956) reviewed attempts to establish a relationship between the luminance of a large uniform field and pupil size, and showed that many complex and varying models have been suggested. Varju (1969) found a nonlinear relationship between pupil size and log stimulus intensity.

Clarke and Ikeda (1985a) found cells in the pretectal olivary nucleus of the rat which increased their maintained firing rates in a graded fashion with graded increases in the level of illumination. The pupil size was found to decrease linearly with the log of the illumination over the same range. They proposed that these cells might provide excitatory input to the Edinger-Westphal nucleus causing the pupil size to reduce as the illumination increased. They also found darkness detectors in the posterior pretectal

nucleus, whose firing rate increased with decreasing levels of illumination, which may inhibit the firing of Edinger-Westphal cells causing the pupil to dilate.

In the pretectal olivary nucleus of monkeys, Gamlin et al (1995) found luminance neurons whose firing rate increased linearly with log retinal illuminance, while pupil size decreased linearly with log retinal illuminance over the same range. They found a mean correlation coefficient of  $r=0.9$  between the firing rate and pupil constriction measured simultaneously for 16 of these luminance neurons.

These cells in the pretectal olivary nucleus appear to be strong candidates for mediating the steady-state pupil size.

In the next section, dynamic pupil responses will be described.

### 1.2.5 Dynamic pupil responses

#### Pupil light reflex

When the eye of a normal human subject is exposed to light, the pupil of that eye (direct response) and the contralateral pupil (consensual response) constrict. The response latency and amplitude are the same. The pupil dilates again shortly afterwards (unless the intensity of the stimulus is very high) and this is referred to as pupillary escape (Cox, 1992). If the stimulus remains on, the diameter to which the pupil returns will be smaller than the prestimulus diameter. However if the stimulus is a brief light flash, the pupil returns to its prestimulus diameter. If both eyes are stimulated, the pupil constriction to a given stimulus is greater than if the stimulus is presented monocularly.

The amplitude of the response will depend on the background adaptation state of the retina, the area of the retina stimulated (the macular and foveal regions are more sensitive to changes in illumination), the direction of the incoming light (cones only respond to quanta of light travelling directly down the cell axis - the Stiles-Crawford effect) and the state of consciousness of the subject (Zinn, 1972).

The relationship between pupil response amplitude and the intensity of a stimulus flash has been studied by Loewenfeld (1966), Lowenstein et al (1968), Webster et al (1968)

and Ellis (1981) among others. The response amplitude is larger for larger stimulus intensity, although ~~as~~ the state of retinal adaptation is also critical. Loewenfeld (1966) showed that the amplitude of pupil constriction varied linearly with the log of the stimulus intensity.

Webster et al (1968) examined the relationship between pupil response amplitude and retinal illuminance, and found large inter-subject variability. Some subjects showed a clear monotonic relationship, while the results of others showed a large standard deviation or large retinal illuminance ranges giving the same constriction amplitude. These findings show possible pitfalls in using the pupil response to establish thresholds as attempted by Schweitzer (1956) and Lowenstein and Loewenfeld (1968), the latter finding that pupillary thresholds were always higher than visual thresholds. Stewart and Young (1989) investigated pupillary and visual thresholds under scotopic conditions and found little difference between them.

The pupillary response to a sinusoidal or periodically presented stimulus has also been investigated by several workers, for example, Troelstra (1968), Varju (1969) and Lowenstein and Loewenfeld (1969). The pupil diameter can follow the stimulus presentation if the frequency is low enough (3 or 4 Hz according to the above studies), but at higher stimulus frequencies the pupillary oscillations tend to fuse, because of the relatively slow action of the iris muscles. The luminance detector cells described by Clarke and Ikeda (1985a) in the pretectal olivary nucleus of the rat were found to modulate their rate of firing according the stimulus frequency up to about 20 Hz (Clarke and Ikeda, 1985b). These cells could also contribute to the pathway mediating pupillary responses to short flashes of light.

#### Pupillary responses to stimulus structure

Stationary sinusoidal gratings have been used extensively to measure the human contrast sensitivity function (Campbell and Robson, 1968) which is effectively the modulation transfer function of the visual system. The highest resolvable spatial frequency gives a measure of visual acuity. Objective methods for measuring visual acuity as the highest resolvable spatial frequency have included the Catford drum (gratings of different spatial frequencies are rotated <sup>in front of</sup> ~~around~~ the subject's head, and the highest spatial frequency

which initiates an optokinetic nystagmus gives a measure of acuity) and pattern electroretinograms and visually evoked cortical potentials, where checkerboards of above threshold spatial frequency no longer evoke a response. Over the last two decades, several workers have used the same principle to examine visual acuity using pupil responses.

Slooter (1981) and Slooter and Van Norren (1980) measured visual acuity with pupil responses to checkerboard stimuli and found a good correlation between pupil acuity and subjective responses to the checkerboards. Slooter (1985) went on to establish that pupil acuities appeared to mirror subjective acuities more closely than acuities obtained from visually evoked cortical potentials, and also measured contrast sensitivity functions as a function of check size measured using pupil responses. These functions were similar to those obtained by psychophysical methods. The work of Slooter and colleagues referred to above was obtained with checkerboards which were alternated with a blank field of the same mean luminance. Ukai (1985) investigated the effect of check size in contrast-reversing checkerboards, and found that check sizes of about 3 minutes of arc gave little or no pupil response.

The assessment of visual acuity by pupil responses to sinusoidal gratings was described by Barbur and Thomson (1987) and a high correlation was found between pupil grating acuity and psychophysical grating acuity. This paper also shows contrast sensitivity functions obtained using pupil responses to gratings, which show similar bandpass characteristics to psychophysical contrast sensitivity functions. A similar correlation between pupil and psychophysical resolution acuities was reported by Cocker and Moseley (1992). Barbur (1991) and Barbur et al (1992b) showed that a pupillary constriction was observed even when the grating presented was of lower luminance than the background field.

Young and Kennish (1993) have used principal component analysis of pupillary responses recorded when a sinusoidal grating was presented for 6 seconds to break down the response into transient and sustained components. They suggest that the transient component is low-pass, while the sustained component is tuned to higher spatial frequencies and may therefore be implicated in the studies described above.

Young et al (1995) used the same technique to established a pupil-based measure of scotopic visual acuity, which agreed well with psychophysical measurements.

It has been found that pupil grating responses are absent in subjects with cortical damage (Barbur and Forsyth, 1986; Barbur et al, 1989, and see section 1.2.6), which suggests that such responses involve the activity of central mechanisms. Pupil responses to spatially-structured stimuli may arise from an increase of cortical activity when the stimulus is presented, which temporarily reduces the supranuclear inhibitory input to the parasympathetic pathways (see section 1.2.2). If the inhibition of the parasympathetic pathways is reduced, the effect is to increase parasympathetic action, which in the pupil causes a pupil constriction.

#### Pupil responses to colour

Loewenfeld (1993) reviews studies investigating pupil behaviour when coloured stimuli are used. She cites Laurens (1923) who showed that pupil response spectral sensitivities demonstrate the Purkinje shift when the subjects are light and dark-adapted. In 1962, Alpern and Campbell showed that pupillary spectral sensitivity bears a close relationship to the CIE spectral scotopic and photopic sensitivity curves if rod contributions are masked using a blue background and if light scatter from the fundus is taken into account. It is therefore clear that both rods and cones contribute to the pupillary response.

Kohn and Clynes (1969) demonstrated pupil constrictions when a stimulus of one colour was presented against a background of a different colour, even if the stimulus was presented at a lower intensity than the background. Young and Alpern (1980) measured pupil responses to alternating monochromatic lights. They eliminated any rod contributions by using a large rod-saturating background, and were able to rule out the possibility that chromatic aberration or chromatic differences in magnification were contributing to the response. They also demonstrated pupil responses when the colour of the target changed, when the second colour was isoluminant with the first colour (established by flicker photometry) or brighter or dimmer than the first colour. Another finding was that the responses produced by the exchange of isoluminant heterochromatic lights had a latency of about 50 ms longer than that evoked by a homochromatic

luminance change, which led them to suggest that these responses could be produced by signals that travel to visual cortex before descending to the pupillomotor nuclei of the midbrain. Barbur et al (1992c) showed that pupil colour responses were absent in achromatopic patients, which also suggests that central mechanisms are involved in generating this response. Young et al (1993) used principal component analysis of pupil responses measured to the exchange of long heterochromatic and achromatic signals. They derived sustained and transient waveforms and suggested that the pupillary responses are a linear sum of these two components. The transient waveform reflects responses to luminance and colour changes, except when the colour changes were isoluminant, and it was therefore proposed that phasic broad-band neurons were mediating these responses.

A colour substitution method was used by Saini and Cohen (1979) to expose chromatic mechanisms of the pupil response. Their findings indicate four mechanisms, which they propose represent the blue, green, red and scotopic mechanisms. Using experimental conditions designed to favour colour-opponent mechanism (large stimuli of 500 ms duration), Krastel et al (1985) showed that pupil increment thresholds arise from colour-opponent mechanisms in the same way as psychophysical spectral sensitivity.

Pupillary spectral behaviour thus appears to mimic spectral sensitivity and colour vision in general. It therefore becomes a candidate for the objective assessment of colour vision. Hedin and Glansholm (1976) measured abnormal spectral sensitivity curves in subjects with protanopia, protanomaly, deuteranopia and deuteranomaly. Young et al (1987) proposed a screening test for protanopes and deuteranopes using a red-green or green-red colour exchange. Protanopes showed little or no response to the green-red change, but large responses to the red-green change, while for deuteranopes, small responses were seen to both changes. Normal subjects showed larger responses to both changes. Barbur et al (1993a) used luminance masking techniques (see Chapters 2 and 4) to measure pupil responses in protanopes, deuteranopes and tritanopes, and showed that no pupillary responses are seen when the coloured stimulus is chosen to fall on the colour confusion line for the class of dichromat examined.

## Other pupillary reflexes

### Near reflex

The oculomotor nerves innervate the ciliary and sphincter pupillae muscles and medial recti and so mediate the so-called near vision triad of accommodation, miosis and convergence that occurs when near vision takes place. The miosis appears to be linked to the convergence mechanism.

### Dark reflex

Pupillary dilation is seen when a reduction in luminance is presented to a subject if the adapting light is moderately bright (Lowenstein and Loewenfeld, 1969). A constriction then occurs when the previous luminance level is restored. The initial dilation is not seen if the adapting light is dim. The dilation is due partly to relaxation of the sphincter pupillae and partly to sympathetic innervation of the dilator pupillae.

### Lid closure (orbicularis) reflex

Miosis occurs when the eyelids are closed, or when a patient is asked to close the eyes while the eyelids are held open. At the same time, the globe rotates upwards (Bell's phenomenon). The pathways mediating this reflex are unclear, but it has been suggested that this reflex indicates direct connections between the seventh (facial) cranial nerve and the oculomotor complex, including the Edinger-Westphal nucleus (Zinn, 1972).

### Trigeminal reflex

Irritation of the eyelids, conjunctiva or cornea results in pupil constriction. Painful stimuli initially cause a mydriasis, but if the pain persists, both pupils constrict, with a greater miosis seen in the affected eye. This reflex is mediated by connections between the sensory trigeminal nerve and the Edinger-Westphal nucleus (Zinn, 1972). The afferent impulses sent along the trigeminal nerve when a painful stimulus is present also cause vasodilation of the capillaries of the iris, which also causes miosis.

### Vestibular reflex

Stimulation of the vestibular apparatus causes ipsilateral mydriasis (Alexandridis, 1985). This is attributed to the passage of some of the sympathetic efferent fibres through the middle ear en route for the iris (see section 1.2.2).

### Psychosensory reflexes

These reflexes are caused by sensory stimulation (for example, touch, pain or sound) which activates the central sympathetic nervous system centres, such as the ciliospinal centre of Budge. From here, impulses are relayed to the superior cervical ganglion and

hence to the dilator pupillae muscle, resulting in mydriasis (Zinn, 1972). Hess (1965) measured pupil responses in men and women to a series of photographs and found pupil dilations to pictures that were thought to be arousing or interesting, for example, 'pinup' figures of the opposite sex, while aversive stimuli, for example, pictures of sharks, caused pupil constriction. He also found some aversive stimuli which caused dilation, for example, pictures of corpses, which was shown to be a 'shock reflex'. On repeated presentation of these 'shock' pictures, the dilation disappeared and the constriction expected with aversive stimuli was seen. Zeitner and Weight (1979) attempted to use pupil responses as an objective measure of self-esteem by measuring responses when subjects observed photographs of themselves or other people. For female subjects, they found a correlation between self-esteem (assessed using psychological tests) and pupil response, but not the relationship that was expected. For these subjects the higher the self-esteem, the smaller the dilation or larger the constriction was seen. No statistically significant correlations were found for male subjects.

#### 1.2.6 Abnormal pupil responses

Pupil examination is an important part of the neuro-ophthalmological investigation, as it provides objective information about the function of the nervous system (Wilhelm, 1994). Abnormal pupil responses can occur following lesions of the afferent or efferent pathways, or lesions of the midbrain and cortical areas.

Because of the large inter-subject variation in pupil responses to light, and in general, the absence of accurate pupil measurement systems, the absolute pupil response does not give a great deal of clinically useful information. However, comparison of the responses in the two eyes can show the presence of a relative afferent pupillary defect (RAPD). An RAPD is most easily seen using the swinging flashlight test, described by Levatin (1959) and is an indication of unilateral or asymmetric optic nerve or severe retinal disease (Wilhelm, 1994). Inflammatory diseases of the optic nerve and optic atrophy have been shown to increase the latency of the pupil light reflex (Alexandridis et al, 1981).

Interruptions of the postganglionic parasympathetic system can cause a tonic pupil, called Adie's syndrome. This may also be associated with an impairment of deep tendon

reflexes or disturbances of thermoregulation and sweating. Tonic pupils must be differentiated from Argyll-Robertson pupils, in which the light reflex is absent, but the near reflex is preserved. This condition is caused by midbrain lesions, once classically associated with neurosyphilis, but probably now more often seen in heroin abusers (Wilhelm, 1994). An interruption of sympathetic innervation causes ipsilateral miosis (Horner's syndrome) which may be associated with ptosis and hypohydrosis.

Routine examination of lesions of the optic chiasm, optic tract or visual cortex tends not to show any difference in the pupillary responses of the two eyes (Alexandridis, 1985). This is because large bright stimuli are used, and direct or scattered light may easily fall on areas of the retinas corresponding to unaffected visual pathway. However, if small dim stimuli are used and measures are taken to avoid scattered light, it has been shown that no pupil responses are seen when the stimuli are presented in affected areas of the visual field, while responses are present when the stimuli are presented in normal areas (Cibis et al, 1975; Thompson et al, 1982). Kardon (1992) reviews the use of pupil responses as an objective method of perimetry, and demonstrates the similarity between visual fields measured subjectively and using pupil perimetry for subjects with anterior ischaemic optic neuropathy, glaucoma and occipital infarct.

Other aspects of vision can be measured using pupil responses and compared with subjective measurements. For example, dark adaptation curves measured using pupil thresholds are similar to those measured using subjective thresholds. Rod monochromats and subjects with night blindness show dark adaptation curves for only rods and cones respectively in the curves measured by pupil thresholds (Alexandridis, 1985).

Contrast sensitivity functions demonstrated using pupil responses have been mentioned above (see section 1.2.5). Barbur et al (1994c) show that abnormal contrast sensitivity functions found subjectively in amblyopic subjects are mirrored by the pupil contrast sensitivity functions.

The pupil grating response has also been investigated in subjects with damaged primary visual cortex and was found to be absent (Barbur and Thomson, 1987), suggesting that

these responses involve input to the midbrain from the visual cortex. Pupil colour responses have also been investigated in these subjects. When small coloured pattern stimuli were presented in the blind areas of their visual fields no pupil responses were measured, although small responses were measured for the sighted fields (Keenleyside, 1989; Keenleyside et al, 1988). When large coloured stimuli were used, responses were measured (Sahraie, 1993; Stoerig et al, 1994) but these may in fact have been contaminated by rod input or luminance changes (see Chapter 4).

The studies described in Chapters 3 and 4 consider some aspects of the pupil light reflex and pupil colour reflex, both in normal subjects and in abnormal subjects, using complex computer-controlled stimuli and accurate measurement of pupil responses. It is hoped that the work described will contribute to the knowledge and current understanding of pupillary behaviour.

## 1.3 Visual function in subjects with cortical lesions

### 1.3.1 Introduction

90% of retinal fibres travel via the geniculostriate pathway. It is well known that lesions of the lateral geniculate nucleus, optic tract or primary visual cortex cause defects in the contralateral visual field, affecting both eyes. These defects may be demonstrated using conventional perimetry.

In patients with cortical lesions causing field defects or in monkeys with artificially induced field defects, some visual functions appear to remain. In human subjects, there may be no consciousness of visual perception and this has been termed 'blindsight' by Weiskrantz et al (1974). In this case indirect methods of testing must be used to expose the visual function, for example, two-alternative forced choice methods. If some awareness of the stimulus employed remains, this has been termed residual vision. 10% of retinal fibres terminate in the midbrain and subcortical regions, and there are also some projections to extrastriate visual cortex (see section 1.1), and it has been proposed that these pathways are involved in mediating blindsight or residual vision (see section 1.3.3)

This section also describes the visual abilities that have been shown to remain when stimuli are presented in perimetrically blind areas of the visual field. Consideration will be given to the studies of some workers who claim that this phenomenon can be explained by scattered light or islands of spared visual cortex. Finally conditions arising from lesions in higher visual areas will be mentioned.

### 1.3.2 Visual abilities that have been described in the absence of striate cortex

#### Monkey studies

Studies by Kluver (1942) led him to the conclusion that destriate monkeys lose the ability to see visual properties such as brightness, colour and shape, but he found that they could distinguish between different targets if the total amount of luminous flux were different. Early experiments by Weiskrantz (described in Weiskrantz, 1980) showed that a destriate monkey could distinguish between spatially different stimuli even though the amount of luminous flux was constant. Schilder et al (1972) showed that

destriate monkeys could discriminate a circle from a triangle, and also found that these animals could choose correctly between red and green targets. A destriate monkey described by Humphrey (1974) initially acted as though she were completely blind, but after 19 months was found to have the ability to look at and reach for moving food targets. Later she became adept at localising and picking up small food targets, and could find her way safely past obstacles towards a current on the floor. Colour discrimination tests gave somewhat confusing results: her ability to detect a red spot on a green background was consistent with a photopic spectral sensitivity function, but red and green spots on a white background became indistinguishable when the green spot was considerably darker than the red one in terms of photopic brightness. Lepore et al (1975) measured spectral sensitivity curves in monkeys before and after the striate cortex was removed. Postoperatively, the scotopic sensitivity curve was normal, while the photopic curve was shifted towards the scotopic curve. They therefore suggested that the geniculostriate system deals with cone information while the <sup>non-geniculostriate</sup> ~~extrastriate~~ structures are dominated by rod input. Keating (1979) found that monkeys could discriminate blue from yellow, and red from green, following removal of striate cortex. He then removed preoccipital areas, and found that the colour discrimination was preserved, which suggests that midbrain structures may be involved in the colour discrimination process. Destriate monkeys could locate visual targets and reach towards them, and they could also perform velocity discrimination (Keating, 1980). These abilities were preserved when preoccipital areas were removed, but were found to be eliminated when the superior colliculus and pretectum were removed in one monkey. Some of the destriate monkeys examined by Dineen and Keating (1981) were able to discriminate complex visual patterns even when local stimulus cues such as amount of contour and number of elements were equal.

A large series of experiments examining visual functions in monkeys following the removal of striate cortex followed by other structures is summarised in Pasik and Pasik (1982). Some aspects of these experiments are summarised in Table 1.7 below. It can be seen that many visual functions may be preserved when striate cortex is removed. Pasik and Pasik (1982) suggest that their findings for destriate monkeys are different from Kluver's (1942) because his lesions included some extrastriate cortex.

Spatial localisation	Preserved in destriate monkeys, but no longer possible when the SC/pretectum were destroyed
Light versus no-light discrimination	Preserved in destriate monkeys and with destruction of SC/pretectum and pulvinars but no longer possible when AOS was destroyed
Discrimination between figures emitting the same luminous flux	Preserved in destriate monkeys
Circle versus triangle	Preserved in destriate monkeys
Red versus green	Preserved in destriate monkeys
Colour versus achromatic	Preserved in one destriate monkey for red and blue but not for green.
Bar orientation discrimination	Preserved in destriate monkeys
Discrimination of sinusoidal gratings versus a homogeneous target	Preserved in destriate monkeys for 0.5, 1.0, 2.0 and 4.0 cycles per degree

Table 1.7 Summary of some aspects of the experiments carried out by Pasik and Pasik (1982). The monkeys were trained on the tasks preoperatively, and then retrained following removal of striate cortex and other structures. SC=superior colliculus. AOS=accessory optic system.

The studies on monkeys described above mainly used two-alternative forced choice methods in which training was given and 'correct' choices were rewarded. In order to succeed at a test, pre- or postoperatively, a large number of trials is carried out and the monkey must reach a criterion level above chance performance. Such experiments therefore give information about performance, but until recently, it has not been possible to surmise whether this performance parallels blindsight or residual vision in humans. If lesion studies are to be helpful in establishing the pathways mediating blindsight, it is important to know whether monkeys also experience blindsight.

An experiment designed by Cowey and Stoerig (1995) demonstrated that hemianopic monkeys experience blindsight. Initially monkeys were rewarded if they correctly touched the position where a light had appeared in the blind or sighted hemifields. Performance levels approached 100% when the lights were about 0.7 log units above the thresholds measured for the blind and sighted fields. The monkeys were then taught to press a rectangle if blank trials were used. The final experiment consisted of stimuli

in the blind and sighted fields and blank trials intermingled. The monkeys pressed the 'blank trial' rectangle both for the blanks and for stimuli presented in the blind hemifield, which implies that these trials were subjectively the same to the monkeys. If stimuli presented in the blind hemifield (which had previously been successfully detected) are indistinguishable from a blank trial, the monkey is exhibiting blindsight.

Moore et al (1995) trained hemianopic monkeys to make saccadic eye movements towards visual targets presented in the blind and sighted hemifields. The monkeys made accurate eye movements towards the stimuli when they were in the sighted field, but made large errors when the stimuli were in the blind field. However, when the fixation target was turned off when the stimulus was turned on, the monkeys were able to saccade towards targets in the blind hemifield. They suggest that this finding provides a parallel to human blindsight, in which patients with striate cortex damage may not report any visual sensation in the blind hemifield, yet they can localise visual targets in the blind area in forced-choice conditions.

Anatomical pathways underlying blindsight and residual vision phenomena will be described in Section 1.3.3.

#### Human studies

Holmes (1918) mapped how cortical lesions relate to visual defects from his studies of soldiers with brain wounds during the First World War. He describes absolute scotomata in which the presence or movement of an object could not be detected, although they were often surrounded by relative scotomata where partial vision was present. Weiskrantz (1986) reviews the work of other First World War investigators, for example, Poppelreuter, who claimed that scotomata were never absolutely blind.

Krieger and Bender (1951) found that it was possible to measure dark adaptation curves in blind and sighted visual fields of subjects with cortical damage. The curves measured in the blind field showed much higher thresholds for the blind field and a greater variation in the thresholds. However the total range of adaptation was similar for normal and affected fields (about 3.6 log units). Krieger (1953) showed that although

threshold values may return to normal if the field defect improves over time, the variation persists.

Two blind patients with total cortical blindness described by Brindley et al (1969) were able to distinguish between darkness and light, provided there was an abrupt change from one to the other, indicating at least some light perception. One of the patients appeared to be exhibiting blindsight, while the other had some residual awareness. The ability to detect stationary targets presented in the blind field of subjects with cortical damage has been investigated by Krieger and Bender (1951), Barbur et al (1980), Stoerig et al (1985), Weiskrantz (1986) and Celesia et al (1991). In general, detection ability depends on stimulus size and luminance. Threshold curves are higher in blind areas than in normal field. Hess and Pointer (1989) were unable to demonstrate greater-than-chance performances when stimuli were presented in the blind field when they were trying to measure contrast sensitivity. They used stimuli weighted with Gaussian functions in space and time, with relatively small areas (standard deviation=2°) and slow onset and offset (standard deviation=250 ms). However, Weiskrantz et al (1991) showed that the stimuli used by Hess and Pointer were ineffective at eliciting blindsight or residual visual responses, and the optimum stimuli were shown to be larger (a standard deviation of 3.3° gave a performance of almost 100%) and with steeper onset and offset (a standard deviation of 200 ms gave 90% performance).

Spatial localisation of stimuli presented in blind areas of visual field has been demonstrated by pointing and eye movements by Poppel et al (1973), Weiskrantz et al (1974), Perenin et al (1980) and Blythe et al (1987). Perenin and Jeannerod (1978) found a significant correlation between the position of bright targets within the hemianopic field and the position of corresponding hand pointing in subjects who had undergone hemispherectomy (removal of the whole neocortex). These results would suggest that spatial localisation in subjects with damaged occipital cortex is mediated by midbrain structures, which remain after hemispherectomy. The superior colliculus has been shown to be involved with eye movements (Schiller and Koerner, 1971; Goldberg and Wurtz, 1972) and was shown to affect spatial localisation in destriate monkeys (Pasik and Pasik, 1982, see Table 1.7). However, King et al (1996) were not able to demonstrate spatial localisation in similar patients, although they used a black target

against a white background, which may not be as effective a stimulus for mediating blindsight.

#### Pattern discrimination

Subject DB, who was extensively investigated by Weiskrantz and colleagues (Weiskrantz et al, 1974; Weiskrantz, 1986) was able to discriminate between horizontal and vertical lines, diagonal and vertical lines and X's and O's if the stimuli were above a certain size and presented for a certain duration. However, if the difference in patterns was small, for example, discriminating between triangles with straight or curving sides, DB's performance was not so good. (Weiskrantz, 1987). Subject GY, who has also taken part in several studies into blindsight and residual vision (including this study, see Chapters 3 and 4), was found to be poor at area discrimination (if the target illumination levels were adjusted to an equal suprathreshold level), orientation discrimination and shape discrimination (Barbur et al, 1980). He was later found to exhibit a bandpass spatial frequency tuning function in his blind hemifield when the contrast of the sinusoidal grating was modulated at 6 Hz (Barbur et al, 1994b). Subjects examined by Blythe et al (1987) were unable to discriminate horizontal and vertical gratings, or triangles and circles. Some of the hemispherectomised patients studied by Perenin (1978) were able to perform simple pattern discrimination, which suggests that some of this ability may be subcortical in origin.

It has been shown that presentation of stimuli in the blind field can affect the perception of what is seen in the sighted field, even if the subject is completely unaware of what is presented in the blind field. For example, when Torjussen (1976) presented a semicircle in the blind field alone, the subjects reported that they had seen nothing. When two semicircles were presented, one in the blind and one in the sighted hemifields, the subjects reported seeing a complete circle. Marcel (1983) presented words in the blind field, which appeared to influence the semantic understanding of words presented in the sighted field.

#### Movement detection

Subject DB was able to detect moving vertical lines and discs (Weiskrantz, 1986). The subject with cortical damage described by Perenin et al (1980) had a "feeling...that

something was moving around him" when he was tested using an optokinetic drum, and this improved over time until he could always indicate correctly the direction of movement. Barbur et al (1980) found that GY could detect a moving target in the blind field, although at low illumination levels, this was only possible if the target was moving faster than 50 degrees per second and if it was at an eccentricity of greater than 17 degrees. His results for speed discrimination ~~results~~ were similar to those of a normal subject. When GY's detection of direction of motion in the blind field was tested in conjunction with positron emission tomography, it was found that area V5 was active without a parallel activation of area V1 (Barbur et al, 1993b). A later study on GY by Weiskrantz et al (1995) showed good performances on discrimination of horizontal and vertical movements, and displacement angles and orientation discrimination for moving targets. GY was aware of the stimuli at higher stimulus speed, displacement and orientation differences (residual vision) but performed well above chance levels even when unaware of the stimuli (blindsight). Blythe et al (1987) also report that detection of slow-moving targets in the blind field required much higher levels of illumination than did faster moving targets.

#### Wavelength discrimination

Barbur et al (1980) measured GY's spectral sensitivity for threshold detection of a moving target, and their results imply that rod signals dominate the responses in the blind hemifield. Brent et al (1994) later showed spectral responses characteristic of red- and green-sensitive cones and post-receptoral colour-opponent mechanism in GY's blind field. They also found that he performed well at a colour naming test, despite complete unawareness of the stimuli, particularly for long wavelengths. Sahraie (1993) showed good performance at colour naming, particularly for highly saturated red and blue stimuli, in GY and FS (who took part in one of the experiments in this study, see Chapter 3). The patient described by Perenin et al (1980) could initially distinguish between some colours, especially red and blue, but this ability deteriorated over time.

Stoerig (1987) showed that six out of ten subjects with cortical damage were able to distinguish between red and green targets presented in blind areas of the visual field. Half of the subjects were able to detect the coloured targets but not an achromatic one

presented at the same eccentricity, suggesting that wavelength and intensity information are treated differently.

She and Cowey went on to investigate wavelength sensitivity in blindsight more fully (Stoerig and Cowey, 1989b, 1991, 1992). The spectral sensitivities found in the blind fields were essentially normal in form, although 1 log unit or less lower than normal. The Purkinje shift was seen between the curves for light and dark adaptation, which indicates rod and cone contributions to the blindsight. They demonstrated characteristic discontinuities in the spectral sensitivity curves, indicating that colour-opponent processes are involved.

The next section describes the anatomical pathways that may be involved in blindsight and residual vision.

### 1.3.3 The neurobiology of blindsight

Figure 1.17 shows a diagram of the known pathways from the eye into the brain, showing possible routes for visual signals to reach secondary cortical visual areas in the absence of striate cortex (Cowey and Stoerig, 1991b). The pathways most often invoked in blindsight are the retinocollicular projection that reaches extrastriate cortical visual areas via the pulvinar nucleus and the direct projection from the LGN to extrastriate areas (Cowey and Stoerig, 1991a). In cases of incomplete striate cortical damage, the imprecise topographical relationships between the optic radiation and striate cortex might allow some information from the field defect to be transmitted to the remaining striate cortex.

The results of Pasik and Pasik (1971, 1982) show that destruction of the superior colliculus and lateral pretectum abolish light discrimination and spatial localisation in destriate monkeys (see Table 1.7). The destruction of extrastriate cortex also reduced performance on light discrimination. Mohler and Wurtz (1977) also demonstrated that the superior colliculus was necessary for spatial localisation in destriate monkeys. From these results, it seems that both midbrain and extrastriate structures are implicated in blindsight and/or residual vision.

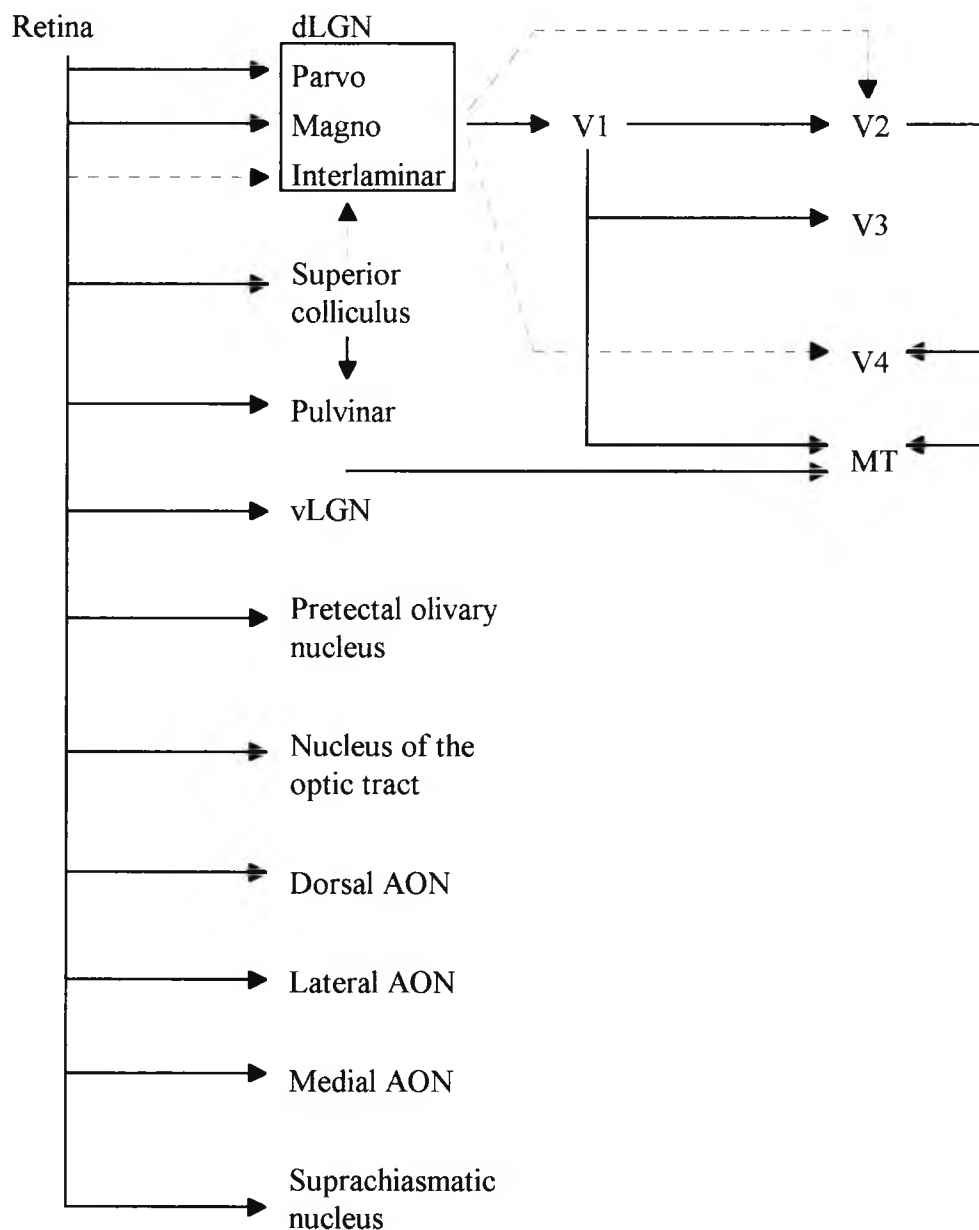


Figure 1.17 The known pathways from the eye into the brain, together with the initial further cortical projections. In the absence of the striate cortex (V1) it is possible for visual signals to reach secondary cortical visual areas. The dotted lines indicated poorly documented pathways, which could theoretically provide signals to extrastriate cortex. AON=accessory optic nucleus. (after Cowey and Stoerig, 1991b)

A comparison may be made between the abilities of patients whose lesions are largely restricted to primary visual cortex and those who have undergone hemidecortication or hemispherectomy (see Payne, 1996, for review). Any residual visual abilities in the latter group are presumably mediated by midbrain structures. These patients could perform spatial localisation tasks (Perenin and Jeannerod, 1978) and coarse pattern discrimination (Perenin, 1978). The patients of Ptito et al (1987) were able to discriminate three-dimensional objects but not two-dimensional patterns. However, King et al (1996) were unable to demonstrate any residual visual abilities in patients with hemispherectomy that were not also associated with discriminable scattered light. More studies using hemispherectomy patients are needed to explain this discrepancy. If these patients have no residual vision and are only using scattered light, it suggests that only extrastriate structures are involved in residual vision. An important feature of this study was that hemispherectomy patients and subject GY (with damaged striate visual cortex) were examined using the same battery of tests, which enables direct comparison between the two types of cortical damage.

Subjects with damage to striate cortex only are able, within limits, to detect, localise or discriminate high contrast stationary stimuli, and also moving stimuli, and they also have wavelength discrimination (see section 1.3.2). These subjects have intact midbrain structures, and in addition, may be using extrastriate cortex. Celesia et al (1991) have measured normal visual evoked potentials (VEPs) to flashes at a frequency of 1 Hz in patients with occipital damage, and in some patients exhibiting residual vision, VEPs to checkerboards with large checks, albeit with longer latencies. These results also suggest that extrastriate cortex is excited by visual stimuli in the absence of striate cortex and conscious awareness of the stimuli.

How does visual information reach extrastriate cortex in the absence of striate cortex? It has been shown (Cowey and Stoerig, 1991b; Weller and Kaas, 1989) that only P-beta retinal ganglion cells are damaged as a result of transneuronal degeneration. Some P-beta ganglion cells survive, however, because they project to parvocellular cells in the LGN which project directly to extrastriate cortex (Yukie and Iwai, 1981; Bullier and Kennedy, 1983) and thus escape retrograde degeneration when striate cortex is destroyed.

Following striate cortex ablation, approximately equal numbers of P-alpha, P-beta and P-gamma retinal ganglion cells survive (Cowey and Stoerig, 1991a). P-alpha cells project to the magnocellular layers of the LGN and to the midbrain and P-gamma cells project to the midbrain, pretectum and S-layers of the LGN. The properties of these cells, together with cells of the superior colliculus, are suitable for the processing of motion and spatial localisation in visual field defects. P-beta cells are important for processing wavelength information, which has been shown to be present in subjects with damaged striate cortex (Stoerig and Cowey, 1989b, 1991, 1992). Their input may be transmitted via the direct geniculo-extrastriate projection mentioned above. Felsten et al (1983) found opponent-colour responses in the lateral pulvinar of the macaque monkey, which could therefore also be involved in wavelength sensitivity in blindsight.

#### 1.3.4 Could blindsight be mediated by scattered light or spared cortex?

Campion et al (1983) reviewed several studies concerned with blindsight and residual vision, including measures taken to control for the possibility of scattered light, such as the inclusion of blank trials, high levels of illumination in the intact visual field and determination of the scattering coefficient. They describe a short series of experiments and claim that their results show that all previous demonstrations of blindsight were attributable to scattered light artefacts or degraded striate vision from spared visual cortex. An open peer commentary following this paper discusses their findings. Barbur and Ruddock point out that subject GY shows temporal characteristics quite different from those of a normal subject, inconsistent with an explanation of scattered light. Cowey argues that complete striate cortex removal in monkeys can be histologically verified, and that destriate monkeys can detect a light stimulus when it is presented in their blind visual field but not when it falls on the blind spot. If scattered light were the basis for detection of these stimuli, they should certainly be detected when falling on the blind spot, a point also made by Bridgeman. Scattered light and small areas of striate cortex are thought to be unlikely explanations for the discrimination of different spatial patterns, for example, Torjussen and Magnussen, and Weiskrantz.

King et al (1996) reported that scattered light could account for the visual performance in hemispherectomy patients rather than residual vision. As mentioned above, this is in opposition to the studies of Perenin (1978), Perenin and Jeannerod (1978) and Ptito et

al (1987). Further studies need to be undertaken to clarify this discrepancy. However, under the same conditions, they found that light scatter could be eliminated as a factor without affecting GY's ability to respond. Clearly, spared cortex is not a possible explanation for patients who have undergone total hemispherectomy.

Fendrich et al (1992) used an image stabiliser to achieve detailed perimetry and found a 1° island of residual vision in the blind field of a hemianope which had been missed by conventional perimetry. Stimuli presented to this island were detected and discriminated, although there was no conscious awareness of the stimuli. They conclude that other instances of blindsight may be mediated by similar islands of functioning cortex. Stoerig (1993) points out that it is unlikely that islands of residual normal cortex could account for the accuracy shown in an eccentricity-dependent target detection paradigm. Weiskrantz (1995) showed that subject GY could follow the path of a moving spot of light presented in his blind field with his arm very accurately and steadily as long as the spot moved above a certain rate. His fixation was monitored throughout. There would have to be many appropriately positioned islands of normal visual cortex if the explanation of Fendrich et al (1992) were to account for this, and a positron emission tomography scan measured when GY was viewing a moving bar showed no activity in V1 at all (apart from the small area associated with the macular sparing). Weiskrantz (1995) therefore concludes that island of striate cortex are not necessary for discrimination of the direction of movement.

### 1.3.5 Effects of non-striate cortical lesions

In the preceding sections, the emphasis has been on blindsight or residual vision in subjects with damage to striate cortex. Lesions in other parts of the cortex can produce specific defects which will be considered briefly here.

Cerebral achromatopsia is a condition which causes patients to lose the ability to acquire information about objects from their reflectances for light of different wavelengths (Zeki, 1993). Such patients can describe their visual environment in terms of greys. It occurs as a consequence of bilateral damage to area V4 of the brain, usually as a result of a stroke. Hemiachromatopsia occurs if the damage is confined to V4 on one side only. In this case, colours are not seen in the visual field contralateral to the damage.

Achromatopsia may not be accompanied by a deficit in form vision. It is however often associated with prosopagnosia, which is an inability to recognise familiar faces.

Prosopagnosia is reviewed by Ruddock (1991b) and Wall (1995). It is thought to be caused by a bilateral lesion of the fusiform and lingual gyri. It has been reported that subjects who are unable to recognise faces may also have problems in distinguishing between other objects belonging to a single generic group, for example, buildings, animals, vehicles and fruit.

Visual form agnosia is an inability to recognise familiar objects (Ruddock, 1991b). It has been divided into two parts: apperceptive agnosia, in which the subject cannot integrate the incoming visual signals to form a percept, and associative agnosia, where there is a failure to identify an object by associating it with previous experience.

An inability to read, or alexia, is caused by a left hemisphere lesion associated with damage to the corpus callosum (Ruddock, 1991b). It may occur in association with prosopagnosia, visual form agnosia and inability to name colours correctly. Patients with this condition may still be able to understand pictures or to read shorthand.

A patient described by Zihl et al (1983) showed a selective impairment of motion vision, or cerebral akinetopsia, following bilateral damage of the lateral temporo-occipital cortex and underlying white matter. She had problems pouring a cup of tea because she could not see the level of the liquid rising, and found it hard to follow a dialogue because she could not see the movements of the mouths of the speakers. When crossing a road, an approaching car would suddenly appear to be very near. This condition is thought to be due to damage to V5.

It is clear that the consequences of brain damage can be many and varied. Lesions in striate cortex which were once thought just to produce areas of blind visual field have now been shown to leave some residual vision if appropriate testing conditions are used. More specific problems, such as those described above, are caused by lesions of higher visual areas, implying specialised functions for these regions.

Subject GY who has been mentioned several times above, and another subject, FS, with cortical damage, took part in some of the experiments described in this study. A subject with partial achromatopsia, LR, also participated in some of the experiments.

## 1.4 Colour vision

### 1.4.1 Introduction

The normal human visual system is equipped to signal information about a large range of colours. Colour vision presumably evolved to aid survival, for example, in the hunt for prey against natural backgrounds where luminance contrast information alone may not be sufficient. The ability to distinguish ripe fruits from unripe ones is another example of the need to process chromatic as well as luminance information.

The intrinsic chromatic properties of objects are described by surface reflectance functions, which represent the fraction of incident illumination reflected from a point on the surface as a function of wavelength. The wavelength radiance distribution of the light reaching an observer from an object will also depend on the spectral power distribution of the illuminant. These are physical parameters which can be measured accurately, but colour vision itself is a perceptual phenomenon. The next section will briefly describe the means by which the normal human visual system analyses information about the chromatic properties of objects, and section 1.4.3 will discuss colour matching and the derivation of chromaticity diagrams.

Section 1.4.4 will describe abnormal colour vision in humans, including congenital and acquired deficiencies, in order to provide a background to the experiments described in Chapter 5. Section 1.4.5 gives a brief summary of various methods that are used for testing colour vision.

### 1.4.2 Physiology of colour vision

The three types of cone present in the normal human retina have been described in Section 1.1.3. These classes of cones contain different visual pigments, and are ideal candidates for the Young-Helmholtz trichromacy theory, first described by Young in the early nineteenth century and later added to by von Helmholtz in the mid-nineteenth century. This theory suggests that the visual system contains three distinct mechanisms that are sensitive to different, but overlapping, regions of the spectrum. Light of a particular colour will excite the mechanisms to different extents, and different lights will be distinguishable from one another if they produce a different pattern of excitation of

the three mechanisms. An important point is that a cone can only respond according to the number of photons absorbed with no regard for wavelength. A single cone or class of cone cannot therefore signal the difference between a change in the number of photons due to an increase in the intensity of light or to a change in the spectral composition of the light. This is known as the principle of univariance.

In 1870, Hering proposed the opponent theory of colour vision. This was based on his observations that colours seemed to operate in opposing pairs. For example, red and green oppose one another and do not blend, that is, there is no 'reddish-green' colour in the same way as there can be 'reddish-yellow' or 'greenish-yellow', and similarly, a bluish-yellow does not exist. He also proposed a third black-white mechanism. These observations are now attributed to the colour-opponent properties of retinal ganglion cells (see section 1.1.3), that is, a second stage in the analysis of colour.

The colour sensitive cells in primary visual cortex have been described in section 1.1.6. Double opponent centre-surround cells, whose centres and surrounds are excited by complementary coloured stimuli, have been described in the blob regions of layers II and III (Livingstone and Hubel, 1984a) and in layer IVC $\beta$  (Michael, 1989). Blob cells project to other blob cells and to the thin stripes in V2, where a high proportion of cells again show colour opponency (Hubel and Livingstone, 1989). These cells might appear to be ideal mediators of the colour perceived by an observer. However, their responses to a coloured stimulus vary according to the colour of the illumination falling on the stimulus, that is, they do not exhibit colour constancy (Zeki, 1980, 1993). Human colour vision clearly incorporates colour constancy, and must therefore reflect the activity of chromatic mechanisms that code the "colour" of a stimulus regardless of the illuminant. Cells exhibiting responses consistent with colour constancy are found in V4, which receives input from V2 (Zeki, 1993).

Cortical simple cells can respond to edges defined by both colour and luminance contrast. This poses an immediate problem since the colour and luminance signals then need to be separated to provide the maximum information to the observer. Models attempting to explain how the chromatic and luminance information is separated or demultiplexed have been described by many authors, for example, Lennie and D'Zmura

(1988), Rodieck (1991), De Valois and De Valois (1993) and a review by Kingdom and Mullen (1995). Models include the combination of the outputs of spatially superimposed receptive-field pairs, the pooling of adjacent receptive fields or extracting colour and luminance information by means of cortical cells with different orientation tuning. Rodieck (1991) has proposed that midget ganglion cells and Type I LGN cells transmit achromatic information, while chromatic information is signalled via bistratified ganglion cells and Type II cells (Wiesel and Hubel, 1966). This theory is considered further in Chapter 5.

#### 1.4.3 Colour matching and chromaticity diagrams

The technique of colour matching using trichromatic colorimetry forms the basis for a colour specification system. A trichromatic colorimeter presents a bipartite field to the observer. In one half of the field is a test colour, while the colour of the other half field is determined by varying the amounts of three primary colours (red, green and blue). If standard red, green and blue primaries are chosen, then colour-matching functions for test patterns of different wavelength can be derived. The CIE 1931 R,G,B system specifies primaries of 700, 546.1 and 435.8 nm (based on transformations of experimental results obtained by Wright and Guild, see account in Wyszecki and Stiles, 1982). The luminous efficiencies of unit quantities of these red, green and blue primaries are in the ratio of 1:4.5907:0.0601, and from these values, new tristimulus units were derived. One new green unit was equivalent to 4.5907 old units, and one new blue unit was equivalent to 0.0601 old units. The standard colour-matching functions are shown in Figure 1.18 in these trichromatic units. With these units an equal-energy white stimulus (that is, a white light consisting of equal amounts of power per small constant-width wavelength interval throughout the spectrum) is matched by an equal amount of each of the primaries, expressed in the new units. These are the standard  $r,g,b$  tristimulus values obtained using the CIE primaries mentioned above, but if other primaries are used, tristimulus values can still be calculated. For example, if a colour is matched by  $R$  units of a red primary,  $G$  units of a green primary and  $B$  units of a blue primary, tristimulus values ( $r,g,b$ ) for that colour are found by calculating  $r=R/R+G+B$ ,  $g=G/R+G+B$  and  $b=B/R+G+B$ . From these calculations it can be seen that  $r+g+b=1$ . The colour to be matched can therefore be specified by any two of the

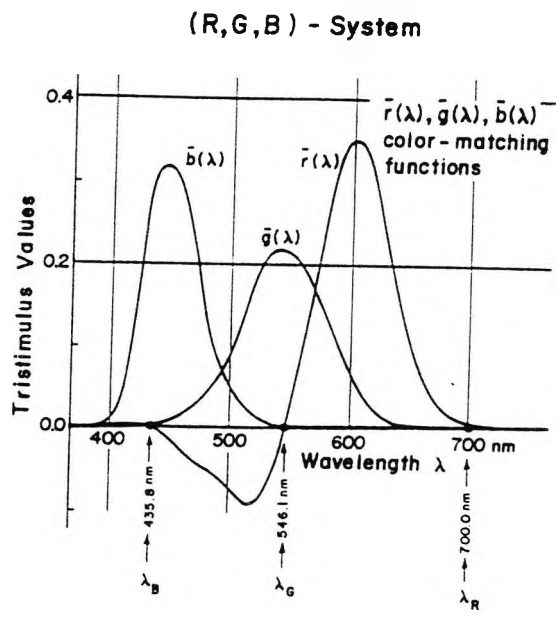


Figure 1.18 Colour matching functions of the CIE 1931 standard colorimetric observer in the system of real primary stimuli R,G and B (Wyszecki and Stiles, 1982)

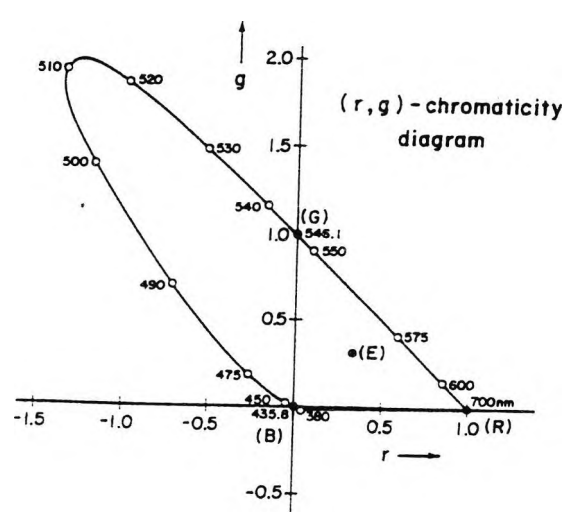


Figure 1.19 (r, g) chromaticity diagram of the CIE 1931 standard colorimetric observer in the system of real primary stimuli R,G and B. The chromaticity point E, of the equal energy stimulus is  $r=1/3$ ,  $g=1/3$ . (Wyszecki and Stiles, 1982)

r, g and b values, and conventionally a diagram of g against r is plotted (see Figure 1.19). The chromaticity of the equal energy stimulus is therefore  $r=1/3$ ,  $g=1/3$ .

The CIE 1931 (X, Y, Z) system is based on imaginary primaries that do not yield negative colour matching functions. The R, G, B tristimulus values can be transformed into X, Y and Z values by a series of equations chosen so that X, Y and Z are positive for all colours, and so that the value of Y for any colour is proportional to the luminance of that colour. The (x,y) chromaticity diagram is shown in Figure 1.20. This diagram was based on matches made using a 2° field. The CIE defined another system in 1964, based on a 10° field, from which comes the ( $x_{10}$ ,  $y_{10}$ ) chromaticity diagram. In 1976, the CIE proposed the uniform chromaticity scale diagram, or ( $u'$ ,  $v'$ ) diagram, which aims to solve the problem of a perceptually non-uniform chromatic discrimination colour space (see Figure 1.21).

The (x,y) diagram is widely used. The colours of stimuli and screen background generated on the equipment used in the studies presented in this thesis were all specified using the (x,y) system (see Chapter 2).

#### 1.4.4 Congenital and acquired colour vision deficiencies

The most common form of colour vision deficiency involves abnormal responses to red and green stimuli, and subjects with this deficiency may be classified into four sub-groups. Protanopes and deuteranopes are able to match any test colour with a mixture of only two matching stimuli, and are referred to as dichromats. Anomalous trichromats require three primaries to match another colour, but their matches are not accepted by normal trichromats, and they will not accept matches made by normal observers. Anomalous trichromats may be protanomalous or deuteranomalous. Classification is often based on the so-called 'Rayleigh match', that is, the amounts of red and green light required by the subject to match a spectral yellow. Normal trichromats make a precise colour match within a small range of red-green ratios. Anomalous trichromats accept a wider range of red-green ratios as matching the yellow, with deuteranomalous subjects needing more green light and protanomalous subjects needing more red. Protanopes and deuteranopes will accept any red-green ratio as a colour match for the yellow. A rarer form of dichromacy is tritanopia.

The underlying spectral response mechanisms for these types of colour vision deficiency are reviewed by Ruddock (1991a). The simplest explanation is that protanopes are missing the red-sensitive photopigment of normal colour vision, and similarly that deuteranopes and tritanopes are missing the green-sensitive and blue-sensitive photopigments respectively. However, this theory does not explain the variability of dichromatic colour matching that has been found, or the fact that normal colour matches are not always accepted by these subjects. Ruddock (1991a) cites the work of Alpern and co-workers and their suggestion that in the case of dichromacy the same photopigment is selected for both 'red-' and 'green-' sensitive cones. Tritanopia is thought to be caused by an absent or non-functioning short wavelength sensitive system (Wright, 1946).

The origin of inherited red-green colour vision deficiencies is an abnormal recessive gene carried on the X chromosome. A male carrying the abnormal gene on the X chromosome will demonstrate the deficiency. Heterozygous females will not exhibit the deficiency if a single abnormal gene is present, because it is recessive. They will pass on the abnormal gene to 50% of any offspring. These females may have slightly abnormal spectral sensitivity, even though colour matching remains normal (Ruddock, 1991a). A female will exhibit the full deficiency only if X chromosomes with the abnormal gene are inherited from both parents, and this is the reason that the incidence of red-green colour vision deficiency is much lower in females than in males. A female possessing two abnormal genes will pass the abnormal gene on to all her offspring.

Tritanopia affects 1.5 to 2 times as many males as females, suggesting that it is not a sex-linked phenomenon. It has been shown to have autosomal dominant inheritance (Piantanida, 1991). A gene encoding the short-wavelength sensitive photopigment believed to be absent or nonfunctional in tritanope has been found on chromosome 7.

For each class of dichromat, a co-ordinate on the chromaticity diagram exists, called the confusion point. If straight lines are drawn through the confusion point across the diagram, they will represent the loci of points confused by that class of dichromat (Figure 1.22, and see Table 1.8).

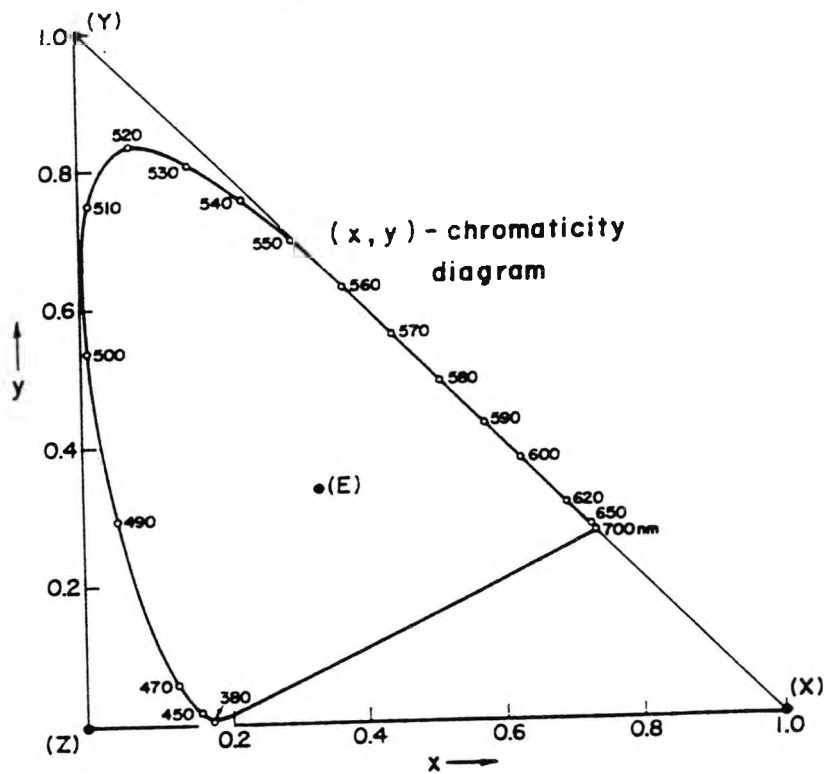


Figure 1.20  $(x,y)$  chromaticity diagram for the CIE 1931 standard colorimetric observer in the transformed system of imaginary primary stimuli  $X$ ,  $Y$  and  $Z$ . The  $(X,Y,Z)$  system constitutes the official CIE 1931 system for practical colorimetry involving colour-matching fields of angular subtense between one and four degrees. The chromaticity point,  $E$ , of the equal energy stimulus is  $x=1/3$ ,  $y=1/3$ . (Wyszecki and Stiles, 1982)

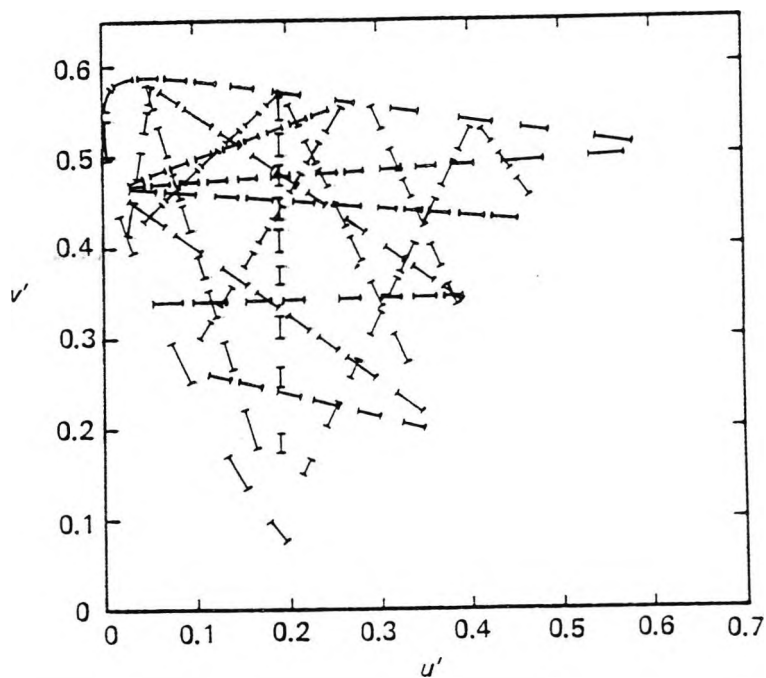
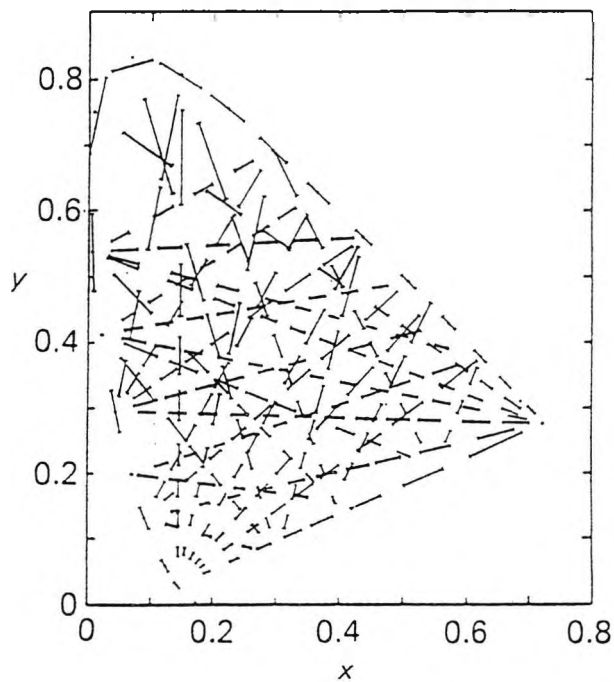


Figure 1.21 Upper graph shows the  $(x,y)$  diagram with lines representing three times the 'just noticeable colour difference'. There is considerable variation in the length of these lines. Lower graph shows the CIE 1976 uniform chromaticity scale  $(u', v')$  diagram with some of the same lines. It can be seen that the variation in the length of the lines is reduced in the lower graph, showing that it represents more perceptually uniform colour space (Hunt, 1991)

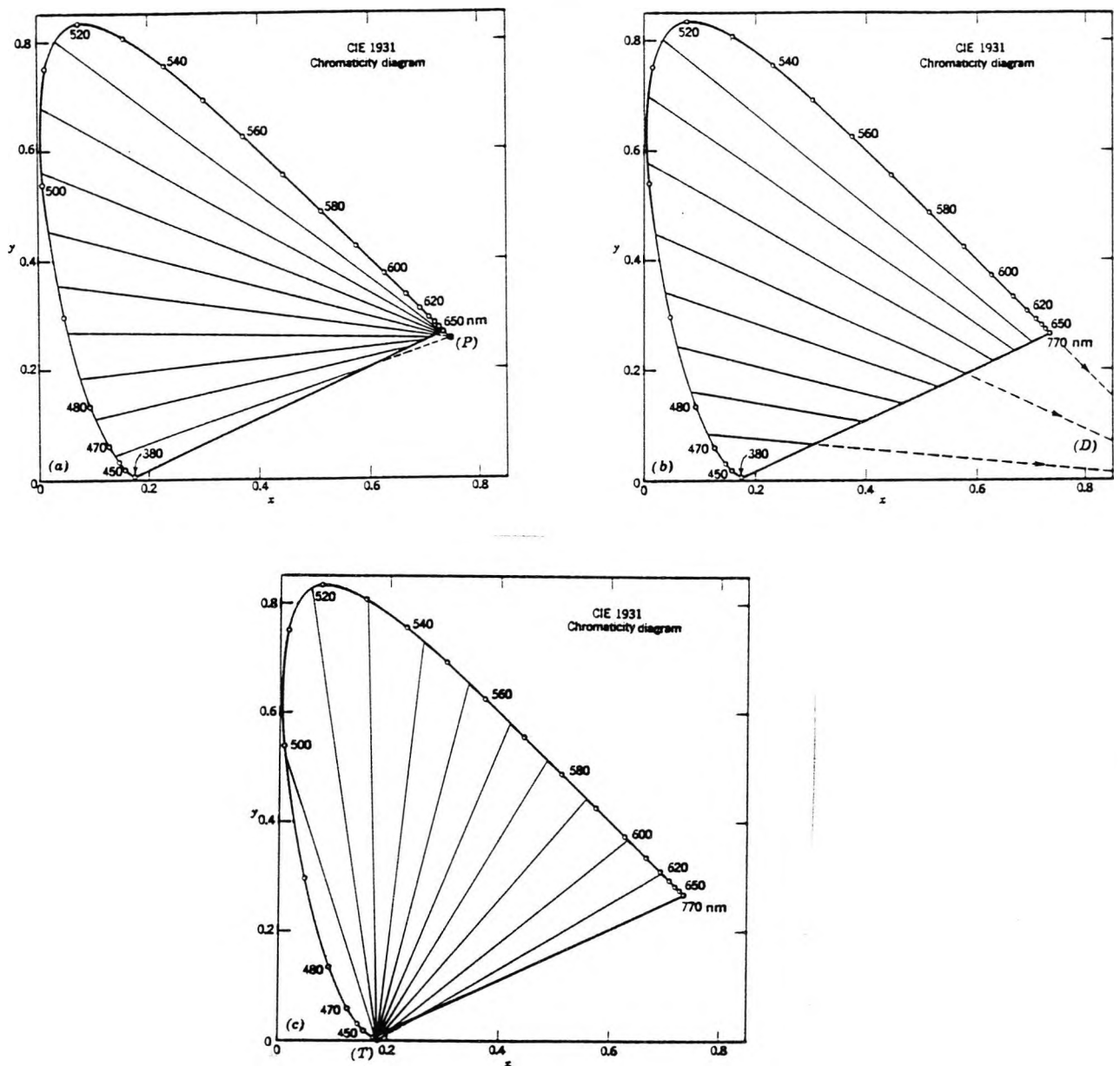


Figure 1.22 Colour confusion lines for dichromats drawn in the normal trichromat's CIE 1931 ( $x, y$ ) chromaticity diagram. For each class of dichromat, all the lines pass through the 'confusion point' and colours represented by points on any given line will be confused by that class of dichromat. (a) Protanope, confusion point is  $x=0.747, y=0.253$ . (b) Deuteranope, confusion point is  $x=1.080, y=-0.080$ . (c) tritanope, confusion point is  $x=0.171, y=0.000$ . (Wyszecki and Stiles, 1982)

Characteristic	Protanomalous	Deuteranomalous	Protanope	Deuteranope	Tritanope
Colour discrimination through the spectrum	Materially reduced from red to yellowish-green but to a varying degree in different cases		Absent from the red to about 520 nm	Absent from the red to about 530 nm	Absent in the greenish-blue to blue (445 to 480 nm)
Neutral point (monochromatic stimulus that matches a fixed 'white' stimulus)	None	None	490-495 nm	495-505 nm	568 and 570 nm
Reduced luminous efficiency of long wavelengths	Yes	No	Yes	No	No
Wavelength of peak of luminous efficiency curve	540 nm	560 nm	540 nm	560 nm	555 nm
Confusion point (CIE x,y co-ordinates)	-	-	x=0.747 y=0.253	x=1.080 y=-0.080	x=0.171 y=0
Frequency of occurrence (%):					
Males	1	4.9	1	1.1	0.002
Females	0.02	0.38	0.02	0.01	0.001

Table 1.8 Features of congenital colour vision deficiencies (from Wyszecki and Stiles, 1982)

The different retinal characteristics found in dichromats alter the luminous efficiency functions of these subjects, particularly for protanopes. This has important implications when isoluminant stimuli are generated since the calibration is usually based on the normal human spectral sensitivity function. For example, stimuli which are meant to be isoluminant with the background may in fact carry luminance contrast for colour defectives. This was the case for the equipment used in the experiments described in this thesis, and so luminance masking techniques were introduced. Figure 1.23 shows spectral luminous efficiency functions for the three classes of dichromats.

Table 1.8 summarises some of the main features of congenital colour vision deficiencies.

Congenital colour vision deficiencies originate from abnormal retinal cones. Acquired colour vision deficiencies on the other hand depend on the location and the pathological process that affects or destroys chromatic processing mechanisms. Table 1.9 lists further differences between congenital and acquired colour vision defects.

Congenital defects	Acquired defects
Present at birth	Onset after birth
Type and severity of defect is stable throughout life	Type and severity of defect may fluctuate
Type of defect can be classified precisely	Type of defect may not be easy to classify. Combined or non-specific deficiencies frequently occur
Both eyes are equally affected	Monocular differences in the type and severity of the defect often occur
Visual acuity is unaffected and visual fields are normal	Visual acuity is often reduced and visual field defects often occur
Predominantly protan or deutan	Predominantly tritan-like
Higher incidence in males	Equal incidence in males and females

Table 1.9 Characteristics of congenital and acquired colour vision deficiencies (Birch, 1991)

Köllner's rule is sometimes applied to the classification of acquired colour vision deficiency. This rule states that conditions affecting the retina will tend to produce blue-yellow defects, while diseases of the optic nerve lead to red-green type of defect

(Gruntzner, 1972). There are however many exceptions to this rule. Other classifications have been suggested (see Krastel and Moreland (1991) for a review).

Colour vision may be affected by the filtering effects of opacities of the crystalline lens or of macular pigment. Cone metabolism and thus colour vision may be affected, for example, in vitamin A deficiency, where tritan-like defects have been found. Optic nerve disorders are likely to affect opponent-colour mechanisms, while lesions of specific layers of the LGN can affect parvocellular mechanisms (also colour-opponent). In the visual cortex, information from the red-green opponent mechanism is used to perceive both colour and fine spatial pattern, and neurons involved in colour processing have been shown to lie in specific areas of V1 and V2 (see sections 1.1.6 and 1.1.7). Lesions of V1 produce scotomata in the corresponding areas of the visual field, but if appropriate methods are used, for example, forced-choice techniques, subjects do show rudimentary colour vision in these areas (see section 1.3.2). Lesions affecting ventral occipito-temporal areas may lead to the condition of achromatopsia, in which colour vision is absent and the world may appear in shades of grey (Plant, 1991; Zeki, 1993). This is thought to be due to damage to V4 cells, which have been shown to respond preferentially to chromatic stimuli. Table 1.10 gives some examples of conditions causing acquired colour vision deficiency.

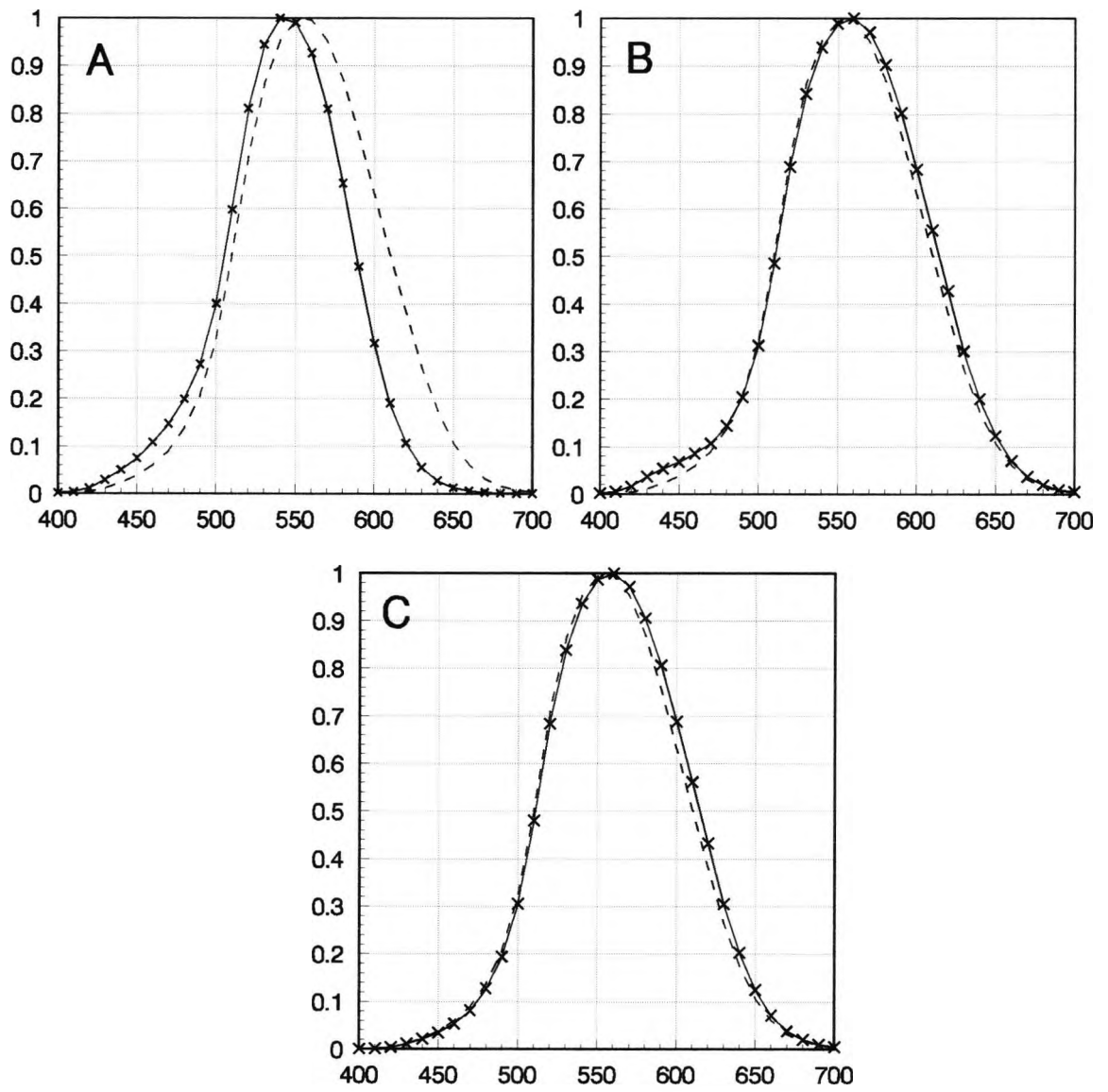


Figure 1.23 Luminous efficiency functions for dichromats (crosses). The luminous efficiency function for normal trichromats is also plotted for comparison (dashed line) A) protanope. B) deuteranope C) tritanope. (Data from Wyszecki and Stiles, 1982)

Condition	Site of damage	Colour vision defect
Vitamin A deficiency	Cone photopigment	Tritan-like
Central serous retinopathy	Photoreceptors	Tritan-like
Chloroquine retinopathy	Retinal pigment epithelium	Impaired discrimination of blue-green and red regions
Choroideraemia	Choroid and outer retinal layers	Blue-green and red-green deficiencies
Retinal effects of digitalis	Retinal photoreceptors	Tritan-like
Cone dystrophy	Retinal cones	Progresses from protanomalous type defect to achromatopsia
Retinitis pigmentosa	Photoreceptor-epithelial complex	Tritan-like
Diabetic retinopathy	Initially inner retinal layers	Loss of blue-green discrimination
Glaucoma	Axons of optic nerve	Tritan-like
Dominant infantile optic atrophy	Retinal ganglion cells	Tritan-like, or occasionally deutan-like
Papilloedema	Swelling of optic nerve head	Blue-yellow deficiency
Optic neuritis	Demyelination and axonal loss in optic nerve	Red-green or unclassifiable
Lesion of V4 / occipito-temporal cortex	V4 / occipito-temporal cortex	Partial or complete achromatopsia

Table 1.10 Examples of acquired colour vision deficiencies (taken from Krastel and Moreland, 1991; Plant, 1991)

#### 1.4.5 Colour vision testing

Colour vision tests are used clinically to identify and differentiate congenital and acquired colour vision defects. Certain occupations have stringent colour vision requirements, and individuals with colour vision deficiencies must be readily identifiable. Colour vision testing can also be a valuable research tool - studying acquired colour vision loss in conjunction with the pathophysiology of certain conditions may give information about the physiology of colour vision or the progression of disease. This approach is discussed further in Chapter 5. Different types of clinical colour vision testing will now be briefly considered.

Colour vision tests may be divided into four categories. Screening tests classify individuals with normal or abnormal colour vision, while grading tests give some indication of the severity of a colour vision defect. Diagnostic tests attempt to classify uniquely certain defects. Vocational tests assess colour ability in practical situations and are often developed specifically for the requirements of a particular occupation.

Anomaloscopes are instruments designed to diagnose different types of colour vision deficiency. Several different anomaloscopes have been designed (for example the Nagel and Neitz anomaloscopes), but the basic principle is that the subject is required to adjust a mixture of red and green to match a yellow field. If a colour vision deficiency is present, a wider than normal range of red-green mixtures is accepted to match the yellow. Anomaloscopes can differentiate between protan and deutan defects, and between dichromats and anomalous trichromats (see section 1.4.4).

Pseudoisochromatic plates are the most widely used clinical colour vision test, and may be used to screen for red-green deficiencies, often with classification into protan and deutan defects. The plates consist of colour coded spots of various sizes and reflectances. Some of the coloured spots are arranged so that numbers or symbols are formed. The colours are chosen so that the numbers and background spots are within isochromatic zones for each class of dichromat. A normal subject usually has little difficulty reading the number or symbol generated, but the defective will not be able to distinguish it from the background. The spots may also be coloured so that a colour deficient subject will see a number different from that seen by normals. Problems with these tests include the accuracy of the printed colours, fading of the colours with time, the level of luminance masking achieved and potential errors if the wrong illumination is used. The Ishihara test is the most widely used pseudoisochromatic test. It does not include any plates to detect tritan deficiencies, and is thus limited as a general test for acquired defects. The American Optical (Hardy Rand and Rittler) plates do include plates for testing tritan defects, and also some superfluous plates to test for a proposed fourth class of congenital deficiency that was thought to exist in the 1940s. The AO test can grade the severity of protan, deutan and tritan defects. Other pseudoisochromatic tests are reviewed by Birch (1991).

Hue discrimination or arrangements tests consist of a range of Munsell samples which the subject is required to arrange into what seems to be a natural colour order. These tests are useful for the examination of acquired deficiency of any type. The D15 test uses 15 colours, and the results are plotted on a circular diagram. A line is drawn from number to number in the order selected by the subject, and errors arising from a colour defect are seen as lines crossing the circle. The axis of these lines indicates the type of defect. The Farnsworth-Munsell 100-Hue test (which actually comprises only 85 colours) involves plotting error scores on a polar diagram. Again the axis of the regions containing the highest error scores indicates the type of defect.

Lantern tests were developed to provide a practical assessment of a subject's ability to recognise and name signal lights correctly, and have particular application in maritime, military, aviation and transport services. Various designs have been suggested, with presentation of one or two lights, in bright or dim illumination, which the subject is required to name (see Birch, (1974,1991) for review).

The City University test does not fit into any of the above categories. It is a useful screening test, incorporating test plates for protan, deutan and tritan deficiencies, with some degree of grading. Each plate consists of a central coloured spot, surrounded by four other spots. The subject is required to indicate which of the four surrounding spots appears to be the closest match to the central spot. The surrounding spots are chosen so that normals, protans, deutans and tritans will all choose a different one to match the central spot.

This section provides a brief outline of clinical colour vision testing methods. As the technology of colour monitors improves, computer-controlled colour vision testing is becoming more widely used, although still mainly as a research tool at present. One such system is described in section 2.4, while Chapter 5 is concerned with the use of this system in testing normal trichromats and subjects with acquired colour vision deficiency.

## **CHAPTER 2 EQUIPMENT AND EXPERIMENTAL METHODS**

### 2.1 Introduction

The equipment employed in this study is described in this chapter. All pupil response measurements (see Chapters 3 and 4) were carried out on the P\_SCAN 100 system. A full description of this apparatus is given in section 2.2. The generation of the stimuli used for the experiments described in Chapters 3 and 4 is outlined in section 2.3.

The chromatic discrimination tests described in Chapter 5 employed the CVTEST program. A description of CVTEST is given in section 2.4. Section 2.5 outlines the experimental room conditions used in the pupillometry and colour vision experiments.

### 2.2 Measurement of pupil responses

The P\_SCAN 100 system was designed for the simultaneous measurement of pupil size and two-dimensional eye movements and has previously been described by Barbur et al (1987) and Barbur (in Alexandridis et al, 1991). A diagram of the apparatus is shown in Figure 2.1. The system uses pulsed infra-red (IR) illumination and measures the diameter of the pupil while the subject views stimuli generated on a high resolution monitor. The illumination is generated using LEDs whose peak spectral emission is 850 nm. The discrete IR sources are positioned to ensure good illumination of the iris, while keeping specular images outside the pupil area. The IR scattered back from the subject's eyes is directed by a 45° IR reflecting mirror down towards the CCD sensors. This mirror transmits 95% of radiation over the visible spectrum, allowing the subject a clear view of the monitor. The subject's head position is fixed by means of head clamps.

Processed IR video signals are generated and displayed on separate video monitors. This allows the examiner to monitor the fixation of the subject. A series of horizontal scan lines overlays the pupil and the co-ordinates of the points of intersection of these scan lines and the pupil margin are extracted by the hardware (Figure 2.2). The number of scan lines that are analysed can be varied, with a maximum of 64. A higher number of scan lines results in a more detailed representation of the pupil margin shape, but

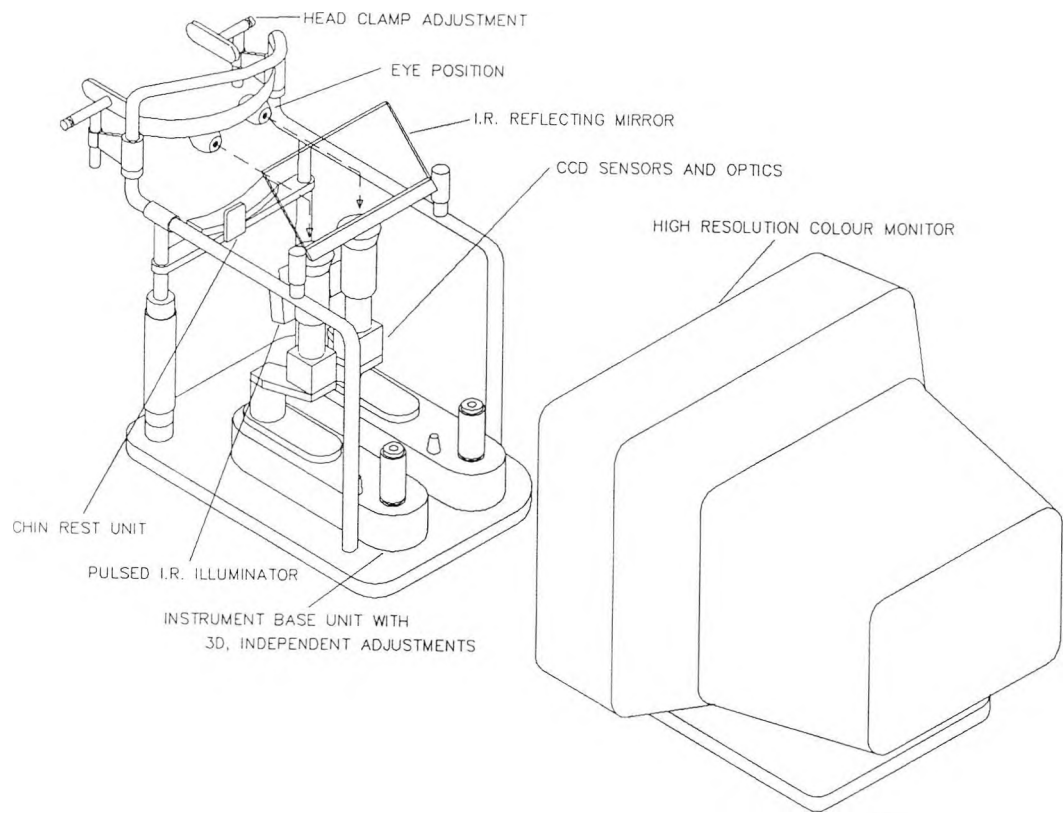


Figure 2.1 Schematic drawing of the P\_SCAN 100 system for the simultaneous measurements of pupil diameter and 2-D eye movements. The diagram shows the instrument base unit which allows easy adjustment of the CCD sensors as required for positioning and focusing of the images of the eyes, and the high resolution colour monitor which is used for generating the visual stimuli

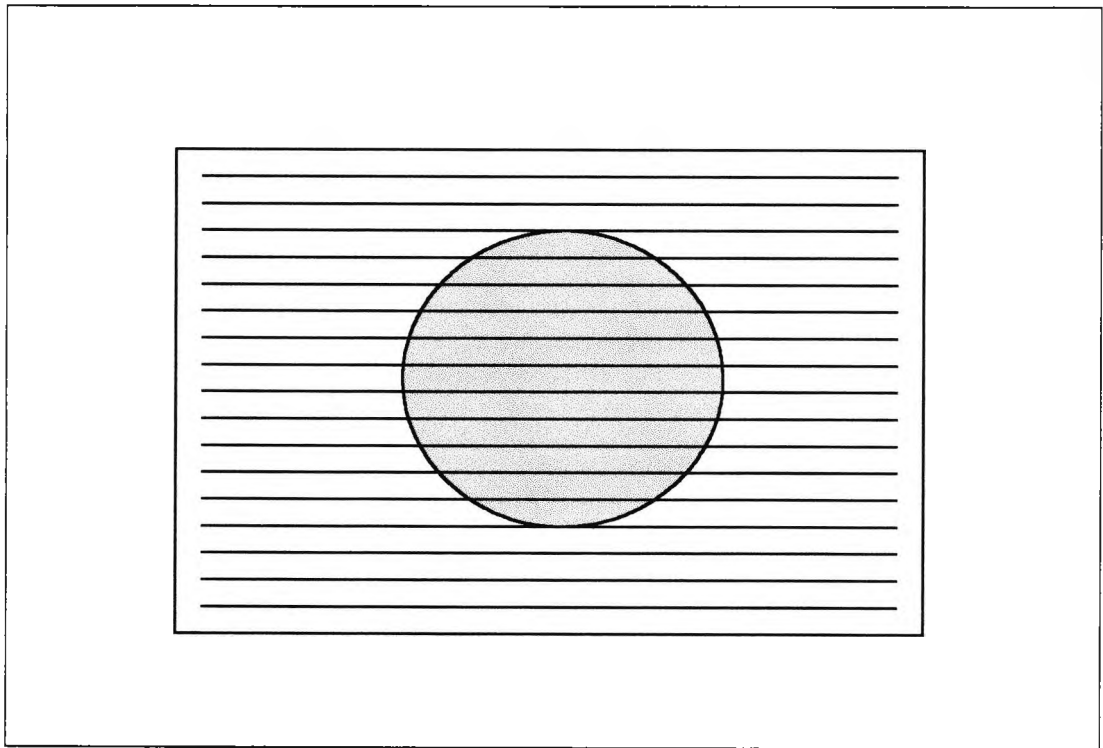


Figure 2.2 Diagram to illustrate appearance of pupil and scan lines in the P\_SCAN 100 system. The co-ordinates of the points of intersection of the scan lines and the pupil margin are extracted by the hardware every 20 ms. The best circle is fitted to the co-ordinates measured, and its diameter and centre position are calculated for each frame.

generates more data points to be processed. In the experiments described in Chapters 3 and 4, 64 scan lines were always used. The points of intersection are established by defining a threshold voltage difference, which will vary between subjects and with different adjustments of the IR illumination. The threshold voltage is automatically defined by the system for the images obtained before each experiment, and may be adjusted manually to achieve an accurate mapping of the pupil margin.

The stimulus parameters are chosen by the examiner at the beginning of each test (see Section 2.3), including the time before, during and after each stimulus for which recording is required. When the subject is ready, the examiner initiates a stimulus using a panel of control buttons. The recording begins as soon as the examiner presses the 'go' button, and consists of video frames measured every 20 ms. For each frame, all the points of intersection of the scan lines and the pupil margin are stored. When the measurement of each trace is complete, a beep is generated and the examiner may encourage the subject to blink or rest before initiating the next stimulus. Because of the intrinsic noise in the pupillary system and the small size of responses measured, each stimulus is presented several times in order that the results may be averaged to increase the signal-to-noise ratio. If several different stimuli have been chosen, they are interleaved and presented in varying order.

At the end of the experimental run, the raw data obtained are processed. For each frame, the best circle is fitted to the co-ordinates measured, and its diameter and centre position are calculated.

The results can then be analysed using the 'pupav' and 'pview' programs. The diameter of the pupil is plotted against time for each stimulus presentation, together with a trace indicating stimulus onset and offset. The error associated with measurements of pupil diameter has been shown to be of the order of 0.2% (Barbur et al, 1987). If more than one stimulus was used, the traces obtained are sorted so that all the traces relating to the same stimulus viewed with the same eye are stored sequentially in the same file. These traces indicate if any blinks occurred during the measurement, or if recording was particularly noisy for any individual presentation (usually if the subject's eyelashes were overlapping the pupil margin and degrading the pupil images). By checking each trace

in turn, the examiner can reject any which might reduce the accuracy of the final result. At the end of each set of traces, the average trace is displayed and analysed. Cursors are used to measure the starting diameter, time at which constriction started and time for maximum constriction to occur. The amplitude and latency of the constriction and the noise variance of pupil measurements are then computed automatically. The system can also be used to monitor eye movements by assessing the movement of the centre of the circle fitted to the pupil margin with time. The two-dimensional eye movement data are stored with the corresponding pupil diameter trace and can be displayed and analysed. When the analysis of results is complete, each trace may be stored for subsequent retrieval, together with details of the experiment, and computation of steady state and noise variance.

All the traces of pupil diameter against time presented in Chapters 3 and 4 are averaged traces. A typical averaged trace is shown in Figure 2.3. *In most cases, the traces are shifted vertically by an arbitrary amount to aid comparison.*

### 2.3 Stimuli used in pupillometry experiments

The stimuli used for the experiments described in Chapters 3 and 4 were generated on a high resolution 20" HP 1187A 60 Hz monitor, with a resolution of 1280 x 1024 pixels. Most of the experiments were carried out with a viewing distance of 700 mm, so that the screen subtended  $28.4^\circ \times 22.7^\circ$ . Each pixel subtended  $0.0222^\circ$  at this distance. The monitor was driven by a Texas Instruments TIGA card providing 256 levels per gun, and the system was calibrated by measuring the luminance for each level for the three guns using an LMT photometer. The stimulus chromaticity and luminance required were achieved by computation of the correct level for each gun. The equipment was recalibrated periodically over the course of the experiments. A warm-up time of at least 45 minutes was always allowed before calibration or experimental measurements were carried <sup>out.</sup> The spectral luminance of the screen phosphors are shown in Figure 2.4.

At the beginning of each experiment, the examiner selected the stimulus parameters required. Within the limits of the screen phosphors and size, any chromaticities and luminances could be chosen, together with the size, shape and position of the stimulus on the screen, and any luminance masking required (see below). Chromaticities were

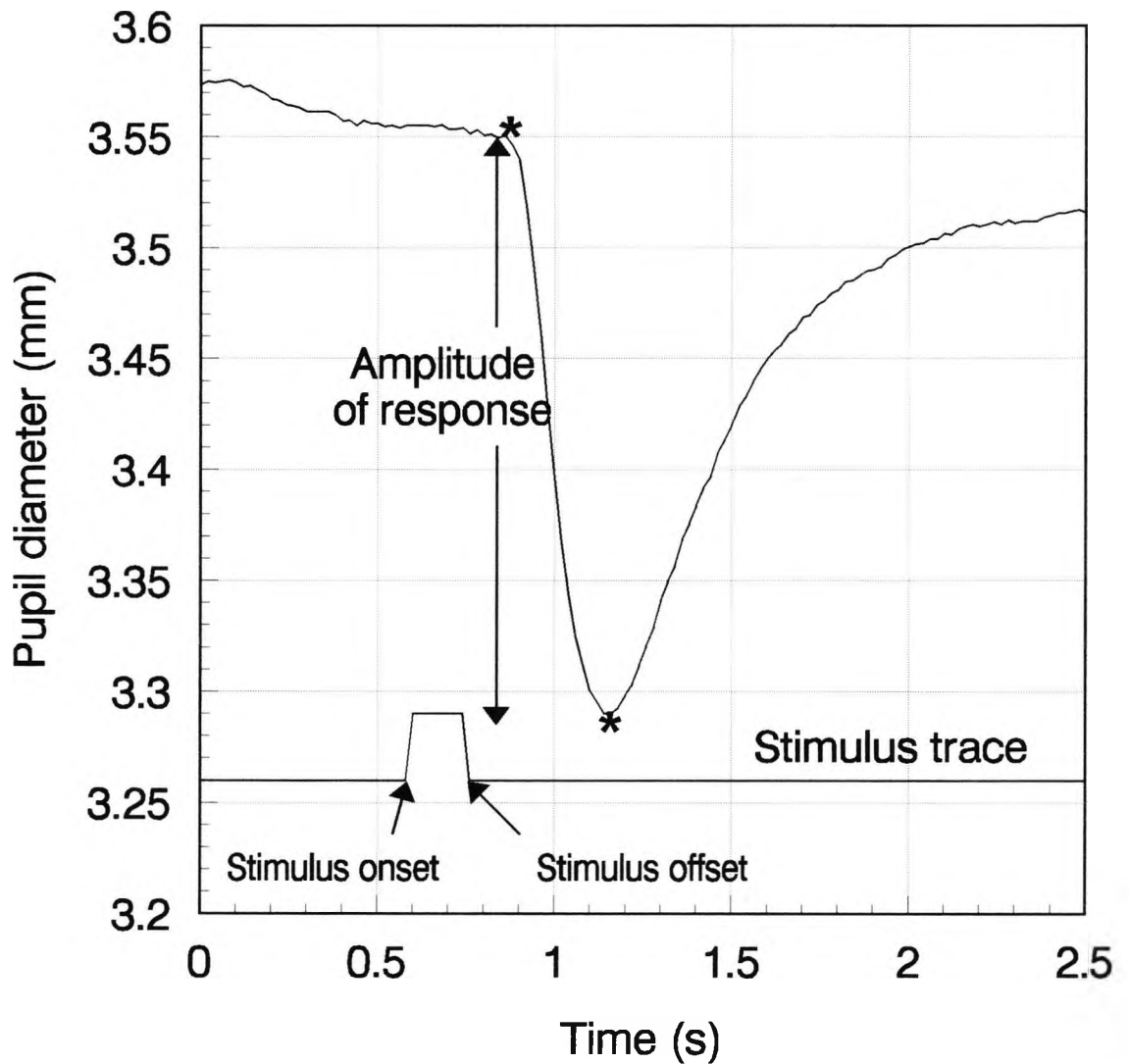


Figure 2.3 A typical averaged trace showing the pupil response to a given stimulus. The lower trace indicates the stimulus onset and offset. The amplitude of response is the difference in the pupil diameters measured at the points indicated by a star, that is, immediately before the constriction starts and at the point of maximum constriction. The analysis program calculates the variance associated with the amplitude of response for the individual traces accepted, and the standard error can be calculated. In the example shown above, 64 individual traces were accepted to create the averaged trace, the amplitude of response was 0.2605 mm with a variance of 0.01048, and therefore a standard error of 0.0128 mm. Results of pupillometry experiments described in Chapters 3 and 4 are presented in this format

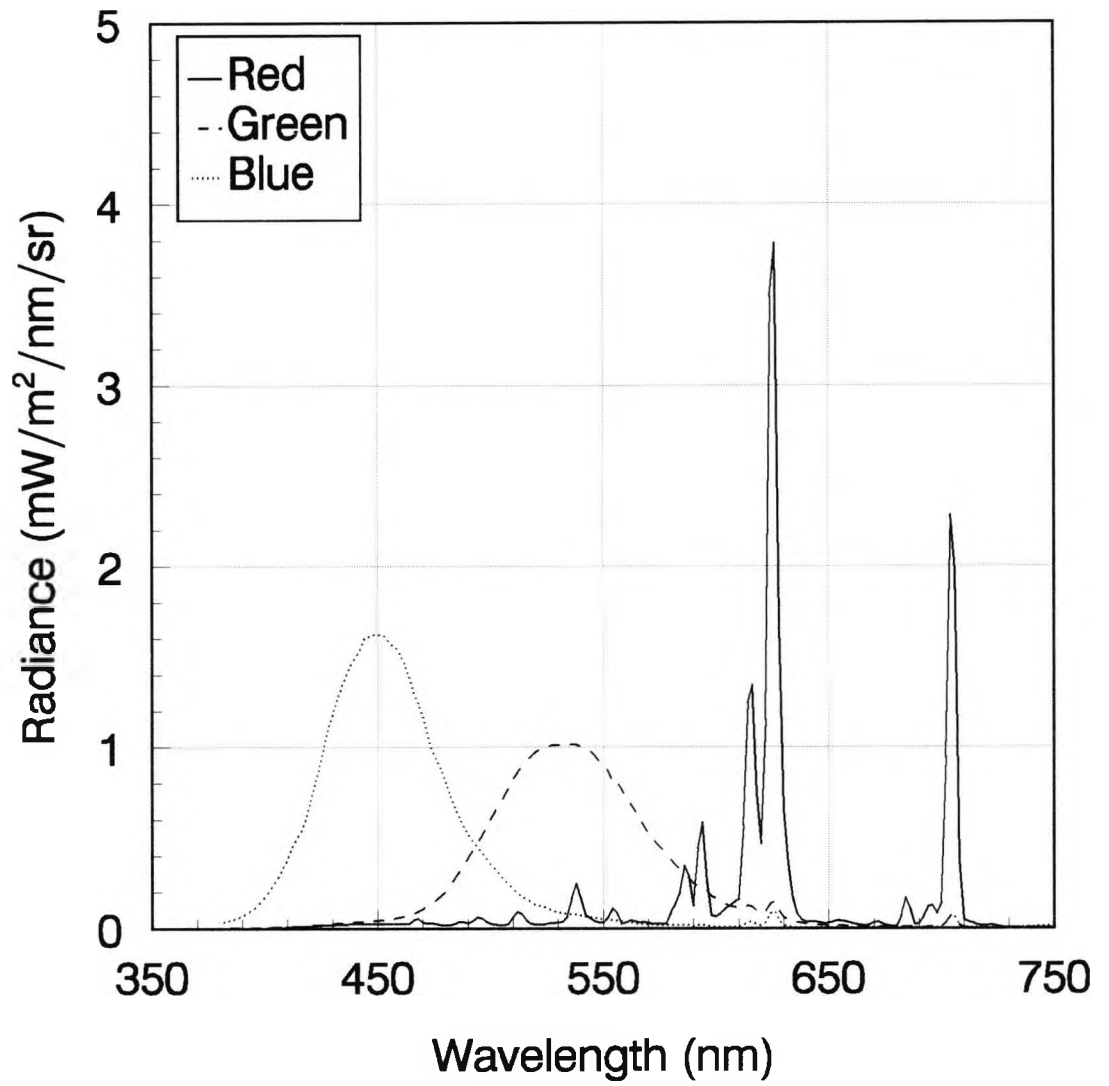


Figure 2.4 Spectral radiance of the three phosphors of the screen used in the experiments described in Chapters 3, 4 and 5

defined by using CIE (x,y) chromaticity co-ordinates. The stimulus was usually positioned as close as possible to the centre of the screen as this is where the gun calibration was carried out, and there may have been slight variations towards the edge of the screen (Mollon and Baker, 1995). The examiner also entered the experimental conditions, such as viewing distance, eye(s) viewing, eye(s) being measured and number of scan lines. The frame group was specified for experiments involving luminance masking (see below). The time course of the stimulus presentation was defined in terms of time before recording, time before stimulus presentation, stimulus duration and time after stimulus.

Many of the experiments described in Chapters 3 and 4 involve the use of random luminance masking (RLM). These are referred to as spatial RLM, or  $RLM_s$ , and temporal RLM, or  $RLM_t$ .

$RLM_s$  has been described in previous papers concerning colour vision testing (Barbur et al, 1992a, 1993a, 1994a,d; Birch et al, 1992; Cole, 1995) and pupil measurement (Barbur et al, 1994d; Barbur, 1995). The stimulus is presented amid an array of achromatic checks. The luminance of each check varies at randomly chosen luminance levels above or below the mean background luminance to maximum and minimum values specified by the examiner as a percentage of the background luminance. The luminances of the checks are calculated so that at any given time the space-averaged luminance over the whole array is equal to the background luminance level, although there are local increments and decrements in luminance. The luminance of each check changes at a frequency specified by the examiner in terms of the frame group (each frame is 16.67 milliseconds, so a frame group of 5 indicates that the luminance of each check varies every  $(5 \times 16.67) \approx 84$  ms). Figure 2.5 shows how the luminance profiles vary spatially across the array for a background luminance of  $24 \text{ cd/m}^2$  for different values of  $RLM_s$ . Figure 2.6a shows how the luminance profile of the checks changes with time for a background luminance of  $24 \text{ cd/m}^2$  and  $RLM_s$  of  $\pm 20\%$ .

$RLM_s$  causes only local changes of check luminance, while the overall space-averaged luminance remains equal to that of the background. During temporal RLM ( $RLM_t$ ), on the other hand, the luminance of the stimulus area varies with time, again according to a frame group set by the examiner, and within limits specified as a percentage of the mean.

RLM<sub>i</sub> may be used alone or in conjunction with RLM<sub>s</sub>. Figure 2.6b indicates how the luminance profile varies with time when RLM<sub>s</sub> and RLM<sub>i</sub> are used together. The local variations defined by RLM<sub>s</sub> are grouped around the mean luminance (as shown for Figure 2.6a with RLM<sub>s</sub> alone) but in this case, the mean luminance varies with time according to the level of RLM<sub>i</sub> chosen.

#### 2.4 Equipment and stimuli used in colour vision measurement

CVTEST, the system of computerised colour vision measurement used for the experiments described in Chapter 5 has been described previously (Barbur et al, 1992a, 1993a, 1994a,d; Birch et al, 1992; Cole, 1995). The same monitor was used as for the pupillometry experiments described in Section 2.3 above. Prior to each experimental run, the stimulus parameters were entered by the examiner or retrieved from a file. These parameters included stimulus size, shape, location, duration, chromaticity (using CIE (x,y) chromaticity co-ordinates) and luminance, and the range and check size of RLM<sub>s</sub> and RLM<sub>i</sub> if required.

CVTEST is a psychophysical test which measures the threshold chromaticity required for a stimulus to be detected from its background. This threshold value is reached by a staircase procedure. This is arranged as follows: the examiner specifies a starting chromaticity, usually chosen to be well above the expected threshold so that the subject knows what stimulus he is required to detect. If the stimulus is seen, the chromaticity is reduced in discrete steps, until a point is reached where the stimulus is no longer seen. The chromaticity is then increased again until the stimulus is seen, and so on. The step size decreases on every reversal according to an exponential function. The number of reversals, and the initial and final step sizes are determined before the experiment. The threshold is taken to be the average of the chromaticities of the last few reversals (for example, the average of the last three points of reversal). CVTEST allows for a 'coarse' and 'fine' staircase to be carried out for the same set of stimulus parameters. The 'coarse' staircase allows reasonably rapid arrival at a threshold value using large step sizes, while the 'fine' staircase starts at this threshold value and uses smaller step sizes to refine the threshold value calculated. Table 2.1 shows a typical set of staircase parameters:

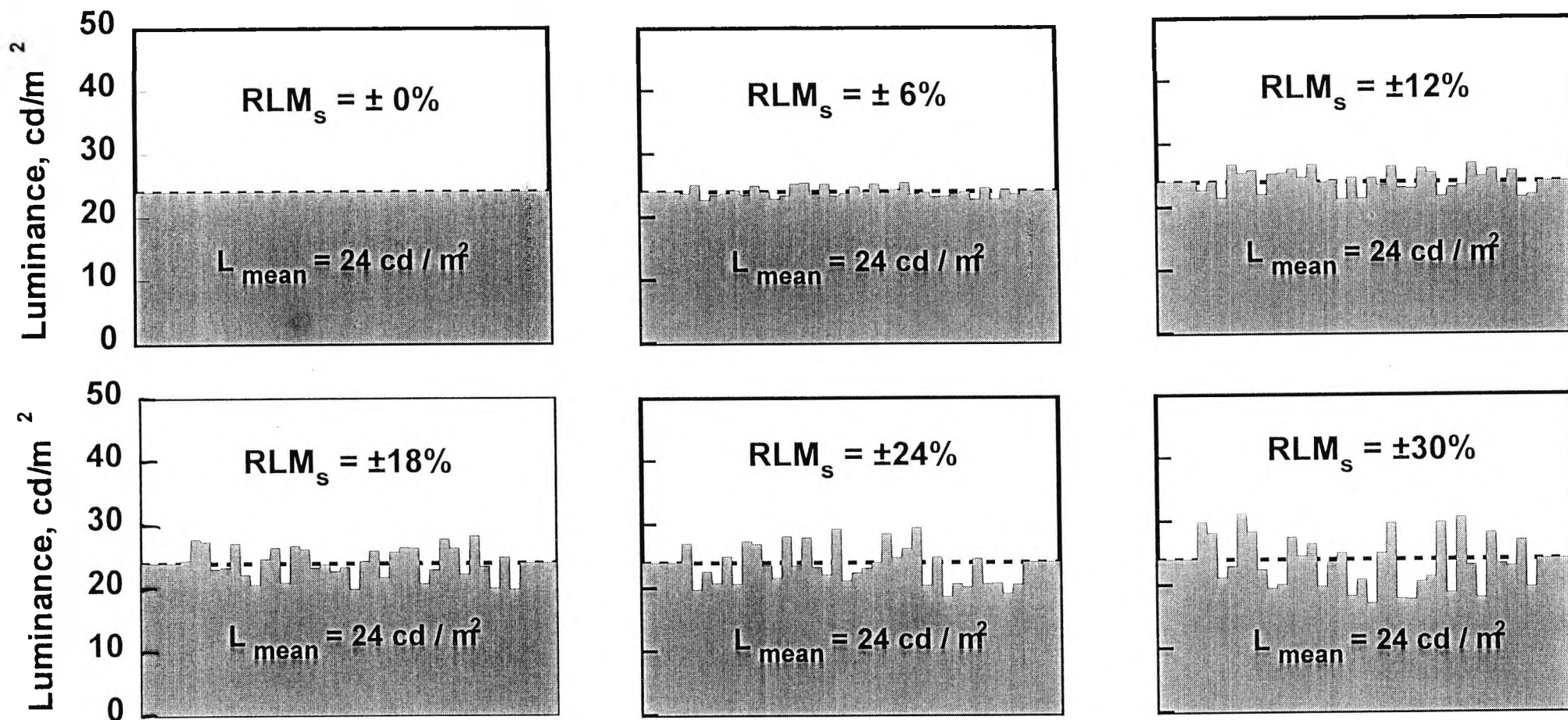
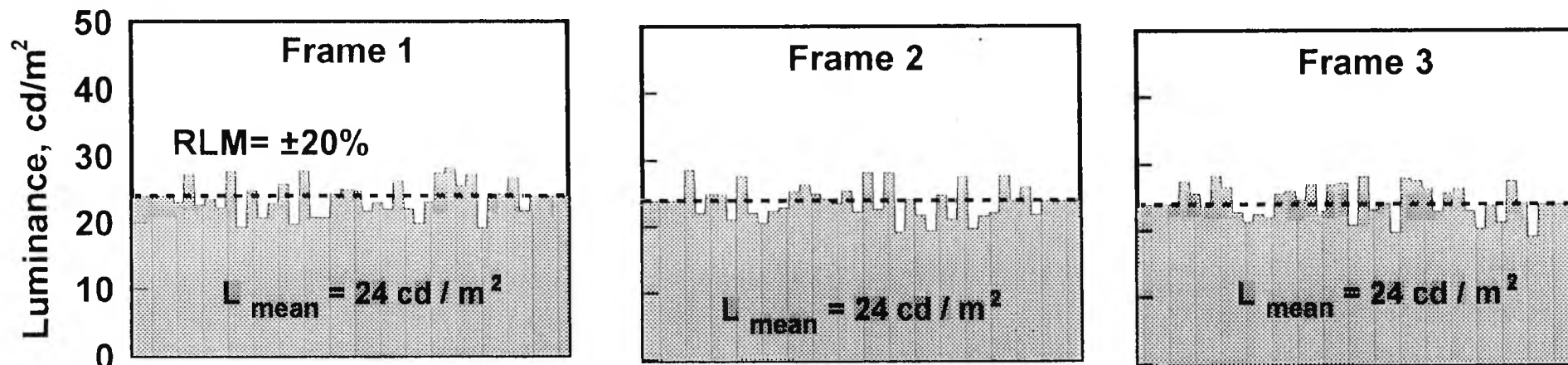


Figure 2.5 Diagram showing luminance profiles for individual frames of spatial random luminance modulation (RLM<sub>s</sub>). Profiles are shown for screen background of 24 cd/m<sup>2</sup> for different RLM<sub>s</sub> amplitudes. The mean luminance across the RLM<sub>s</sub> display indicated by a dotted line is 24 cd/m<sup>2</sup>. The check luminances vary according to the RLM<sub>s</sub> selected, for example, for a RLM<sub>s</sub> of **±30%** the checks may have luminances between 31.2 cd/m<sup>2</sup> and 16.8 cd/m<sup>2</sup>

## A Spatial random luminance modulation (RLMs)



## B Temporal random luminance modulation (RLMt)

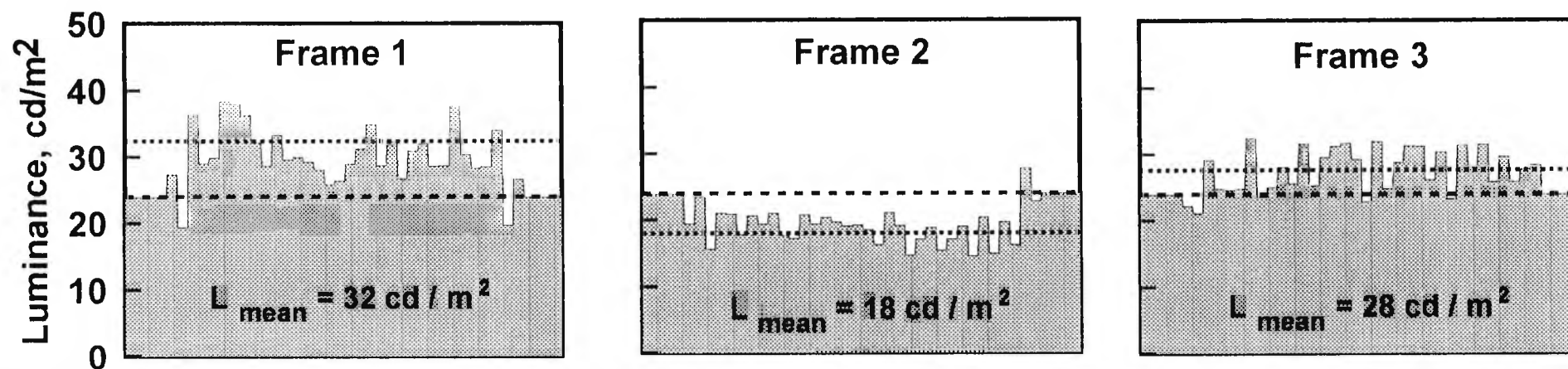


Figure 2.6 (A) Luminance profiles of RLM<sub>s</sub> only, showing how the luminance of the checks varies about a constant mean luminance from frame to frame. (B) Luminance profiles for RLM<sub>s</sub> and RLM<sub>t</sub> showing how mean luminance changes from frame to frame

Staircase	Coarse	Fine
Number of reversals	5	6
Reversals ignored	2	3
Start increment	0.012	0.006
End increment	0.006	0.001

Table 2.1 Typical staircase parameters (increments are in CIE (x,y) chromaticity units)

## 2.5 Experimental room conditions

The same room conditions were used for both pupil and colour measurement experiments. The subject was separated from the examiner and the control PC by a black curtain. The only illumination on the subject's side of the curtain came from an extended Lambertian surface on the ceiling above the display monitor. This arrangement provided diffuse illumination, but contributed only about 0.2 cd/m<sup>2</sup> to the luminance of the display. The walls and the ceiling of the experimental room were painted matt black. The subject's eyes and pupillometer cameras were shielded from scattered light by a matt black horizontal shade, and the pupillometer base and monitor units were covered with black velvet.

## 2.6 Definition of contrast

The contrast used to define stimulus intensity is given by:

$$\text{Contrast} = \frac{L_s - L_b}{L_b}$$

where  $L_s$  = luminance of the stimulus

$L_b$  = luminance of the background

## **CHAPTER 3 A STUDY OF PUPIL LIGHT RESPONSE COMPONENTS IN HUMAN VISION**

### 3.1 Introduction

The dynamic pupil light reflex has been described by Lowenstein and Loewenfeld (1969), Loewenfeld (1993) and see section 1.2.5. Some workers have shown that it increases linearly with the log of the stimulus intensity, although Webster et al (1968) found large inter-subject variability. Subjects with lesions of the optic chiasm, optic tract or visual cortex exhibit abnormal pupil responses if appropriate stimuli are used (section 1.2.6).

This chapter describes the discovery of what appear to be two separable components of the pupil light reflex, isolated using the Random Luminance Modulation (RLM) techniques described in Chapter 2. Preliminary experiments are described for a normal subject, followed by subsequent experiments carried out on normal subjects, a subject with damaged primary visual cortex and a subject with optic nerve drusen. The effects of stimulus contrast and area have also been examined for normal subjects and subjects with damaged primary visual cortex, and are described in sections 3.6 and 3.7.

From the results obtained, two components of the pupil light reflex are proposed, one of which is absent or reduced in subjects with cortical damage. This hypothesis is consistent with the abnormal responses found in such subjects when small, dim stimuli are used.

### 3.2 Initial experiments - RLM<sub>s</sub> alone

#### Introduction

The RLM<sub>s</sub> technique was originally developed as a luminance masking technique for psychophysical colour vision testing (Barbur et al, 1992a; Birch et al, 1992; Barbur et al, 1993a, and see section 2.3). It has also been used to eliminate luminance changes when measuring pupil colour responses, thus isolating the true response to coloured stimuli (Barbur et al, 1993a). The work described in this chapter is based on the following

hypothesis: if the  $RLM_s$  is effective at eliminating luminance contrast changes, then it is reasonable to expect that any 'contrast-based component' of the PLR should also be reduced when  $RLM_s$  is used.

### Subjects

Complete sets of results will be given for a normal subject JB, who is a 42 year old emmetropic male, an experienced participant in pupil measurement experiments. Similar results have been obtained with 20 more normal subjects by Shaila Chaudry (unpublished data). Subject GY is 38, and has damaged left primary visual cortex as a result of a road accident at the age of 8, leaving him with a right homonymous hemianopia with macular sparing (see Barbur et al, 1980, for visual field map). At the beginning of this investigation, GY was approximately emmetropic and the experiments were carried out with no correction for refractive error. Later, it was found that his right eye had become hyperopic and for later experiments he wore a correction of R:+3.00 DS L:+1.00 DS, which included an allowance of +1.00 DS for the viewing distance.

### Experimental procedure

The P\_SCAN 100 system was used for all the pupil measurement experiments described in this chapter (see section 2.2). The subjects viewed the screen from a distance of 700 mm. At this distance the screen subtended  $28.4^\circ \times 22.7^\circ$ . The background luminance of the screen was  $24 \text{ cd/m}^2$  with CIE (x,y) chromaticity co-ordinates of (0.305, 0.323) and the stimulus was a square of  $13^\circ \times 13^\circ$ , presented as shown in Figure 3.1, for 167 ms. The target was positioned so that its centre was  $16.9^\circ$  from the fixation target. The PLR was measured to the stimulus alone, and then with increasing levels of  $RLM_s$ . Each condition was presented 64 times. The pattern for the  $RLM_s$  consisted of  $1^\circ$  checks, and a border one check wide was presented round the stimulus as shown in Figure 3.1b. For subject GY the above stimulus conditions were used to test the blind hemifield, and a mirror image of this configuration with respect to the vertical meridian (ie, stimulus above and to the left of fixation) was used to test the sighted hemifield. Viewing and recording were binocular, and 64 traces from the right and left eyes were averaged.

## Results

Figure 3.2 shows the pupil responses measured in subject JB for a stimulus contrast of 30%, and the amplitudes of the responses are plotted in Figure 3.3. The largest response was obtained when the stimulus was presented with zero  $RLM_s$ . The results show that increasing the  $RLM_s$  contrast reduces the amplitude of the response until a contrast of 35%  $RLM_s$  is reached. Increasing the contrast of the  $RLM_s$  above this level appears to cause no further reduction of response amplitude. In general though, for stimuli of this size and contrast the response amplitude is smaller with  $RLM_s$ .

Figure 3.4 shows results obtained for subject GY for a stimulus contrast of 30%, with and without  $RLM_s$  of 45%, in the blind and sighted hemifields. The response amplitude obtained by presenting the stimulus with zero  $RLM_s$  in the blind hemifield is smaller than that obtained with the same stimulus in the sighted hemifield. As in the normal subject, the amplitude is reduced when  $RLM_s$  is introduced in the sighted field. However, for the blind field, introduction of the  $RLM_s$  does not greatly reduce the amplitude for this stimulus.

## Conclusion

For the stimulus configuration used in this experiment, the PLR reduces asymptotically as the  $RLM_s$  amplitude is increased. The  $RLM_s$  is constructed so that although there are local variations in luminance, the total light flux level on the retina is constant and independent of  $RLM_s$  amplitude. The total light flux on the retina only increases when the stimulus is presented. If the PLR were only mediated by neurons responding to local luminance increments (ie within each check), the  $RLM_s$  should eliminate all of the response. If the PLR were only mediated by neurons which sum up light increments over the entire stimulus, the  $RLM_s$  should have no effect at all. The results suggest that in normal subjects both types of neurons are present. Increasing the range of possible  $RLM_s$  contrasts gradually reduces that part of the response mediated by neurons responding to local luminance increments until this component is made ineffective. The remaining part of the response must be mediated by neurons that can sum up over large areas of the stimulus.

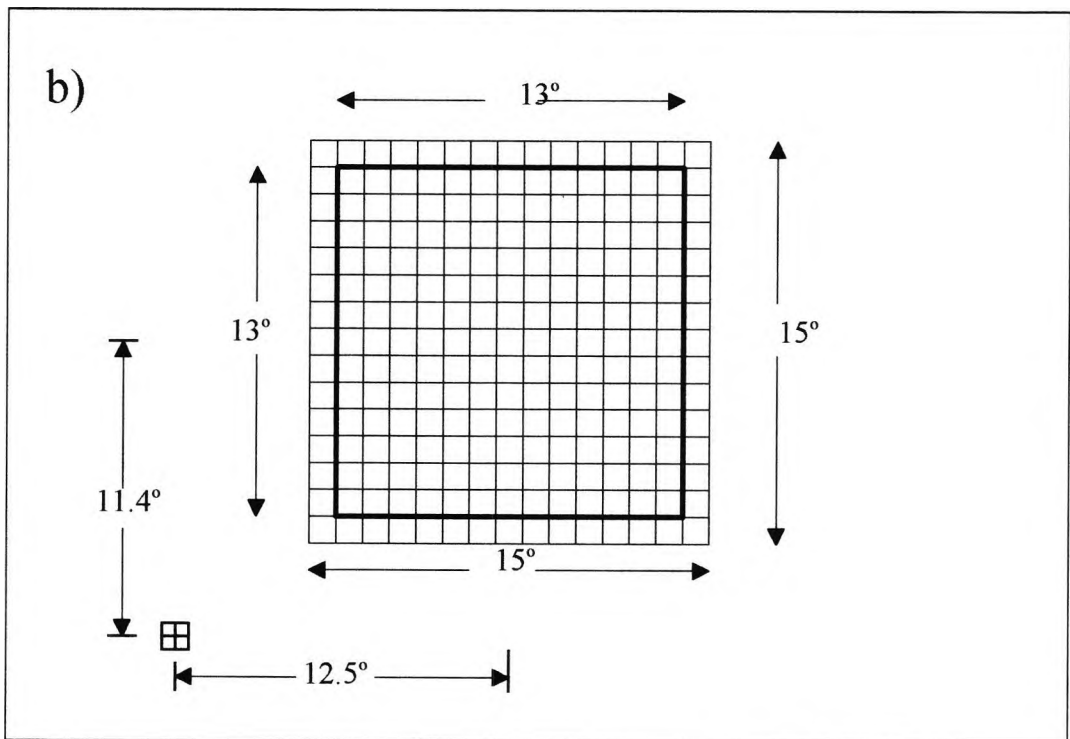
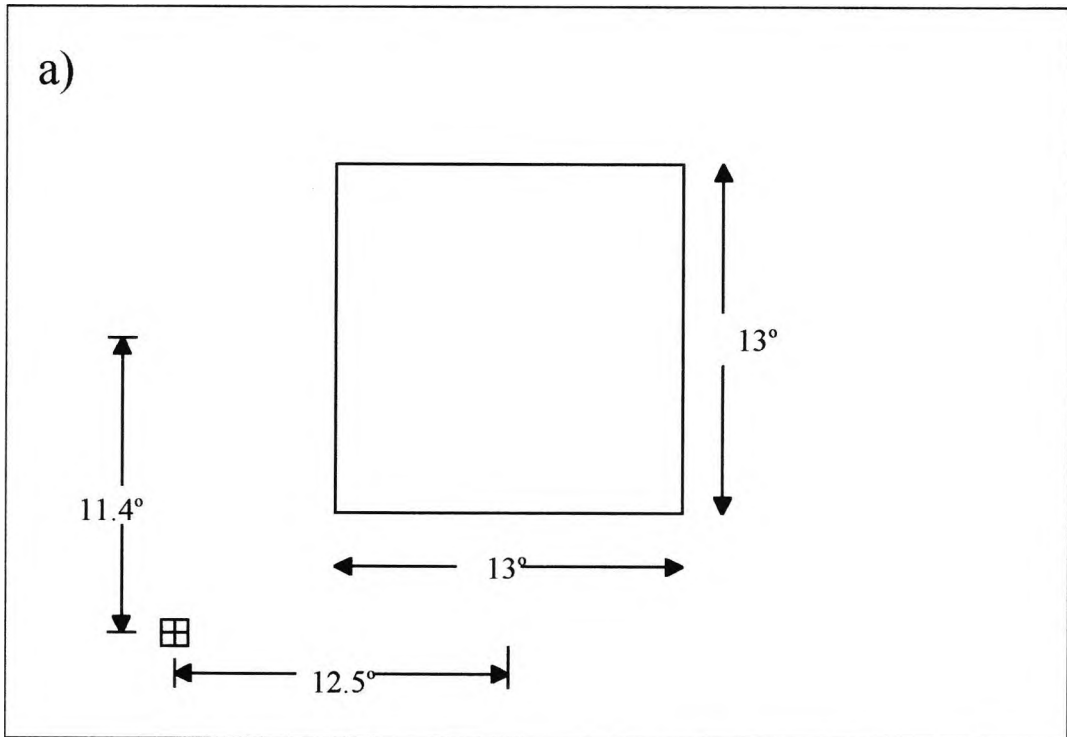


Figure 3.1 Stimulus configuration for initial pupil light reflex experiments  
 a) without and b) with RLM<sub>s</sub>.

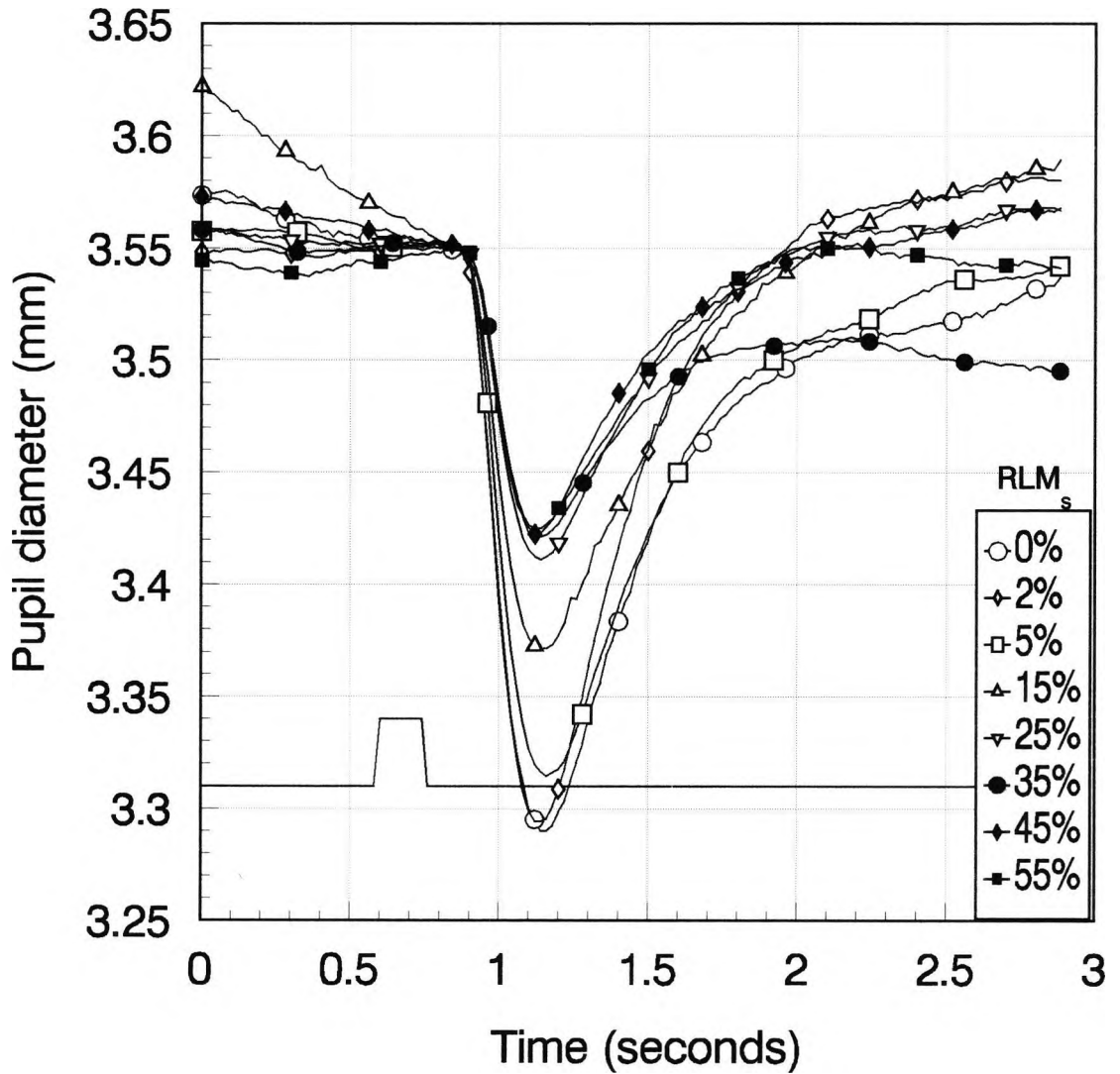


Figure 3.2 Pupil responses measured using different  $RLM_s$  contrasts for subject JB. Stimulus configuration as shown in Figure 3.1, stimulus contrast=30%. The traces have been shifted vertically by an arbitrary amount to aid comparison.

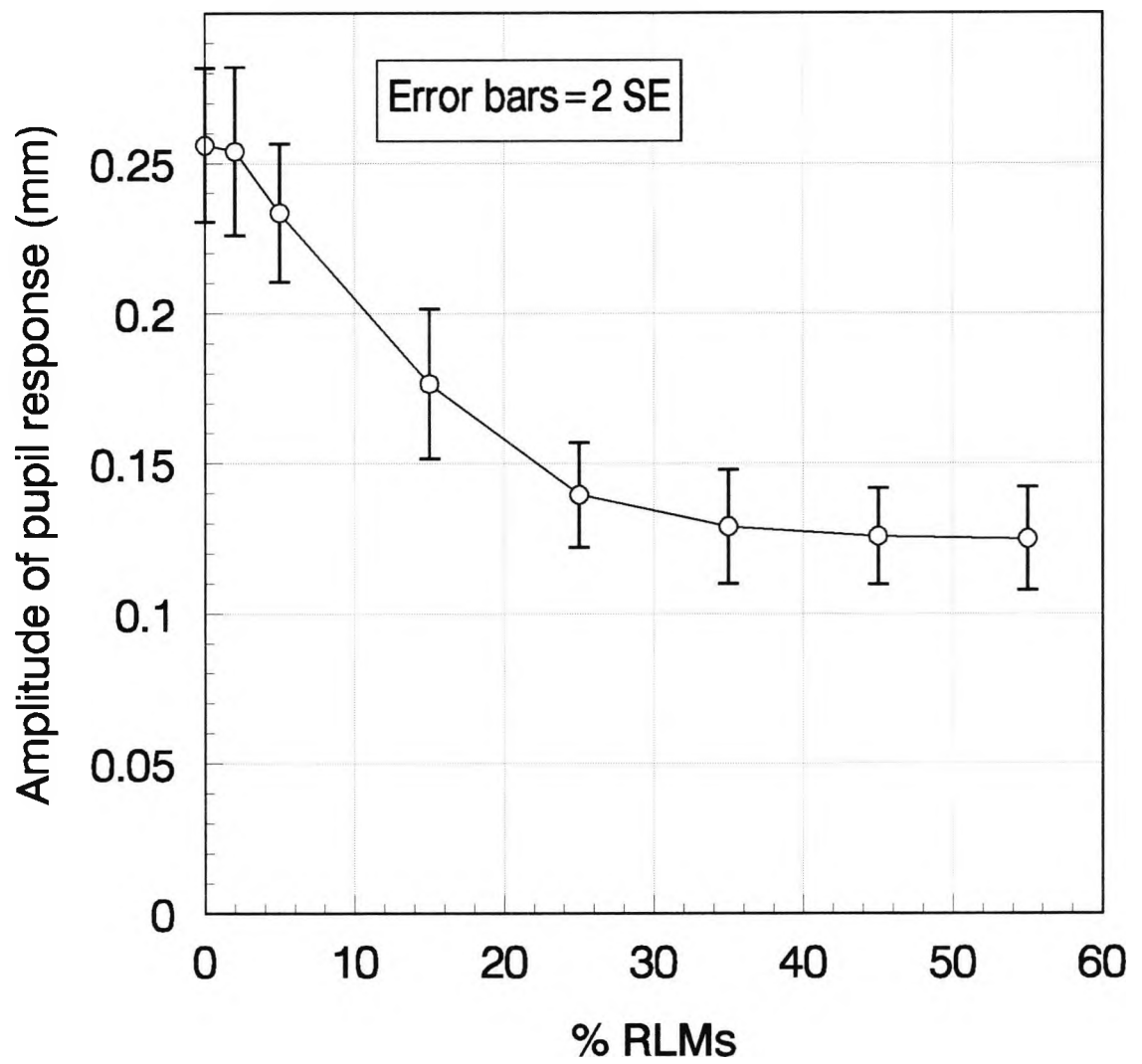


Figure 3.3 Effect of increasing RLM<sub>s</sub> contrast on pupil response amplitude, subject JB. Measurements were taken from the traces shown in Figure 3.2, stimulus configuration as shown in Figure 3.1, with stimulus contrast=30%

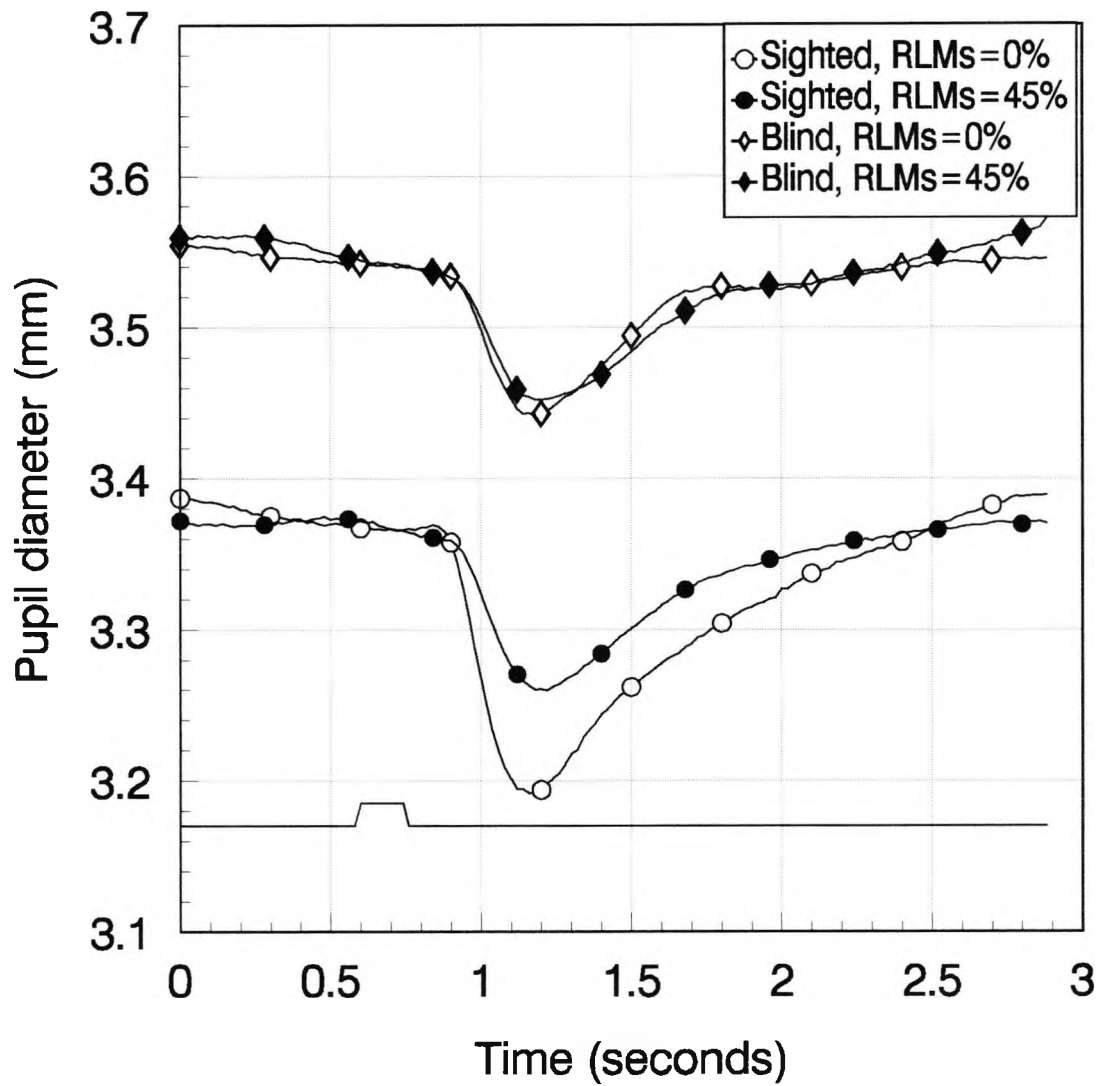


Figure 3.4 Pupil responses measured with and without  $RLM_s$  of 45% for stimuli presented in subject GY's blind and sighted hemifields. Stimulus configuration was as shown in Figure 3.1 for the blind hemifield, and a mirror image about the vertical meridian was used for the sighted hemifield. Stimulus contrast was 30%.

For GY's blind field, the use of  $RLM_s$  makes little difference for this stimulus, which suggests that the component affected by the  $RLM_s$  is reduced or absent for his cortically blind hemifield.

### 3.3 Introduction of $RLM_t$

#### Introduction

It has been shown in section 3.2 above that the response to a luminance increment could not be completely eliminated using  $RLM_s$  alone (for the stimuli used in this experiment), and it was suggested that this was because the pupil response pathways can sum up light flux over the whole stimulus area. A new form of luminance masking that causes the mean luminance of the whole stimulus to change randomly within specified limits was therefore introduced (see section 2.3). Since the luminance change is uniform over the whole pattern and changes only as a function of time, this modulation has been called temporal random luminance modulation ( $RLM_t$ ).  $RLM_t$  was introduced in order to test the hypothesis that part of the PLR is mediated by neurons that sum up over the whole stimulus area. In addition to local contrast changes, the random changes in the mean luminance of the whole test stimulus should mask the response of neurons summing up over the stimulus area and therefore the response obtained for a given stimulus should be smaller with  $RLM_s$  and  $RLM_t$  than with  $RLM_s$  alone.

#### Experimental procedure

The same stimulus configuration was used as shown in Fig 3.1, with stimulus contrast of 30%.  $RLM_s$  was kept constant at  $\pm 35\%$ , which from section 3.2 gives maximum reduction of amplitude for this stimulus, and the PLR was measured for different  $RLM_t$  contrasts. Each condition was presented 64 times, and traces for the right and left eyes were averaged. For subject GY, the stimulus was presented with and without  $RLM_s=25\%$  and  $RLM_t=45\%$  in the blind and sighted hemifields.

#### Results

The responses measured for subject JB are shown in Figure 3.5 and the amplitudes plotted in Figure 3.6. The response is almost completely eliminated for  $RLM_t$  contrasts of  $\pm 35\%$  and above.

Figure 3.7 is a summary of the pupil traces obtained for JB with no RLM, RLM<sub>s</sub> only and with both types of masking; Figure 3.8 and 3.9 show the corresponding results obtained for subject GY in the blind and sighted hemifields.

## Conclusions

The results show that the addition of random luminance masking over the whole stimulus eliminates the pupil light reflex completely. This observation supports the idea that this reflex response has at least two components. One component can be removed by local contrast masking, but it takes large area light flux masking to remove the remaining response.

For the subject GY, pupil responses to stimuli presented in the blind field are small compared with responses to stimuli presented in the <sup>Sighted</sup>Blind field, but the local contrast masking does not appear to reduce the amplitude of response further (section 3.2). The results for stimuli presented in the sighted hemifield are similar to those of the normal subject. Using both types of RLM eliminates the response in the blind as in the sighted fields (Figures 3.8 and 3.9). This suggests that while the component affected by the RLM<sub>s</sub> is absent in GY, his PLR is eliminated by large area contrast masking as in a normal, and therefore involves summation over the stimulus area. It may be that the first component involves neurons affected by the loss of V1, while the rest of the response is mediated similarly to that of a normal subject, probably through the classical subcortical pathways.

## 3.4 Repeatability of readings

### Introduction

For the initial experiments described in sections 3.2 and 3.3, each trial run consisted of repeated presentations of the same stimulus with or without RLM. These two conditions were randomly interleaved. To change the experimental conditions (for example, to change the contrast of the stimulus or the RLM) it was necessary to stop and input the new conditions required, before commencing the next run. Usually, a series of conditions was presented consecutively. It was possible that the responses might change between runs, for example, the response amplitudes might decrease

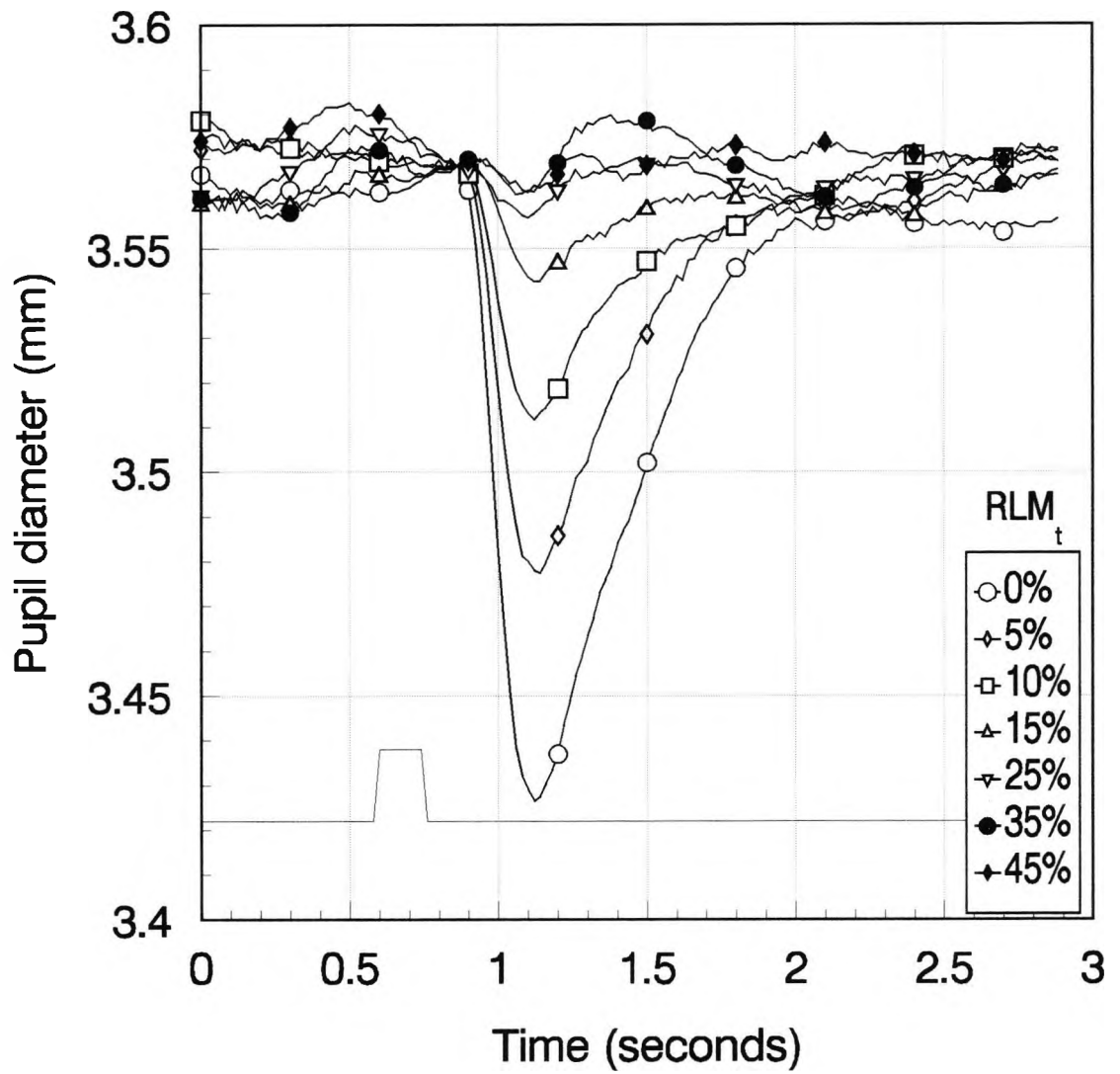


Figure 3.5 Pupil responses measured using different  $RLM_t$  contrasts for subject JB. Stimulus configuration as shown in Figure 3.1, with  $RLM_s=35\%$  and stimulus contrast=30%

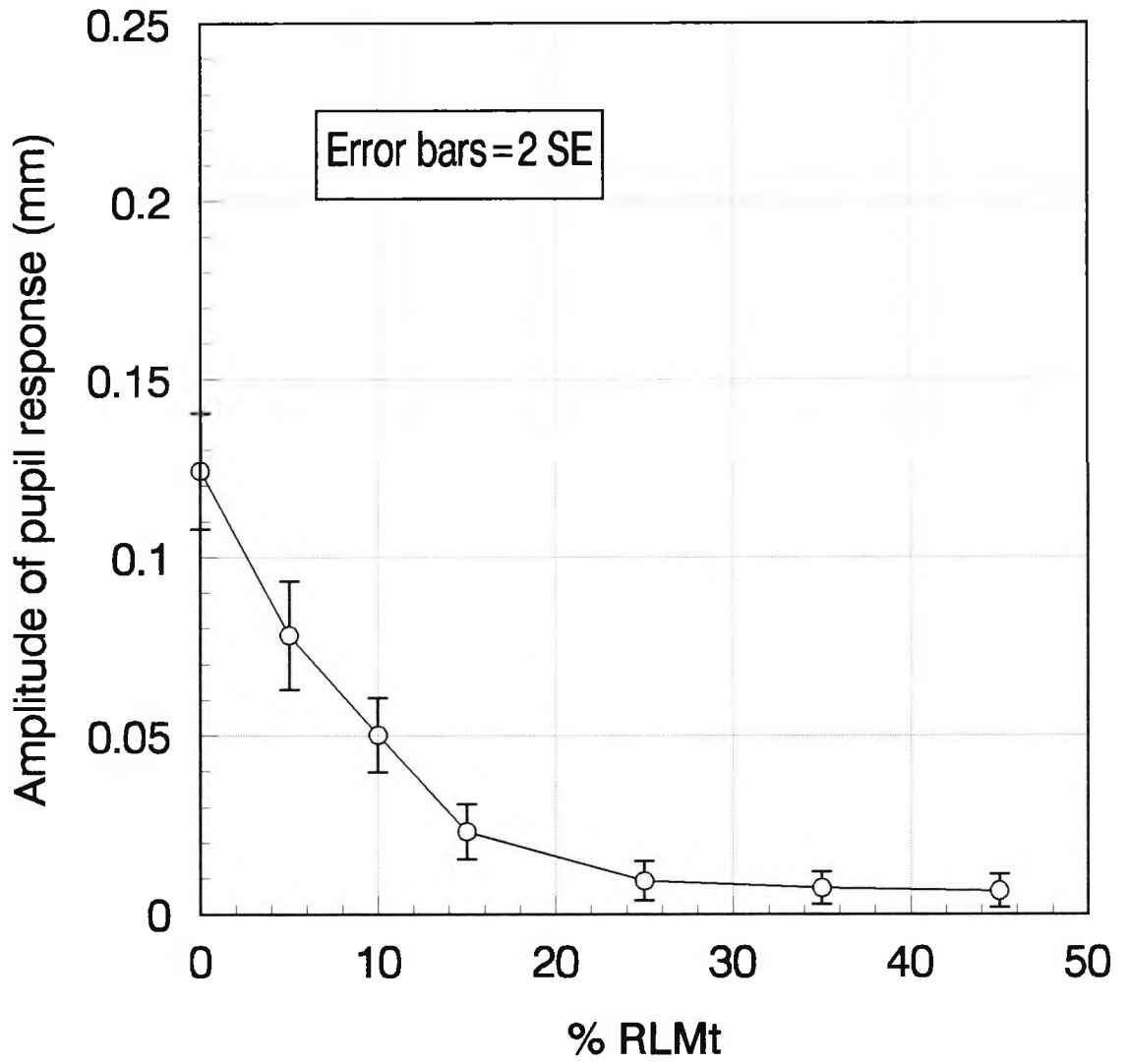


Figure 3.6 Effect of increasing  $RLM_t$  contrast on pupil response amplitude, subject JB. Measurements were taken from the traces shown in Figure 3.5, stimulus configuration as shown in Figure 3.1, with  $RLM_s=35\%$  and stimulus contrast=30%

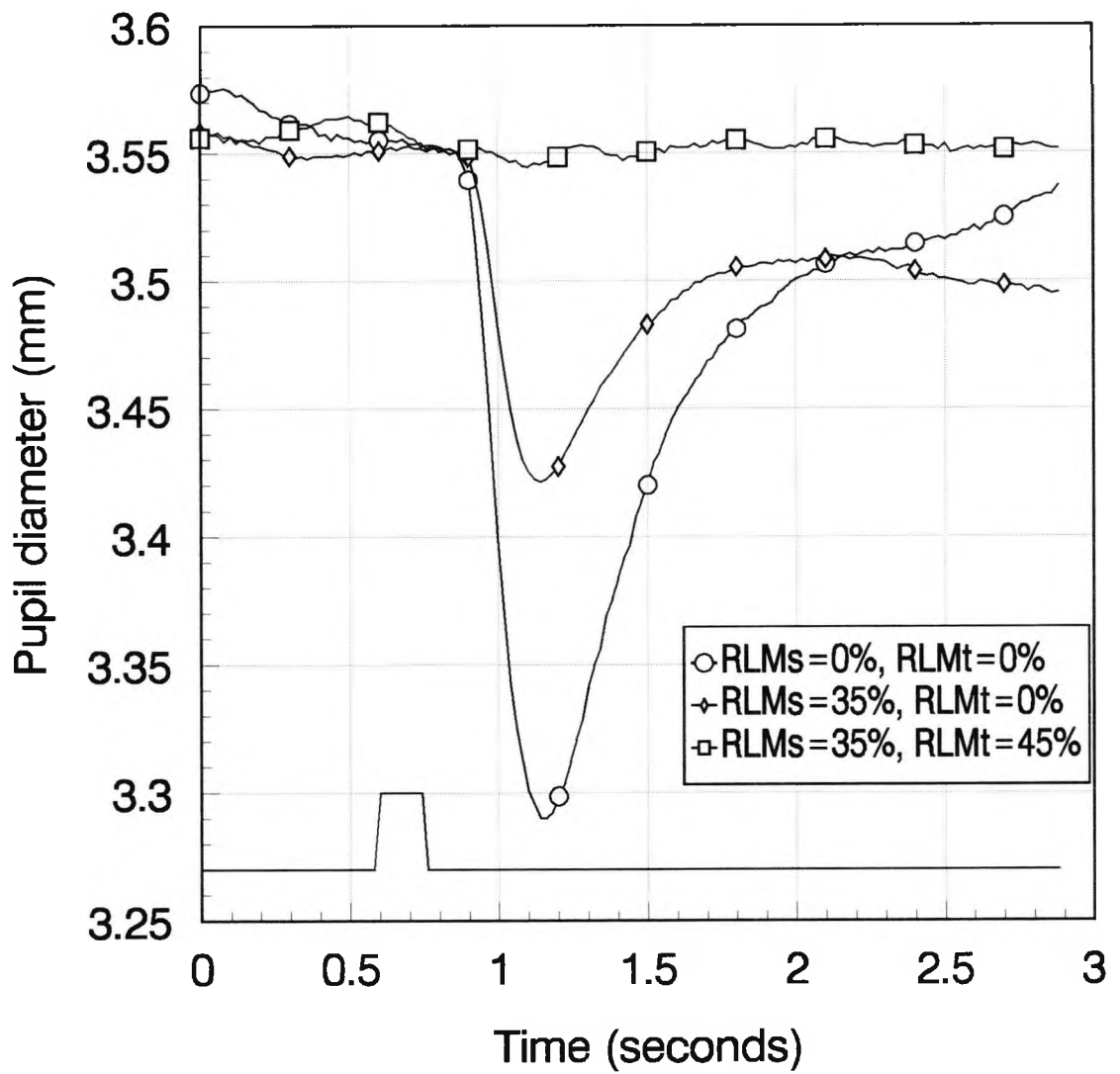


Figure 3.7 Summary of the pupil traces obtained for subject JB with no RLM, RLM<sub>s</sub> only and with both types of masking; Stimulus configuration was as shown in Figure 3.1 with stimulus contrast of 30%

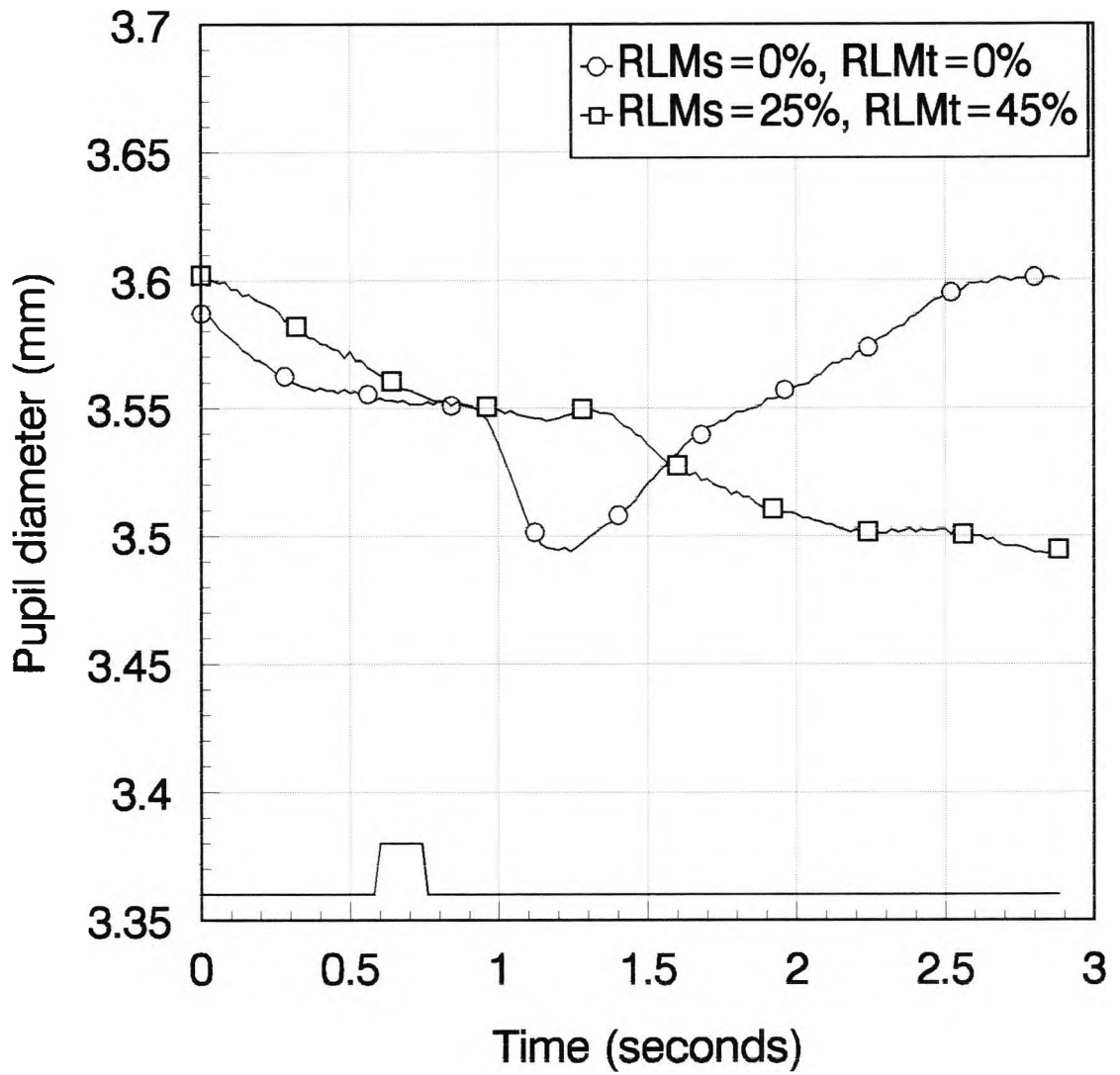


Figure 3.8 Pupil responses measured for GY's blind hemifield with no masking, and with both  $RLM_s$  and  $RLM_t$ . Stimulus configuration as shown in Figure 3.1, with stimulus contrast=30%

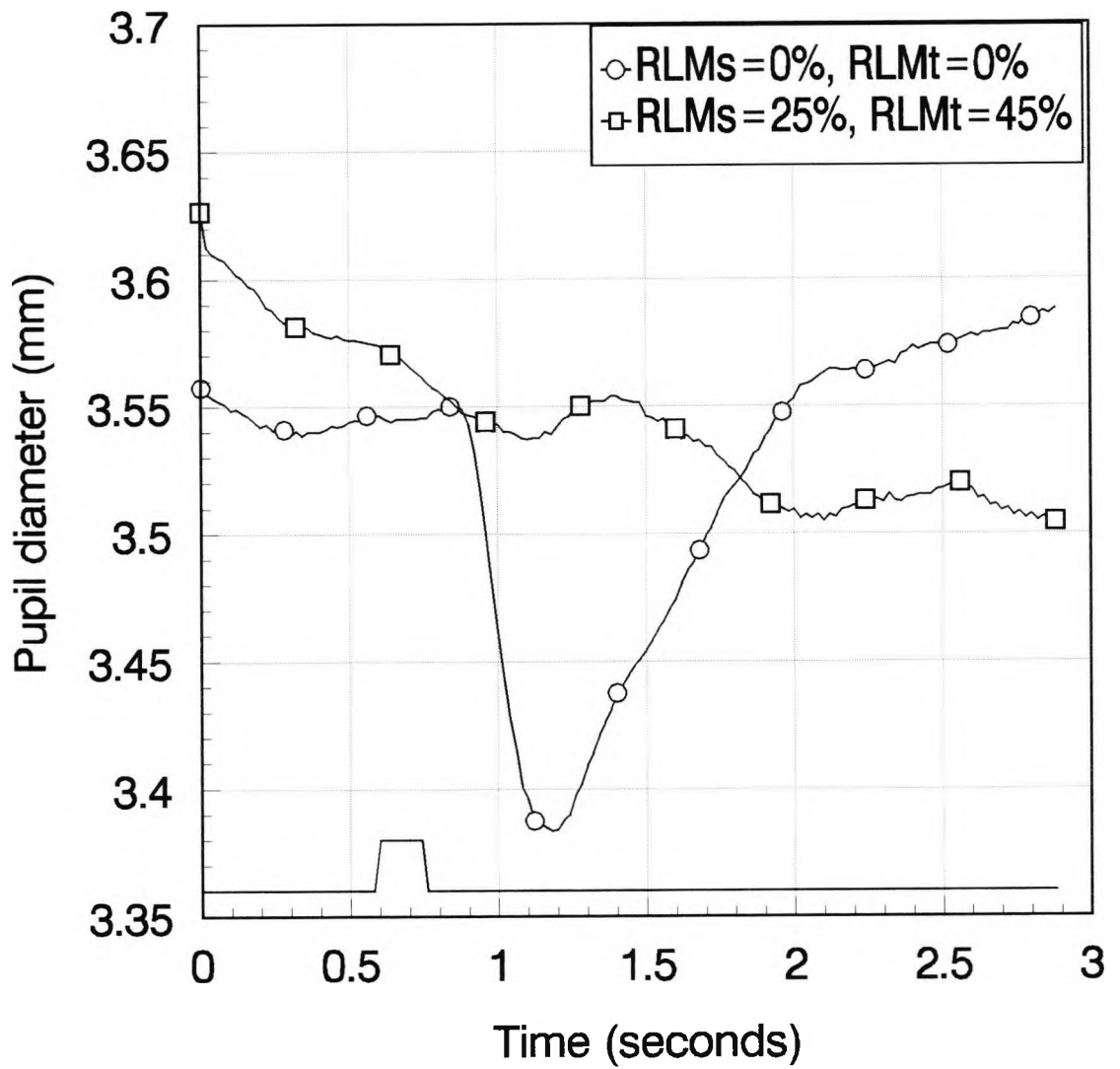


Figure 3.9 Pupil responses measured for GY's sighted hemifield with no masking, and with both  $RLM_s$  and  $RLM_t$ . Stimulus configuration a mirror image of that shown in Figure 3.1, with stimulus contrast=30%

throughout an experimental session due to subject fatigue. To prevent any trends in amplitude being mistaken for a true effect, the conditions were not usually presented in a consecutive order, for example, in order of increasing RLM contrast. To check between-run reliability for subjects JB and GY, the following experiment was conducted.

#### Experimental procedure

The stimulus configuration was as shown in Figure 3.1a. The background luminance was  $24 \text{ cd/m}^2$ , and the stimulus contrast was 60%. For subject JB the stimulus was presented with and without  $\text{RLM}_s$  of 60%. Each trial run consisted of 32 presentations, and 6 consecutive identical trial runs were carried out. Viewing and recording were binocular and the traces from the right and left eyes were averaged.

An experiment to assess variability was also carried out on subject GY. The test involved the use of identical stimulus conditions in consecutive runs, and these were selected in order to assess the repeatability of results in this subject. The experimental conditions were the same as those for JB above, but in this case only the "without  $\text{RLM}_s$ " condition was repeated in consecutive runs. The stimulus was presented in the sighted and blind hemifields (4 and 3 identical runs respectively) and the results were analysed separately for these two conditions.

#### Results

The response amplitudes and variances associated with each condition for JB are listed in Table 3.1. One-way analysis of variance has been used to examine whether there is a significant difference between individual runs for the two conditions with and without  $\text{RLM}_s$ , and the statistical findings are presented in Table 3.2. The null hypothesis states that there is no difference between the mean amplitudes obtained in each run for the same experimental conditions. The amplitude obtained for each run is a mean of 32 traces, and the variance associated with each amplitude is given by the analysis programme, 'pview'. The mean and standard deviation for the 6 runs have been calculated. For the two conditions (that is, without and with  $\text{RLM}_s$ )  $F_{\text{obt}} < F_{\text{crit}} (\alpha=0.05)$  so the null hypothesis is retained.

The analysis of GY's results (shown in Tables 3.3 and 3.4) also show that the null hypothesis is retained.

### Conclusions

As the null hypothesis was retained for the conditions with and without RLM<sub>s</sub>, it can be concluded that there was no significant difference between the consecutive runs for both conditions. Similarly, for GY there is no significant difference between the consecutive runs when the stimulus is presented in the sighted and blind hemifields.

In later experiments, the software was changed so that it was possible to interleave several different stimulus conditions in the same run, for example, different stimulus and RLM contrasts or stimulus area or position could all be interleaved. This has the advantage that any external factors influencing the results over time should affect all the different stimuli equally. This was available when testing was carried out on other normal subjects (Shaila Chaudry, unpublished data). However the results presented in this section show that even when interleaving several different stimulus conditions was not possible, reliable results were obtained from these subjects on consecutive runs.

### 3.5 Further investigation of the effects of RLM<sub>s</sub> on the pupil light reflex

#### Introduction

Following the results of the experiments described in section 3.2 and 3.3, it was decided to investigate more thoroughly the effect of RLM<sub>s</sub> contrast on the PLR when different stimulus contrasts were employed.

#### Experimental procedure

For subject JB a hemianular stimulus was used as shown in Figure 3.10. This type of stimulus configuration was also used in the investigation of effect of stimulus area (see section 3.7). When RLM<sub>s</sub> was used, the check size was 0.33° x 0.33° and a border of approximately 1 check was surrounded the stimulus. The luminances of the checks varied every 83 ms (every 5 frames). The viewing distance was 700 mm. The background luminance of the screen was 24 cd/m<sup>2</sup>, with CIE (x,y) chromaticity co-ordinates of (0.305, 0.323). A range of RLM<sub>s</sub> contrasts (from 0% to 75%) was

Run	Amplitude without RLM <sub>s</sub> (mm)	Variance without RLM <sub>s</sub>	Amplitude with RLM <sub>s</sub> (mm)	Variance with RLM <sub>s</sub>
1	0.3126	0.006923	0.1679	0.001765
2	0.3062	0.003144	0.1857	0.002267
3	0.2865	0.003762	0.1811	0.001897
4	0.2938	0.004214	0.1885	0.001809
5	0.2953	0.00433	0.168	0.003218
6	0.2872	0.006501	0.1835	0.003191
Mean	0.2969		0.1791	
Std dev	0.0105		0.00899	

Table 3.1. Summary of amplitudes and variances measured for 6 identical consecutive runs, subject JB. See text for experimental conditions.

Without RLM<sub>s</sub>:

Source	Degrees of freedom	s <sup>2</sup>	F <sub>obt</sub>
Between runs	5	3.50336 x 10 <sup>-3</sup>	0.728*
Within runs	26	4.812333 x 10 <sup>-3</sup>	

\*with  $\alpha=0.05$ , F<sub>crit</sub>=2.98.

With RLM<sub>s</sub>:

Source	Degrees of freedom	s <sup>2</sup>	F <sub>obt</sub>
Between runs	5	2.585152 x 10 <sup>-3</sup>	1.096*
Within runs	26	2.357833 x 10 <sup>-3</sup>	

\*with  $\alpha=0.05$ , F<sub>crit</sub>=2.98.

Table 3.2. The results shown in Table 3.1 were subjected to one-way analysis of variance in order to discover whether there is a significant difference between the means of each run (each of which is a mean of 32 traces). The null hypothesis states that there is no difference between the mean amplitudes obtained in each run for the same experimental conditions. In each case, F<sub>obt</sub> < F<sub>crit</sub>, so the null hypothesis is retained.

Run	Sighted hemifield		Blind hemifield	
	Amplitude (mm)	Variance	Amplitude (mm)	Variance
1	0.3586	0.0133	0.2178	0.01187
2	0.3526	0.01315	0.2262	0.009809
3	0.2964	0.007308	0.1714	0.007788
4	0.339	0.01399		
Mean	0.3367		0.2051	
	0.0281		0.0295	

Table 3.3. Summary of amplitudes and variances measured for identical consecutive runs in GY's sighted and blind hemifields. See text for experimental conditions.

Sighted hemifield:

Source	Degrees of freedom	$s^2$	$F_{obt}$
Between runs	3	0.025193	2.1105*
Within runs	28	0.011937	

\*with  $\alpha=0.05$ ,  $F_{crit}=2.95$ .

Blind hemifield:

Source	Degrees of freedom	$s^2$	$F_{obt}$
Between runs	2	0.027875	2.838*
Within runs	29	0.009822	

\*with  $\alpha=0.05$ ,  $F_{crit}=3.33$ .

Table 3.4. The results shown in Table 3.3 were subjected to one-way analysis of variance in order to discover whether there is a significant difference between the means of each run (each of which is a mean of 32 traces). The null hypothesis states that there is no difference between the mean amplitudes obtained in each run for the same experimental conditions. In each case,  $F_{obt} < F_{crit}$  so the null hypothesis is retained.

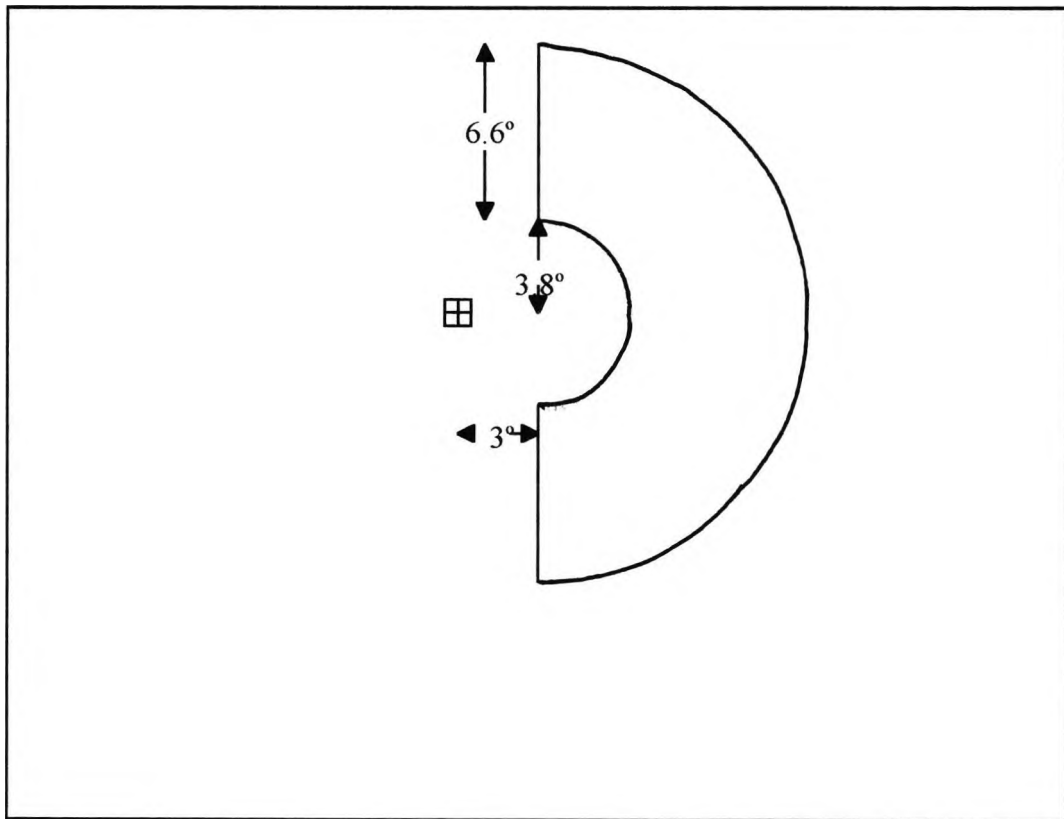


Figure 3.10. Stimulus configuration for subject JB, for further investigation of effect of  $RLM_s$  contrast. For full details, see text.

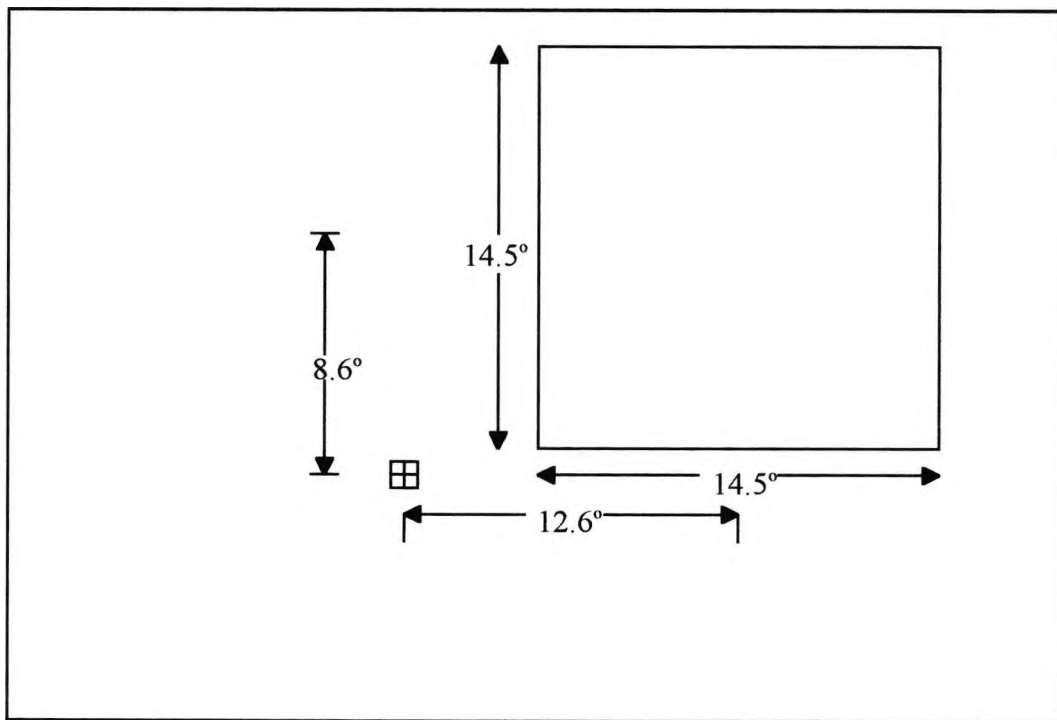


Figure 3.11. Stimulus configuration for subject GY, for further investigation of effect of  $RLM_s$  contrast. For full details, see text.

used in combination with stimulus contrast of 15%, 20%, 30%, 45% and 60%, and the stimulus duration was 172 ms. The response to a stimulus contrast of 120% with  $RLM_s$  of 0% was later measured. Each stimulus condition was presented 36 times, the average trace for each eye was calculated, and these were then also averaged.

For subject GY the stimulus configuration shown in Figure 3.11 was used for presentation in the blind hemifield, and a mirror image with respect to the vertical meridian was used for presentation in the sighted field. The  $RLM_s$  check size was  $0.9^\circ$ , and the stimulus size was  $14.5^\circ \times 14.5^\circ$  positioned so that its centre was  $15.3^\circ$  from the fixation point. A range of  $RLM_s$  contrasts (from 0% to 75%) was used with stimulus contrasts of 20%, 40%, 80% and 137% and stimulus duration was 246 ms. Again the mean of 36 presentations was found, and the results for the right and left eyes averaged together.

## Results

The results for JB are shown in Figure 3.12. It can be seen that for a stimulus contrast of 15% the  $RLM_s$  does in fact eliminate the response almost entirely. However, for greater stimulus contrasts, results similar to those described in section 3.2 are seen, namely that increasing the  $RLM_s$  amplitude reduces but does not entirely eliminate the PLR.

Similar results are seen for GY's sighted field, as shown in Figure 3.13. When the stimuli are presented in his blind field, the responses are usually smaller than for the corresponding stimulus in the sighted field, and the  $RLM_s$  does not reduce the PLR amplitude as in the sighted field. Very little response is measured for a stimulus contrast of 20% presented in the blind field.

## Conclusions

The hypothesis put forward in Section 3.2 was that the pupil light reflex may consist of two or more components, one of which can be eliminated by  $RLM_s$ . The results for subject JB shown in Figure 3.12 support this idea as the PLR amplitude is reduced as  $RLM_s$  contrast is increased. For low contrast stimuli, the  $RLM_s$  appears to eliminate the

response entirely, suggesting that the main component involved in mediating PLRs for low contrast stimuli is the one eliminated by the RLM<sub>s</sub>.

It has been suggested from the initial results (section 3.2) that GY may not have the component that is eliminated by the RLM<sub>s</sub> on his affected side. If this component dominates the response to low contrast stimuli, GY should show little or no response to these stimuli presented in his blind field. Figure 3.13 shows that this is the case for a stimulus contrast of 20%. For high contrast stimuli a significant response is measured in the blind field, which can approach the amplitude measured when the corresponding stimulus is presented in the sighted field. This suggests that the contribution of the component eliminated by the RLM<sub>s</sub> becomes proportionately less as stimulus contrast is increased. This is consistent with rapid saturation of the low contrast component above a given contrast level. Stimulus contrast and the two components of the PLR will be considered further in the next section.

### 3.6 The effect of stimulus contrast on the pupil light reflex

#### Introduction

The effect of stimulus contrast on response amplitude when no RLM<sub>s</sub> is present is shown in Figures 3.14 and 3.15 (subjects JB and GY), which are plotted from data taken from Figures 3.12 and 3.13 respectively. The point (0,0) has been included in each case, based on the assumption that in the absence of a stimulus the pupil response is zero. Figure 3.14 also includes the amplitude measured for subject JB for stimulus contrast of 120%.

Figure 3.14 shows that, for subject JB, the data points appear to fall on two straight lines of differing slopes. This suggests the possibility of two mechanisms with different contrast gains; one mechanism effective at low contrasts with a high contrast gain, and a second with a lower contrast gain that covers a larger change in light level. Similar contrast gain characteristics have been described by Kaplan and Shapley (1986) for M and P retinal cells.

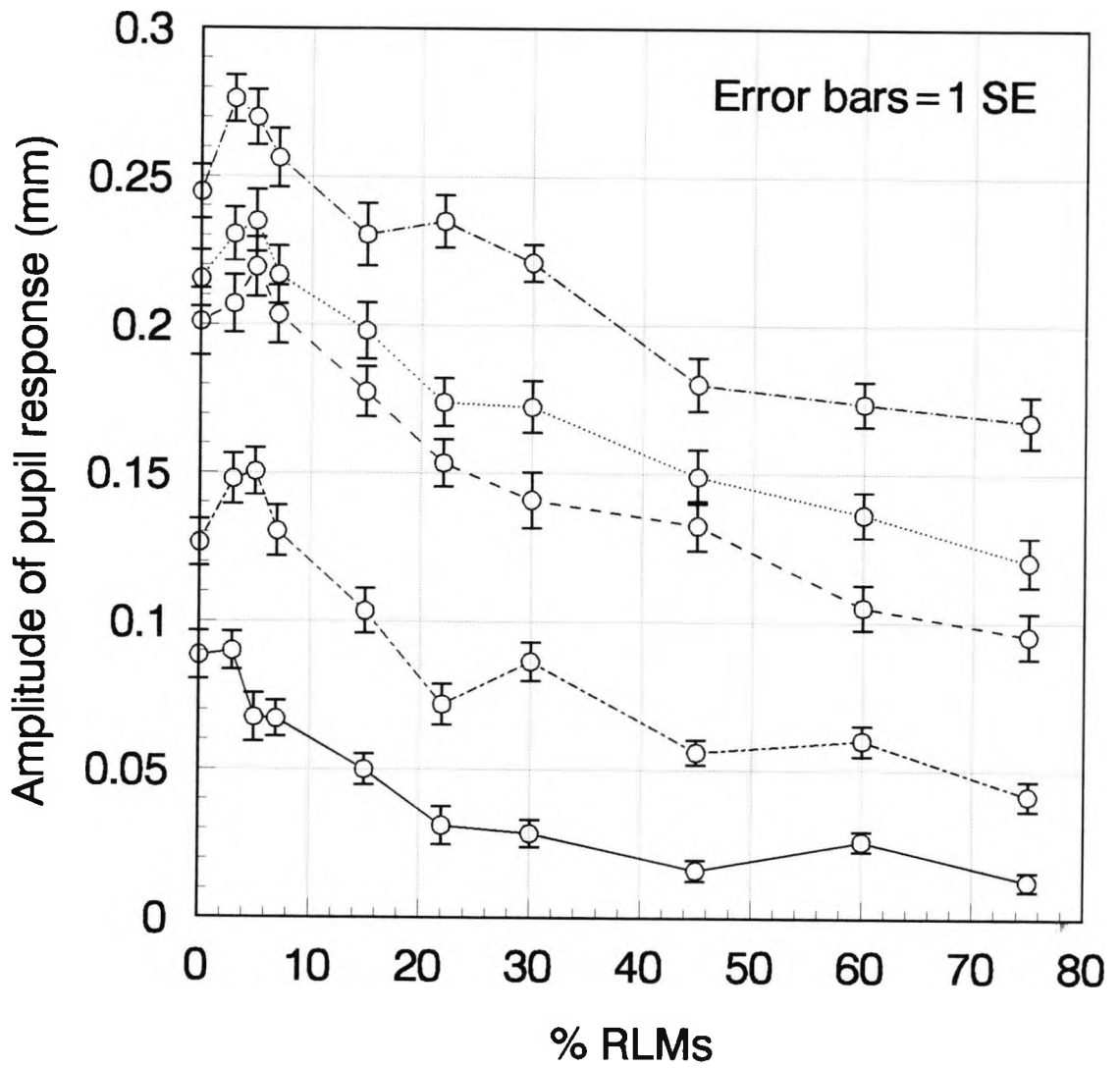
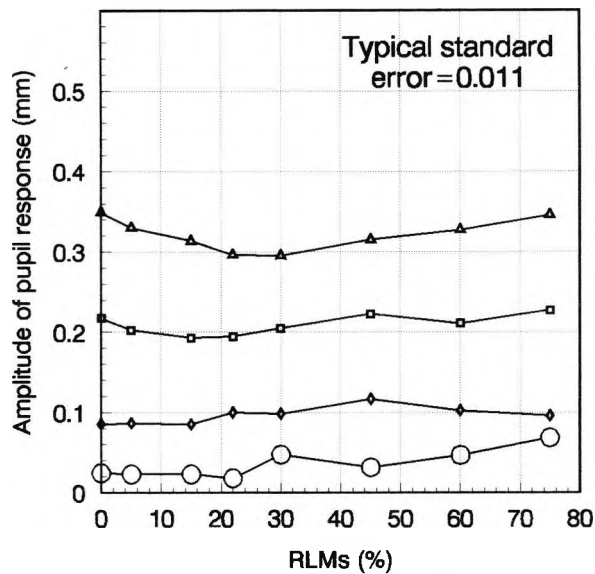
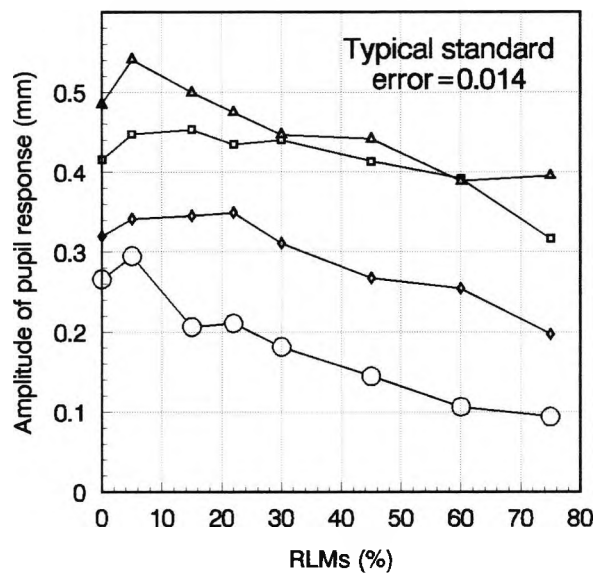
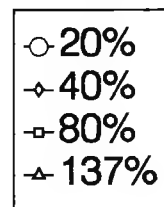


Figure 3.12. Effect of RLM<sub>s</sub> contrast on pupil response amplitudes for stimuli of different contrasts, subject JB. Stimulus configuration as shown in Figure 3.10. Stimulus contrasts, from bottom trace to top trace: 15% (solid line), 20% (short and long dashes), 30% (dashed line), 45% (dotted line) and 60% (dots and dashes)



**A. Blind hemifield**

**Stimulus contrast**



**B. Sighted hemifield**

Figure 3.13. Effect of  $RLM_s$  contrast on pupil response amplitudes for stimuli of different contrasts, subject GY. Stimulus configuration as shown in Figure 3.11. Stimulus contrasts 20%, 40% 80% and 137% as indicated in the legend. A) Blind hemifield B) Sighted hemifield

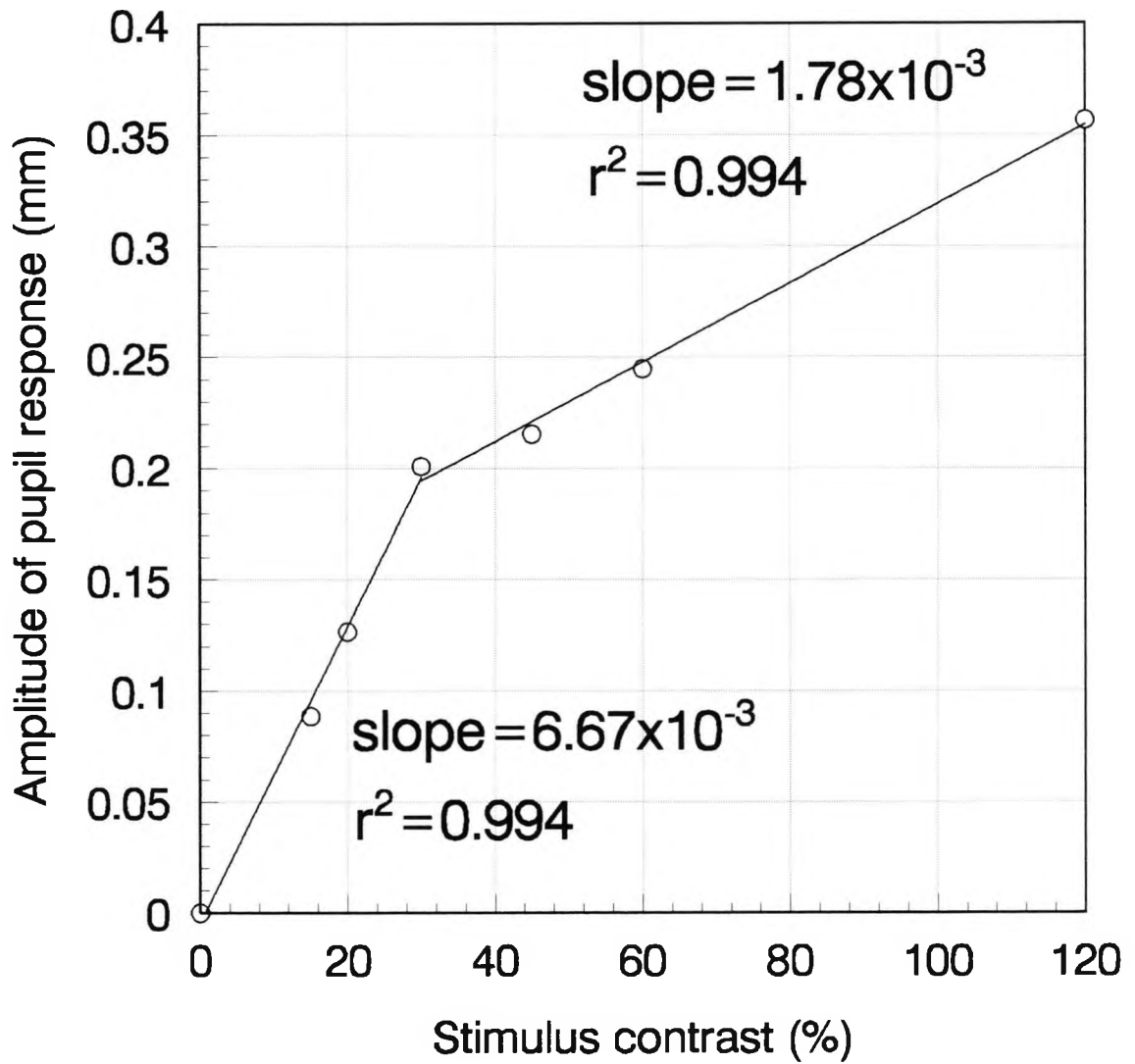


Figure 3.14 Pupil response amplitude as a function of stimulus contrast with no  $RLM_s$ , subject JB. Measurements taken from Figure 3.12, stimulus configuration as shown in Figure 3.10. The data points appear to lie on two straight lines, for which the slopes and  $r^2$  values have been calculated

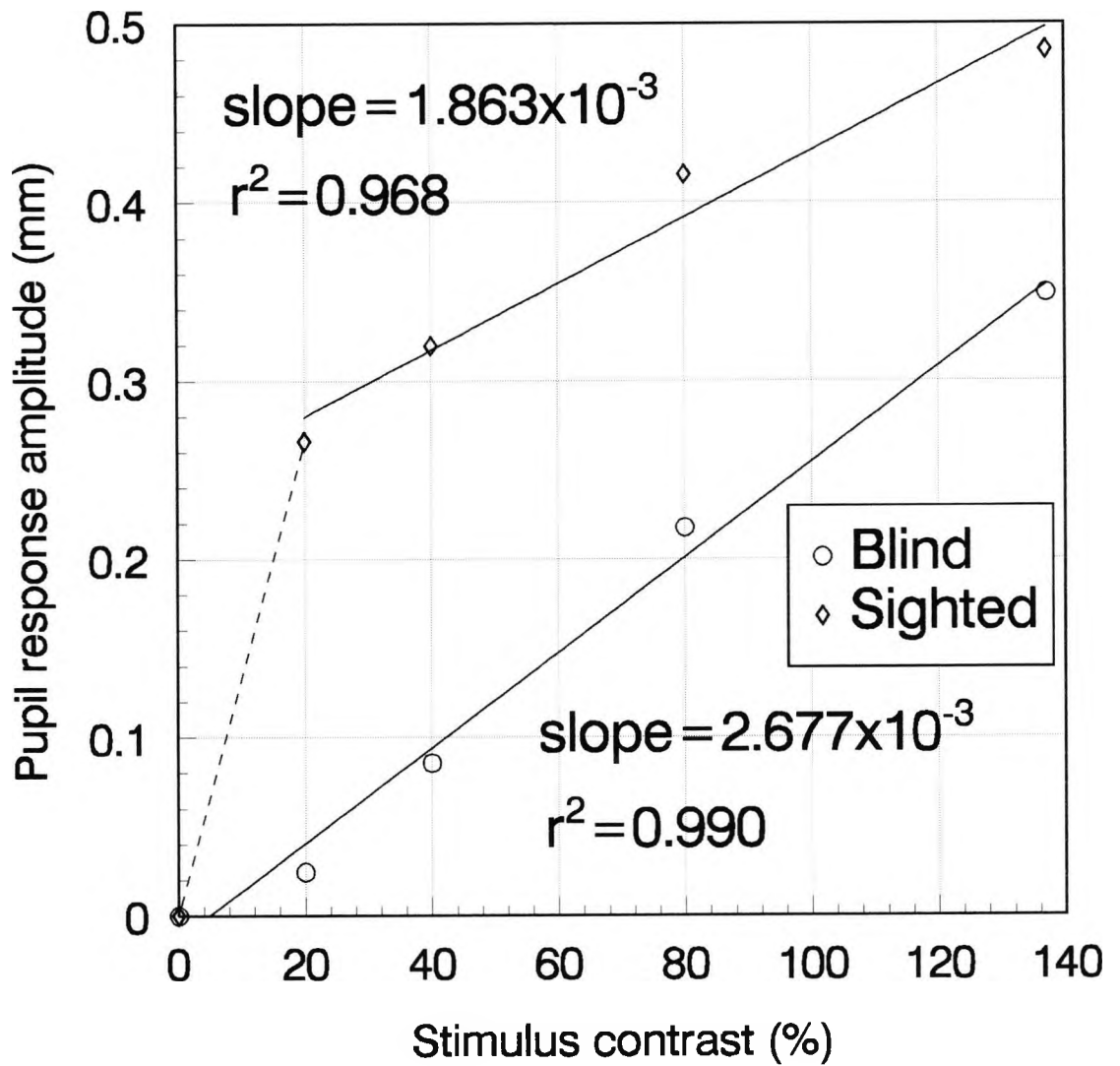


Figure 3.15 Pupil response amplitude as a function of stimulus contrast with no  $RLM_s$ , subject GY, blind and sighted hemifields. Measurements taken from Figure 3.13, stimulus configuration as shown in Figure 3.11. For the sighted field the data points appear to lie on two straight lines, for which the slopes and  $r^2$  values have been calculated. For the blind field, the data points are best fitted by a single regression line

Figure 3.15 shows similar results for GY's sighted field, but for the blind field the data points are best fitted by a single regression line, which has a shallow slope of similar magnitude to the second 'low contrast gain' component described in his sighted field and for JB. The component missing in GY could thus be the 'high contrast gain' component, which is eliminated by the RLM<sub>s</sub>, leaving him with only the 'low contrast gain' mechanism to mediate PLRs.

Experiments were carried out to measure the responses to different stimulus contrasts in the blind and sighted fields of GY and a subject with damage to the left optic radiations and a right homonymous field defect, FS. This subject has been investigated by Stoerig, (see Stoerig and Cowey (1989a) for a visual field plot (their subject F)). If little or no response is measured with low contrast stimuli in the affected fields, it would be consistent with the idea that these patients only have a low contrast gain mechanism, as this would not give large responses to low contrast stimuli. If the responses in the blind and sighted fields become more similar as stimulus contrast increases, such an observation would suggest that the high contrast gain component present in the sighted field saturates, and that the low contrast gain component (presumed to be unaffected in these patients) becomes dominant.

#### Experimental procedure

For GY, a sector shaped stimulus was used, similar to that shown in Figure 3.10, except that the extent of the sector was 60° above and below the horizontal, giving a total sector extent of 120°. A mirror image was used to present stimuli in the sighted hemifield. Background luminance was 24 cd/m<sup>2</sup>, with CIE (x,y) chromaticity co-ordinates of (0.305, 0.323). Each stimulus was presented 32 times and the results for the right and left eyes were averaged. The stimulus duration was 263 ms.

For FS, a smaller sector of total extent 40° was used, with a sector width of 9.8° positioned so that its inner edge was 2.6° from the fixation point. This stimulus was chosen so that it fell in his field defect. The stimulus duration was 263 ms. Background luminance and chromaticity was the same as for GY. Only the right eye viewed and was measured.

## Results

The results for GY are shown in Figure 3.16, and those for FS in Figure 3.17. It can be seen from Figure 3.16 that there is almost no response to the 15% contrast stimulus in GY's blind hemifield. There is a significant difference between the responses in the blind and sighted fields for contrasts of 15% and 90% ( $p < 0.001$ , two-tailed t-test). However, for contrasts of 180% and 340% the responses in the blind and sighted field are not significantly different ( $p > 0.05$ , two-tailed t-test).

A similar pattern of results can be seen for FS in Figure 3.17. There is a significant difference between the results for blind and sighted fields for contrasts of 30% and 150% ( $p < 0.01$ , two-tailed t-test), but no significant difference at 340% ( $p > 0.05$ , two-tailed t-test).

## Conclusions

The results obtained for both subjects are consistent with the hypothesis that the component that dominates the PLR at low contrasts is missing. For high contrast stimuli they have PLRs similar to normals, which suggests that the component they are missing plays little part in the response to such stimuli.

### 3.7 The effect of stimulus area on the pupil light reflex

#### Introduction

The two component hypothesis has been described above in terms of stimulus contrast. It was of interest to see what effect stimulus area had on these two components. The advantage of a low contrast gain component is continued response over an extended range of light flux changes. If the function of this component is to contribute to the control of pupil size, then large area summation would also be required. If this hypothesis is correct, PLRs measured with RLM<sub>s</sub> should be small for small stimuli and increase with stimulus area as they are dominated by a component which exhibits area summation. If GY only has the lower gain component, he should get little or no response to small stimuli in his blind field, but these responses should increase as the stimulus size increases.

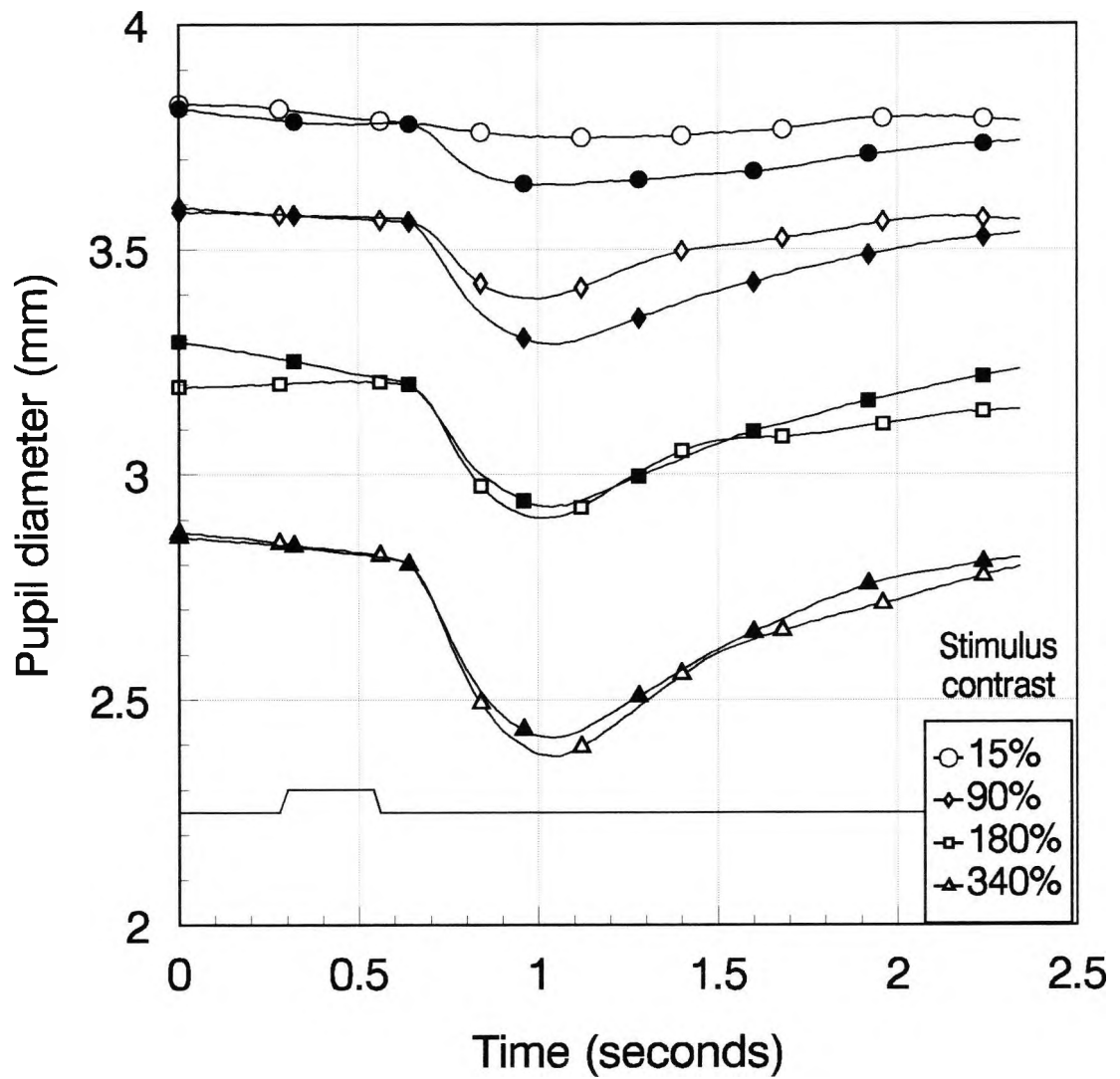


Figure 3.16 Pupil responses to sector stimuli (angular extent 120°) for the blind (open symbols) and sighted (filled symbols) for subject GY. Stimulus contrasts as indicated in the legend

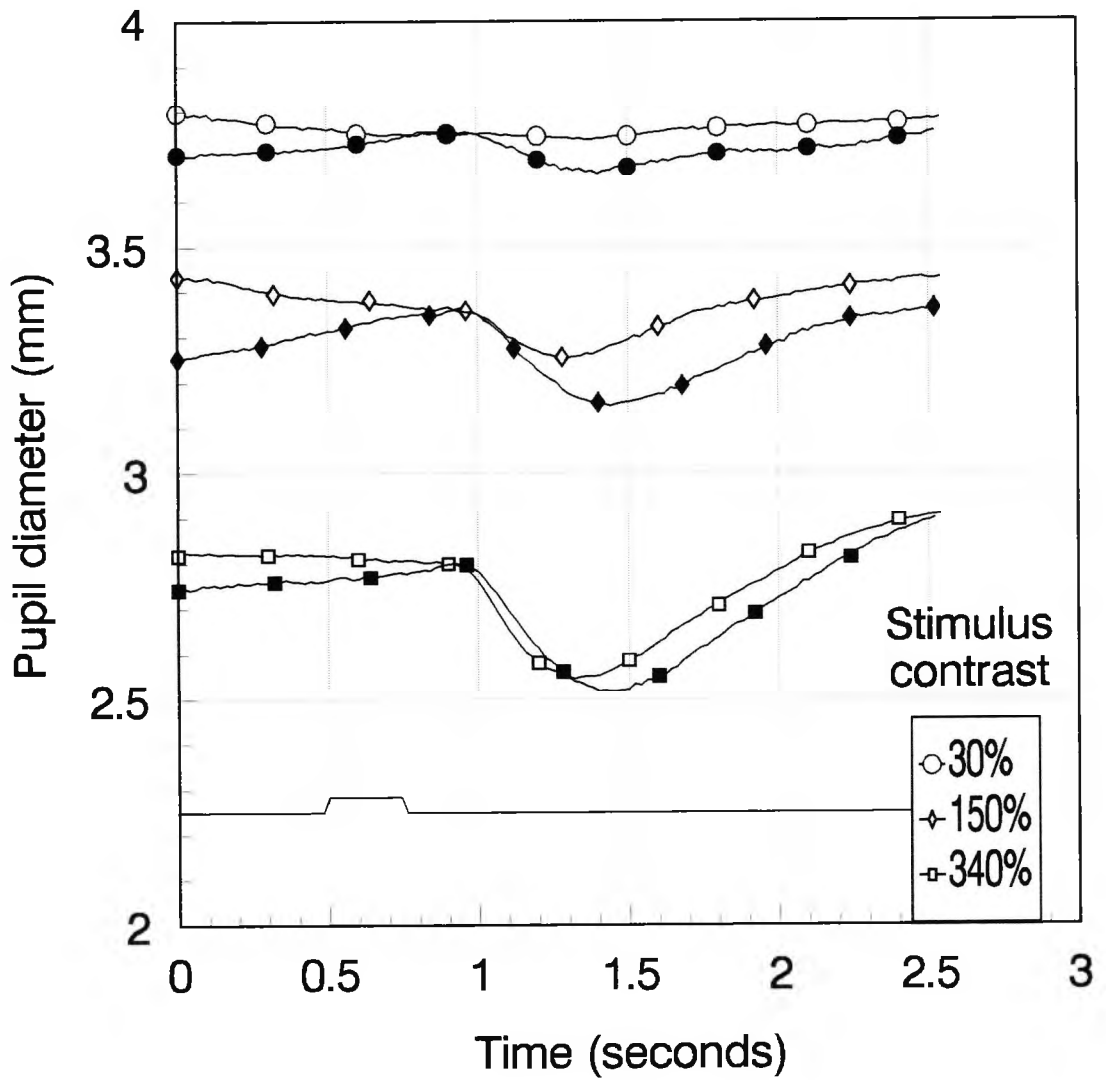


Figure 3.17 Pupil responses to sector stimuli (angular extent  $40^\circ$ ) for the affected (open symbols) and unaffected (filled symbols) areas of visual field for subject FS. Stimulus contrasts as indicated in the legend

## Experimental procedure

An annular stimulus was used to eliminate the effects of any variation with retinal eccentricity. For normal subject JB, the stimuli were portions of an annulus centred on the fixation point, whose inner radius was  $3.7^\circ$  and outer radius was  $10.3^\circ$ . The angular extent varied from  $60^\circ$  to  $360^\circ$  to provide stimuli of different areas. Background luminance was  $24 \text{ cd/m}^2$  and two different stimulus contrasts were used; 30% and 90%. The stimuli were presented for 263 ms with or without  $\text{RLM}_s$  of 75%, with a check size of  $0.3^\circ$ . A high  $\text{RLM}_s$  contrast was chosen in order to achieve maximum elimination of the high contrast gain component. Each stimulus was presented 32 times and the results for the right and left eyes were averaged.

For GY the maximum angular extent of the stimulus was  $180^\circ$  in order to position it within either the blind or sighted hemifields, and the centre of the annulus was set  $4^\circ$  to the right of fixation (blind field) or to the left (sighted field) in order to avoid the preserved macular area. The stimulus contrast was 30%, and was presented without  $\text{RLM}_s$  in the blind and sighted fields. Otherwise all experimental parameters were as for JB.

## Results

The results for JB are shown in Figures 3.18 and 3.19, and Figure 3.20 shows the results for GY.

The amplitudes in Figure 3.18 (stimulus contrast=30%, subject JB) have been measured and plotted against log stimulus area in Figure 3.21. Considering the amplitudes of responses with  $\text{RLM}_s$  (dashed line in Figure 3.21), there is no significant response for the smallest stimulus size ( $p > 0.1$ , one tailed t-test), but for larger stimulus areas there is a significant response ( $p < 0.01$ , one tailed t-test) which increases as the stimulus area increases. This corresponds to the proposed low contrast gain, high spatial summation component only. The difference between responses with and without  $\text{RLM}_s$ , thought to be the high contrast gain component and indicated by a dotted line in Figure 3.21, has a shallower slope than the low gain component when plotted against stimulus area, for this stimulus contrast.

Figure 3.22 shows the amplitudes for JB when the stimulus contrast was 90%. In this case, significant responses are seen with  $RLM_s$  for all stimulus areas ( $p < 0.01$ , one tailed t-test). The responses with  $RLM_s$  (dashed line) show a clear increase with stimulus area, while difference between with and without  $RLM_s$  (dotted line) increases very little with stimulus area.

The amplitudes measured for GY shown in Figure 3.20 are plotted in Figure 3.23. The data are not as clear as for JB, but response amplitudes appear to increase for both blind and sighted fields increases as stimulus area increases (solid and dashed lines). However, unlike the results for JB, no statistically significant correlation is seen between the amplitude of response and log stimulus area for the number of points obtained.

### Conclusions

The results for JB are consistent with the idea proposed above that the low contrast gain component (measured with  $RLM_s$ ) shows spatial summation, while the high contrast gain component (the difference between responses without and with  $RLM_s$ ) shows spatial summation, but with a smaller gain per log unit area. The results obtained for GY are less clear. The response amplitudes appear to increase with stimulus area for both the blind and sighted fields with a slightly greater slope for the sighted field. This is not inconsistent with the hypothesis that only the low contrast gain component is functioning for GY's blind field, while both components are contributing to the response for his sighted field. However, this experiment should be repeated for GY, preferably with more data points, before any firm conclusions can be drawn.

The results for JB described in this section support the idea of two components of the PLR. This will be summarised and discussed further in the next section.

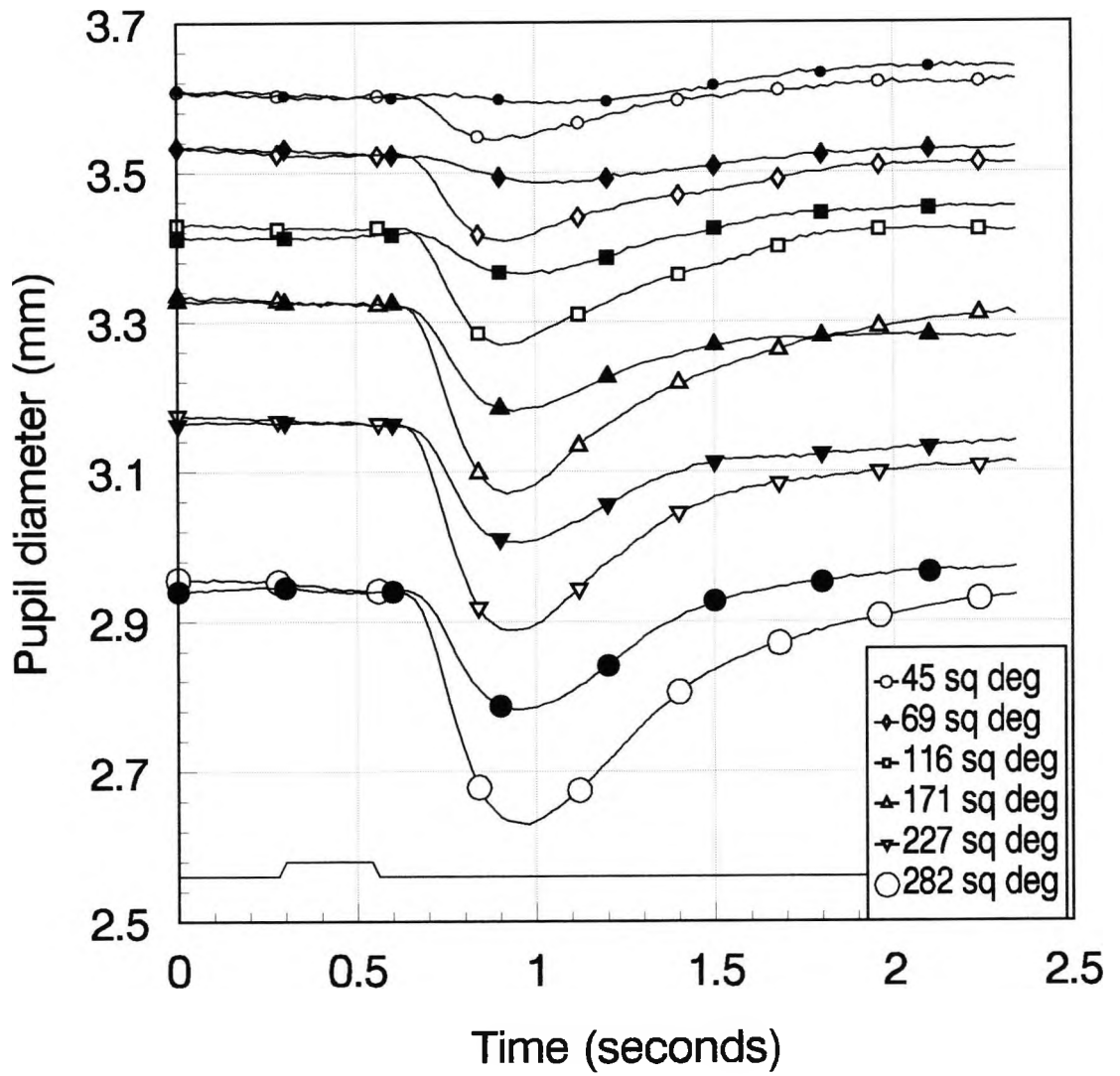


Figure 3.18 Pupil responses for sector stimuli of varying angular extent for subject JB. Stimulus contrast was 30%, and responses are shown with no RLM<sub>s</sub> (open symbols) and with RLM<sub>s</sub>=75% (filled symbols)

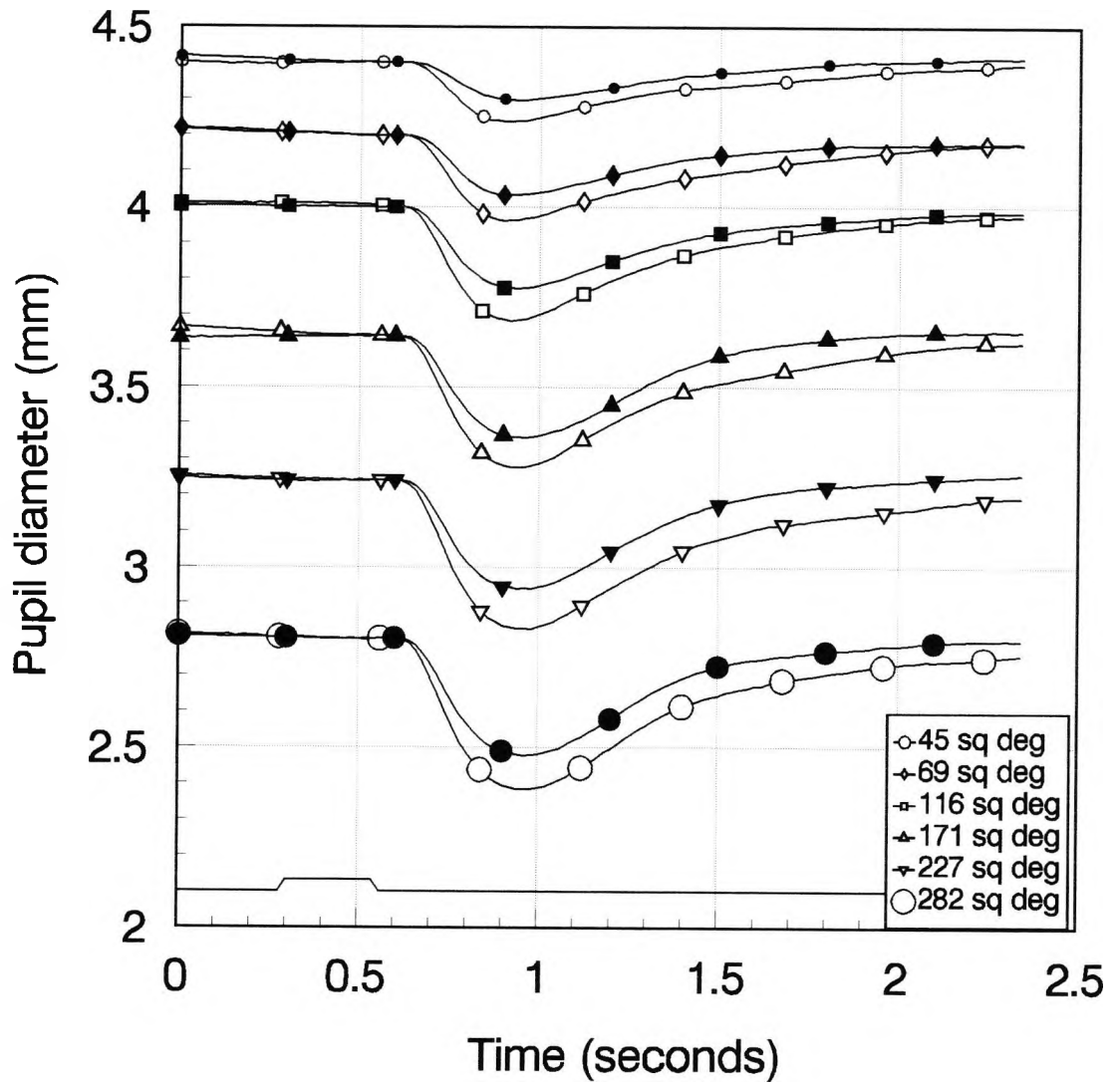


Figure 3.19 Pupil responses for sector stimuli of varying angular extent for subject JB. Stimulus contrast was 90%, and responses are shown with no RLM<sub>s</sub> (open symbols) and with RLM<sub>s</sub>=75% (filled symbols)

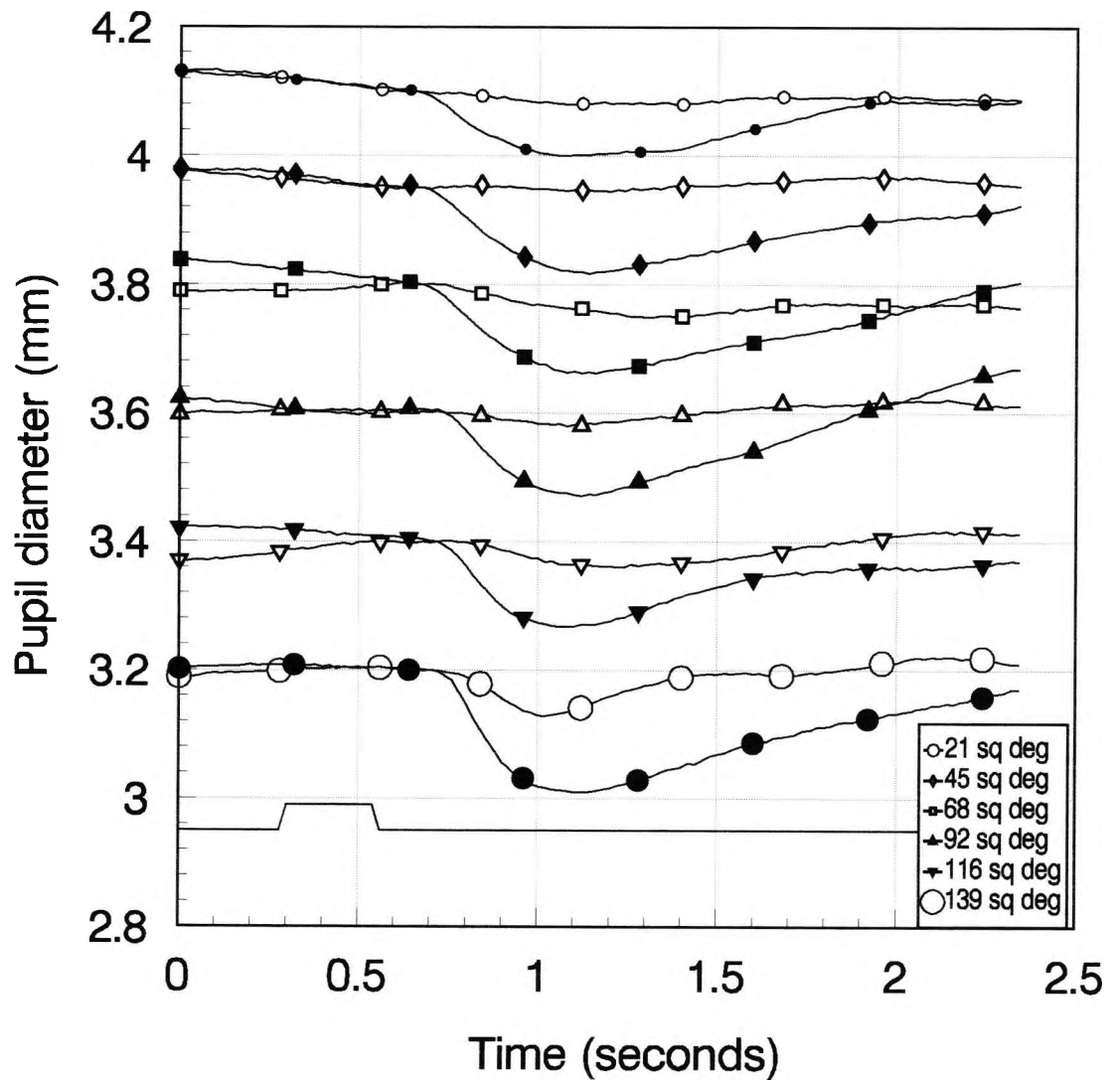


Figure 3.20 Pupil responses for sector stimuli of varying angular extent for subject GY. Stimulus contrast was 30%, and responses are shown for the blind (open symbols) and sighted (filled symbols) hemifields

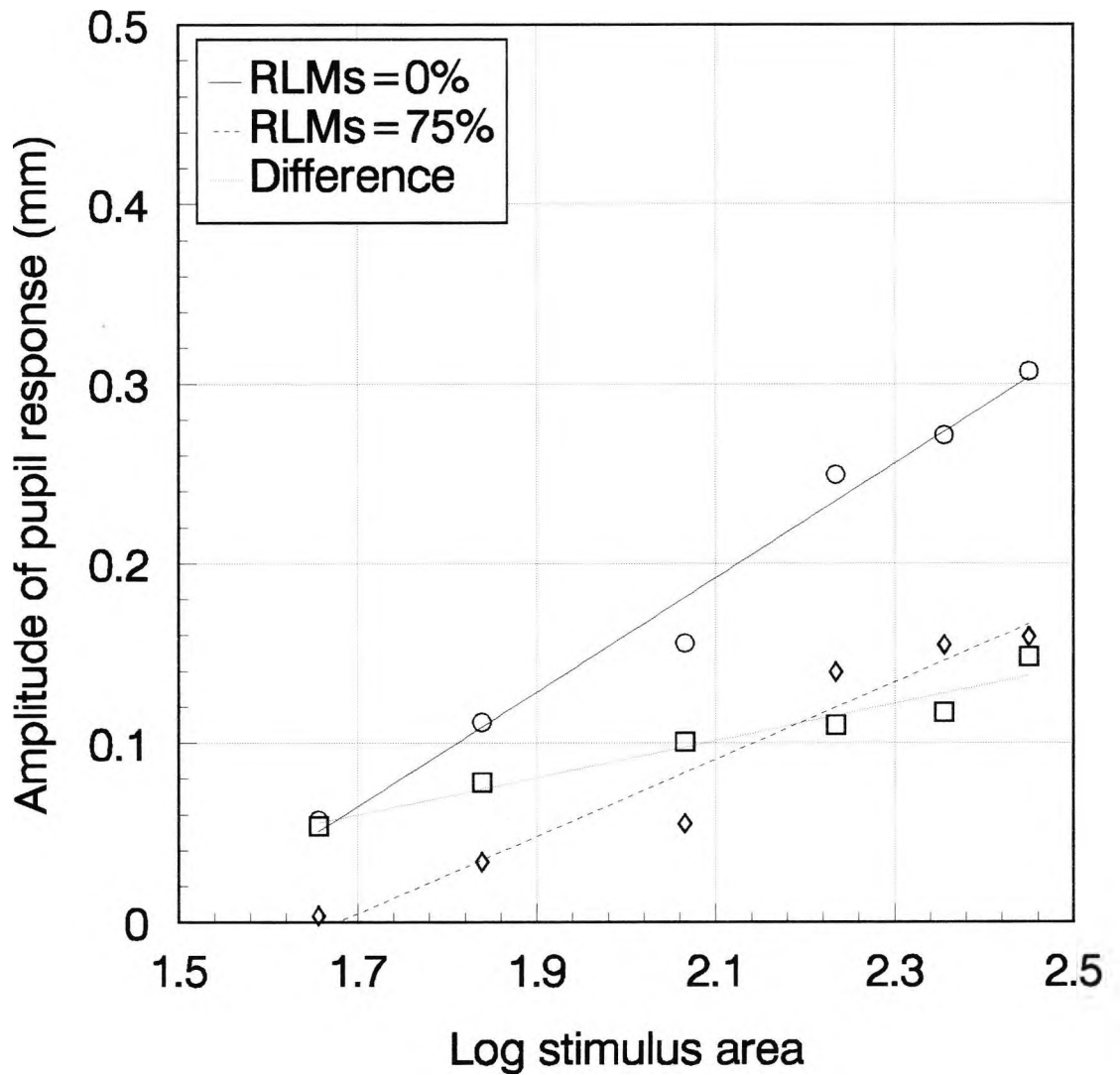


Figure 3.21 Pupil response amplitude as a function of log stimulus area for subject JB, contrast=30%. Measurements taken from Figure 3.18. The dashed line indicates the regression line fitted to the data points (diamonds) when  $RLM_s$  of 75% was used ( $r^2=0.91$ ,  $p<0.01$ ). This line may indicate the proposed low contrast gain, high spatial summation component of the pupil response. The dotted line and square symbols ( $r^2=0.93$ ,  $p<0.01$ ) indicate the difference in responses with and without  $RLM_s$ , and correspond to the proposed high contrast gain component

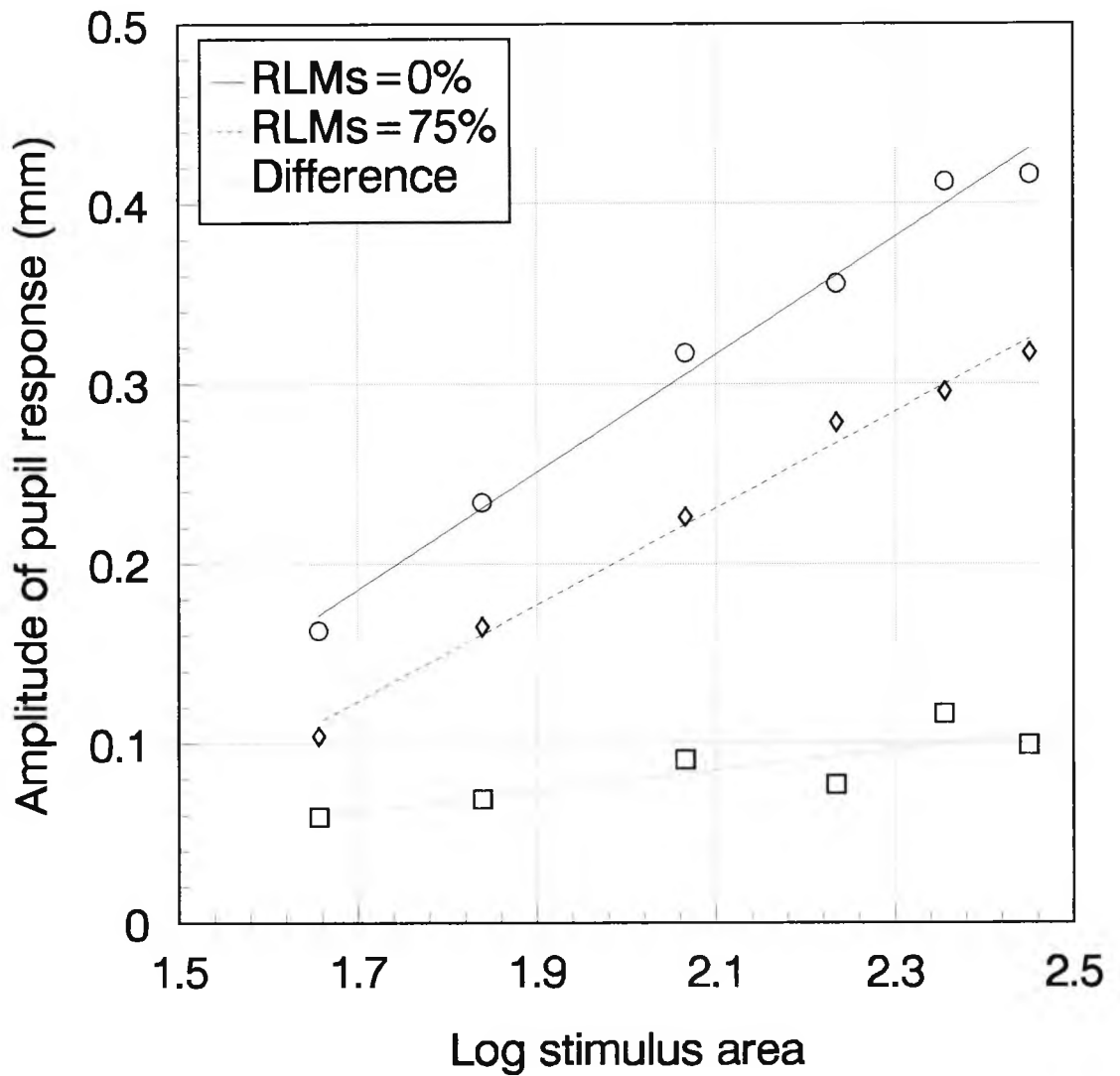


Figure 3.22 Pupil response amplitude as a function of log stimulus area for subject JB, contrast=90%. Measurements taken from Figure 3.19. The dashed line indicates the regression line fitted to the data points (diamonds) when  $RLM_s$  of 75% was used ( $r^2=0.90$ ,  $p<0.01$ ). This line may indicate the proposed low contrast gain, high spatial summation component of the pupil response. The dotted line and square symbols ( $r^2=0.66$ ,  $0.02<p<0.05$ ) indicate the difference in responses with and without  $RLM_s$ , and correspond to the proposed high contrast gain component

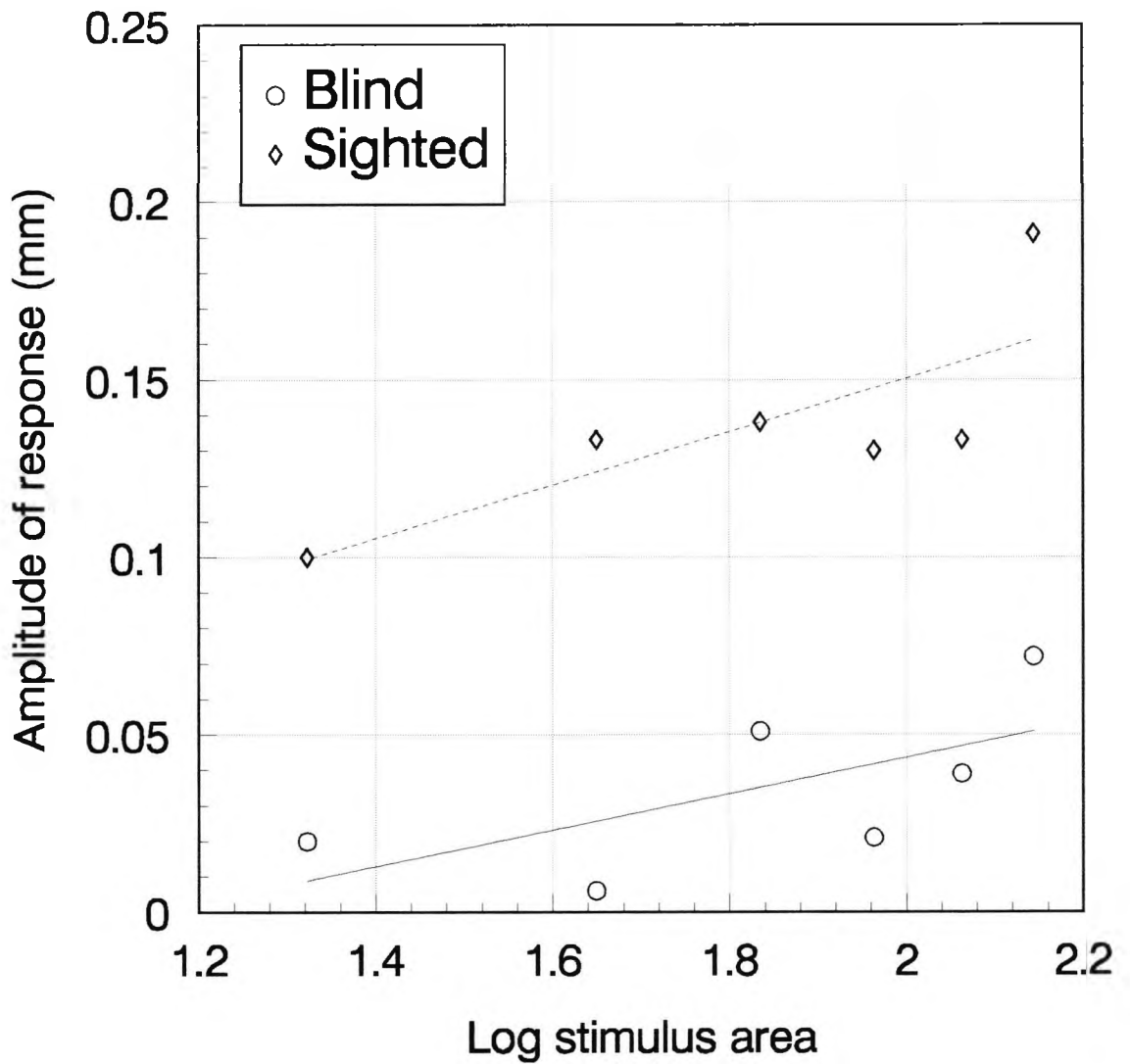


Figure 3.23 Pupil response amplitude as a function of log stimulus area for subject GY, contrast=30%. Measurements taken from Figure 3.20. The dashed line indicates the regression line fitted to the data points (diamonds) for the sighted hemifield, while the solid line and circles indicate the amplitudes measured for the blind hemifield. There is no statistically significant correlation between the amplitude of response and log stimulus area for the blind hemifield ( $p > 0.2$ ), while for the sighted field,  $r^2 = 0.59$ ,  $0.02 < p < 0.05$

### 3.8 Two proposed components of the PLR

#### Introduction

The results in the preceding sections support the idea of two separable components that contribute to the PLR. From examining the effects of  $RLM_s$  contrast, stimulus contrast and stimulus area and considering normal subjects and subjects with cortical damage, a pattern is emerging of a high contrast gain cortical component with low 'area gain' and a low contrast gain, subcortical component with extensive spatial summation.

In this section, some brief experiments will be described. The experimental findings contribute further information about the properties of the two proposed components.

#### a) Is the same effect present foveally?

So far all experimental stimulus configurations considered have used peripheral stimuli, so that comparisons can be made with the results of subjects with cortical damage. The effect of  $RLM_s$  and  $RLM_l$  for subject JB for a foveally presented stimulus was investigated.

#### Experimental procedure

A circular stimulus of radius  $3.3^\circ$  and contrast 55% was presented, centred on the fixation point. Background luminance was  $16 \text{ cd/m}^2$ . The stimulus was presented with no masking, with  $RLM_s=65\%$ , and with  $RLM_s=20\%$  and  $RLM_l=65\%$ , each being presented 36 times. Binocular viewing and measurement was used, and the results from the right and left eyes were averaged.

#### Results

The results are shown in Figure 3.24. It can be seen that  $RLM_s$  alone reduces the PLR amplitude, while the response is almost completely eliminated with a combination of  $RLM_s$  and  $RLM_l$ .

#### Conclusions

Comparing Figure 3.24 with Figure 3.7 shows that similar responses are obtained for stimuli presented foveally and in the periphery.

b) Does the  $RLM_s$  have to be dynamic to have its effect?

So far all the experiments involving  $RLM_s$  have used dynamic  $RLM_s$ , that is, the luminance of the checks varies every few frames (see Chapter 2). An experiment was carried out to see what was the effect of using static  $RLM_s$  that is, with the pattern of checks appearing and remaining at their initial luminances while the stimulus is presented. If static  $RLM_s$  does not reduce the PLR amplitude, it suggests that the proposed cortical component requires dynamic  $RLM_s$  to mask it.

#### Experimental procedure

An annular stimulus was used, of inner radius  $3.3^\circ$  and outer radius  $10.3^\circ$ , presented with and without static  $RLM_s$  of 45%. The background luminance was  $24 \text{ cd/m}^2$ . The stimulus duration was 197 ms, and each stimulus condition was presented 24 times. Subject JB viewed the stimulus binocularly and results from the right and left eyes were averaged.

#### Results

The results obtained are shown in Figure 3.25. It can be seen that the introduction of static  $RLM_s$  makes no difference to the PLR amplitude ( $p < 0.05$ , two-tailed t-test).

#### Conclusions

The proposed cortical component is eliminated by dynamic  $RLM_s$  but not by static  $RLM_s$ . The PLR must arise from neurons signalling a luminance increment when the stimulus appears, and the two components that have been described are presumably mediated by different groups of neurons. When no masking is used, both components can signal a luminance increment. When dynamic masking is used, one component or group of neurons cannot signal the stimulus onset within the  $RLM_s$  and the PLR is therefore reduced. In effect, the dynamic  $RLM_s$  makes the stimulus invisible to this group of neurons. Static  $RLM_s$  however does not reduce the PLR, so presumably the groups of neurons associated with both components can detect the stimulus onset.

These results may indicate that the two components have different temporal characteristics. For example, if the high gain cortical component exhibits a bandpass temporal frequency curve, it would not be eliminated by static  $RLM_s$  which is associated

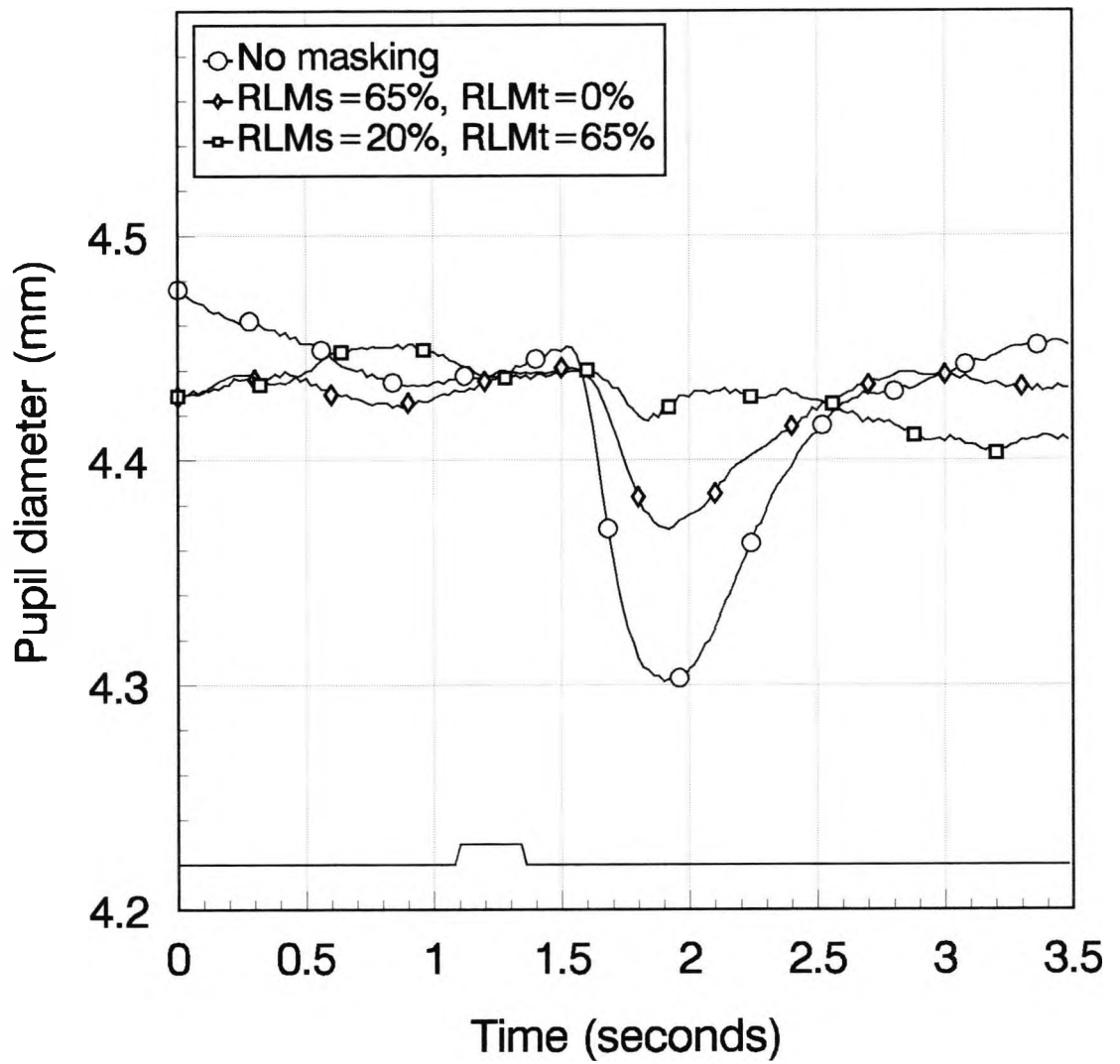


Figure 3.24 Pupil responses measured for subject JB, for foveal presentation of a circular stimulus  $3.3^\circ$  in radius and contrast=55%. The stimulus was presented with no masking, with  $RLM_s=65\%$ , and with  $RLM_s=20\%$  and  $RLM_t=65\%$

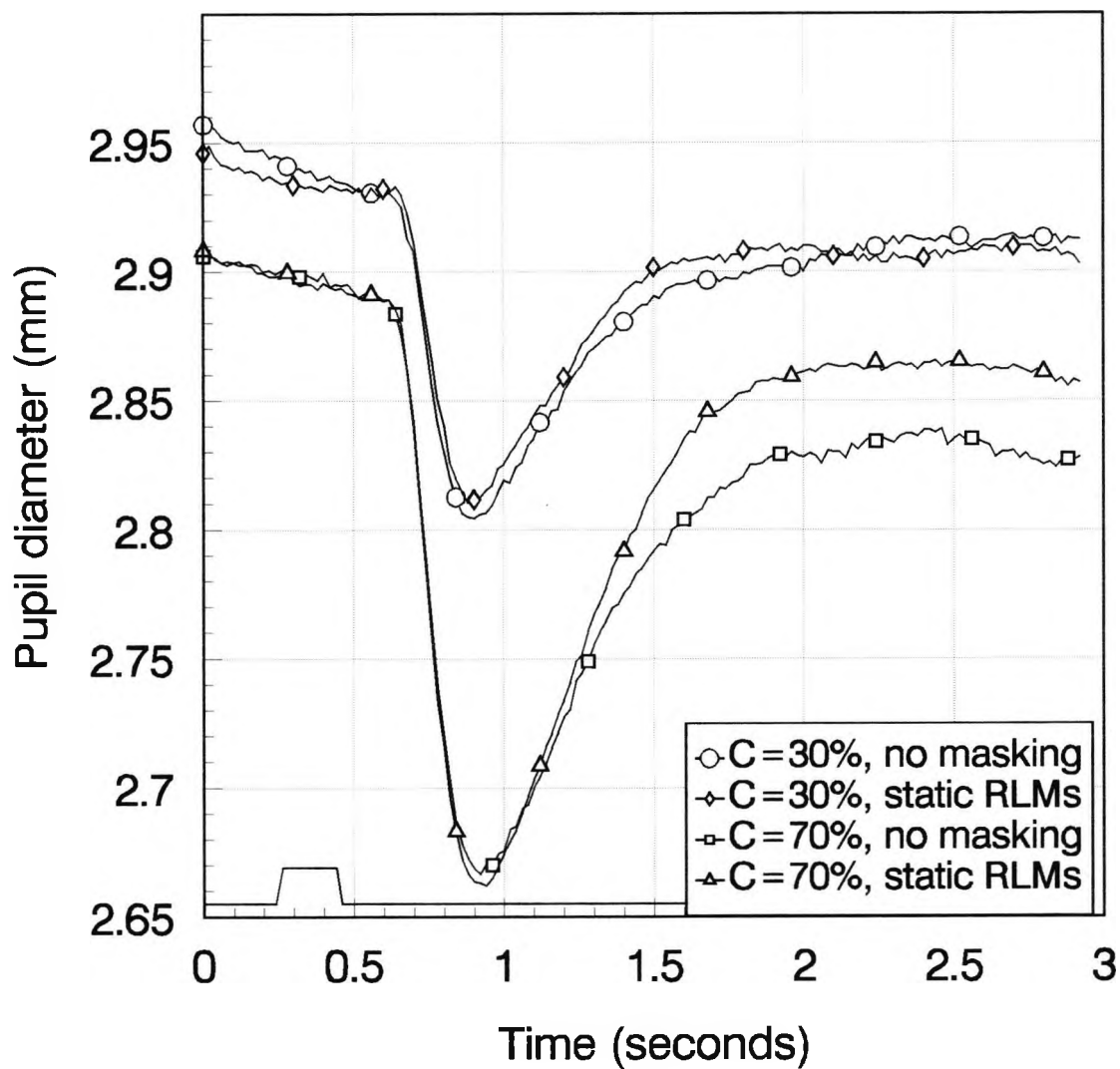


Figure 3.25 Pupil responses measured for subject JB with and without static RLMs of 45%. An annular stimulus was used (inner radius 3.3° and outer radius 10.3°) with contrasts of 30% and 70%

with a low temporal frequency, but would be affected by rapidly changing  $RLM_s$ . The temporal frequency characteristics could be further investigated by using  $RLM_s$  with different frame groups, preferably with Gaussian onset and offset of luminance.

c) If there are two separable components, can they be lost selectively?

If subjects can be found with selective loss of one or other of the two proposed components, this would provide additional evidence to support the hypothesis that separate neural substrates are involved in mediating these components. The experiments above show that GY appears to have lost the cortical component of the PLR to stimuli presented in his blind field. This section describes experiments on a subject who appears to have lost the other component. Some of these results have been presented in Barbur et al (1996).

#### Experimental procedure

AB is a 12 year old male subject who has bilateral optic nerve drusen which have affected the left eye more severely than the right eye. His visual acuity was 6/5 unaided in both eyes, but there was marked visual field loss for the left eye and mild loss for the right eye. He was referred for pupillary testing because he was thought to have a left relative afferent pupillary defect. Little or no anisocoria was seen in normal binocular viewing.

The stimulus was a square of side  $12.5^\circ$  and contrast of 30% presented foveally for 187 ms against a background of luminance  $24 \text{ cd/m}^2$ . The first investigation was to measure the PLR to this stimulus, with no  $RLM_s$ , with monocular and binocular viewing. 16 presentations were averaged for each condition.

The effect of  $RLM_s$  was also investigated, using the stimulus as described above, with and without  $RLM_s$  of 45% and check size of about  $1^\circ$ . Monocular viewing and recording was used, and 32 presentations were averaged for each condition. Results were also obtained for normal subject JB with monocular viewing for comparison.

## Results

The PLRs measured monocularly and binocularly are shown in Figure 3.26. The traces have *not* been shifted vertically, so this graph shows the absolute measurements of pupil diameter. The pupil traces in the first 0.5 seconds, before the stimulus has been presented, show that there is a much larger pupil diameter when the left eye is viewing monocularly than when the right eye is viewing monocularly. This increase in steady state pupil size is consistent with a left afferent pupillary defect. However, when both eyes are viewing the left pupil is only very slightly bigger than the right pupil, which suggests that the left consensual response is intact and that the efferent pathways are unaffected. When the stimulus is presented, constrictions corresponding to the normal PLR are seen in both eyes for monocular and binocular viewing, although the amplitude of response is slightly smaller when the left eye is viewing monocularly.

The effect of RLM<sub>s</sub> is shown in Figure 3.27. The traces have been shifted vertically for ease of comparison. For AB's left eye viewing monocularly, the RLM<sub>s</sub> eliminates most of the PLR, leaving a response of 0.039 mm. When his right eye is viewing monocularly the response obtained with RLM<sub>s</sub> is 0.083 mm, that is, about twice what is measured with left eye viewing. JB also shows a reduced response when RLM<sub>s</sub> is used, consistent with previous results described in this chapter.

## Conclusions

AB's left eye defect is probably caused by selective neural damage caused by compression of the optic nerve by the disc drusen. Figure 3.26 shows that there is an abnormality of the mechanism involved in determining the steady state size of the pupil when the left eye is viewing, but that the transient constriction of the pupil when a stimulus is presented is virtually normal. Figure 3.27 shows that for monocular viewing with the left eye, the RLM<sub>s</sub> eliminates most of the PLR of the left eye. The previous sections have shown that a residual response would be expected with RLM<sub>s</sub> for a stimulus of this area and contrast, supplied by the proposed low contrast gain component. The fact that the residual response is very small suggests that this component is defective or missing for AB's left eye. The residual response measured with RLM<sub>s</sub> with his right eye is smaller than that measured for JB, which may indicate some optic nerve damage for this eye as well, caused by the disc drusen.

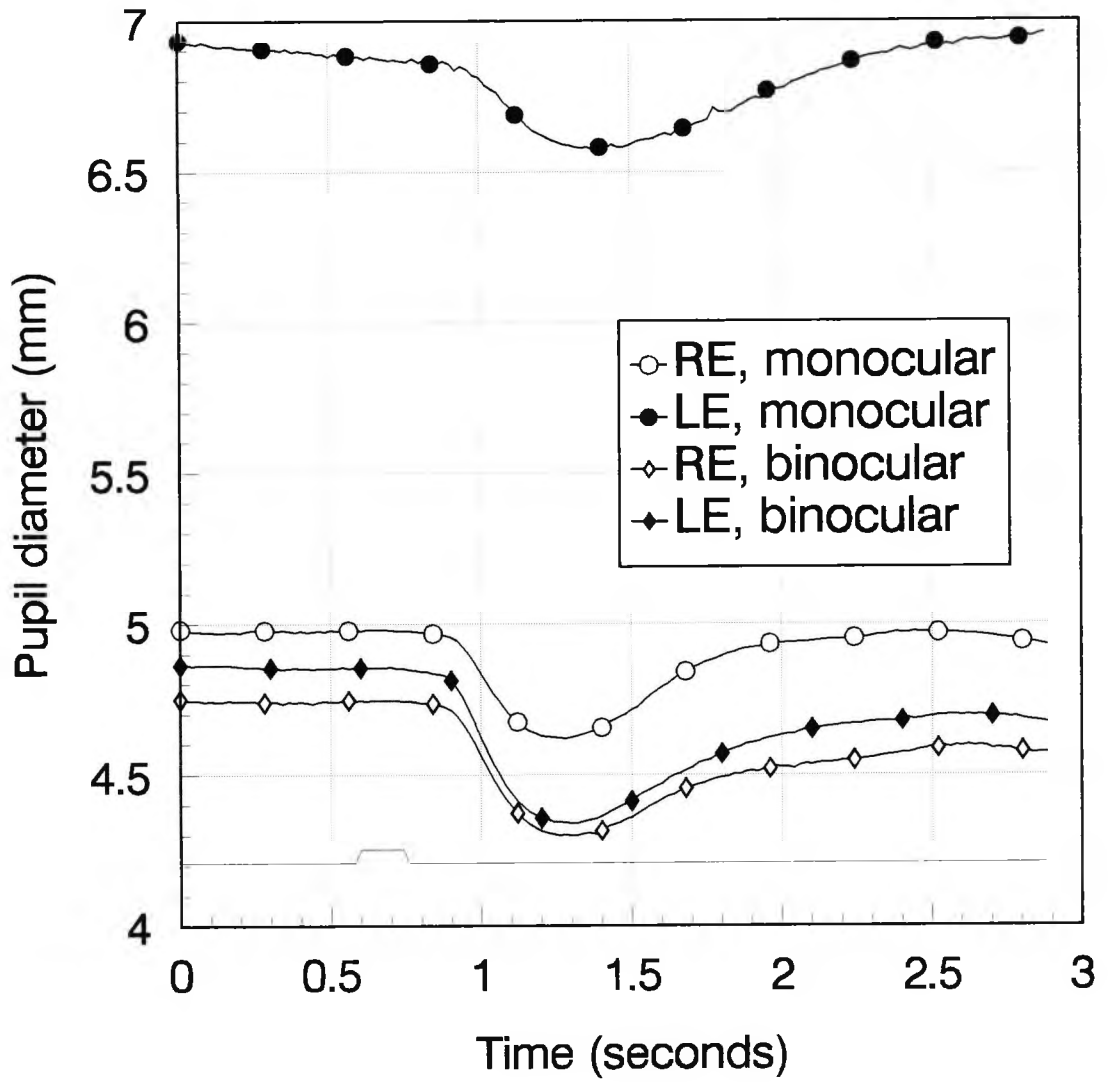


Figure 3.26 Pupil responses measured for subject AB for monocular and binocular viewing. The stimulus was a square of side  $12.5^\circ$  and contrast 30%, presented foveally. The traces have *not* been shifted vertically. The initial difference in pupil diameter when the right and left eyes are viewing monocularly indicates the left afferent pupillary defect

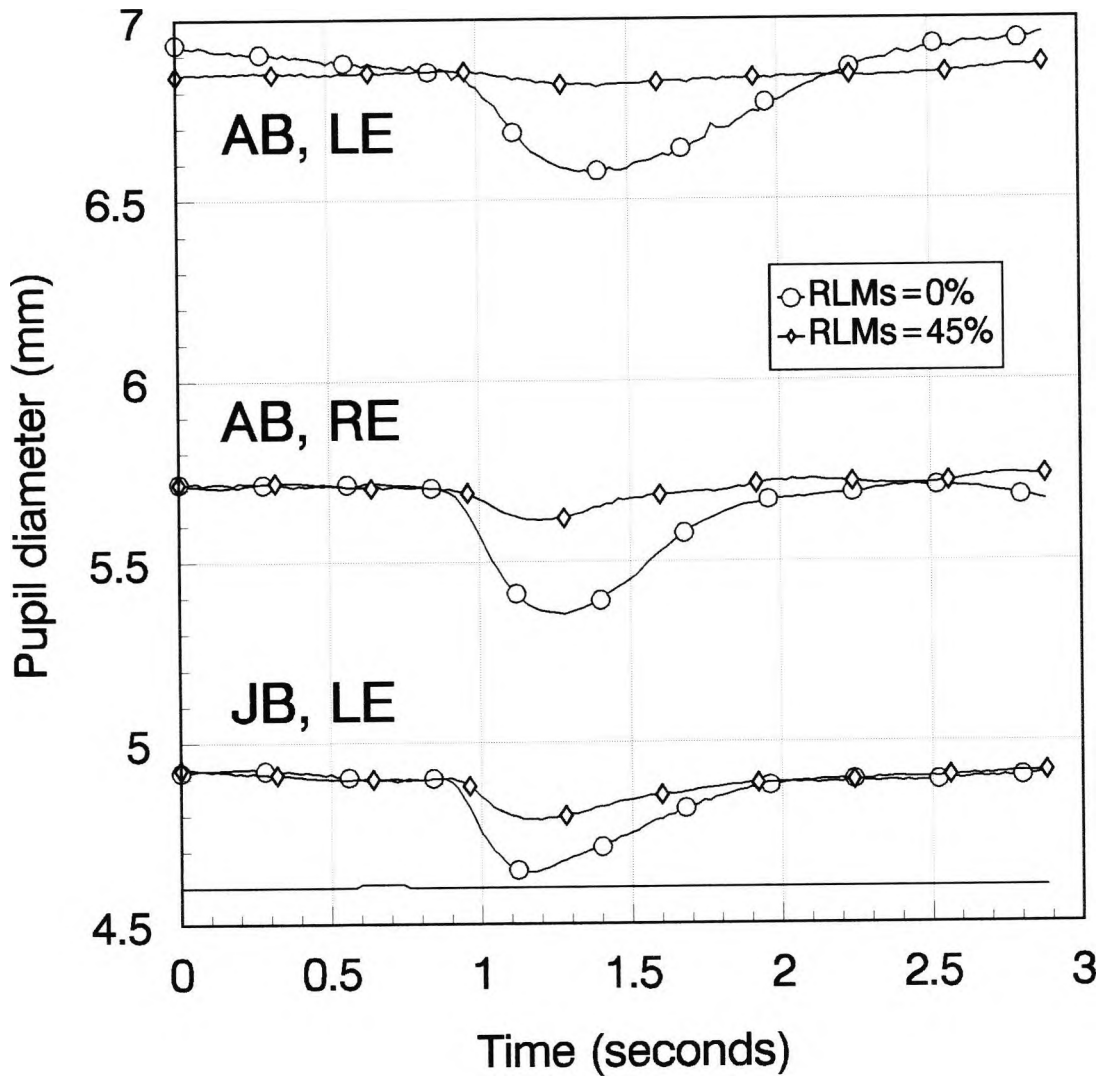


Figure 3.27 Pupil responses measured for subject AB for a square stimulus of side  $12.5^\circ$  and contrast 30%, presented foveally, with and without RLMs of 45%. Results are shown for monocular viewing and recording, and the traces have been shifted vertically for ease of comparison. Monocular results are included for normal subject JB for comparison

AB thus appears to have an abnormality of the mechanism controlling the steady state pupil size, and also to lack the low contrast gain component. Could these be the same thing? This component has already been compared to the classical subcortical part of the pupil pathways, which is involved with steady state pupil size (Clarke and Ikeda, 1985a; Gamlin et al, 1995), and AB's results are consistent with the proposal that the component unaffected by RLMs is subcortical and contributes to steady state pupil size.

These results also show that it is possible to find subjects with selective damage to one or the other of the two proposed pathways, which is evidence that they may be mediated by separate neural substrates.

### 3.9 Summary

The experimental results described in this chapter have built up a picture of two components contributing to the PLR measured to a luminance increment of short duration, whose properties are summarised in Table 3.5.

	'Cortical' component	'Subcortical' component
Contrast gain	High Saturates (above 30%)	Low Large luminance range
Area summation	Yes Low increase per log unit area	Yes High increase per log unit area
Time characteristics	Transient	More sustained
Effect of RLM	Eliminated by $RLM_s$ alone	Not eliminated by $RLM_s$ alone, is eliminated by $RLM_t$

Table 3.5. Summary of the two PLR components described in Chapter 3.

The first component is eliminated by  $RLM_s$ , and so is thought to be concerned with local contrast increments. The effects of  $RLM_s$  contrast amplitude on this component suggest that this is a high contrast gain mechanism which saturates above 30% contrast. Kaplan and Shapley (1986) described similar contrast gain characteristics for retinal M ganglion cells. Its contribution to the total PLR amplitude increases linearly with log stimulus area, but with a low 'area gain' slope. It is not affected by static  $RLM_s$  suggesting that it

is a transient mechanism (again similar to the properties of M-type ganglion cells). It does not appear to be present in subject GY with damaged primary visual cortex, suggesting that it involves neurons of the primary visual cortex or that have undergone retrograde degeneration as a result of his cortical lesion.

The second component is normally not eliminated by RLM<sub>s</sub>, perhaps because it signals luminance increments over a large area. It is a low contrast gain mechanism, and is therefore not particularly effective at low contrasts. It shows a clear ~~linear~~<sup>straight-line</sup> relationship with log stimulus area. GY's PLRs appear to consist entirely of contributions from this system, so there is presumably no cortical involvement. This component appears to exhibit extensive spatial summation and responds to a large range of luminance increments, properties that would be useful in controlling steady state pupil size. The results obtained with AB suggest that this component contributes to the steady state size of the pupil. Although the contrast gain characteristics are similar to those described for P retinal ganglion cells by Kaplan and Shapley (1986), it is unlikely that this pathway involves P cells. Firstly, P cells do not project to the midbrain (Perry and Cowey, 1984) and secondly, damage to visual cortex causes a loss of most P cells (Cowey and Stoerig, 1991b). It is therefore unlikely that P cells contribute to GY's PLR. Although this pathway may be related to steady state pupil size control, it can still cause a short-lived constriction to brief light increments, as these can be measured in GY with sufficiently high stimulus contrast.

The two components described above may be compared with the transient and sustained components of the PLR suggested by Young et al (1993) based on principal component analysis of pupil response data. Their transient component dominates the PLR at low stimulus luminances, and has a relatively high contrast gain, but saturates at higher luminance increments. It therefore shows similar characteristics to the 'cortical' component described above. Their sustained component increases monotonically with the stimulus luminance increment, as does the 'subcortical' component described above.

Subjects with damage beyond the LGN may demonstrate abnormal pupil responses clinically only if suitable stimuli are used (section 1.2.6). The results described for GY and FS show that there are clear differences between PLRs measured in normal and

affected fields, for small and/or low contrast stimuli. This must be the case since it is possible to map out field defects in such subjects with pupil perimetry (Kardon, 1992). However, it has been shown that for high contrast stimuli there does not appear to be any difference between PLRs in affected and normal fields (Figures 3.16 and 3.17). Pupillary responses are often tested clinically with a pen torch which is a large high contrast stimulus, and might not be expected to show the differences that have been described. A further consideration is that in the experiments described in this chapter eliminating the high contrast gain component only reduces the PLR amplitude by 0.2 mm or less, which is not enough to be observed without specialised recording equipment. With the use of appropriate stimuli and suitable recording devices, subtle aspects of the PLR have been observed, and these may turn out to be clinically useful in neuro-ophthalmology.

Further experiments could be carried out to investigate in greater detail the properties of these two components. The effect of stimulus eccentricity could be examined, for example, to see if there is any relationship between the proposed cortical component and cortical magnification factor or ganglion cell distribution. It has been suggested that the cortical component may be a transient component, so the effect of stimulus duration could be investigated for normals and for subjects such as GY. Perhaps normal subjects would get responses for very short stimulus durations while the subcortical pathway would have a longer threshold time for a constriction to occur. If similar components could be demonstrated in monkey studies, it may then become possible to investigate the effect of different lesions on the two components.

## **CHAPTER 4 INVESTIGATION OF THE PUPIL COLOUR RESPONSE**

### 4.1 Introduction

The pupil is known to respond to isoluminant chromatic exchanges (see section 1.2). It has been demonstrated that the pupil colour response (PCR) could be used as an objective colour vision test (Young et al, 1987; Barbur et al, 1993a). In subjective colour vision testing it is essential to remove any luminance contrast cues that the subject could use for discrimination or recognition of the stimulus. If PCRs are to be used as an objective test it is also necessary to remove or make ineffective luminance changes generated by the stimulus as these would cause a pupil light reflex constriction. This could be done by establishing equiluminant stimuli prior to the colour vision test, for example, by heterochromatic flicker photometry or minimally distinct border methods, but this is time-consuming and may require special apparatus. It may also be difficult to set isoluminance with saturated chromatic stimuli. Objective tests are often useful for subjects where communication is restricted, for example, in infants or patients unable to perform subjective tests. Such methods for obtaining equiluminance are obviously inappropriate for these subjects.

Previous studies have used stimuli of approximately equal luminance (Young et al, 1993) or coloured stimuli of lower luminance than the background (Barbur et al, 1989). Barbur et al (1993a) used a random luminance masking technique identical to the RLMs described in Chapters 2 and 3, and showed that dichromatic subjects do not demonstrate a PCR when the stimuli used lie on their principal colour confusion lines.

Pupil responses measured using chromatic targets have also been investigated in subjects with cortical damage. Keenleyside (1989) found little or no response in these subjects when isoluminant chromatic gratings were used. Sahraie (1993) measured pupil responses when large highly-saturated coloured targets were used. Comparing results of these subjects with those of normal subjects may give useful information about the neural pathways involved in mediating pupil responses to coloured stimuli.

When measuring pupil responses to chromatic stimuli, it is important to consider the possible explanations for the responses measured. Accommodation and/or convergence at stimulus onset would cause a pupil constriction as part of the 'near vision triad', which could be mistaken for a response to the stimulus itself. Keenleyside (1989) has shown that no significant accommodation or convergence was found using the P\_SCAN 100 system for presentation of coloured and grating stimuli. It is also possible that a chromatic stimulus could be associated with a light flux increase, despite efforts to the contrary, causing a pupil constriction. The RLM<sub>s</sub> technique used in these experiments is thought to be sufficiently good at masking luminance changes to eliminate this effect for stimuli consisting of small coloured elements (see above). If larger stimuli are used, RLM<sub>t</sub> has been shown to eliminate luminance contrast effectively (section 3.3). If large stimuli are used in the peripheral field, care must be taken to avoid rod-driven pupil responses, for example, by light adaptation (Alpern and Campbell, 1962). The responses to large coloured stimuli found in subjects with cortical damage by Sahraie (1993) may have been contaminated by rod intrusion. The RLM<sub>t</sub> technique should prevent rod intrusion, by masking light flux changes summed up over the stimulus area and by changing the mean light flux level too rapidly for the rods to follow.

If precautions are taken to eliminate these factors, the resulting responses should be pure responses to the chromatic signals, or pupil colour responses (PCRs). These may be cortical event-driven responses, in that the appearance of a coloured stimulus interrupts the supranuclear inhibitory impulses acting on the Edinger-Westphal nucleus allowing parasympathetic action on the pupil and causing a pupil constriction (see section 1.2.2).

This chapter will describe work using the technique of Barbur et al (1993a) to carry out more detailed investigation of the PCR in normal subjects and dichromats. PCRs were also investigated in subjects GY and FS, who have been mentioned in Chapter 3, and LR, a subject with incomplete cerebral achromatopsia.

## 4.2 PCRs in normal subjects

### Introduction

Barbur et al (1992a, 1993a) describe psychophysical and pupillometric colour vision testing in normal subjects and dichromats. In this technique the coloured stimulus is presented on a neutral background amid random luminance masking which should mask any luminance increment associated with the onset of the stimulus, leaving the subject to respond either subjectively or objectively to the chromatic change only. Barbur et al (1992a, 1993a) show that increasing the amplitude of the RLM<sub>s</sub> has no effect on the chromatic discrimination thresholds determined subjectively in normal subjects. In dichromats, however, increasing the RLM<sub>s</sub> amplitude reveals the true extent of the isochromatic region in each class of colour deficient subject. If RLM<sub>s</sub> is used with achromatic targets, the threshold luminance contrast required to detect the target increases with RLM<sub>s</sub> amplitude (Barbur et al, 1994a), demonstrating that the introduction of RLM<sub>s</sub> is effective at masking the luminance contrast of the stimulus. This section describes experiments using RLM<sub>s</sub> to investigate the PCR in normal subjects more fully.

### Experimental procedure

Three normal trichromatic subjects participated in this study. Details of these subjects are summarised in Table 4.1. Subjects viewed the screen from a distance of 700 mm, wearing an appropriate correction if required. The background luminance of the screen was 28 cd/m<sup>2</sup>, with CIE (x,y) chromaticity co-ordinates of (0.305, 0.323).

The stimulus configuration is shown in Figure 4.1. The RLM<sub>s</sub> formed an array of 15 x 15 checks of side 0.4° and was set at 25%. The coloured stimulus was formed by a subset of these checks undergoing a chromatic displacement in addition to the ongoing random luminance changes such that a pattern of seven vertical bars was formed as shown in Figure 4.1. The dimensions of the bars were 0.4° x 5.2°, and thus they were easily resolved by all the subjects. The chromatic displacement was 0.09 units which was the maximum that could be achieved with the screen used. Twelve different colours were used with angles of chromatic displacement from 0° to 330° at 30° intervals. The stimulus duration was 250 ms, and each of the twelve stimuli were

Subject	Age	Sex	Visual acuity	Eye measured
JB	40	M	R: 6/6 L: 6/6	Binocular
MH	24	F	R: 6/5	Right
RT	32	M	R: 6/5 L: 6/4	Binocular

Table 4.1. Details of normal trichromatic subjects participating in PCR experiments

Subject	Age	Sex	Colour vision defect	Visual acuity	Eye measured
PE	26	M	Protanope	L: 6/6	Left
SA	33	M	Protanope	L: 6/9	Left
RV	45	M	Deutanope	L: 6/6	Left
JF	43	M	Tritanope	L: 6/4	Left

Table 4.2. Details of dichromats participating in PCR experiments

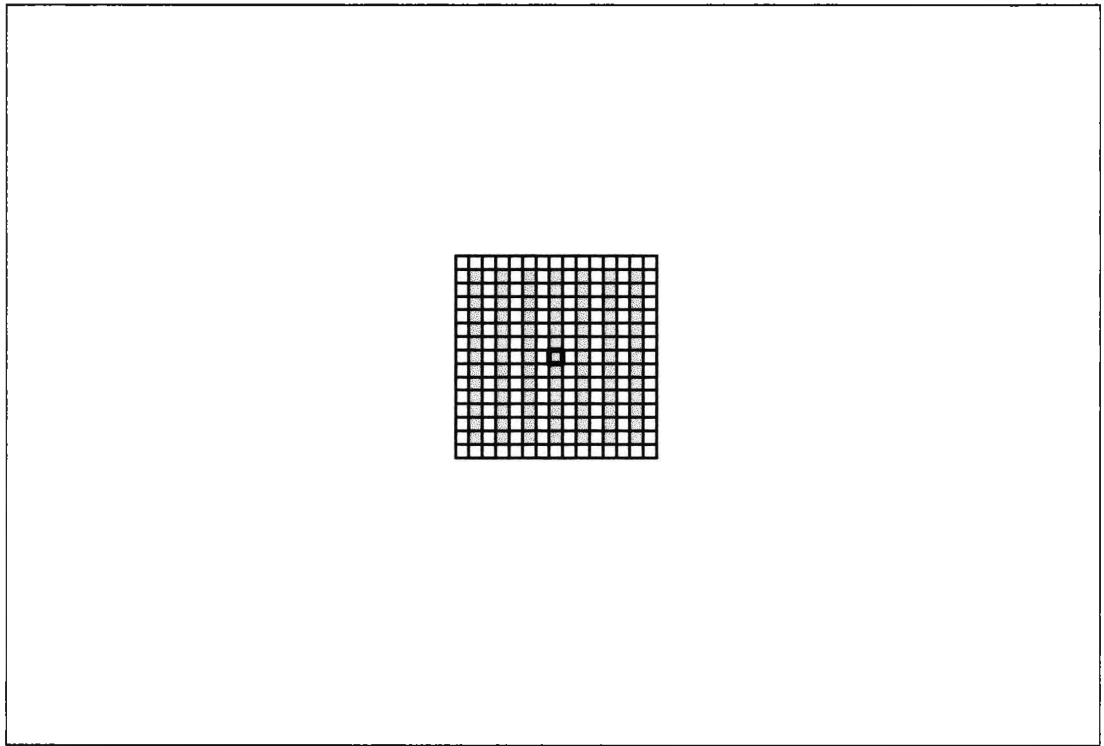


Figure 4.1 Stimulus configuration for measuring PCRs in normal subjects and dichromats. Shaded bars indicate coloured stimulus, small checks indicate RLMS checks (approximately  $0.4^\circ \times 0.4^\circ$ ). The fixation target was positioned in the centre of the middle bar as indicated by the small square

presented 36 times. Subjects JB and RT viewed the stimulus binocularly and the results shown are the average for the right and left eyes. No useful traces were recorded for subject MH's left eye because her eyelashes obscured part of the pupil margin, so the results shown are for the right eye only.

## Results

The average traces obtained for subject MH are shown in Figure 4.2. The amplitudes were measured from these graphs as explained in Chapter 2, and the standard errors associated with each amplitude were calculated. The amplitudes are plotted in Figure 4.3. Similarly, the amplitudes for each colour were calculated from the average traces measured for subjects RT and JB, and these results are shown in Figures 4.4 and 4.5 respectively.

The smallest response obtained for each subject was shown to be significant using a one-tailed single sample t-test; in each case,  $p < 0.0005$ . It can therefore be concluded that significant responses were measured for all the colours tested. There is some inter-subject variability, but there are generally minima for angles of chromatic displacement in the region of  $60^\circ$  and  $240^\circ$ , consistent with the results found by Barbur et al (1992a). Psychophysical measurements taken with this type of stimulus show that for normal subjects the chromatic discrimination threshold ellipse has its major axis in the direction  $60^\circ$ - $240^\circ$  (Birch et al, 1992; Barbur et al, 1992a, 1993a, and see Chapter 5).

## Conclusions

The results show that significant PCRs can be measured using this experimental procedure for all the colours tested in normal subjects. A constant chromatic displacement well above threshold was used for each colour, and it was generally found that the colours to which the subjects are least sensitive produced a minimum on the PCR amplitude graph, reflecting the opponent-colour contributions to the pupil (Hedin and Glansholm, 1976; Krastel et al, 1985).

This experiment confirms and extends the work described by Barbur et al (1992a, 1993a) for normal subjects, and the next section describes an extension of their work on dichromats.

### 4.3 PCRs in dichromats

#### Introduction

The use of PCRs as an objective means of assessing colour vision has been mentioned in section 4.1, and has already been investigated, for example, by Young et al (1987) and Barbur et al (1992a, 1993a). This section describes experiments to investigate more fully the PCRs obtained in dichromatic subjects.

#### Experimental procedure

Four dichromatic subjects took part in these experiments; two protanopes, a deuteranope and a tritanope. The protanopes and deuteranope were found to have severe colour vision defects using an Ishihara test. The colour vision of the tritanope was assessed using the computerised colour vision test described by Birch et al (1992) and see Chapter 5, and the results are shown in Figure 4.6. Details of these subjects are given in Table 4.2. The stimulus configuration was as shown in Figure 4.1. The background luminance in this case was  $34 \text{ cd/m}^2$ , and the chromatic displacement was 0.042 units. The RLM<sub>s</sub> used was 25%. For all these subjects only the left eye results were measured. Each colour was presented 36 times and the resulting traces were averaged.

For the normal subjects described in section 4.2 twelve equally spaced directions of chromatic displacement were used. For the dichromats, a range of angles was chosen so that there were relatively more colours near the directions of the colour confusion axis. The angles used are shown in Tables 4.3 to 4.6. Because of the extremely narrow chromatic discrimination threshold ellipse obtained for the tritanope, 16 different angles were used to establish the PCR for this subject.

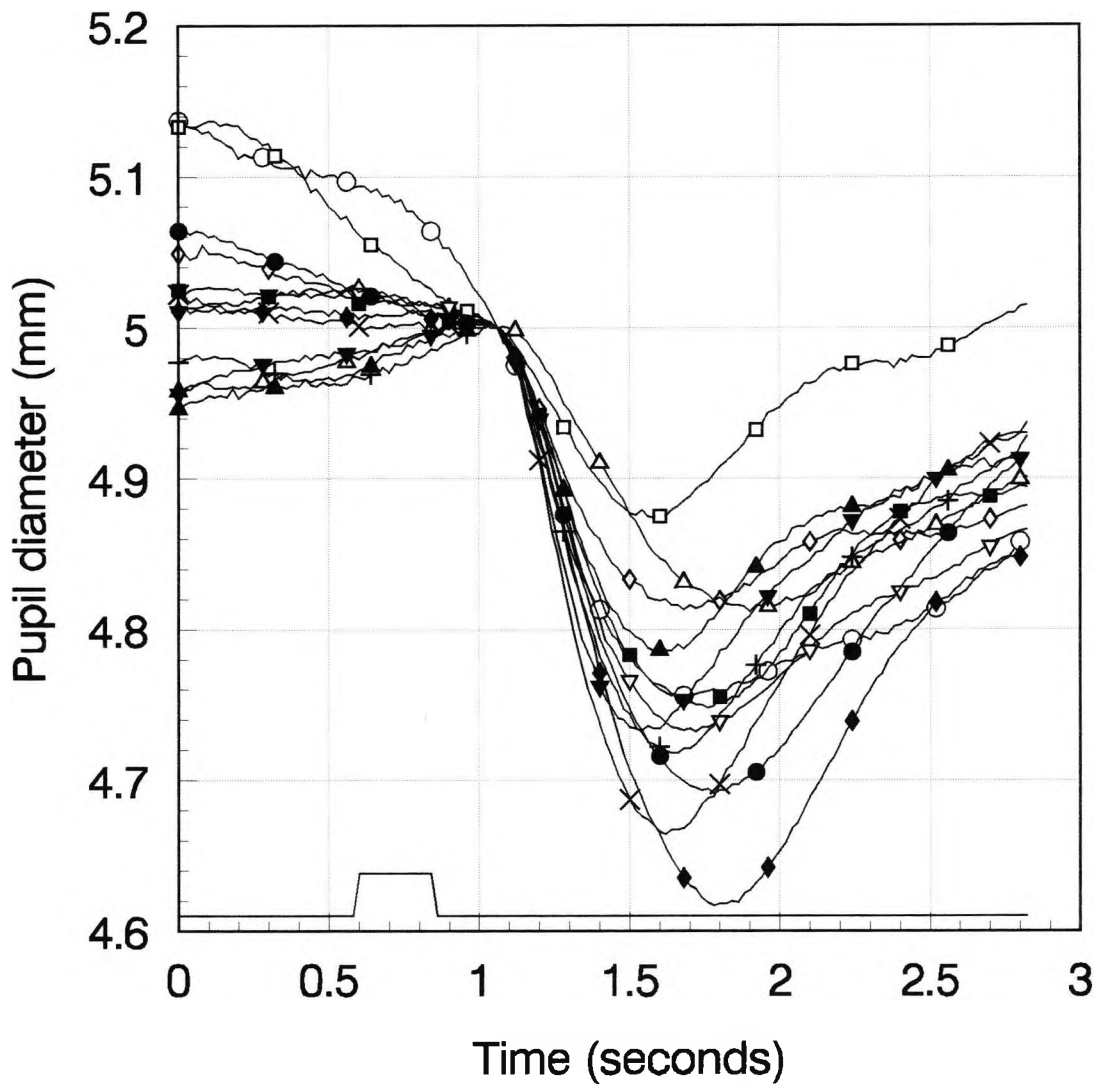


Figure 4.2 Pupil responses measured for normal subject MH. Stimulus configuration as shown in Figure 4.1. Angles of chromatic displacement from  $0^{\circ}$  to  $330^{\circ}$  at  $30^{\circ}$  intervals. The response amplitudes associated with the different angles of chromatic displacement have been measured and are plotted in Figure 4.3.

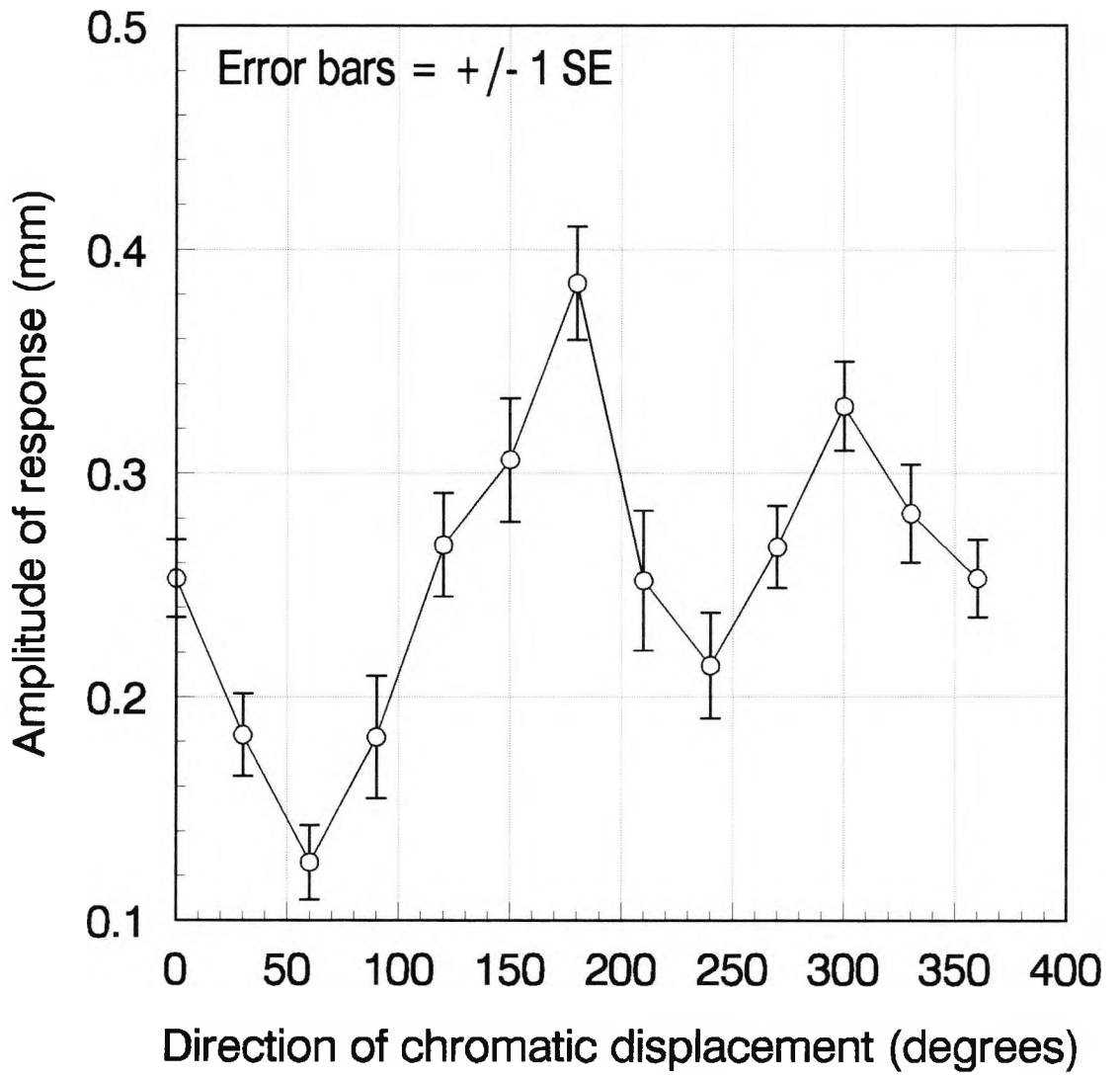


Figure 4.3 Pupil response amplitudes measured for normal subject MH, stimulus configuration as shown in Figure 4.1

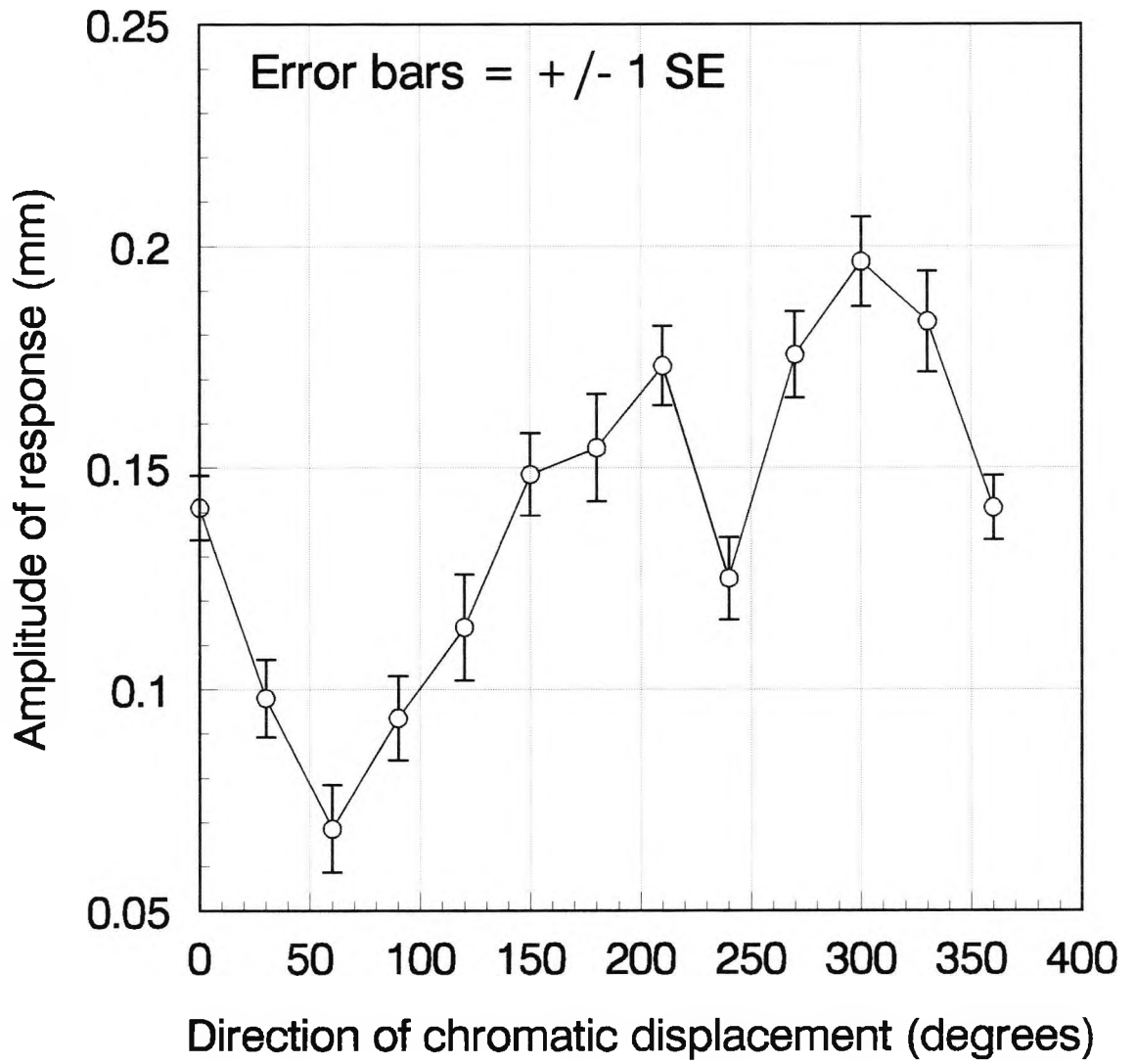


Figure 4.4 Pupil response amplitudes measured for normal subject RT, stimulus configuration as shown in Figure 4.1

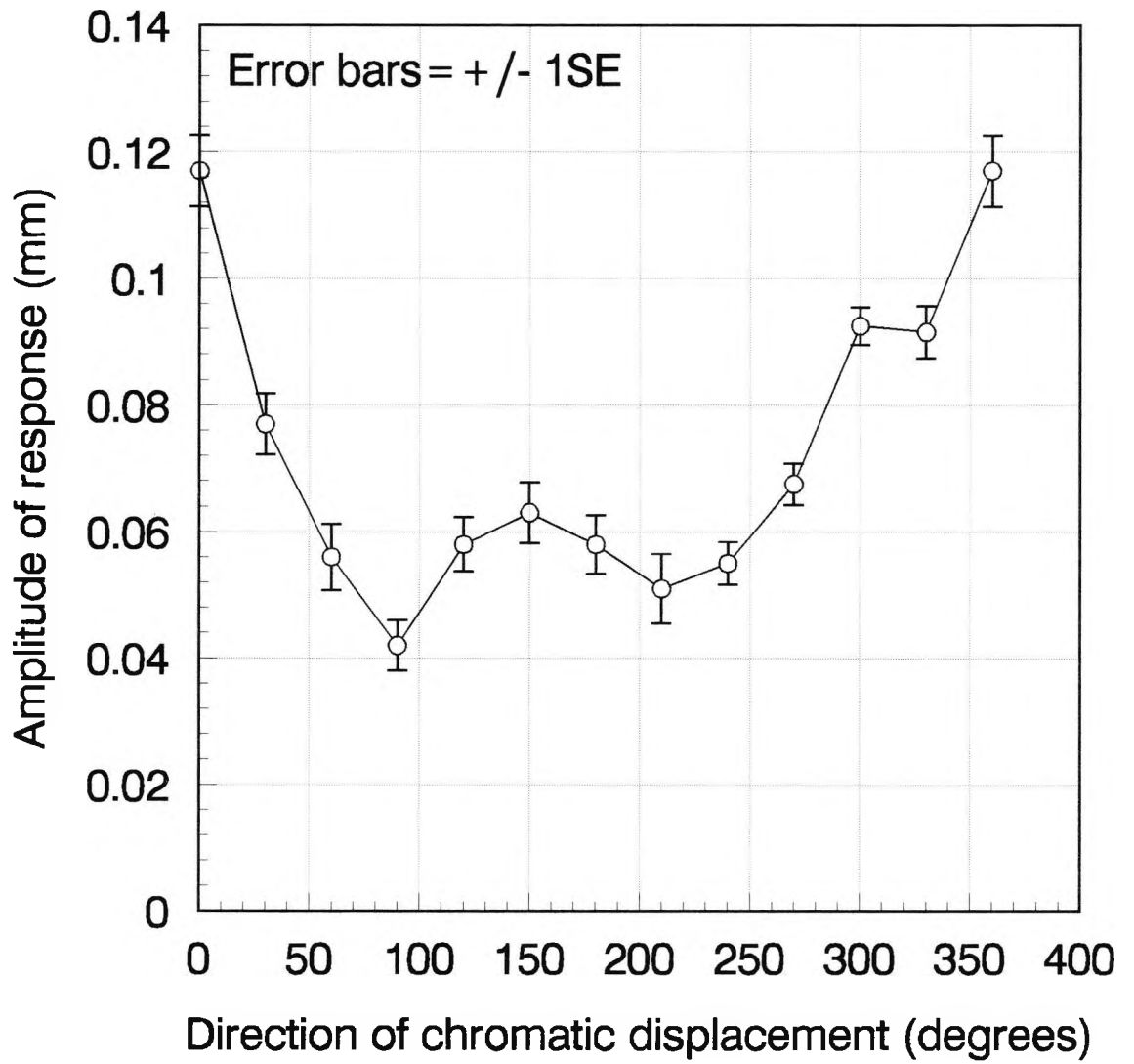


Figure 4.5 Pupil response amplitudes measured for normal subject JB, stimulus configuration as shown in Figure 4.1

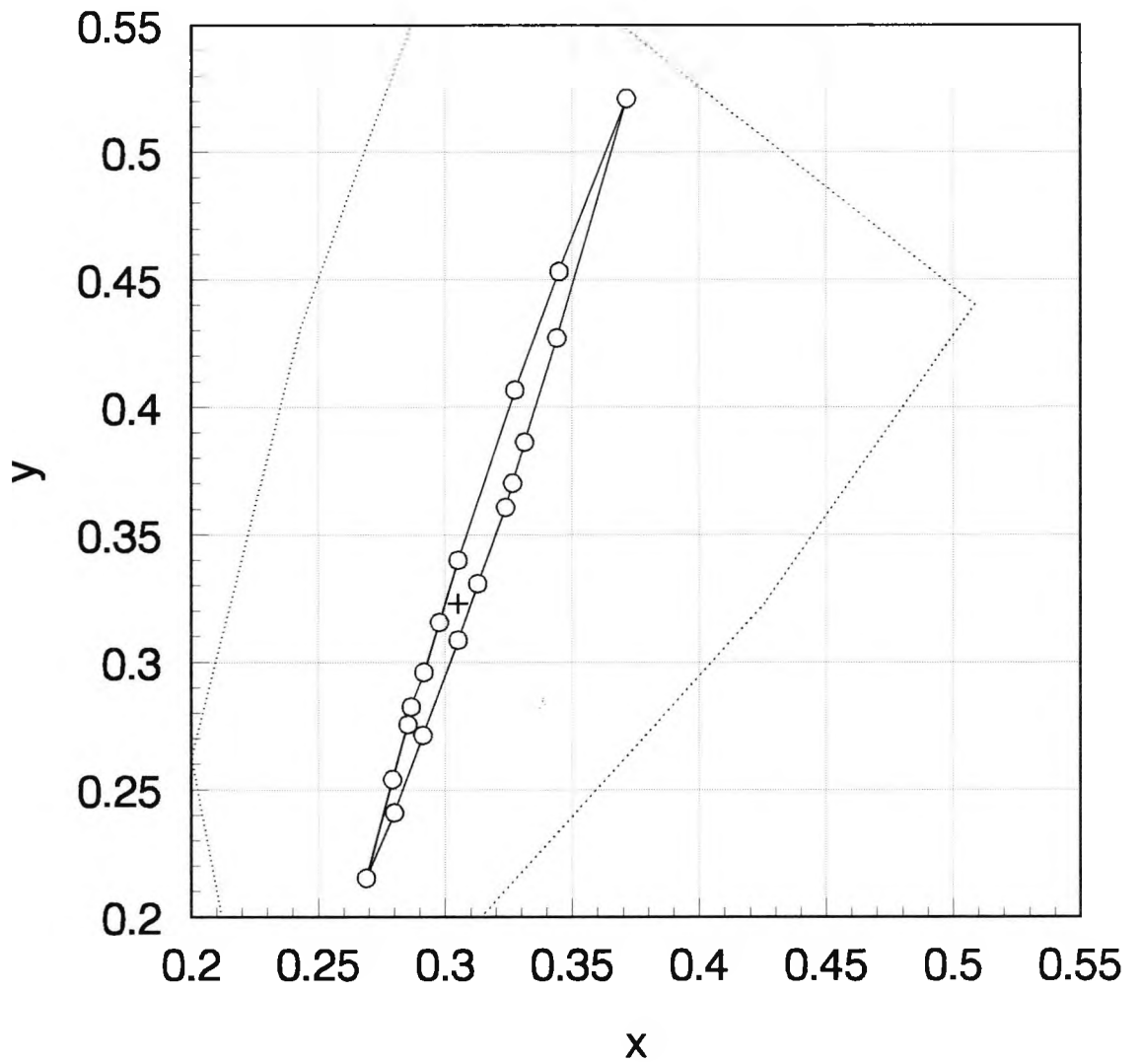


Figure 4.6 Chromatic discrimination ellipse for tritanope JF, measured using the computerised colour vision test described in Chapters 2 and 5 (stimulus configuration as shown in Figure 4.1). Dotted line shows the phosphor limits of the screen

Angle of chromatic displacement	p (one-tailed t test for single samples)
45	<0.0005
90	<0.0005
135	<0.0005
167	>0.05
170	>0.1
173	>0.1
225	<0.0005
270	<0.0005
315	<0.0005
347	<0.005
350	>0.1
353	>0.1

Table 4.3 Angles of chromatic displacement used for SA (protanope) and significance of results obtained.

Angle of chromatic displacement	p (one-tailed t-test for single samples)
45	<0.0005
90	<0.0005
135	<0.005
167	>0.1
170	>0.1
173	<0.025
225	<0.0005
270	<0.0005
315	<0.01
347	>0.1
350	<0.01
353	>0.1

Table 4.4 Angles of chromatic displacement used for PE (protanope) and significance of results obtained.

Angle of chromatic displacement	p (one-tailed t-test for single samples)
60	<0.0005
120	<0.0005
127.5	>0.1
142.5	>0.1
157.5	>0.1
172.5	<0.0005
240	<0.0005
300	<0.0005
307.5	<0.0005
322.5	<0.025
337.5	>0.1
352.5	>0.1

Table 4.5. Angles of chromatic displacement used for RV (deuteranope) and significance of results obtained.

Angle of chromatic displacement	p (one-tailed t-test for single samples)
0	<0.0005
25	<0.0005
45	<0.0005
67.4	>0.1
67.8	>0.1
68.2	<0.005
90	<0.0005
135	<0.0005
180	<0.0005
205	<0.0005
225	<0.0005
247.2	>0.1
247.6	>0.1
248	>0.1
270	<0.0005
330	<0.0005

Table 4.6 Angles of chromatic displacement used for JF (tritanope) and significance of results obtained.

## Results

The average traces obtained for subject SA are shown in Figure 4.7. The amplitudes were measured from these graphs as explained in Chapter 2, and the standard errors associated with each amplitude were calculated. The amplitudes are plotted in Figure 4.8. Similarly, the amplitudes for each colour were calculated from the average traces measured for subjects PE, RV and JF, and these results are shown in Figures 4.9, 4.10 and 4.11 respectively.

The significance levels of the amplitudes obtained for these subjects are shown in Tables 4.3 to 4.6. For subject SA, the stimuli for which no significant response (at the 0.01 level) was measured were those with angles of 167, 170, 173, 350 and 353. For PE, no significant responses were obtained for 167, 170, 173, 347 and 353. A small but significant response was obtained for the 350 stimulus, which was unexpected. For the deuteranope, RV, the angles for which no significant responses were obtained were 127.5, 142.5, 157.5, 322.5, 337.5 and 352.5. The tritanope showed no significant responses for 67.4, 67.8, 247.2, 246.7 and 248.

## Conclusions

From the results described above, it is clear that there are certain angles of chromatic displacement which do not evoke a PCR in dichromats, and the angles are different for different classes of colour vision deficiency as would be expected. These angles presumably do not cause a PCR because they are isochromatic with the background and are not detected by the subjects.

These results support the view that it is possible to use the PCR as an objective colour vision test. An abbreviated form of the above experiment was used by Birch et al (1992) in which PCRs were measured only to 'protan', 'deutan' and 'tritan' axes. Clearly this would be more practical for a clinical test than using 12 or more colours per subject. However, it would be necessary to gather data from a larger sample of dichromats to ascertain what the appropriate axes to test would be. This would be particularly important for tritanopes as the isochromatic region is so narrow (for example, subject JF described here gets no significant response for 67.8 but does get a response for 68.2).

#### 4.4 PCRs in subjects with cortical damage

##### Introduction

This section describes experiments carried out in subjects with cortical damage. It was hoped that examining the PCRs in these subjects and comparing the results with those of normal subjects may shed some light on the neural mechanisms underlying the PCR.

Previous work has shown that subjects with damaged primary visual cortex may have some residual colour vision remaining (Stoerig, 1987; Stoerig and Cowey, 1992; Sahraie, 1993; Barbur et al, 1994d; Brent et al, 1994) revealed by two-alternative forced choice methods. However, it is not so clear whether these subjects have PCRs. Keenleyside (1989) used 8° Gaussian targets of lower luminance than the background or chromatic gratings of 1.2 and 3.5 cycles per degree to investigate PCRs in subjects with cortical lesions, including GY. She did not measure any significant responses when these stimuli were presented in the subjects' affected fields. Sahraie (1993) used circular stimuli of 7°, of equal or lower luminance than the background, and of varying levels of saturation. He found that GY demonstrated measurable pupil responses when these stimuli were highly saturated, while for a medium saturation level a response was only measured to the red stimulus. However these results may have been contaminated by rod-driven light responses (see section 4.1).

Barbur et al (1994d) systematically investigated the PCRs of subject GY using the stimulus paradigm described in sections 4.2 and 4.3 (that is, using coloured stimuli isoluminant with the background with RLM<sub>s</sub> to eliminate any luminance contrast contribution). Figure 4.12 plots their results for GY's PCRs when the stimulus is presented foveally and Figure 4.13 plots their results for the stimulus presentation in the blind and sighted hemifields. It can be seen that significant PCRs are measured for each of the 12 stimulus colours used for foveal and sighted hemifields ( $p < 0.0005$  for all colours except 60 in the sighted hemifield where  $p < 0.025$ ) and these follow the same broad pattern as those measured for normal subjects in section 4.2. However little or no responses were measured in the blind field with this stimulus configuration ( $p > 0.05$  for all colours except 180 where  $0.05 > p > 0.025$ ). The coloured elements of this stimulus are much smaller than those considered by Sahraie (1993) so it seems

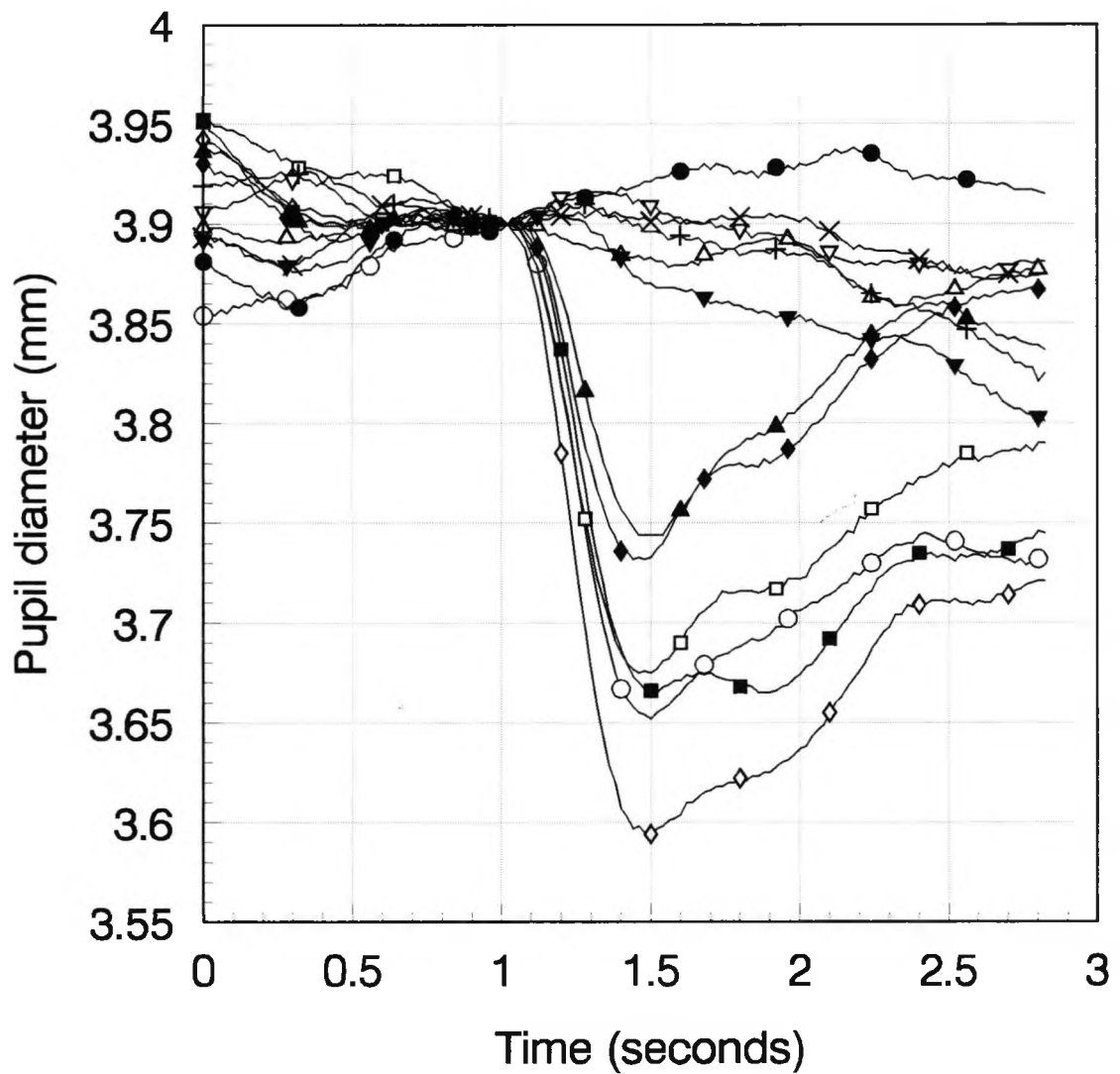


Figure 4.7 Pupil responses measured for protanope SA. Stimulus configuration as shown in Figure 4.1 Angles of chromatic displacement as listed in Table 4.3 *The response amplitudes associated with the different angles of chromatic displacement have been measured and are plotted in Figure 4.8.*

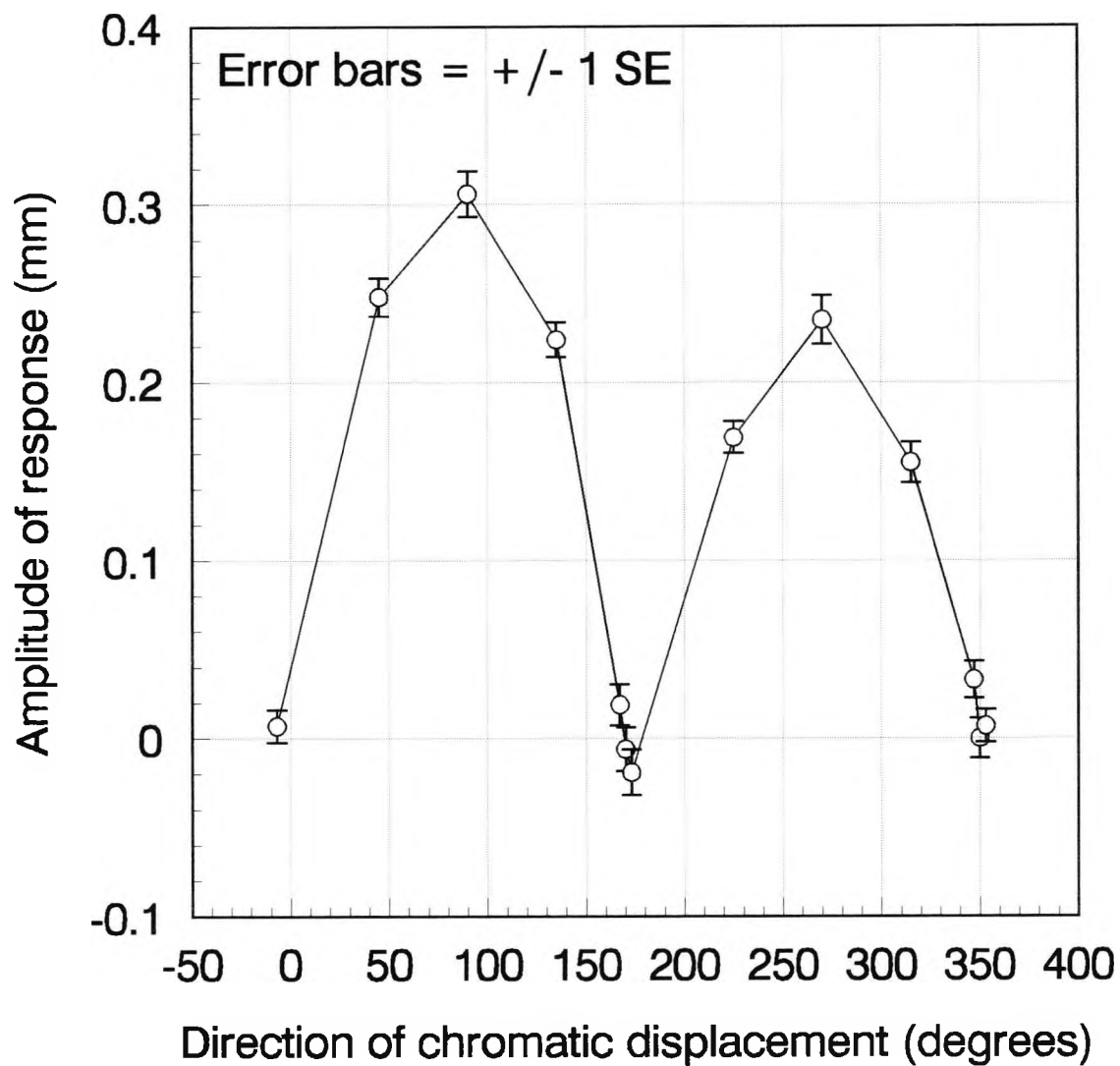


Figure 4.8 Pupil response amplitudes measured for protanope SA. Stimulus configuration as shown in Figure 4.1 Angles of chromatic displacement as listed in Table 4.3

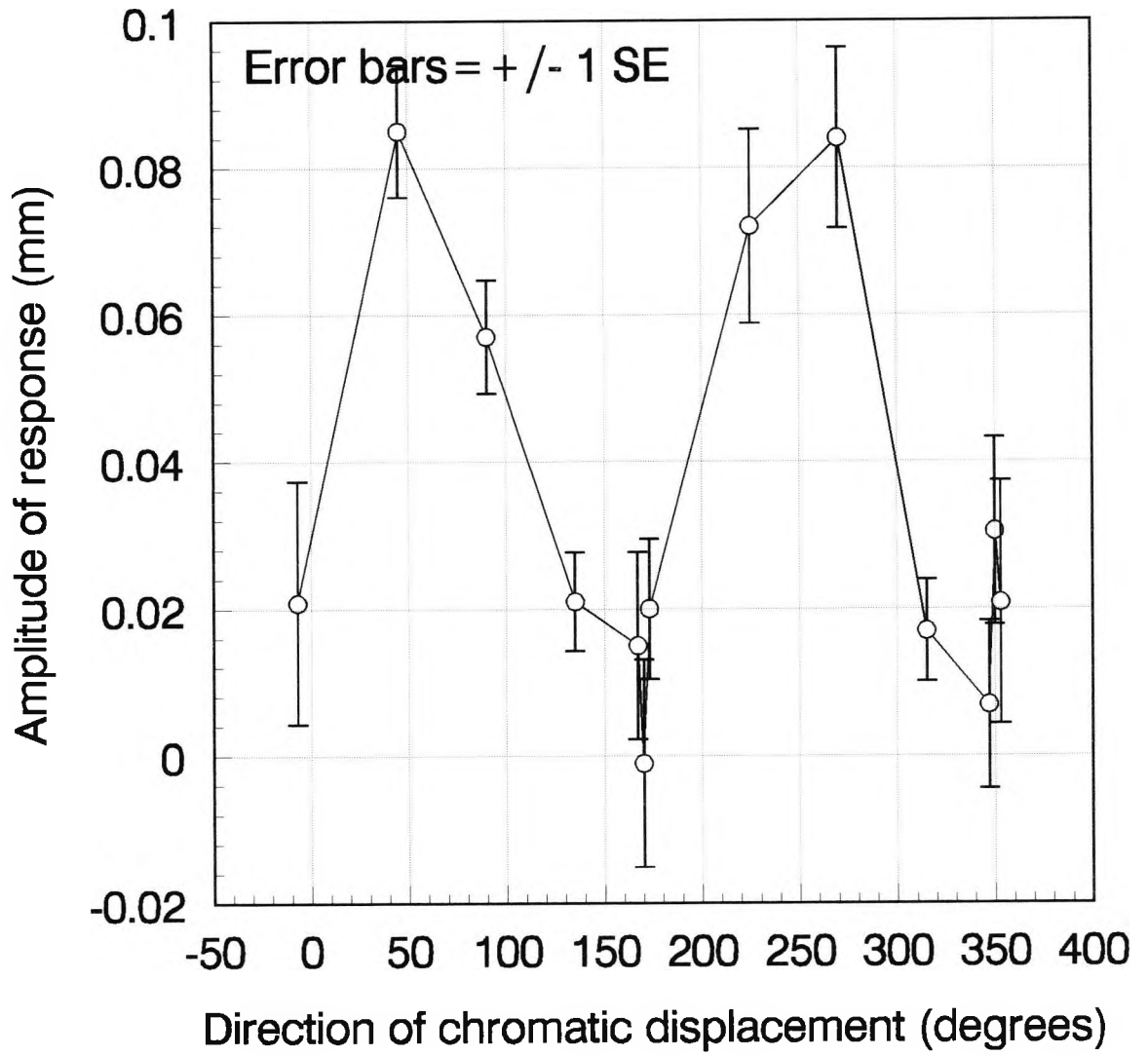


Figure 4.9 Pupil response amplitudes measured for protanope PE. Stimulus configuration as shown in Figure 4.1 Angles of chromatic displacement as listed in Table 4.4

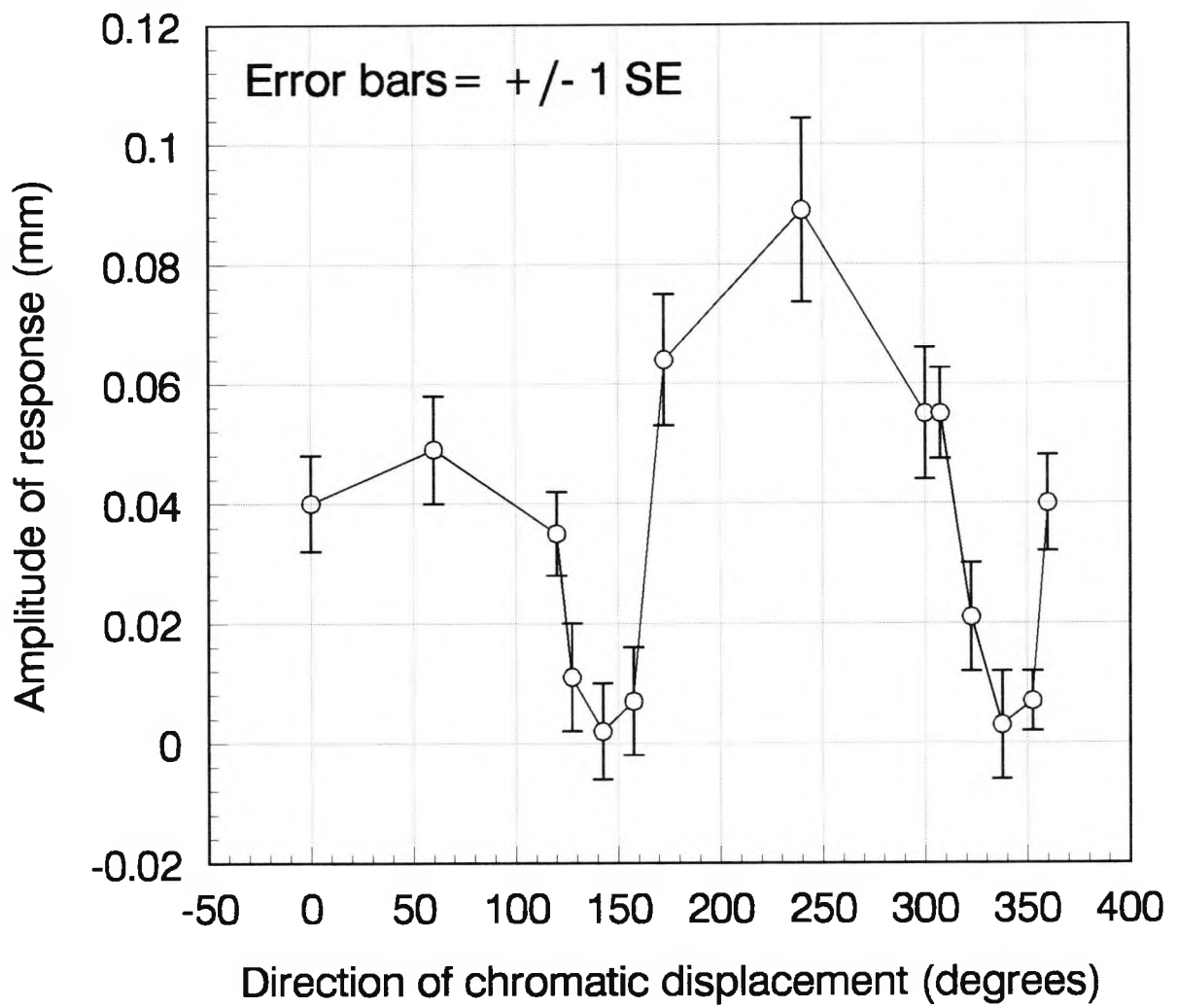


Figure 4.10 Pupil response amplitudes measured for deuteranope RV. Stimulus configuration as shown in Figure 4.1 Angles of chromatic displacement as listed in Table 4.5

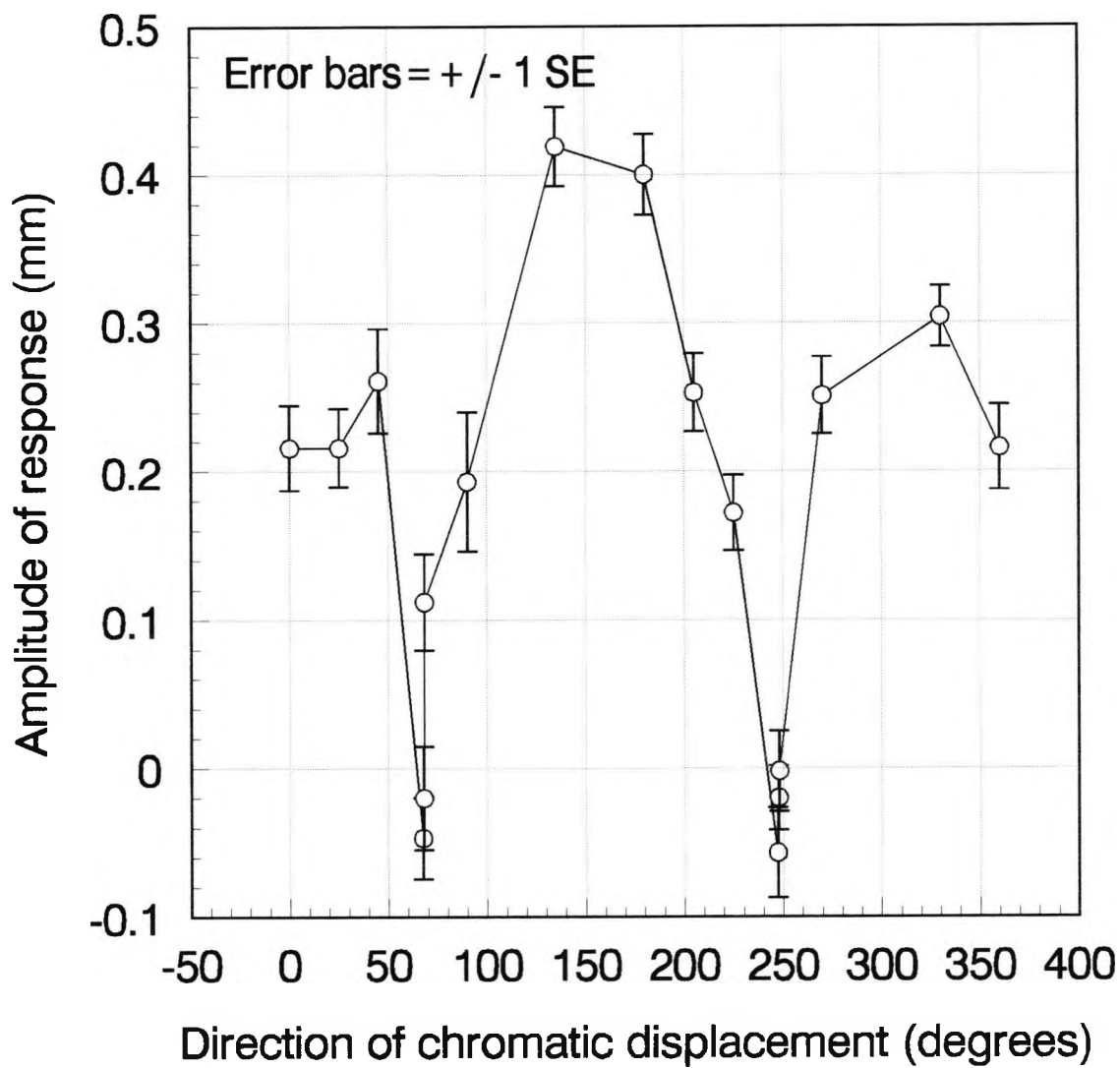


Figure 4.11 Pupil response amplitudes measured for tritanope JF. Stimulus configuration as shown in Figure 4.1 Angles of chromatic displacement as listed in Table 4.6

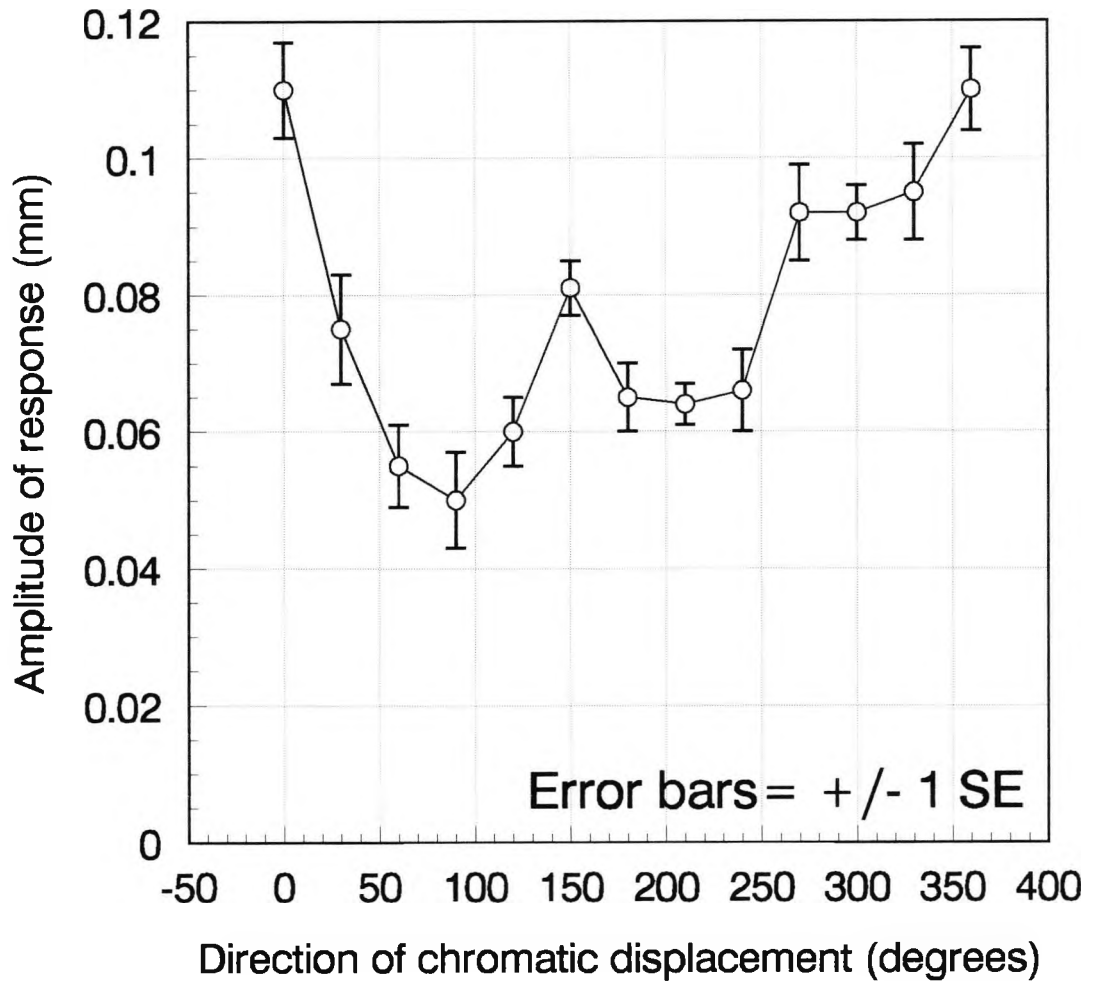


Figure 4.12 Pupil response amplitudes measured for subject GY, foveal presentation (Barbur et al, 1994d). Stimulus configuration as shown in Figure 4.1 Angles of chromatic displacement from 0° to 330° at 30° intervals

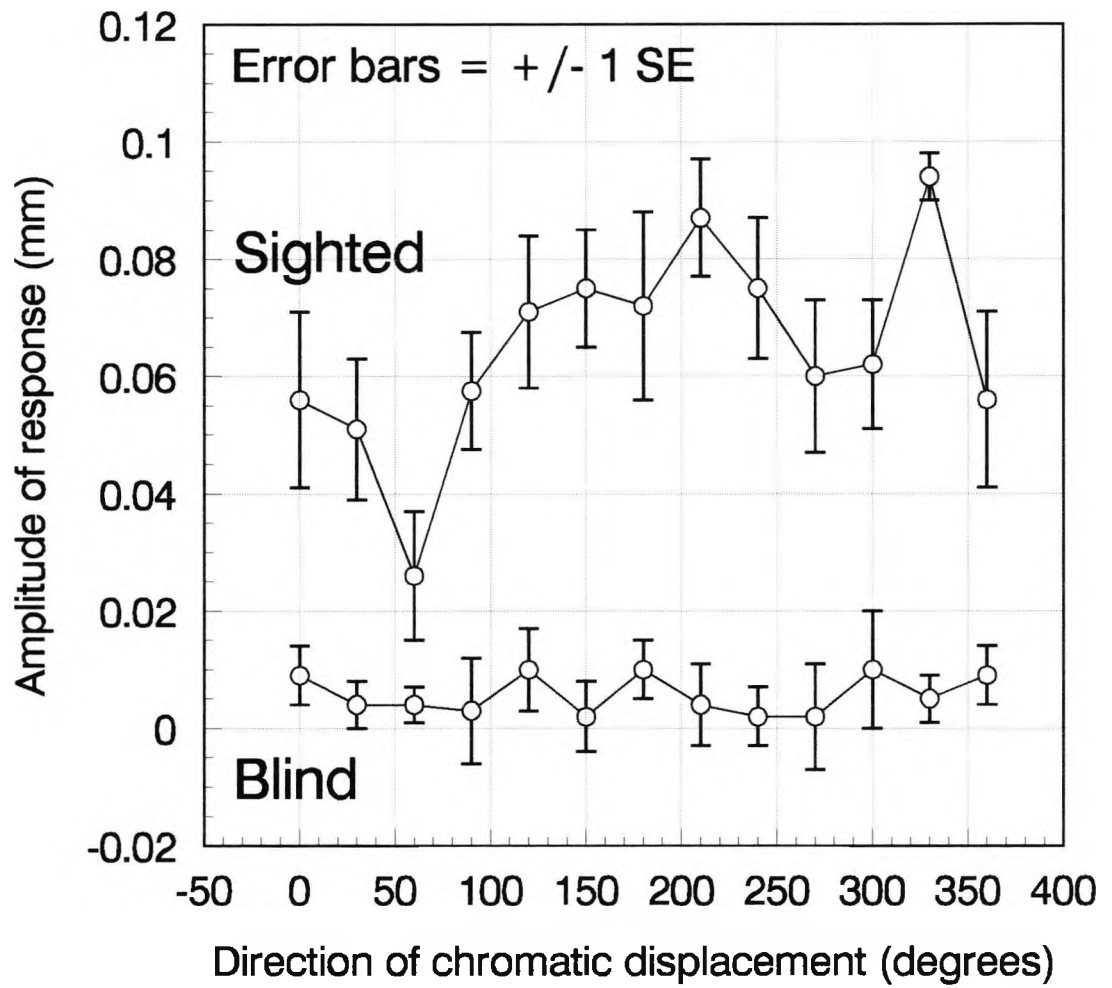


Figure 4.13 Pupil response amplitudes measured for subject GY, presentation in blind and sighted hemifields (Barbur et al, 1994d). Angles of chromatic displacement from 0° to 330° at 30° intervals

likely that stimulus size is an important factor in the measurement of PCRs in these subjects.

Barbur et al (1992c) used a similar test to examine the PCRs of a subject with cerebral achromatopsia, CAG, who has also been investigated by Barbur et al (1994a) and Williams (1995). The results are shown in Figure 4.14. No significant PCRs were measured ( $p > 0.1$ , except for 60 where  $0.05 > p > 0.025$ ).

In the light of the work described in Chapter 3, RLM<sub>s</sub> alone may not be sufficient to mask the detection of light flux increments associated with onset of a large stimulus. This section describes an experiment designed to investigate further the PCR in subject GY using a large stimulus size, in conjunction with local contrast (RLM<sub>s</sub>) and large field (RLM<sub>t</sub>) light flux masking.

A similar technique has been used to measure the PCRs in subject LR, a subject with partial cerebral achromatopsia. LR is a 69 year old male with a history of ischaemic heart disease, who suffered an occipital infarct 6 months before these tests were carried out. An MRI scan showed a left inferior occipital lesion and smaller focal lesions in both thalami and superficial cerebral white matter, which were likely to be of ischaemic origin (G.T.Plant, personal communication). Initially, he had a right homonymous quadrantic field defect, and reported that colours appeared grey, and he was only able to read the control plate of the Ishihara test with either eye. A month later the visual fields had improved apart from a small heteronymous defect in the right upper quadrant (more pronounced in the right eye). At this stage he passed all the Ishihara test plates with the left eye, but misread four plates with the right eye, with no particular pattern of errors. He was unable to see coloured targets in the upper right field. Six months after the infarct the visual fields were full, but there was still a homonymous region in the right superior field in which he perceived no colour. The colour vision in the right and left upper quadrants was subjectively investigated using CVTEST (see Chapters 2 and 5). The stimulus was a 2° square, and the results are shown in Figure 4.15 (indicated by circles). LR was unable to see the coloured stimulus even at the maximum chromatic displacement possible when it was presented in the right upper quadrant, although he performed quite well when the stimulus was

presented in the unaffected field (indicated by diamonds). Contrast sensitivity was measured in this region and in the corresponding left superior field using a computerised sinusoidal grating test, and the results are shown in Figure 4.16. It can be seen that contrast sensitivity is lower in the affected area than for the non-affected area for all spatial frequencies tested. However, there is certainly some achromatic vision present in this area.

#### Experimental procedure

The stimulus configuration used to measure PCRs in subject GY was similar to that shown in Figure 3.1, that is, a square target of  $13^\circ \times 13^\circ$  presented so that its centre was  $16.9^\circ$  from the fixation point. A mirror image was used to present the stimulus in GY's sighted hemifield. The viewing distance was 700 mm. The screen luminance was  $24 \text{ cd/m}^2$ , with CIE (x,y) chromaticity co-ordinates of (0.305, 0.323). Three stimulus colours were used with a chromatic displacement of 0.153 units on the CIE (x,y) diagram. The angles used were 5 (red), 96 (green) and 225 (blue), giving (x,y) co-ordinates of (0.457, 0.336), (0.289, 0.475) and (0.197, 0.215). The luminance of the coloured stimuli was  $24 \text{ cd/m}^2$ , that is, isoluminant with the background according to the CIE standard observer.. However, because this was a large stimulus presented away from the fovea, the stimulus and background were almost certainly not isoluminant. Each stimulus was presented with no luminance masking, with  $\text{RLM}_s$  only of 45% and with  $\text{RLM}_s$  of 25% and  $\text{RLM}_t$  of 45%. It was hoped that this latter condition would prevent the response of the pupil to a luminance increment associated with stimulus onset, as this would be masked by the combined spatiotemporal modulation. Each stimulus condition was presented 32 times and since binocular measurements were made, the results for the right and left eyes were averaged. PCRs were measured using the same stimulus configuration and methods for normal subject JB's right hemifield, and for GY's blind and sighted hemifields.

For subject LR, it was first necessary to establish a stimulus configuration that allowed as large a stimulus size as possible while confining it to the area of field in which there was no colour perception. Using CVTEST the optimum configuration was found to be an  $8.6^\circ$  square, whose centre was positioned  $10^\circ$  above and to the right of fixation. A mirror image was used to measure the PCRs on the unaffected side. The colours used

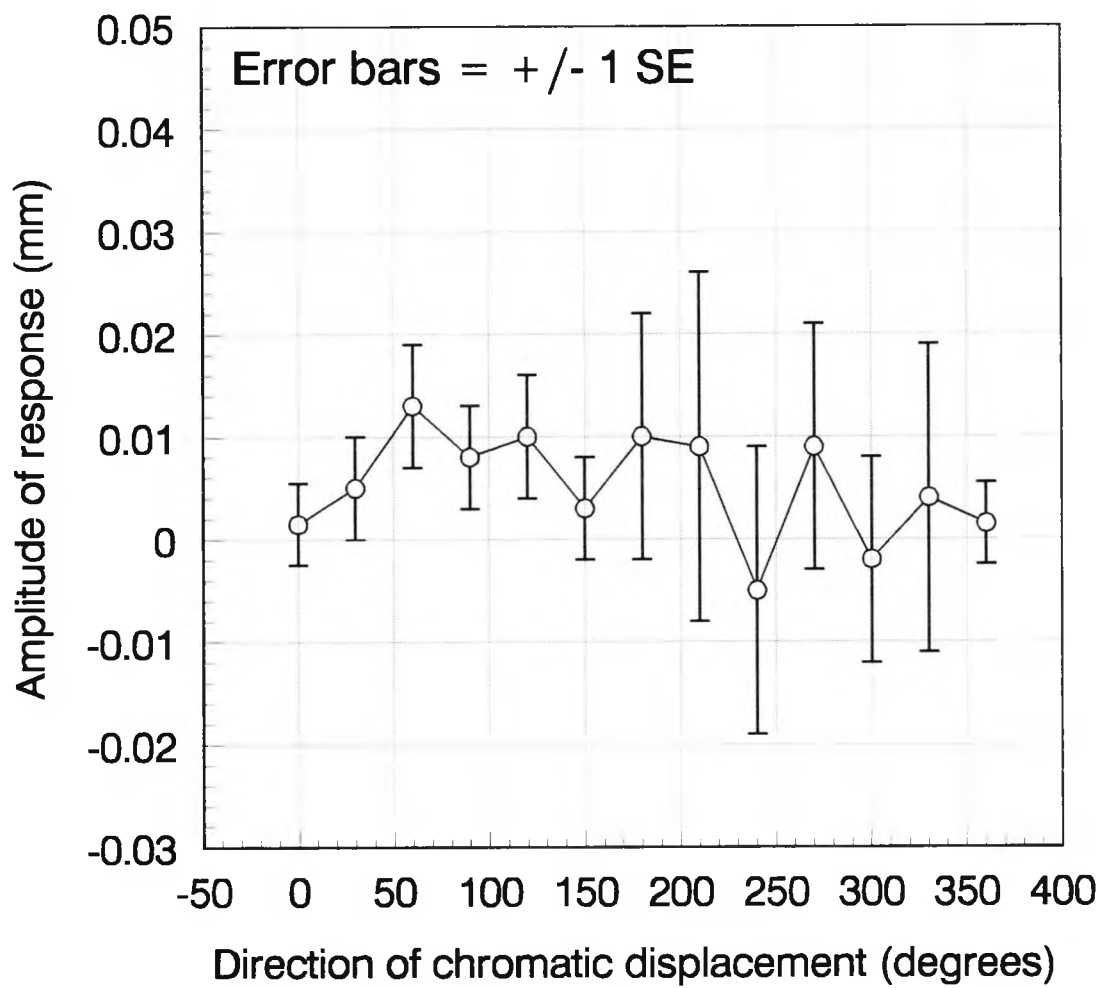


Figure 4.14 Pupil response amplitudes measured for cerebral achromatopsic subject CAG (Barbur et al, 1992c). Angles of chromatic displacement from 0° to 330° at 30° intervals

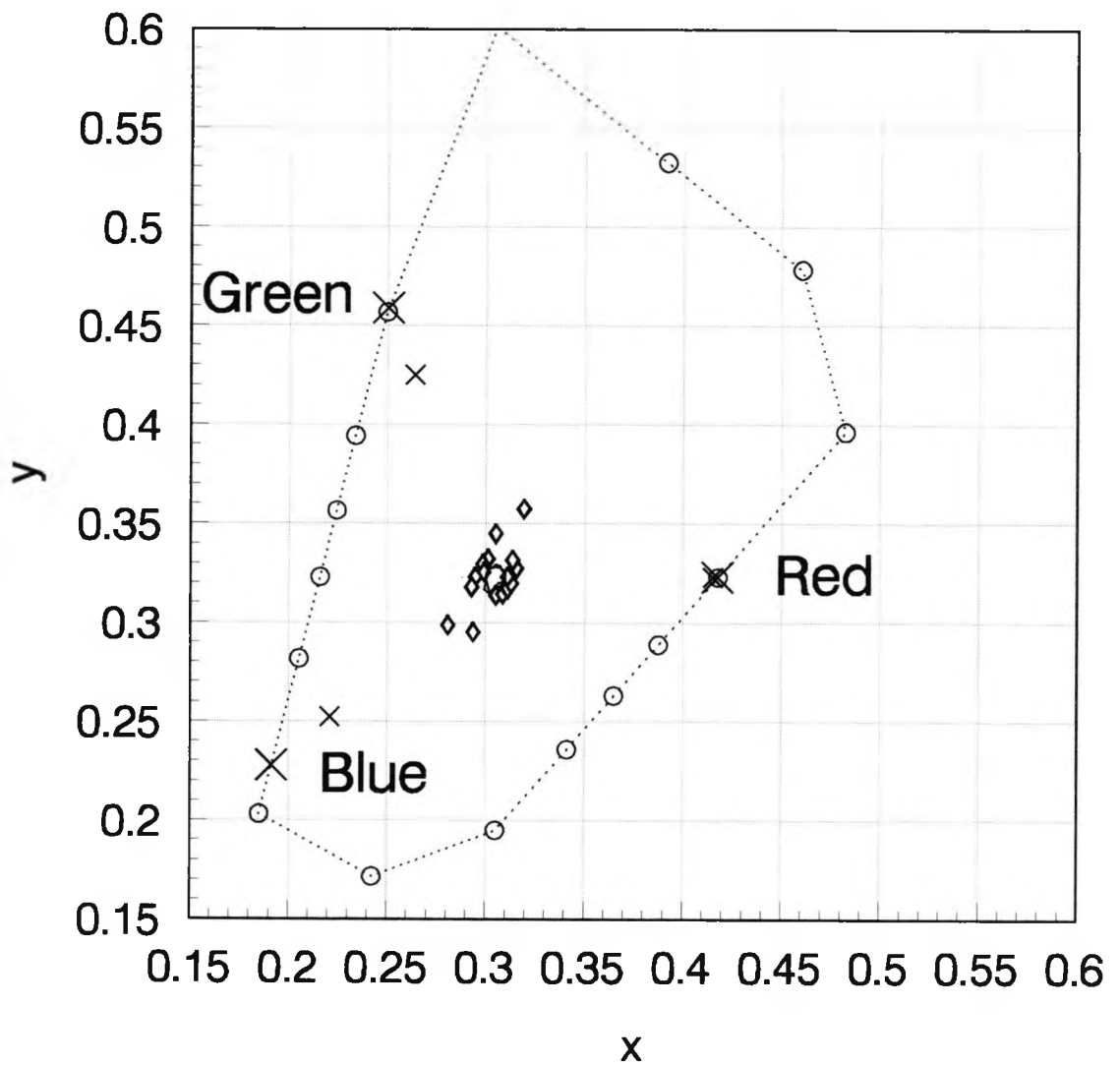


Figure 4.15 Chromatic discrimination thresholds for subject LR (incomplete cerebral achromatopsia) in his affected and unaffected fields, using the computerised colour vision test described in Chapters 2 and 5. A 2° square was presented in the affected field, which was not perceived even at the maximum chromatic displacement (circles), although it was seen readily when presented in the mirror image position in the opposite field (diamonds). The large crosses indicate the thresholds for an 8.6° square (presented so that its centre was 10° above and to the right of fixation) for angles of 0° (red), 112° (green) and 220° (blue). This stimulus was not perceived by LR at the maximum saturation that the screen would allow. The small crosses indicate the stimulus chromaticities used for the pupil colour response experiments, which were also unperceived by the subject

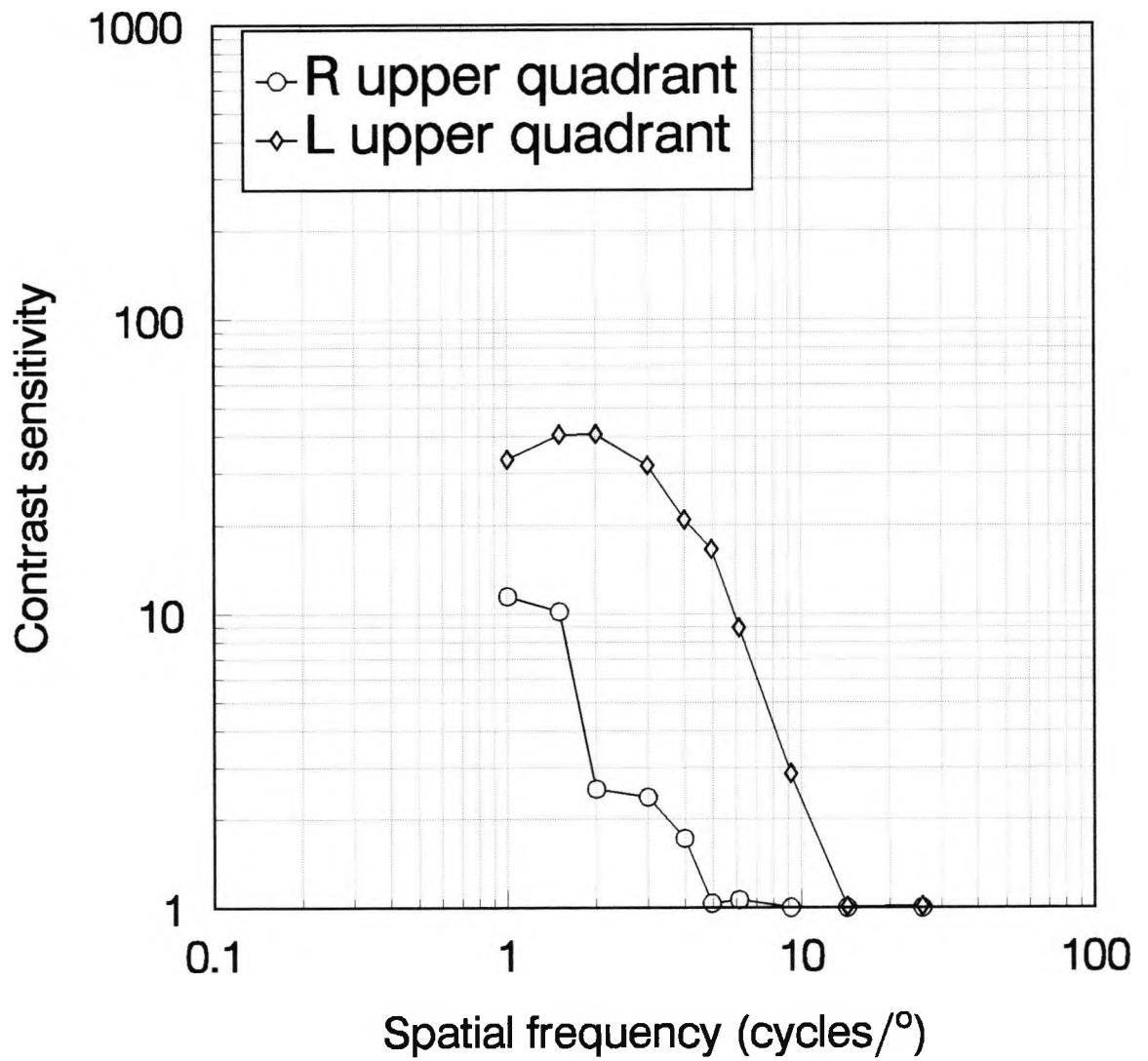


Figure 4.16 Contrast sensitivity for subject LR (incomplete cerebral achromatopsia). Contrast sensitivity was measured to achromatic sinusoidal gratings presented in the part of the right superior field affected by the brain lesion (circles) and in the corresponding part of the normal left superior field (diamonds)

had angles of chromatic displacement of 0 (red), 112 (green) and 220 (blue). LR was unable to perceive these colours even at the maximum saturation that the screen would allow, indicated by the large crosses in Figure 4.15. The stimulus conditions used for the pupillometry were a chromatic displacement of 0.11 (x,y) units in these directions, indicated by the small crosses in Figure 4.15. The (x,y) co-ordinates for these colours were therefore (0.415, 0.323), (0.264, 0.425) and (0.221, 0.252). The coloured stimuli were presented with  $RLM_s$  of 30% and  $RLM_t$  of 15%. Interleaved with the three coloured stimuli was an achromatic stimulus whose contrast was 60%. This was to ensure that a normal PLR was present, and the stimulus was presented with no luminance masking. Each stimulus was presented 36 times, and the average result taken. The results obtained for LR's left eye were marred by unwanted infra-red reflections from his spectacles, so only the data obtained from his right eye could be used.

## Results

The results obtained for normal subject JB are shown in Figure 4.17. It can be seen that large responses are measured when the coloured stimulus is presented alone. When  $RLM_s$  and  $RLM_t$  <sup>are used</sup> the amplitudes of the responses are smaller, but they are significant for all three colours ( $p < 0.0005$ , with one-tailed t-test, for all three colours). Very similar results are obtained for GY's sighted field, shown in Figure 4.18 ( $p < 0.0005$ , for all three colours). For his blind field (Figure 4.19), large responses are measured to the red and blue stimuli when they are presented without luminance masking. When  $RLM_s$  and  $RLM_t$  are used, the response amplitudes are smaller, especially for the green and blue stimuli, but the responses are all significant ( $p < 0.0005$ ).

The responses measured for stimuli presented in the unaffected and affected regions of LR's field are shown in Figures 4.20 and 4.21 respectively. Significant responses are seen for all four stimuli when they are presented in the normal field ( $p < 0.0005$ ). Figure 4.20 shows that the responses to the coloured stimuli have a longer latency than the response to the achromatic stimulus, which supports the view that they are different from a pupil constriction evoked by a luminance increment. For the affected side, a significant response is seen to the achromatic stimulus ( $p < 0.0005$ ). Small but

significant responses are seen for the red and blue stimuli ( $p < 0.005$ ) while for the green stimulus, the significance level is lower ( $0.05 < p < 0.025$ ). There is a greater difference between the latencies of the PCRs and that of the PLR than for the unaffected side.

## Conclusions

The results described in this section show that pupil responses can be measured to coloured stimuli for both subjects. It seems likely that these are true PCRs because of the luminance masking used.

It has not been shown anatomically what neural mechanisms are involved in the generation of the PCR. From the results described above and in previous work, it is clear that there is some cortical input to the PCR, as coloured stimuli which produce large responses in normals do not elicit any response in subjects with cortical lesions. It may be that presentation of a coloured stimulus causes excitation in the cortex which reduces the supranuclear inhibitory input to the pupillomotor nucleus, which in turn causes a pupillary constriction.

However, if large saturated coloured stimuli are used, the results for GY show that PCRs can be demonstrated in subjects lacking primary visual cortex. If measures are taken to prevent any response to luminance increments contaminating the results, information about the stimulus wavelength must be reaching the pupillomotor system without passing through the striate cortex.

Pupil responses in normal subjects have been shown to display colour-opponent mechanisms (Hedin and Glansholm, 1976; Krastel et al, 1985). Primate studies of chromatic properties of superior colliculus cells indicate that no chromatic opponency is found (Marrocco and Li, 1977) although cells responding preferentially to certain wavelengths have been found (Kadoya et al, 1971; Marrocco and Li, 1977). It may be that the subcortical pathway can carry residual chromatic information when the stimuli are sufficiently large and saturated. Such signals may still reach extrastriate areas that are normally involved in processing chromatic signals received via intact primary visual cortex. The signals would have to use an alternative neural route to reach the extrastriate cortex when primary cortex is damaged (see below). Once the chromatic

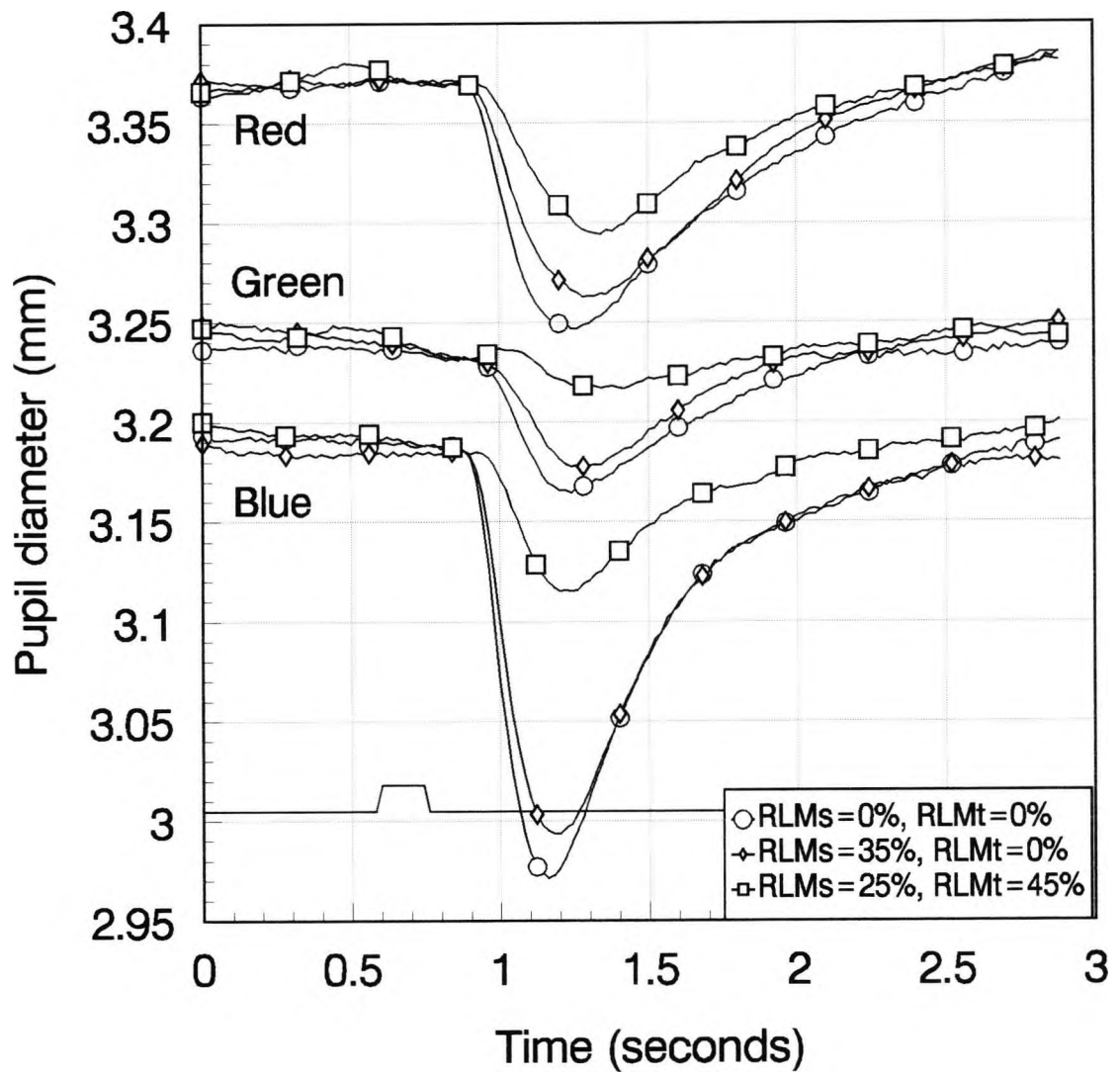


Figure 4.17 Pupil responses measured for subject JB to coloured stimuli. Stimulus configuration as shown in Figure 3.1 (a  $13^\circ$  square presented so that its centre was  $16.9^\circ$  from fixation), angles of chromatic displacement were  $5^\circ$  (red),  $96^\circ$  (green) and  $225^\circ$  (blue)

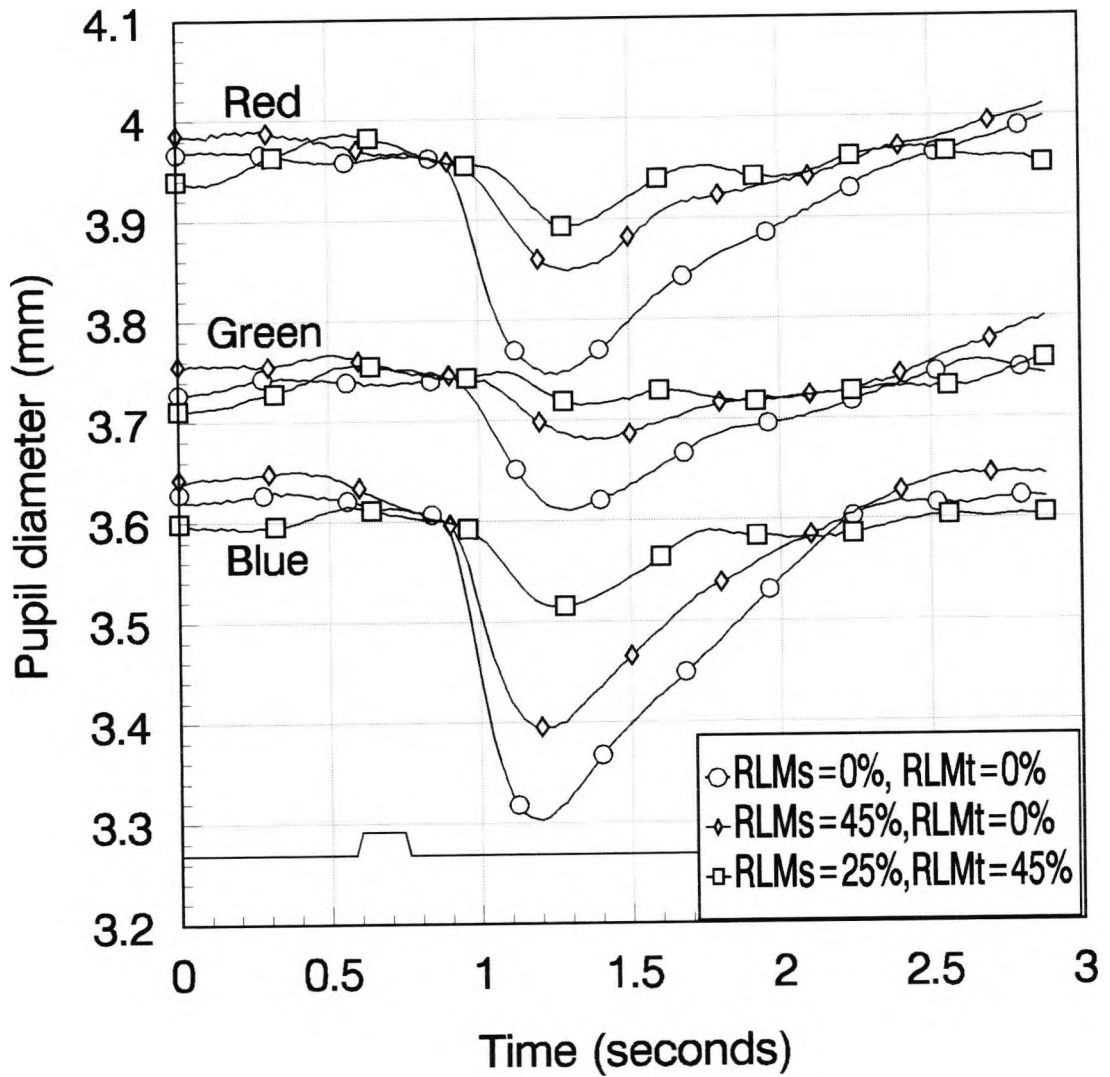


Figure 4.18 Pupil responses measured for subject GY to coloured stimuli presented in his sighted hemifield. Stimulus configuration was a mirror image of that shown in Figure 3.1 (a  $13^\circ$  square presented so that its centre was  $16.9^\circ$  above and to the left of fixation), angles of chromatic displacement were  $5^\circ$  (red),  $96^\circ$  (green) and  $225^\circ$  (blue)

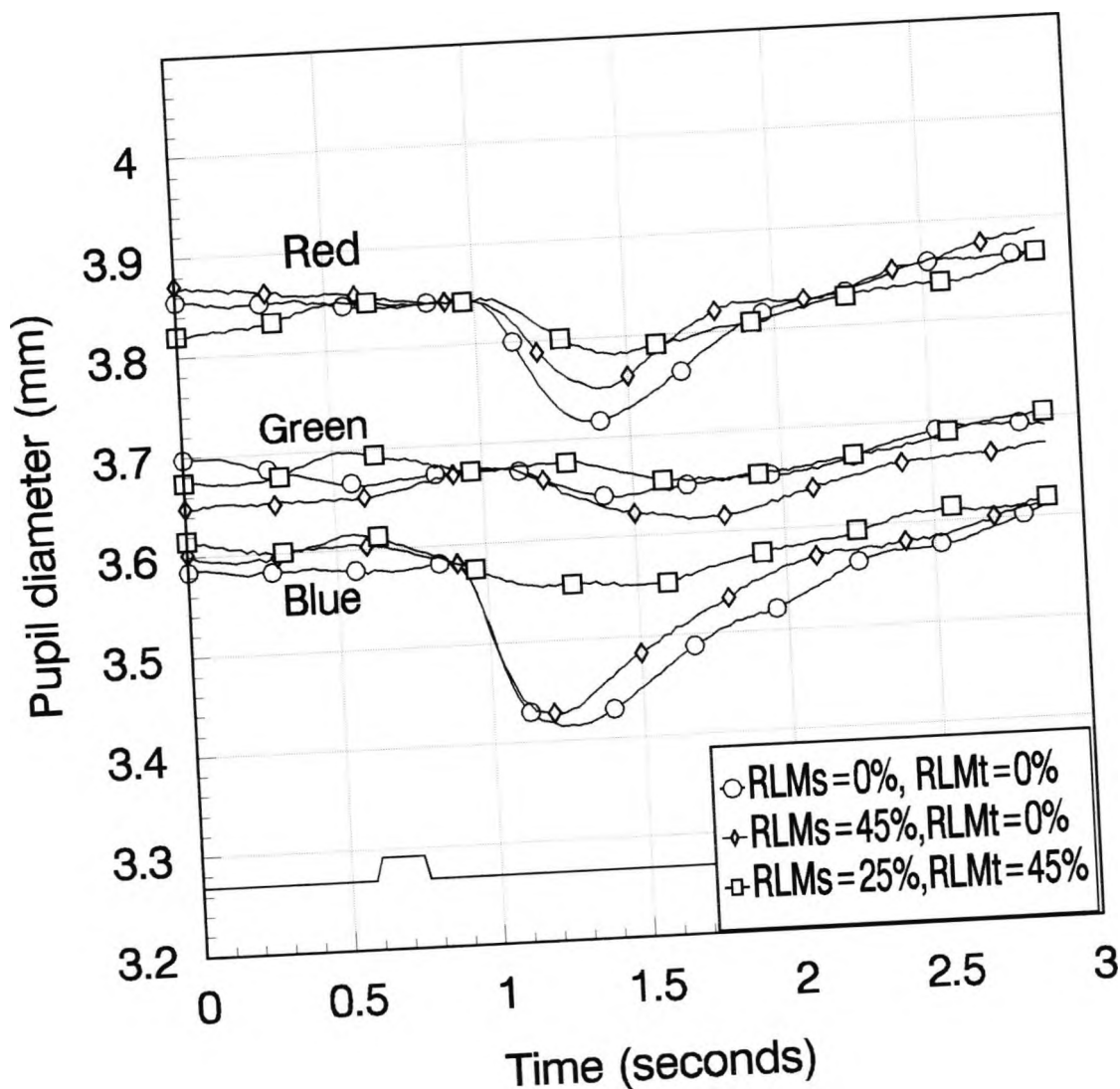


Figure 4.19 Pupil responses measured for subject GY to coloured stimuli presented in his blind hemifield. Stimulus configuration was as shown in Figure 3.1 (a  $13^\circ$  square presented so that its centre was  $16.9^\circ$  above and to the right of fixation), angles of chromatic displacement were  $5^\circ$  (red),  $96^\circ$  (green) and  $225^\circ$  (blue)

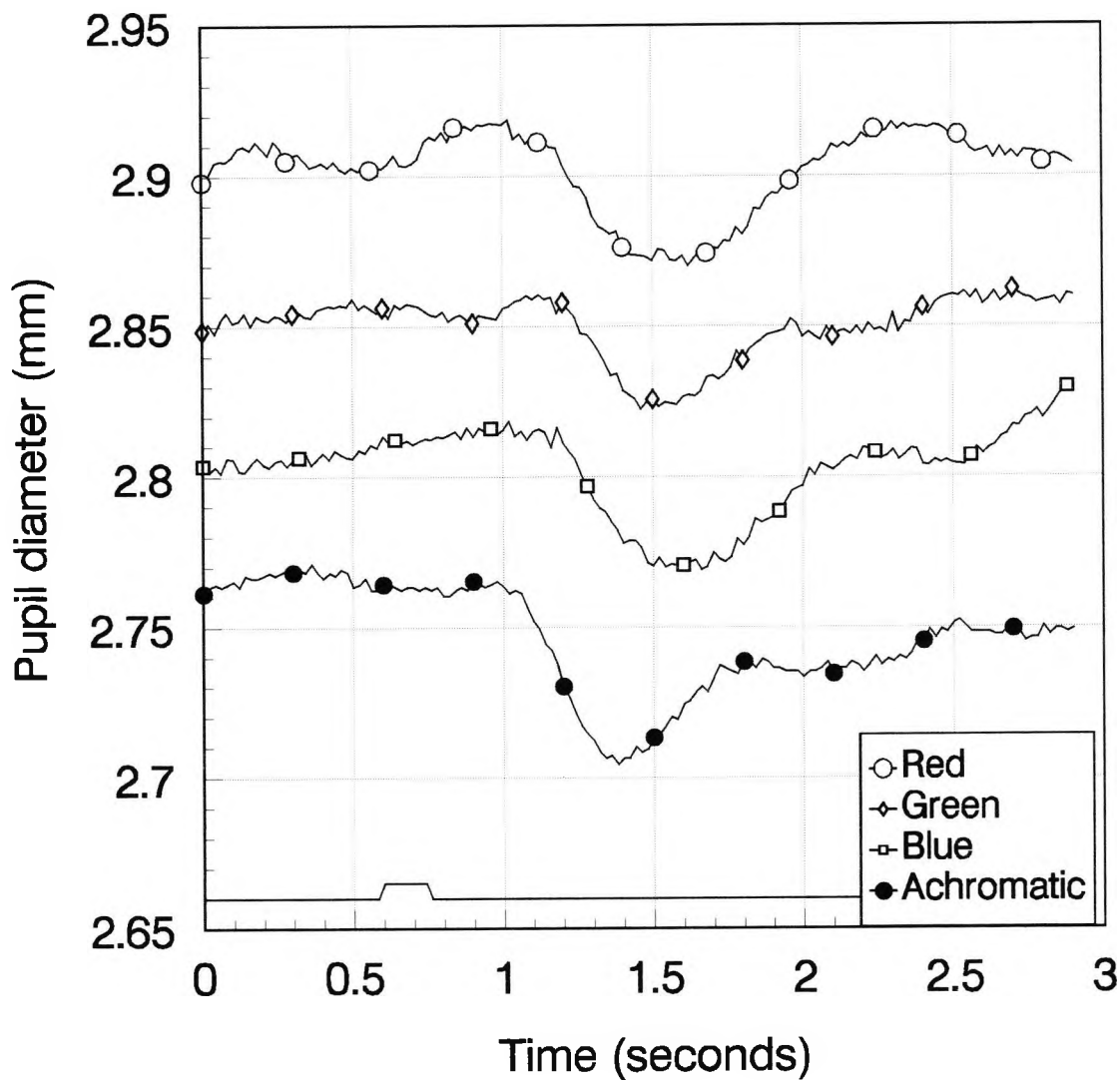


Figure 4.20 Pupil responses measured for subject LR to coloured stimuli presented in his unaffected visual field. Stimulus configuration was an  $8.6^\circ$  square presented so that its centre was  $10^\circ$  above and to the left of fixation, angles of chromatic displacement were  $0^\circ$  (red),  $112^\circ$  (green) and  $220^\circ$  (blue),  $RLM_s=30\%$ ,  $RLM_t=15\%$

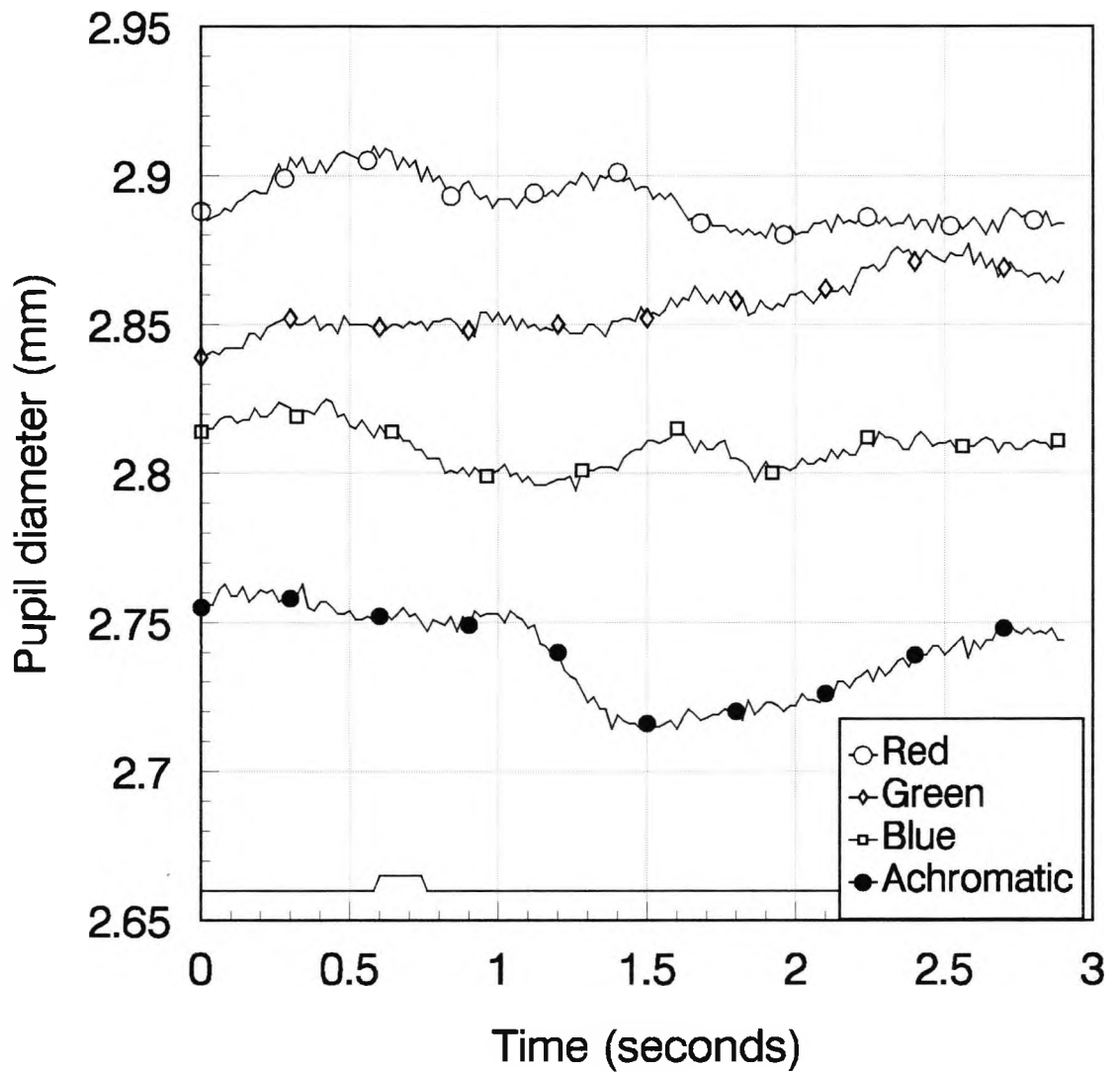


Figure 4.21 Pupil responses measured for subject LR to coloured stimuli presented in his affected visual field. Stimulus configuration was an  $8.6^\circ$  square presented so that its centre was  $10^\circ$  above and to the right of fixation, angles of chromatic displacement were  $0^\circ$  (red),  $112^\circ$  (green) and  $220^\circ$  (blue),  $RLM_s=30\%$ ,  $RLM_t=15\%$

information reaches the extrastriate areas and is processed, the PCR may be initiated in the normal way by interruption of the inhibitory action on the Edinger-Westphal nucleus. A recent study by Barbur et al (in press) using fMRI brain imaging found that GY's superior colliculus showed significant activation when a red stimulus was presented in his blind hemifield, as well as areas of the brain outside the classical visual areas. This finding is consistent with the possibility that subcortical structures channel information to other areas of the brain which mediate GY's residual colour vision and PCRs.

Cowey and Stoerig (1991a,b) and Kisvarday et al (1991) discuss the neural pathways which could provide an indirect pathway from the retina to extrastriate cortex. Cowey and Stoerig (1991b) have shown that while most LGN cells degenerate following cortical ablation in monkeys, a few remain which project to the V4 region. P-beta retinal ganglion cells are subject to transneuronal retrograde degeneration, leaving the affected retina with approximately equal numbers of alpha, beta and gamma ganglion cells. It has been shown that retinal ganglion cells project to LGN interneurons which project to the remaining LGN P and M cells. There is also input to the LGN from the superior colliculus which receives direct retinal input which is apparently anatomically normal. So despite the degeneration of the LGN when V1 is destroyed, there is still a pathway for information to travel from the retina to LGN (via LGN interneurons or superior colliculus) to extrastriate cortex (V4). V4 could be the source of cortical influence over the PCR in normals and subjects with damaged striate cortex. If V1 is intact there is likely to be a greater input to V4 than if the information has to travel via a few surviving neurons, which could account for the reduced PCRs found in subjects with damaged striate cortex.

What of subjects with preserved V1 but (presumably) damaged V4 causing achromatopsia? If V4 is the source of PCRs, then these patients should not have measurable PCRs. The results for LR show that, again with large saturated stimuli, it is possible to measure small but significant PCRs. In this experiment the largest response is seen to the red stimulus, then blue, then green. These are qualitatively similar to the results measured for GY's blind field, which may indicate a common underlying mechanism, and this could be the subcortical pathway described above. It would be

useful to test PCRs in more subjects with achromatopsia to see if this is a common finding. fMRI techniques in such patients may give more information about the pathways involved.

#### 4.5 Summary

The work described in this chapter builds on the results of previous studies which have measured PCRs. A computerised luminance masking technique has been used to ensure that the responses measured are not contaminated by PLRs.

Section 4.2 describes the PCRs measured in normal subjects. Responses were clearly present for all the coloured stimuli used. However, there was inter-subject variability in terms of amplitude and to some extent the minima of the graphs. It would be useful to extend this study to include more normal subjects to build up a picture of this inter-subject variability.

Section 4.3 describes the abnormal PCRs found in dichromatic subjects. In contrast to the PCRs measured in normal subjects, dichromats do not demonstrate PCRs to those colours which fall in the same isochromatic zone as the background. By extending this work to larger numbers of dichromatic subjects it may be possible to select a few critical colours which will distinguish between normals, protanopes, deuteranopes and tritanopes and which could form the basis of a rapid objective colour vision test. Difficulties may be encountered for tritanopes because of the extremely narrow isochromatic zone. The equipment required to extract such small pupillary responses probably excludes this method from widespread clinical use, but it could prove a valuable research method for studying colour vision objectively, for example, in infants.

There is also potential for this method to be used as a tool to investigate neural pathways involved in the PCR by comparing normal results with those obtained from subjects with known lesions. Section 4.4 attempts to do this by comparing the PCRs measured in subjects with damage to V1 or V4. In both cases, no PCRs are measured

when small stimuli are used of medium saturation, which suggests that there is cortical involvement in the generation of PCRs to such stimuli, perhaps in V4. However, when much larger, highly saturated stimuli are used, small but significant PCRs can be measured which are qualitatively similar in the two subjects investigated. This may indicate a common underlying mechanism, which could be subcortical.

There is some difficulty in obtaining subjects with clearly defined brain lesions who are able to participate in the long experiments required for a thorough investigation of colour vision by means of pupil measurement. Ideally, this study should be extended to cover a whole range of colours for patients with different lesions to try to build up a clearer picture. For example, from the experiments described in Section 4.4, it is not possible to conclude whether there is any colour-opponent input to the PCRs. If more colours were measured, the presence or absence of the minima and maxima such as those seen in Figures 4.3, 4.4 and 4.5 could give a clue as to whether any colour-opponent mechanisms are involved. If they are, it is unlikely that the normal subcortical pupillary pathway is solely involved in generating PCRs, and cortical areas or perhaps the pulvinar (Felsten et al, 1983) may be implicated.

It would also be interesting to investigate spatial tuning of the PCRs in these subjects, since it appears that no responses are measurable for small stimuli, but that they are present if large stimuli are used. This could be achieved by varying stimulus size to find a threshold size for which PCRs are measured. It might be possible to compare these findings with receptive field sizes of neurons in the different areas that have been implicated in the generation of PCRs.

Gamlin et al (in press) have carried out a study into the presence of PCRs in rhesus monkeys. Pupil responses were measured for twelve different directions of chromatic displacement, although there was less variation between colours than found for the human subjects in this study (section 4.2). The rod contrast associated with the chromatic stimuli was calculated, and it did not appear that the responses measured were related to rod input. The measurement of PCRs in monkeys could be used as a basis for selective lesion studies to explore more fully the relationship between different cortical areas and the PCR.

## **CHAPTER 5 COLOUR VISION IN SUBJECTS WITH DAMAGE AFFECTING THE EARLY-STAGE VISUAL PATHWAYS**

### 5.1 Introduction

The chromatic discrimination ability of an observer may be measured by establishing a range of chromatic changes that cause no change in perceived colour. In subjects with poor colour discrimination, a larger range of colours will appear to be identical than for subjects with normal colour vision. The Nagel anomaloscope uses this principle to assess the severity of protan and deutan defects - an observer with a severe protanopia, for example, will accept a large range of red/green ratios as matching a given yellow (Wyszecki and Stiles, 1982). MacAdam (1942) plotted chromatic discrimination ability as a series of ellipses in the CIE (x,y) chromaticity diagram, and his results for one normal observer are shown in Figure 5.1. Colours defined by chromaticity co-ordinates within each ellipse appear to be identical. Relatively small ellipses are obtained for a normal observer. However, a dichromatic observer will not perceive any colour difference over a larger range of chromaticity changes, and the normal chromatic discrimination ellipse extends into an isochromatic zone.

The colour vision test used for experiments in this chapter was developed at City University and has been previously described by Birch et al (1992) and Barbur et al (1992a, 1993a). It presents isoluminant coloured stimuli on a high resolution colour display (see Chapter 2) and the task of the observer is to say whether or not the stimulus is seen. A staircase procedure, which varies the chromatic displacement of the test object from the background, is used to determine the chromatic discrimination threshold. The size, shape, colour and luminance of the stimulus, and the colour and luminance of the background can be selected by the examiner within the limits of the program and the screen phosphors.

With all colour vision testing, it is the chromatic information which is of interest, and it is therefore vital to remove any luminance contrast cues associated with the stimulus presentation which could be used by the subject to detect the target. This has been achieved by using luminance masking, for example, using spots of different

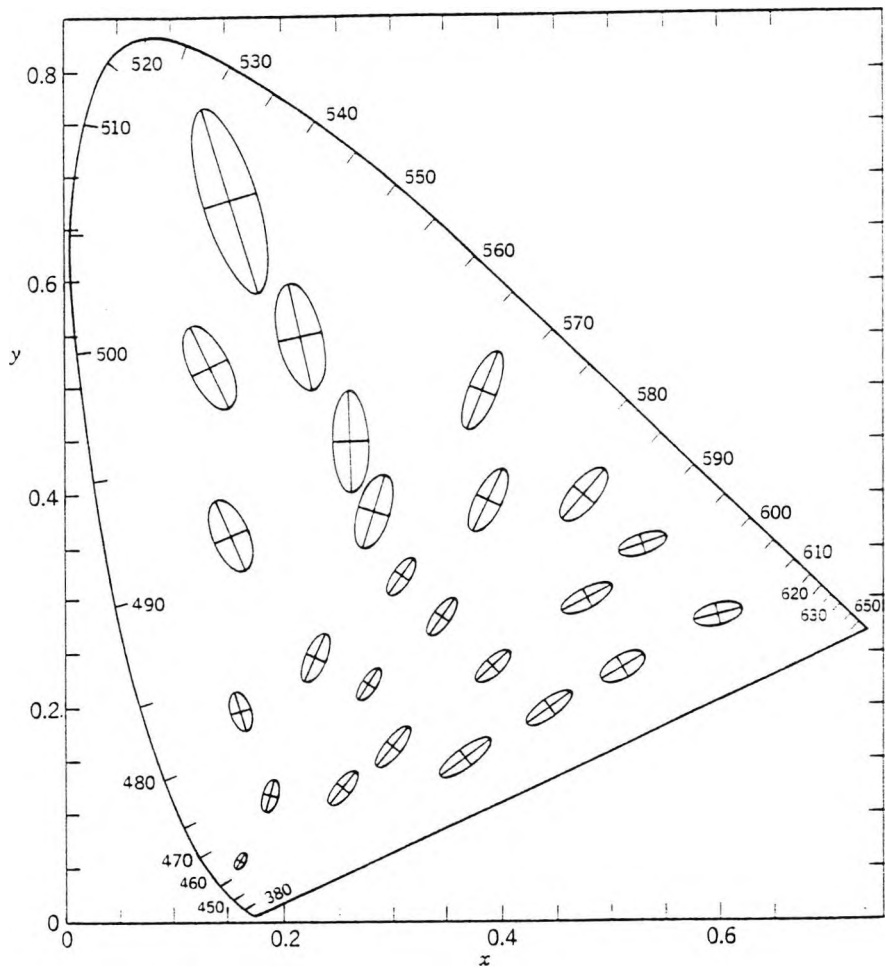


Figure 5.1 MacAdam (1942) ellipses plotted on the CIE 1931 (x,y) chromaticity diagram. The axes of the plotted ellipses are ten times their actual lengths. The centre point of each ellipse represents a test colour formed from a fixed combination of red, green and blue primaries. Observers were required to form a match for the test colour using the same three primaries, and the ellipses show the standard deviations of the measurements made (in x,y chromaticity units). The 'just noticeable colour differences' were found to be about three times as large as the corresponding standard deviation. (Wysecki and Stiles, 1982)

reflectances in tests based on pseudoisochromatic plates (such as the Ishihara and HRR tests), or patches of different luminance in computer based tests (Mollon and Reffin, 1989). In the test described here, the luminance masking is achieved by presenting the coloured stimulus embedded in an array of checks whose luminance changes randomly every few milliseconds (see Chapter 2), that is, there is Random Luminance Modulation (RLM<sub>s</sub>) of the checks. The coloured stimulus is formed by a subset of these checks undergoing a chromatic change as well as the ongoing luminance changes. It has been shown that increasing the RLM<sub>s</sub> increases the threshold luminance required for detection of an achromatic stimulus, but has no effect on colour discrimination thresholds in normal observers (Birch et al, 1992; Barbur et al, 1992a, 1993a).

A major advantage of this test is that the subject is not required to set isoluminance, and that any type of colour vision deficiency can be investigated. Acquired colour vision defects are relatively common in diseases of the retina and optic nerve (Grutzner, 1972; Birch et al, 1979; Krastel and Moreland, 1991; Plant 1991) and as such may be useful in diagnosis and/or monitoring the progression of a condition. Conventional tests used in colour vision screening, such as the Ishihara and City University tests, do not give a detailed picture of the colour vision deficiency and may in some cases miss a colour vision abnormality altogether.

This computerised test has been used to investigate colour vision in the absence of V1 (Barbur et al, 1994d) and in achromatopsic subjects (Barbur et al, 1994a). This chapter describes an investigation of the residual colour discrimination in two subjects referred for visual assessment, where other colour vision tests had given confusing results (Cole (1995) and section 5.3). The results obtained for these subjects suggested some kind of optic neuropathy. Similar investigations were carried out with subjects who had had optic neuritis to see if the same results were obtained (section 5.4).

It was necessary first to establish in detail the pattern of results expected in normal subjects. An experiment was carried out to this end and is described in section 5.2.

## 5.2 Chromatic discrimination ability in normal subjects

### Introduction

Two different types of stimulus were used by Barbur et al (1994a) to examine the way in which chromatic signals are used, and the same conditions were used to examine the colour vision of the two abnormal subjects described in the next section. It was necessary to establish the results expected for normal subjects using the same conditions.

The first test pattern is a set of vertical coloured bars which 'pop up' amid the background of the RLM<sub>s</sub> when a chromatic displacement is generated. This test arrangement will be referred to as the pattern test. The subject is required to say whether or not he can see the vertical bars. He should only be able to detect the bars if he can discriminate the colour of the bars from that of the background, that is, the detection of spatially structured objects is based on chromatic signals only. Results for a typical normal trichromat for this type of stimulus were given in Barbur et al (1993a). Similar results were obtained with six other subjects.

The second stimulus configuration used by Barbur et al (1994a) and in this chapter is based on a block of colour defined by luminance contrast and undergoing a chromatic displacement. In this case, the block is always at a higher luminance than the background and is thus always visible to the subject. The same RLM<sub>s</sub> affects both the block and the surrounding border of checks. The task is to detect a colour change in the central block. Results for a normal trichromat are given by Barbur et al (1994a). This test will be referred to as the colour test.

This section describes a more extensive investigation of results obtained in normal subjects undergoing the pattern and colour tests.

### Experimental procedure

Colour discrimination thresholds were measured for eleven subjects, (four female and seven male, ages ranging from 22 to 42). The subjects viewed the screen from 700 mm, wearing an appropriate spectacle correction if required. The stimuli were

presented foveally and were viewed binocularly in the centre of the display, which subtended a visual angle of  $26^\circ \times 21^\circ$ . The CIE (x,y) chromaticity co-ordinates of the uniform background field were (0.305, 0.323), the same as the background used by MacAdam (1942) in his original experiments..

The stimulus configurations used are shown in Figure 5.2. For the pattern test an array of  $15 \times 15$  achromatic checks appeared forming the random luminance modulation (RLM<sub>s</sub>, see Chapter 2). For these colour vision tests the RLM<sub>s</sub> used was 20% and the luminance of each check changed every 83 ms. The check dimensions were approximately  $0.4^\circ \times 0.4^\circ$ . The coloured stimulus was formed by a subset of the checks changing chromaticity so as to form seven vertical bars (Figure 5.2, upper diagram) whose dimensions were approximately  $3.0^\circ \times 0.4^\circ$ . The achromatic RLM<sub>s</sub> appeared for 333 ms and the coloured bars then appeared within the RLM<sub>s</sub> for a further 333 ms. For this test the background luminance was  $34 \text{ cd/m}^2$ . The subject's task was to report whether he was aware of any vertical bars, and not whether he thought there was a colour change.

Before measuring colour vision using the pattern test, it was necessary to establish that the acuity of the subject was sufficient to resolve the bars. This was achieved by measuring luminance contrast thresholds for detection of achromatic bars of the same dimensions as the coloured bars used in the pattern test amid the same RLM<sub>s</sub> (Barbur et al, 1994a). None of the subjects studied had any difficulty in detecting the achromatic bars.

For the colour test, the same array of  $15 \times 15$  checks was presented, this time at a luminance of  $15 \text{ cd/m}^2$ , apart from a central block of  $5 \times 5$  checks whose luminance was  $34 \text{ cd/m}^2$  (Figure 5.2, lower diagram) The central block subtended about  $2^\circ \times 2^\circ$  and was always clearly visible to the subject because its luminance was higher than that of the surrounding checks. For this test, the coloured stimulus was formed by the checks of the central block undergoing a chromatic displacement, and the subject was required to say whether or not the block had changed colour. As in the pattern test, the checks again changed luminance values every 83 ms, and the coloured stimulus was

presented after 333 ms for a duration of 333 ms. The RLM<sub>s</sub> was again set at 20% of the specified luminances for the central and surrounding checks.

For both tests a range of test target colours were generated (specified by the angle of chromatic displacement in the CIE (x,y) diagram) surrounded by the background chromaticity of (0.305, 0.323). In most cases, sixteen colours were used, from 0° to 337.5° in 22.5° steps, but for four of the subjects only twelve colours were used, from 0° to 330° in 30° steps. In each experimental run, half of the colours were presented in a randomly interleaved order, and a threshold chromatic displacement was found using a staircase procedure. For each set of stimuli, a rough approximation of the threshold was found using the 'coarse' staircase setting, the result being taken as the starting point for the 'fine' setting (see section 2.4). The results shown in the next section are the thresholds obtained with the 'fine' setting.

## Results

The results for the pattern test are shown in Figure 5.3. The solid line shows the mean chromatic displacement threshold for all the subjects tested and the dotted lines indicate two standard errors either side of the mean. The different numbers of subjects for each colour considered were taken into account when calculating the standard errors. The ellipse indicated by the solid circles is the best fit ellipse for the mean data.

The results for the colour test are shown in Figure 5.4, with the same notation as in Figure 5.3 above.

Comparison of the mean thresholds found for the normal subjects for the pattern and colour tests shows that there is no significant difference between them ( $p > 0.2$ , t-test for paired samples).

For both tests, the chromatic discrimination thresholds are reasonably small, and the best fit ellipse is of similar magnitude and orientation in each case. The best chromatic discrimination is seen in the 150°-330° axis, with thresholds around 0.003 CIE (x,y) units, while the threshold is higher (around 0.01 units) in the 60°-240° axis. The

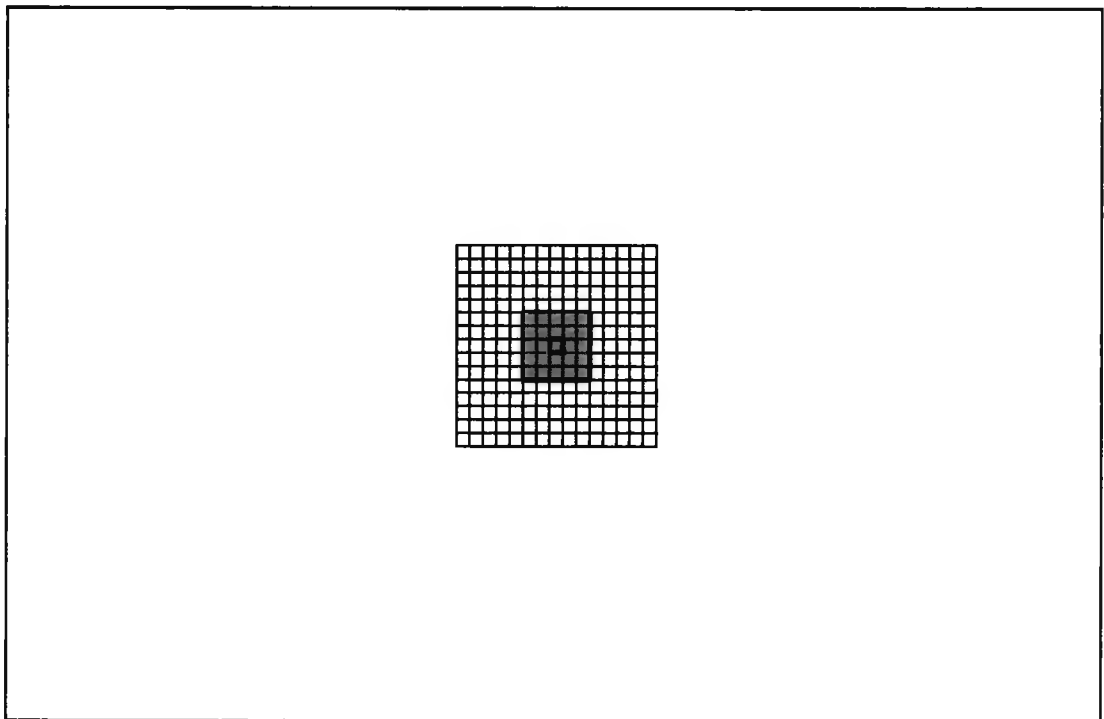
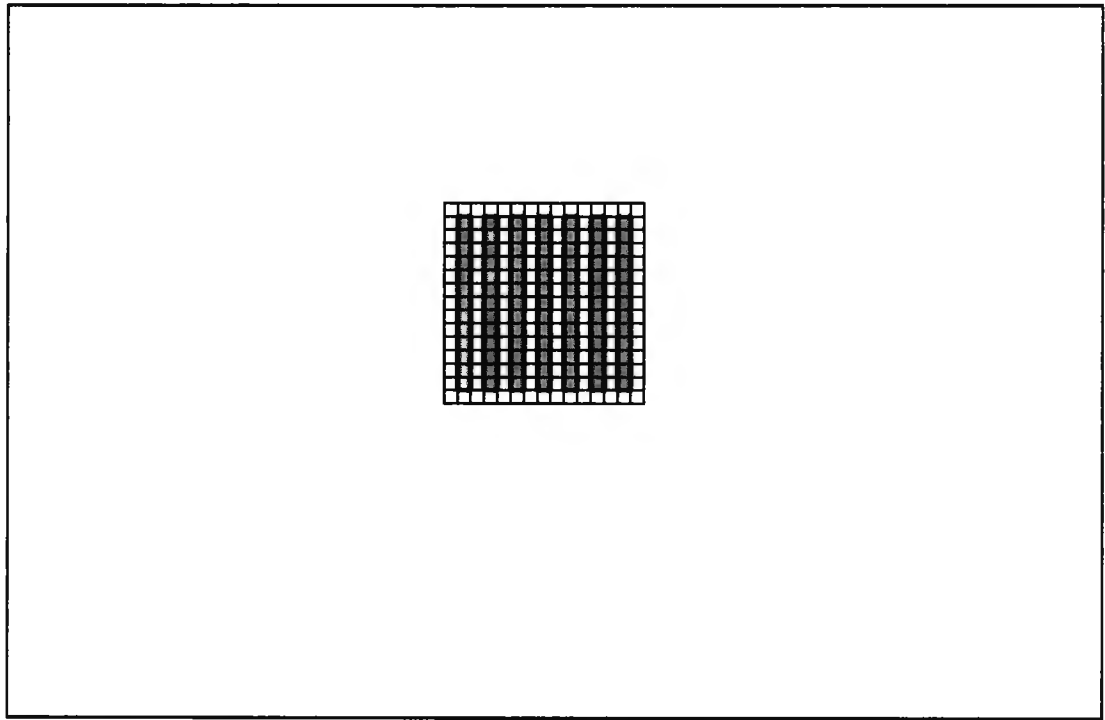


Figure 5.2 Stimulus configurations used for the 'pattern' test (upper diagram) and 'colour' test (lower diagram). Each check (indicated by the small squares) was  $0.4^\circ \times 0.4^\circ$

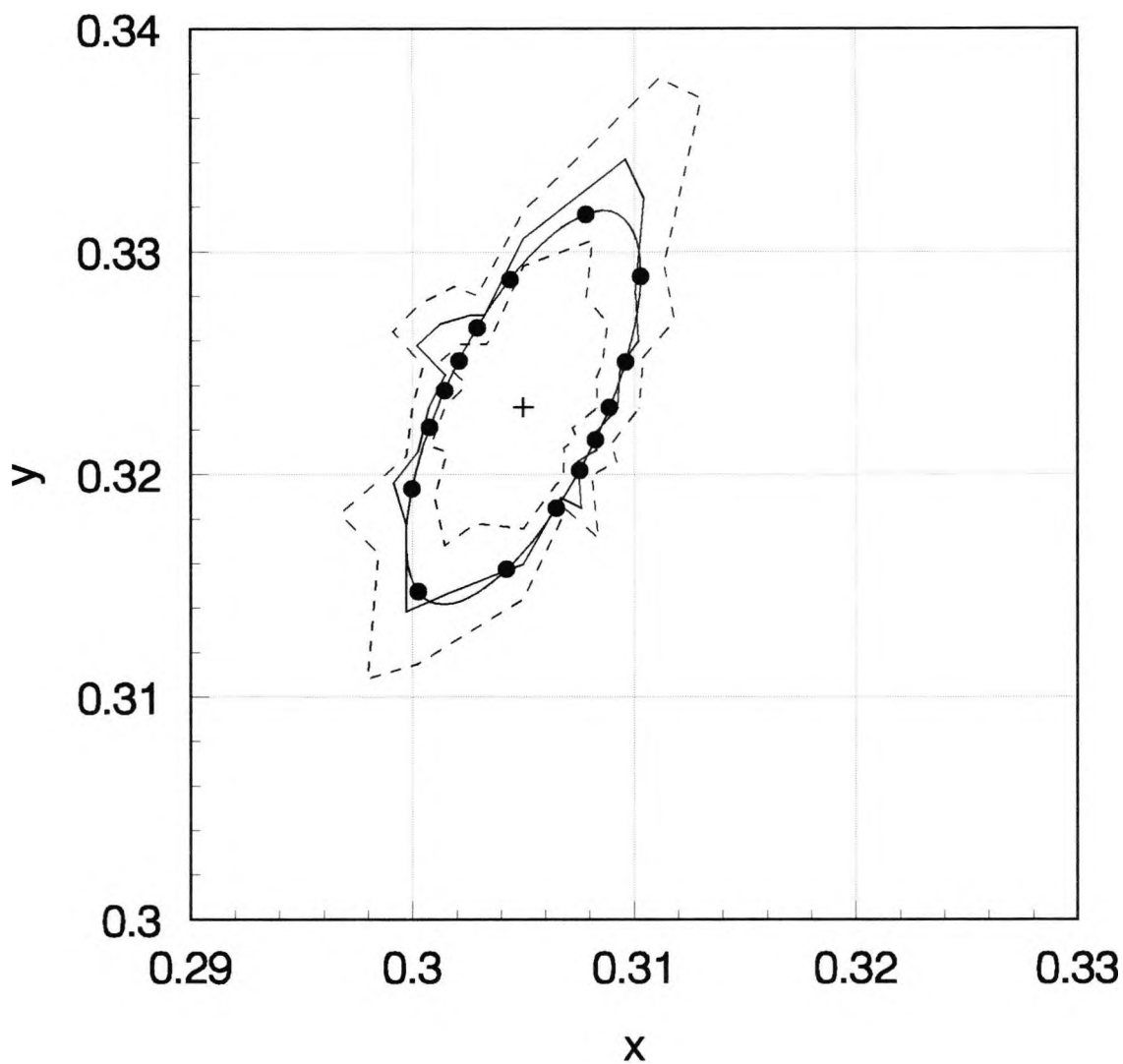


Figure 5.3 Chromatic discrimination thresholds for normal observers for the pattern test. The solid line shows the mean threshold values, with the dashed lines indicating two standard errors either side of the mean. The ellipse indicated by the solid circles is the best fit ellipse for the mean data

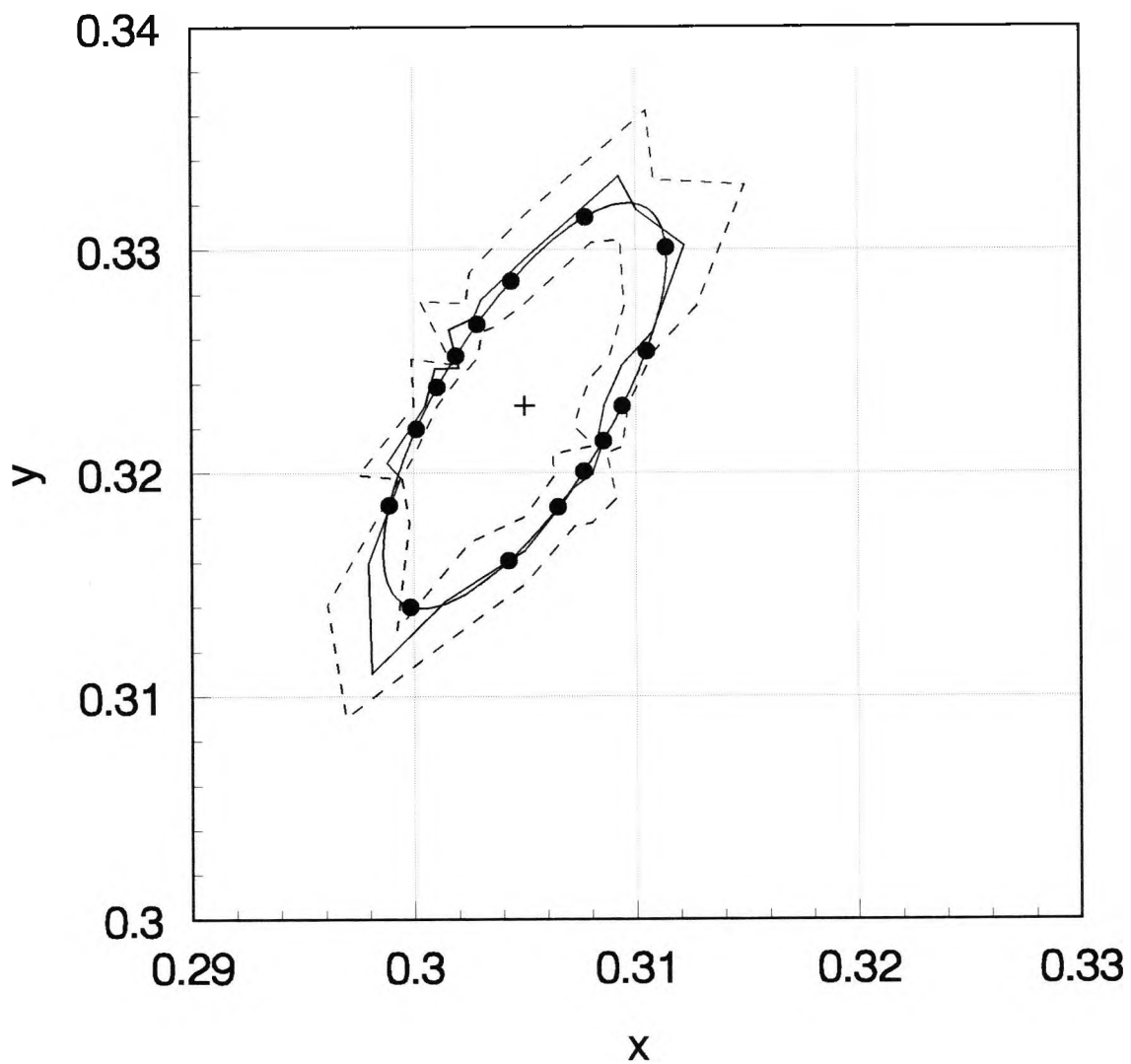


Figure 5.4 Chromatic discrimination thresholds for normal observers for the colour test. The solid line shows the mean threshold values, with the dashed lines indicating two standard errors either side of the mean. The ellipse indicated by the solid circles is the best fit ellipse for the mean data

ellipse is centred on the point corresponding to the background chromaticity, which is indicated by a cross in Figures 5.3 and 5.4.

## Conclusions

The mean data points and best fit ellipses are replotted in Figure 5.5, along with the results obtained for a normal subject by Barbur et al (1993a) for comparison. The results obtained in this study are very similar to those of Barbur et al (1993a). MacAdam (1942) plotted the standard deviations of colour matching thresholds and found that the just-noticeable difference was about three times as large as the corresponding standard deviations (Wyszecki and Stiles, 1982). His best fit ellipse for the point (0.305, 0.323) is also shown in Figure 5.5. The measurements performed using this experimental set-up (Barbur et al, 1993a, and the present study) give chromatic discrimination thresholds approximately four times higher than those obtained by MacAdam, although the orientation of the ellipses is very similar. In the latter study, the subject was required to match the two halves of a bipartite 2° field, which had luminance of 48 cd/m<sup>2</sup>, surrounded by a background field of 24 cd/m<sup>2</sup>. The thresholds found using the computerised test are higher than expected from MacAdam's data (standard deviation multiplied by four, instead of three). This may be due to the higher luminance and the fact that the subject controlled the colour of the matching field, rather than the forced-choice staircase procedure employed here.

These results give an idea of the chromatic discrimination thresholds obtained by normal observers. The next sections will compare these results with those obtained in subjects with suspected retinal or optic nerve pathology.

## 5.3 Colour vision in subjects with acquired selective colour vision loss

### Introduction

The pattern and colour tests described in Section 5.2 were used to investigate the colour vision of two subjects who were referred for visual assessment. This section describes these subjects and the results obtained, and attempts to account for the findings in terms of neural damage. Some of these results have been described previously in Cole (1995) and Barbur et al (1997).

## Subjects

The first subject to be tested was a 69 year old male (GW). He complained of difficulties with the vision in the right eye following what was thought at the time to be a series of small cerebral vascular lesions, which had also caused some difficulties with speech and walking. The visual acuity was only very slightly worse in the right eye (R:6/9<sup>+3</sup>, L:6/6<sup>-1</sup>) and clinical ophthalmological investigation (fundus examination, perimetry and pupillometry) had failed to show any reason for the symptoms he was experiencing. He had normal visual evoked potentials to achromatic checkerboard patterns in each eye.

Clinical colour vision tests (Ishihara, City University and HRR tests) suggested protanopia but failed to discriminate between the two eyes. The Farnsworth-Munsell 100-hue test showed some difference between the two eyes (Figure 5.6) and a tentative diagnosis was made of an acquired defect in the right eye and a protanomalous defect in the left eye. He did not remember having colour vision tests in the past, and had not been previously diagnosed as having any colour deficiency.

The investigation of his colour vision described in this section began about a year after these problems were first noticed. The problems with speech and walking had improved, but GW still felt that there was 'something wrong' with the right eye.

Some time after the tests described here had been carried out, GW underwent further neurological assessment at the National Hospital. An MRI scan showed multiple lesions in the white matter that are normally associated with multiple sclerosis (MS) of late onset. Analysis of spinal fluid showed evidence of inflammation also compatible with MS (G.T.Plant, personal communication).

The second patient (DM) was a 58 year old male, who had noticed that objects seemed blurry and a different colour with the right eye six months before the tests described here were carried out. He had undergone a thorough ophthalmological investigation, that confirmed the observed decrease in colour saturation and light sensitivity for the right eye suggestive of a right optic nerve lesion, although there were no supportive clinical signs. An MRI scan showed ethmoidal sinus mucosal disease only with no

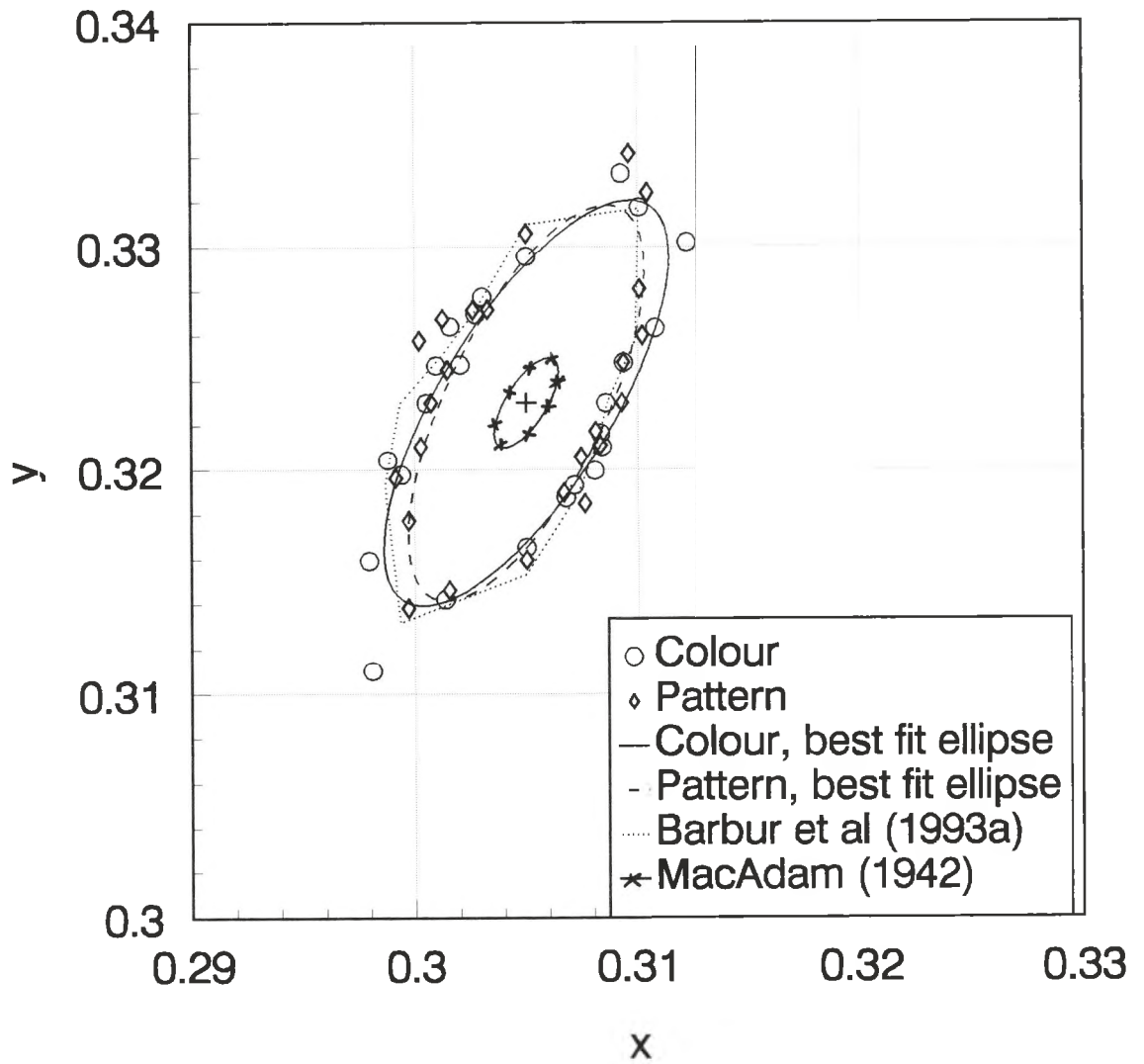


Figure 5.5 Comparison of chromatic discrimination thresholds found for normal observers for the pattern and colour test (Figures 5.3 and 5.4) with the results of Barbur et al (1993a) and MacAdam (1942)

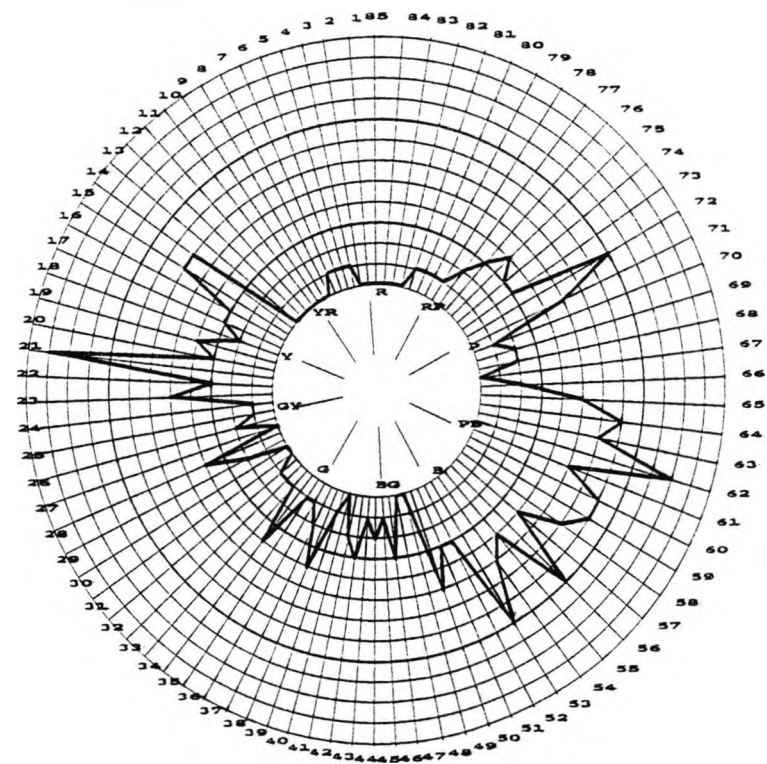
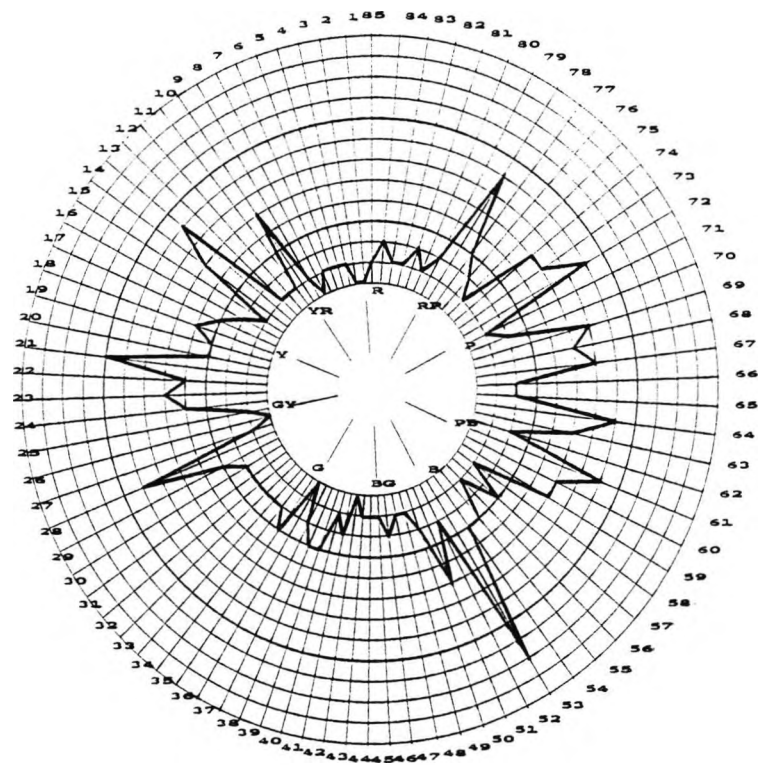


Figure 5.6 GW's results for Farnsworth-Munsell 100-hue test. Upper plot shows results for his right eye (total error score =232, tentative diagnosis of acquired defect). Lower plot shows results for his left eye (total error score =220, tentative diagnosis of protanomaly)

evidence of a neurological lesion, and Humphrey visual field analysis suggested the possibility of bilateral arcuate scotomata (personal communication from DM's general practitioner). The field plots are shown in Figure 5.7.

The visual acuity was good in both eyes (R:6/5<sup>-3</sup>, L:6/5). He failed most plates of the Ishihara test with the right eye and passed them all with the left eye. His contrast sensitivity was measured using a computerised test presenting achromatic sinusoidal gratings of different spatial frequencies, and the results are shown in Figure 5.8. He has lower contrast sensitivity than normal in both eyes particularly for the low and high spatial frequencies tested.

#### Experimental procedure

The pattern and colour tests were performed by each subject. The tests were performed monocularly, first a 'coarse' run and then a 'fine' run for each set of colours. The results shown in the next session are the thresholds measured with the fine run. Both subjects both wore appropriate spectacle corrections.

From preliminary results with the pattern test and also the results of the 100-hue test it seemed likely that GW was protanomalous, so the colours chosen for this subject were the optimum for investigating this type of defect, that is, with more colours along the isochromatic zone for a protanope and fewer perpendicular to it. The twenty colour directions tested are shown in Table 5.1. Subject DM appeared to have normal colour vision in his unaffected eye, so twelve equally spaced colour directions were used.

The RLM<sub>s</sub> used was 35%. In all other respects the pattern and colour tests were carried out as described in Section 5.2. Achromatic bars were also presented to ensure that the subjects' achromatic visual acuities were sufficient, and neither subject had any difficulty in seeing the achromatic bars.

A subject with congenital protanopia (TM, aged 31) also carried out the colour and pattern tests so that his results could be compared with those of GW.

Subject	Directions of chromatic displacement tested (degrees)
GW	0, 7.5, 15, 22.5, 30, 90, 150, 157.5, 165, 172.5, 180, 187.5, 195, 202.5, 210, 270, 330, 337.5, 345, 352.5
DM	0, 30, 60, 90, 120, 150, 180, 210, 240, 270, 300, 330
TM (protanope)	0, 7.5, 15, 22.5, 30, 90, 150, 157.5, 165, 172.5, 180, 187.5, 195, 202.5, 210, 270, 330, 337.5, 345, 352.5

Table 5.1 Directions of chromatic displacement tested for subjects GW and DM (subjects with acquired colour vision deficiency) and TM (congenital protanope)

## Results

Figure 5.9 shows the results for GW for the pattern test. The data for TM are also plotted for comparison. It can be seen that the chromatic discrimination ellipse for TM is extended along the isochromatic zone for a protanope in good agreement with previous results (Birch et al, 1992). The ellipse for GW's left eye is enlarged compared with the protanope ( $p < 0.0001$ , t-test for paired samples) particularly for the range 172.5 to 345. The ellipse for GW's right eye is much larger than the protanope for all angles ( $p < 0.0001$ ) and it extends to the limit imposed by the phosphors of the screen for 11 of the 20 colours tested.

Figure 5.10 shows the results for the colour test for GW and TM. There is a significant difference between the results of GW's right eye and TM ( $p < 0.001$ ) and, at a lower significance level, GW's left eye and TM ( $p = 0.0143$ ).

Comparison of Figures 5.9 and 5.10 shows that the results for GW's left eye are broadly similar to those of the protanope. This observation strongly suggests that GW may have a congenital protan defect. The right eye shows a marked difference from the protanope for the pattern test, and a smaller difference for the colour test. This difference in performance between the two tests is not found to any great extent in the protanope (Figure 5.11). It seem likely that the right eye shows a protan defect overlaid with an acquired defect, which accounts for the confusion in the diagnosis with conventional colour vision screening test.

Figure 5.12 and 5.13 show the results for DM for the pattern and colour tests respectively with the best fit ellipses for the mean normal data obtained in Section 5.2. All the ellipses measured for DM are significantly different from the mean data

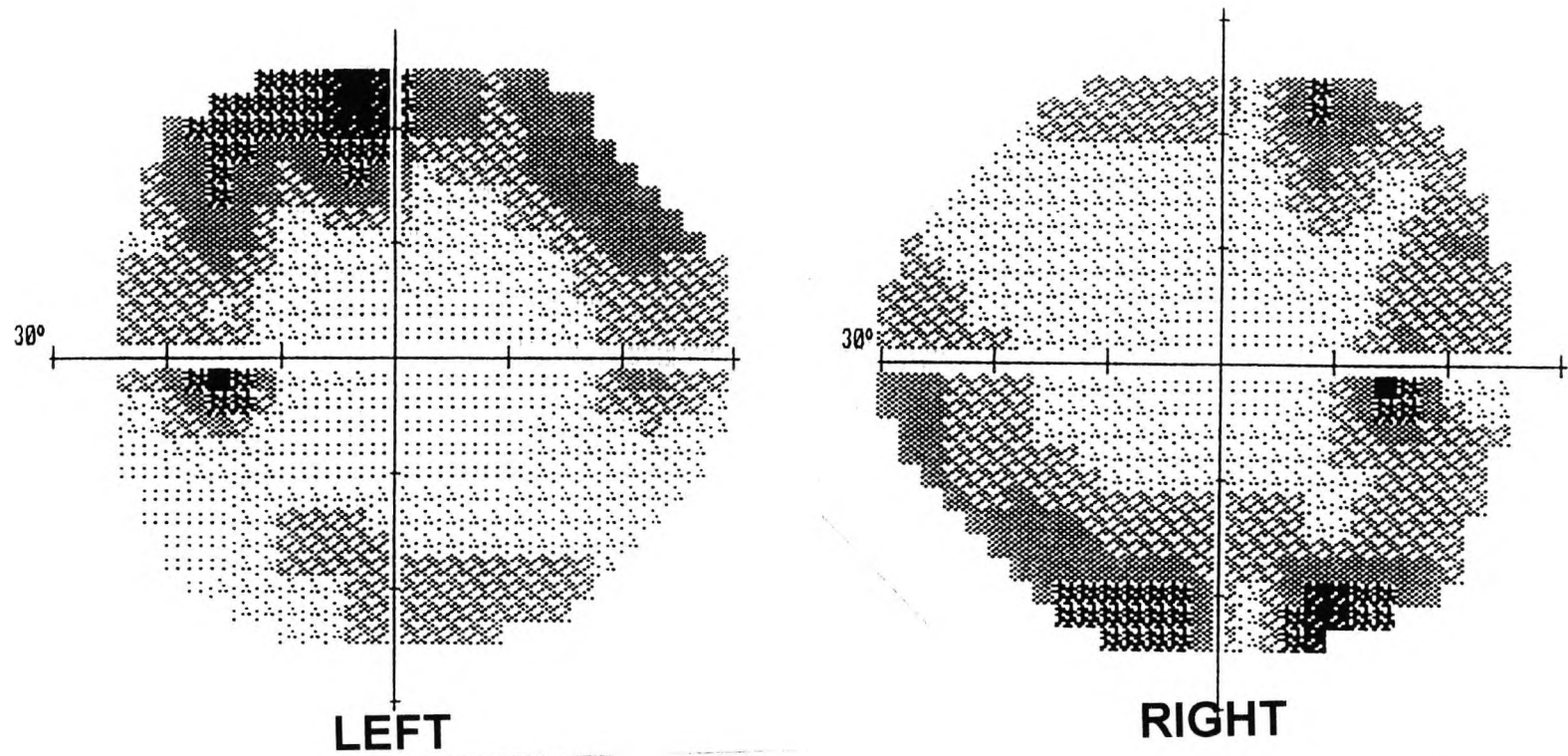


Figure 5.7 Humphrey visual field plots obtained for DM, showing bilateral arcuate defects

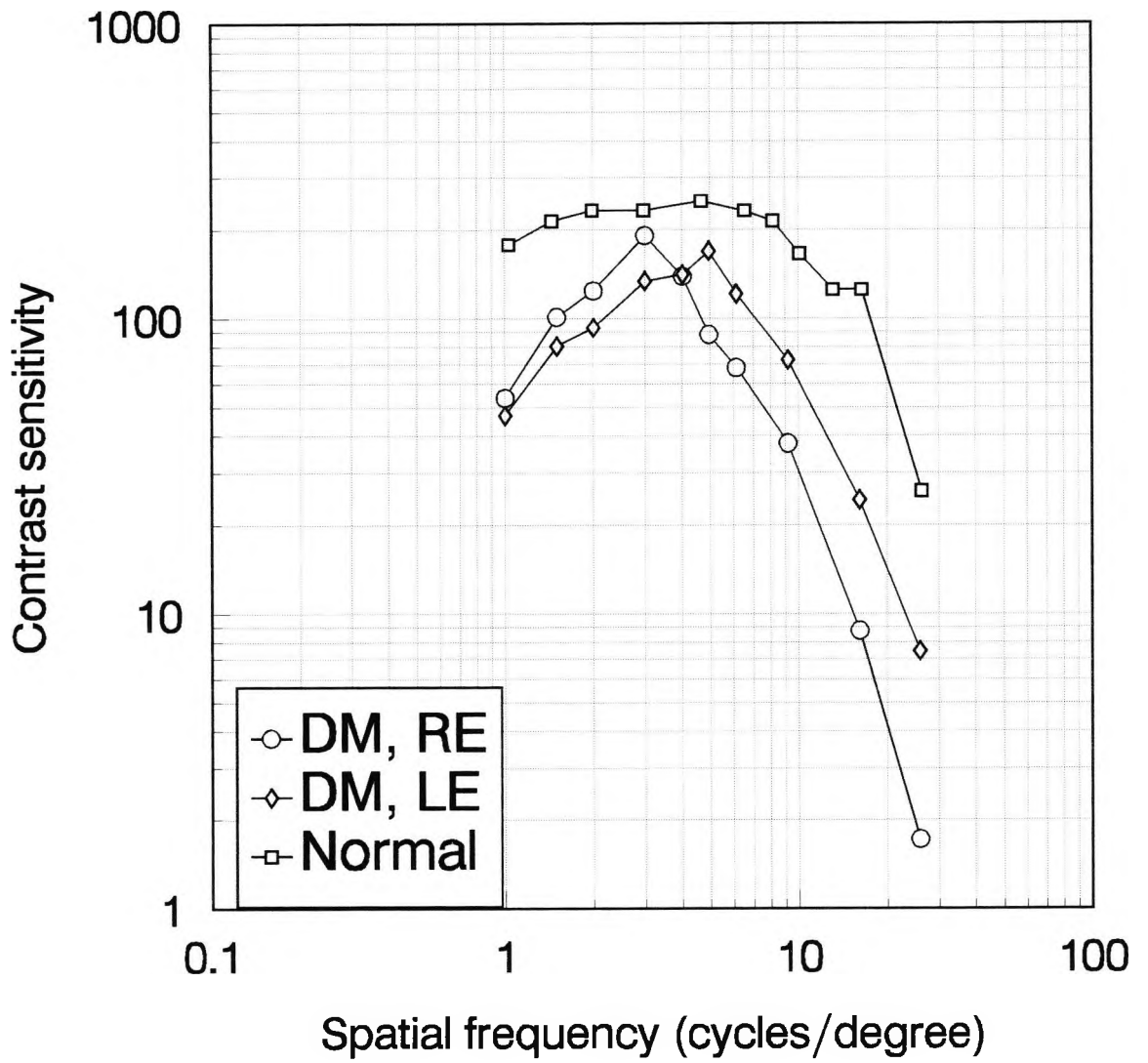


Figure 5.8 Contrast sensitivity functions for subject DM

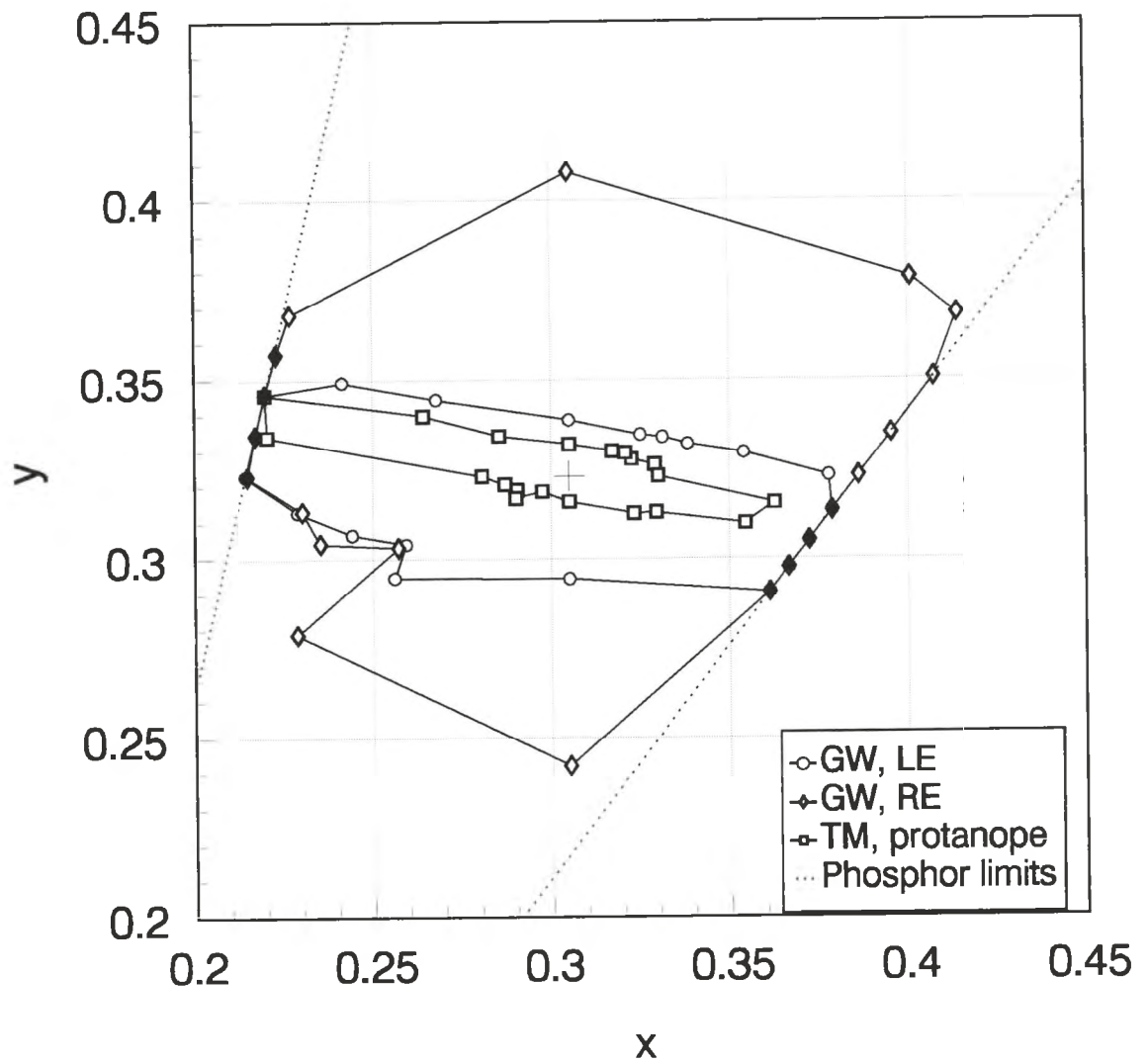


Figure 5.9 Chromatic discrimination ellipses for subject GW, pattern test, with data for a congenital protanope, TM, for comparison. Stimulus configuration as shown in Figure 5.2, upper diagram. The filled symbols indicate points which could not be discriminated at the limits of the screen phosphors.

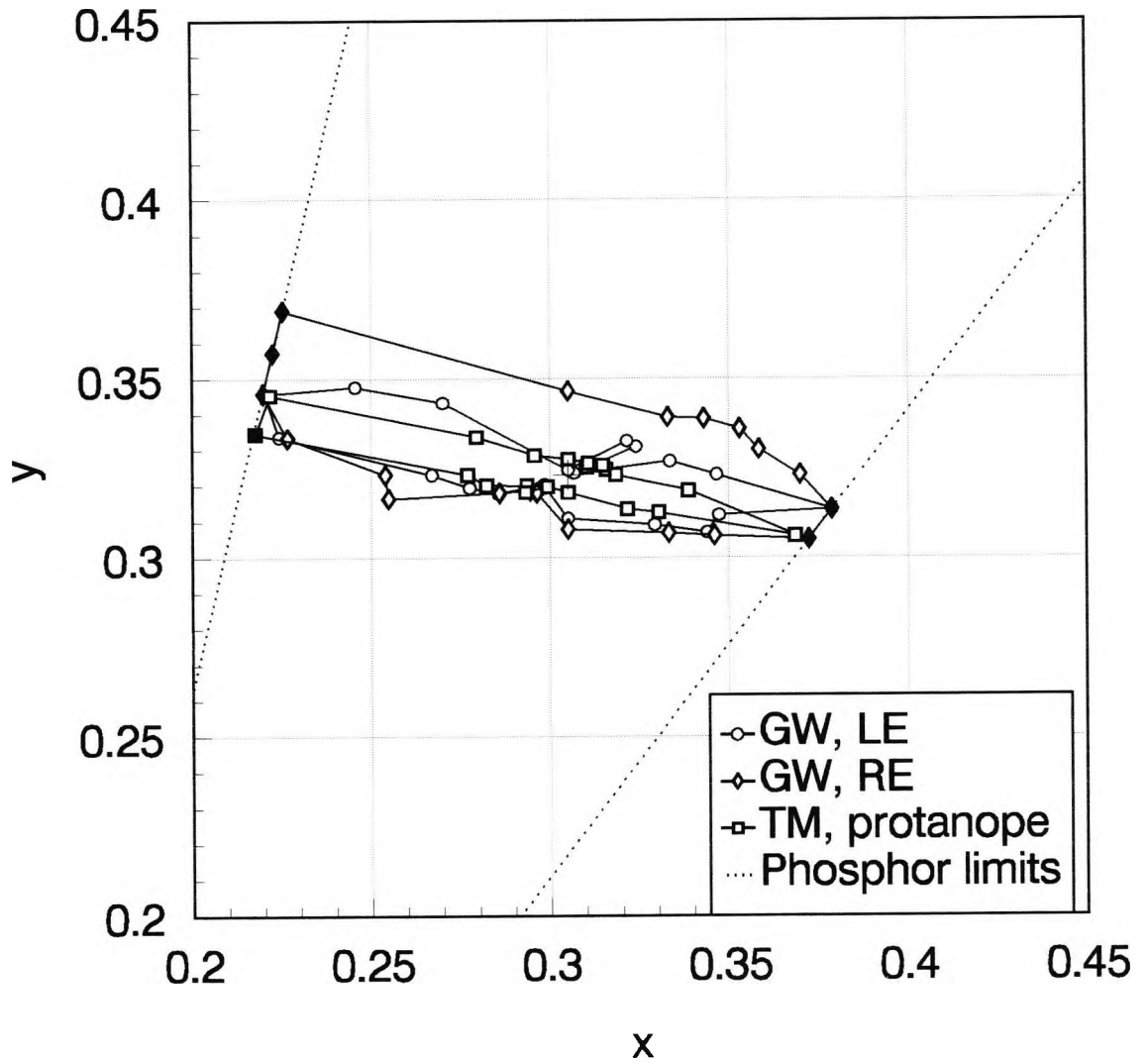


Figure 5.10 Chromatic discrimination ellipses for subject GW, colour test, with data for a congenital protanope, TM, for comparison. Stimulus configuration as shown in Figure 5.2, lower diagram. The filled symbols indicate points which could not be discriminated at the limits of the screen phosphors.

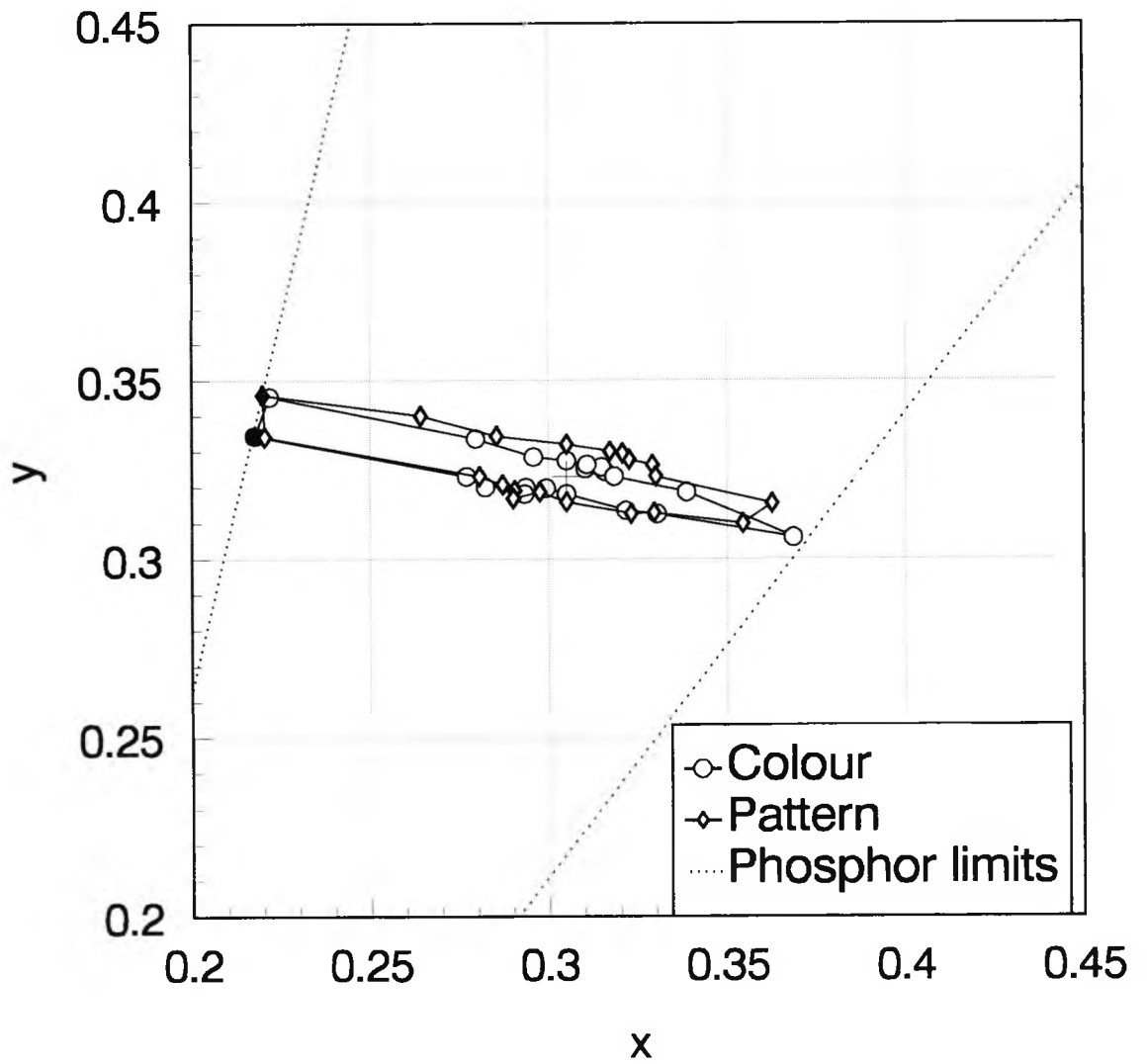


Figure 5.11 Chromatic discrimination ellipses for subject TM (congenital protanope) for the pattern and colour tests. Stimulus configuration as shown in Figure 5.2. *The filled symbols indicate points which could not be discriminated at the limits of the screen phosphors.*

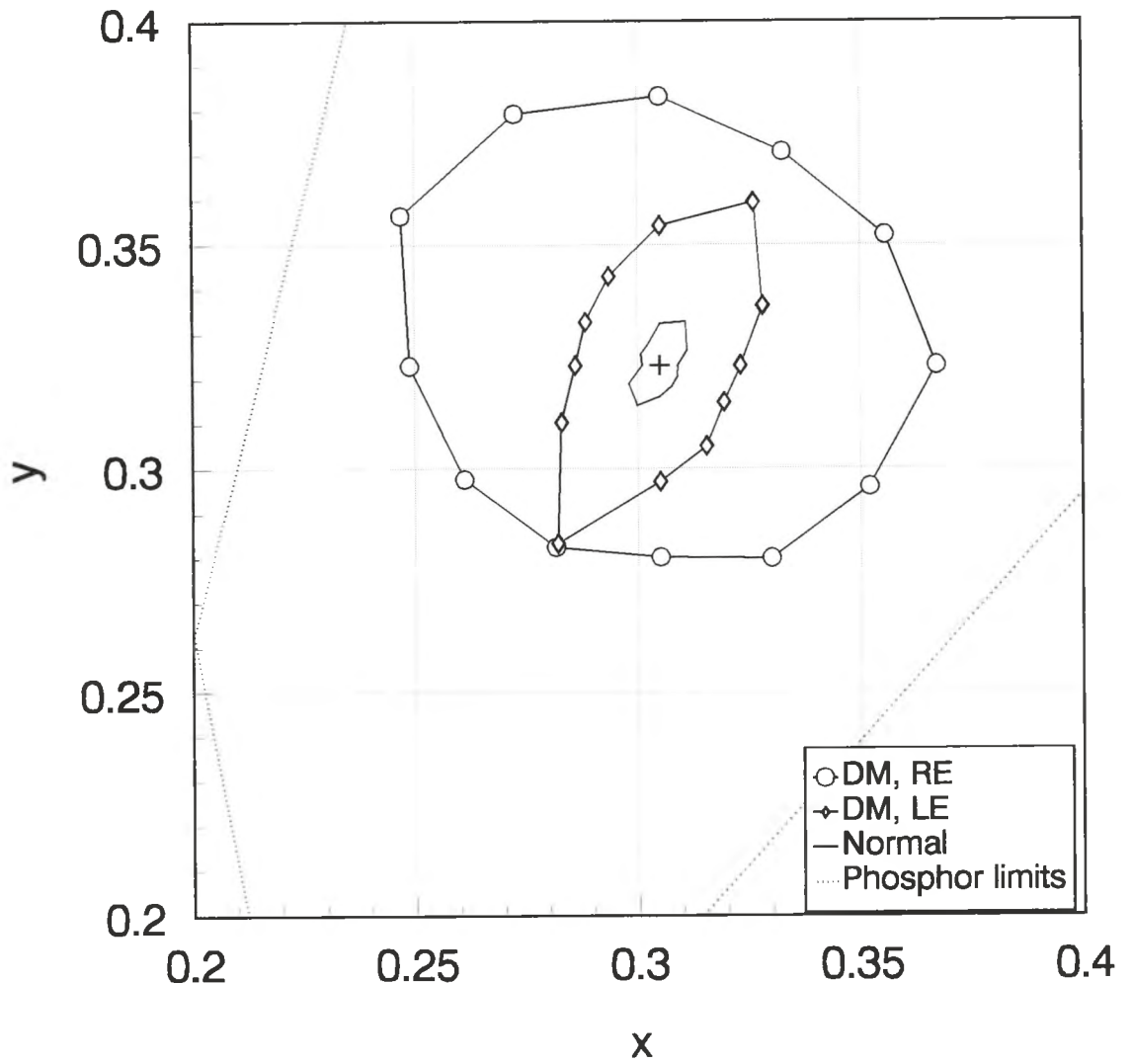


Figure 5.12 Chromatic discrimination ellipses for subject DM, pattern test, with the normal data from Figure 5.3 for comparison. Stimulus configuration as shown in Figure 5.2, upper diagram

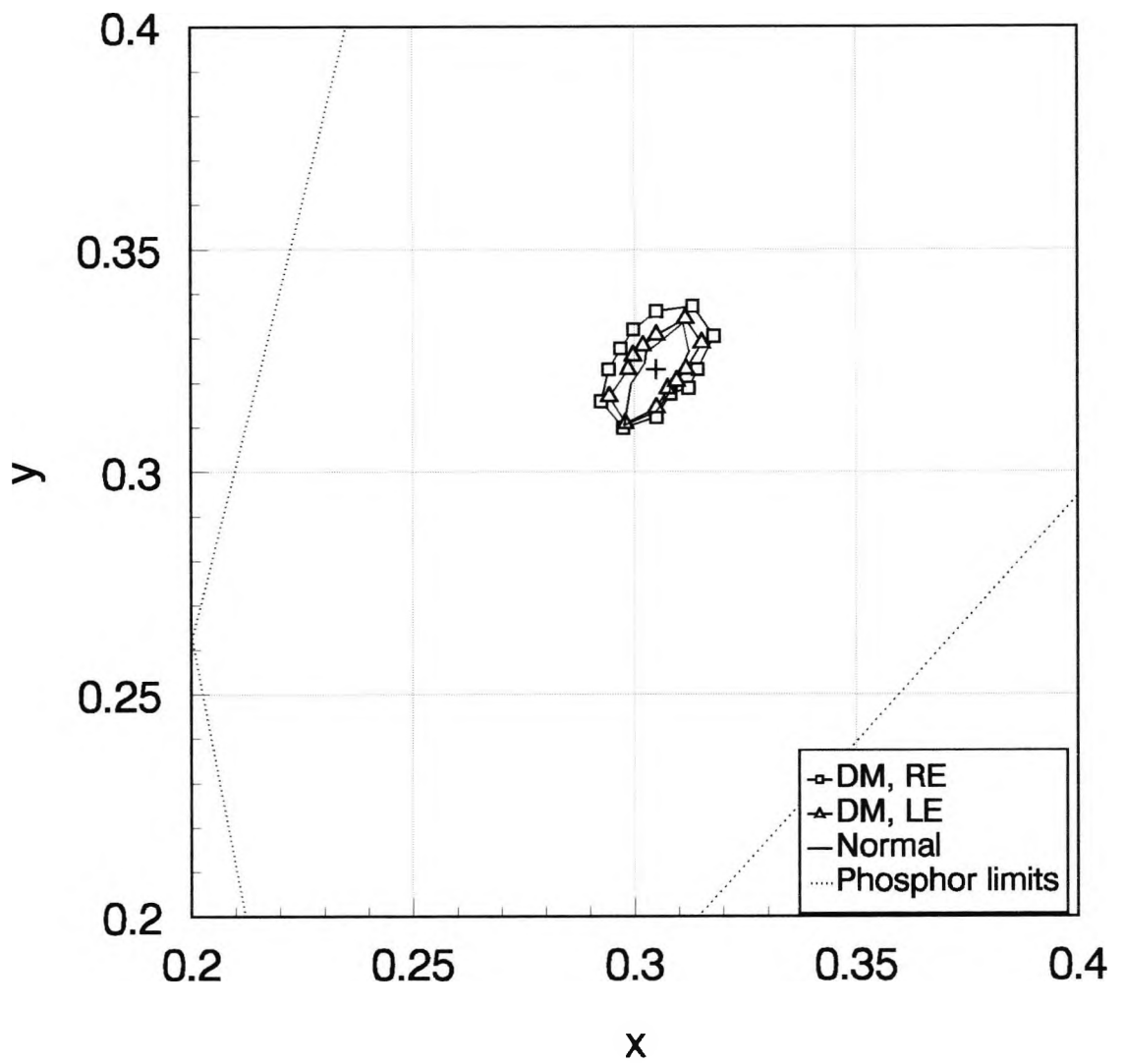


Figure 5.13 Chromatic discrimination ellipses for subject DM, colour test, with the normal data from Figure 5.4 for comparison. Stimulus configuration as shown in Figure 5.2, lower diagram

( $p < 0.005$ , t-test for paired samples, for each eye and each test). However, it can be seen from Figure 5.13 that the results for the colour test for both eyes are much nearer to normal than the results for the pattern test shown in Figure 5.12. The symptomatic right eye performs much worse than the left eye for the pattern test, but there is also a clear impairment of performance for the asymptomatic left eye at this test. The presence of bilateral visual field defects and the impaired colour vision performance in both eyes support the view that there is some underlying pathology in both eyes, even though the left eye is asymptomatic.

### Conclusions

The pattern test is designed to isolate the use of pure chromatic signals for detection of stimulus bars, while masking any luminance contrast changes associated with the stimulus. The results therefore reflect the subject's ability to perceive spatial structure defined only by chromatic signals. In the colour test, the subject can only use chromatic signals to detect a colour change since the target is defined by luminance contrast.

Both of the patients described in this section show poor performance at the pattern test with their affected eyes. However they show relatively normal colour discrimination when the colour test is used. They must therefore be suffering from a loss of ability in using chromatic signals to define spatial structure, while the use of chromatic signals to detect a colour change remains relatively unaffected.

What could be the mechanisms for these changes? Since one eye is affected more severely than the other for both these patients, the mechanisms must involve neurons early in the visual pathway, anterior to the optic chiasm.

Colour information is carried by parvocellular neurons which have been described in section 1.1.5. The bulk of the parvocellular cells examined by Wiesel and Hubel (1966) were Type I cells, with centre-surround colour-opponent properties. These cells can signal information about the luminance and chromaticity of the retinal image, and are responsible for discrimination of fine spatial detail. It has been proposed that the information about luminance and colour is separated at a higher stage of processing

(Lennie and D'Zmura, 1988; De Valois and De Valois, 1993) by the appropriate combination of outputs derived from different colour-opponent cells. Type I cells are good candidates for signalling the information required to perform the pattern test described here.

Wiesel and Hubel (1966) also described Type II cells which show spectral opponency but no centre-surround receptive field organisation. These cells only comprised 7% of the cells they examined. Such cells would be able to signal chromatic information but not fine spatial detail, and would presumably be able to signal information about a colour change as in the colour test described here. They would be too sparse to account for the chromatic acuities of 11-12 cycles/deg found by Mullen (1985), which are presumably mediated by Type I cells.

There are two possible explanations for the results obtained with the two subjects described in this section. The first is that the affected eye has lost enough of its Type I neurons to be unable to signal the spatial information required to detect the bars in the pattern test, but that enough Type I cells remain to signal a colour change over a larger area.

A second possible explanation is that all the Type I cells have been destroyed leaving only the Type II cells, whose large, spatially co-extensive colour-opponent receptive fields are ideal for signalling chromatic information (Rodieck, 1991). A possible drawback here is that both subjects retained good visual acuity in their affected eyes, and resolution of fine detail has been attributed to Type I parvocellular cells. However, recent studies have shown that there is little difference in the size of receptive field centres in parvocellular and magnocellular retinal ganglion cells, and that the magnocellular system may have virtually the same spatial resolution as parvocellular cells (discussed in Merigan and Maunsell, 1993). The good acuity could therefore be mediated by the magnocellular system, even if Type I parvocellular cells were destroyed.

The results presented in this section do not provide sufficient evidence to decide which of the above explanations is the more likely.

GW was subsequently diagnosed as having MS, and since about 70% of patients with this condition have episodes of optic neuritis (McDonald, 1986) it was a possibility that the acquired colour vision deficiency could have a similar pathogenesis to that commonly found in optic neuritis (see section 5.4). If the colour vision of subjects who had previously suffered optic neuritis was found to be affected in the same way as GW and DM, it would add weight to the idea that there was a similar underlying neuropathy. The next section describes an investigation into six such subjects.

#### 5.4 Colour vision in subjects who have had optic neuritis

##### Introduction

McDonald (1986) states:

the term *optic neuritis* refers to a clinical syndrome in which visual impairment develops over a matter of days, usually to the accompaniment of discomfort in or around the eye which is increased by eye movement. The visual loss persists for a few weeks then recovers over a matter of a month or two in 90% of cases. At the height of the illness, there is usually a central scotoma: the optic disc is swollen in rather less than 50% of patients, and impairment of colour vision is present in almost all.

Optic neuritis is commonly associated with multiple sclerosis, whose pathology is characteristically the predominant destruction of myelin with relative preservation of axons, which causes abnormalities of conduction along the fibres. Some axons of the optic nerve are lost in optic neuritis and this may account for the range of visual and psychophysical symptoms that may be experienced during or following an episode of optic neuritis.

Hess and Plant (1986) review spatial and temporal consequences of optic neuritis. These patients may suffer from decreased contrast sensitivity, over a wide range of spatial frequencies, or at high, intermediate or low frequencies only. There may also be orientation-specific loss. Temporal dysfunction results in a lower critical flicker frequency in these subjects, and the temporal contrast sensitivity is often reduced.

Foster (1986) reviews the effect optic neuritis has on luminance and colour perception. There may be an increased luminance threshold which can be variable, reduced

temporal resolution of two flashes presented ~~subsequently~~ <sup>successively</sup> and a delay in transmission leading to a relative perceptual latency in the affected eye.

Colour vision is almost always affected during an episode of optic neuritis, and there may be residual changes in colour perception following an attack, when the visual acuity has returned to normal and any central scotoma has subsided (see Plant (1991) for a review).. The colour vision defect is usually described as deutan-like (Grutzner, 1972) or red-green (Birch et al, 1979), although Mullen and Plant (1986) found that red-green and blue-yellow stimuli were affected equally. Fallowfield and Krauskopf (1984) and Mullen and Plant (1986) suggested that colour vision was more severely affected than luminance vision, although Foster et al (1985) found colour and luminance vision to be equally affected.

Subject GW described in section 5.3 was thought to have an acquired colour vision defect. He did not have the clinical features associated with an attack of optic neuritis, such as reduced visual acuity, pain or a central scotoma. However, since he was later found to have MS, the cause of the defect in the right eye is likely to have resulted from a demyelinating optic neuropathy.

This section describes the investigation of the colour vision of six subjects who have had optic neuritis, using the pattern and colour tests described above. If these subjects were to show poor performance at the pattern test, while achieving near normal results on the colour test as GW did, such findings might suggest that there could be a similar underlying mechanism causing the acquired defect in GW.

#### Experimental procedure

The colour vision of six subjects who had suffered optic neuritis in the past was examined using the pattern and colour tests. The test conditions were exactly as those described in section 5.2, except that measurements for both eyes were taken monocularly.

Details of the subjects are given in Table 5.2.

Subject	Age	Sex	Affected eye	Time since optic neuritis	Visual acuity
RH	32	M	Left	3 years	R:6/5 L:6/9 <sup>+3</sup>
PL	39	F	Left	8 months	R:6/4 L:6/4
POL	36	F	Left	15 months	R:6/4 L:6/5 <sup>-3</sup>
RA	38	M	Left	14 months	R:6/4 L:6/4
CH	23	F	Both (worse in left eye)	2 years	R:6/4 L:6/4
AM	36	M	Right	15 months	R:6/4 L:6/4

Table 5.2. Details of subjects who have had optic neuritis

### Results

The thresholds measured for the optic neuritis patients for the colour and pattern tests are shown in Figures 5.14, 5.15 and 5.16. The best fit ellipses for normal subjects (see section 5.2) are also shown for comparison.

The results were analysed using a t-test for paired samples between left and right eyes as shown in Table 5.3.

Subject	Pattern	Colour
RH	$t_{obt} = 7.11, p < 0.001$	$t_{obt} = 6.63, p < 0.001$
PL	$t_{obt} = 3.99, p < 0.01$	$t_{obt} = 4.05, p < 0.01$
POL	$t_{obt} = 3.31, p < 0.01$	$t_{obt} = 7.13, p < 0.001$
RA	$t_{obt} = 3.21, p < 0.01$	$t_{obt} = 0.77, p > 0.2$
CH	$t_{obt} = 13.5, p < 0.001$	$t_{obt} = 5.89, p < 0.001$
AM	$t_{obt} = 1.27, p > 0.2$	$t_{obt} = 2.69, 0.01 < p < 0.02$

Table 5.3. Comparison of left and right eyes of optic neuritis patients for pattern and colour tests.

In section 5.3, subject GW with acquired colour vision deficiency of unknown origin in one eye had higher chromatic discrimination thresholds in the affected eye for the pattern test, but not the colour test. Only subject RA showed the same results, with significantly higher thresholds for the affected eye in the pattern test, but no significant difference between the eyes for the colour test. Four of the six subjects participating in

this study (RH, PL, POL and CH) showed a significant increase in threshold for both the pattern and colour tests for the affected eye (or more severely affected eye in the case of CH). Subject AM showed no difference between the eyes for the <sup>pattern</sup> colour test, while for the <sup>colour</sup> pattern test, thresholds are raised for the affected eye ( $0.01 < p < 0.02$ ). Inspection of the lower <sup>left</sup> right-hand graph of Figure 5.16 and t-test analysis shows that there is no significant difference between the affected eye and the results for normal subjects ( $p > 0.2$ ), while the unaffected eye performs better than normal ( $p < 0.01$ ). <sup>for colour</sup>

A comparison of performance between the colour and pattern tests was also carried out. This analysis is shown in Table 5.4 below.

Subject	Unaffected eye	Affected eye
RH	$t_{obt} = 0.23, p > 0.2$ No significant difference	$t_{obt} = -2.94, p < 0.01$ Colour worse
PL	$t_{obt} = -1.79, p > 0.05$ No significant difference	$t_{obt} = -1.91, p > 0.05$ No significant difference
POL	$t_{obt} = -4.21, p < 0.001$ Colour worse	$t_{obt} = -2.42, 0.02 < p < 0.05$ Colour worse at 0.05 level
RA	$t_{obt} = 2.39, 0.02 < p < 0.05$ Pattern worse at 0.05 level	$t_{obt} = 1.97, p > 0.05$ No significant difference
CH	$t_{obt} = 6.24, p < 0.001$ Pattern worse	$t_{obt} = 16.4, p < 0.001$ Pattern worse
AM	$t_{obt} = 3.89, p < 0.01$ Pattern worse	$t_{obt} = 4.75, p < 0.001$ Pattern worse

Table 5.4. Comparison of performance of optic neuritis patients at the pattern and colour tests for affected and unaffected eyes (for CH, the left eye is taken to be the affected eye).

For subjects GW and DM described in section 5.3, performance was worse at the pattern test than for the colour test in the affected eye, while for normal subjects there was no difference in performance between the two tests (see section 5.2). In this

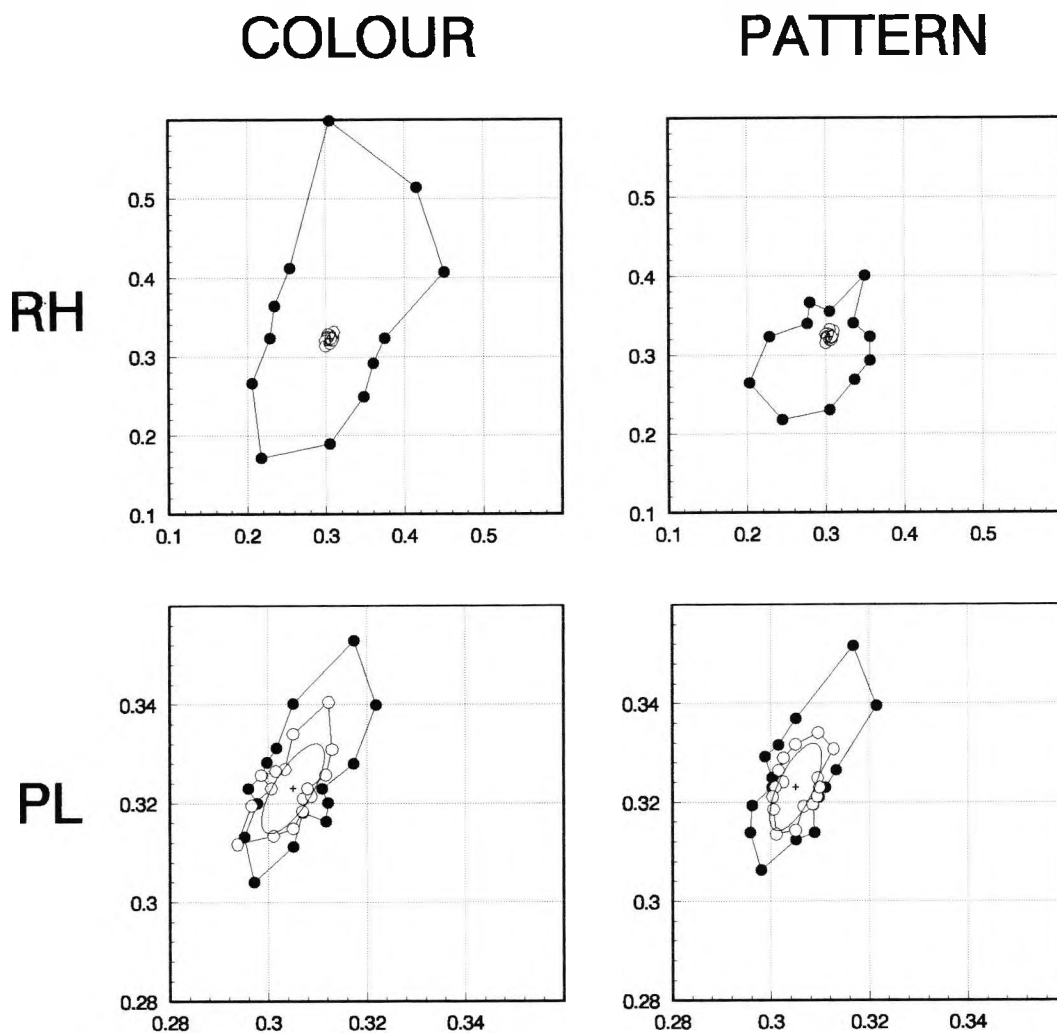


Figure 5.14 Chromatic discrimination ellipses for colour and pattern tests for RH and PL, optic neuritis patients (affected eye shown by filled circles, unaffected eye shown by open circles). The best fit ellipses for normal data (from Figures 5.3 and 5.4) are included for comparison. Stimulus configurations as shown in Figure 5.2. Note the different scales for these two patients

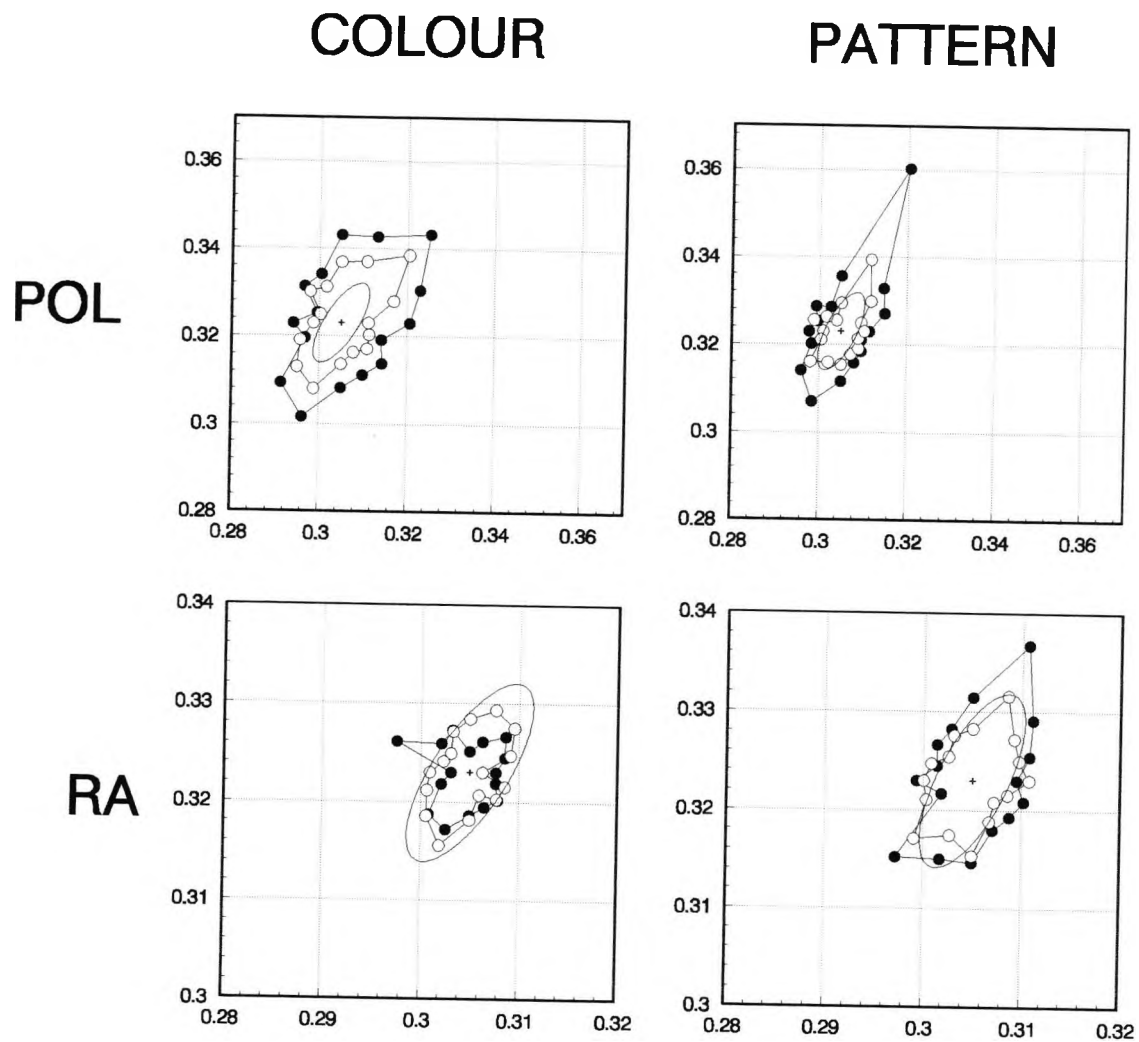


Figure 5.15 Chromatic discrimination ellipses for colour and pattern tests for POL and RA, optic neuritis patients; (affected eye shown by filled circles, unaffected eye shown by open circles). The best fit ellipses for normal data (from Figures 5.3 and 5.4) are included for comparison. Stimulus configurations as shown in Figure 5.2

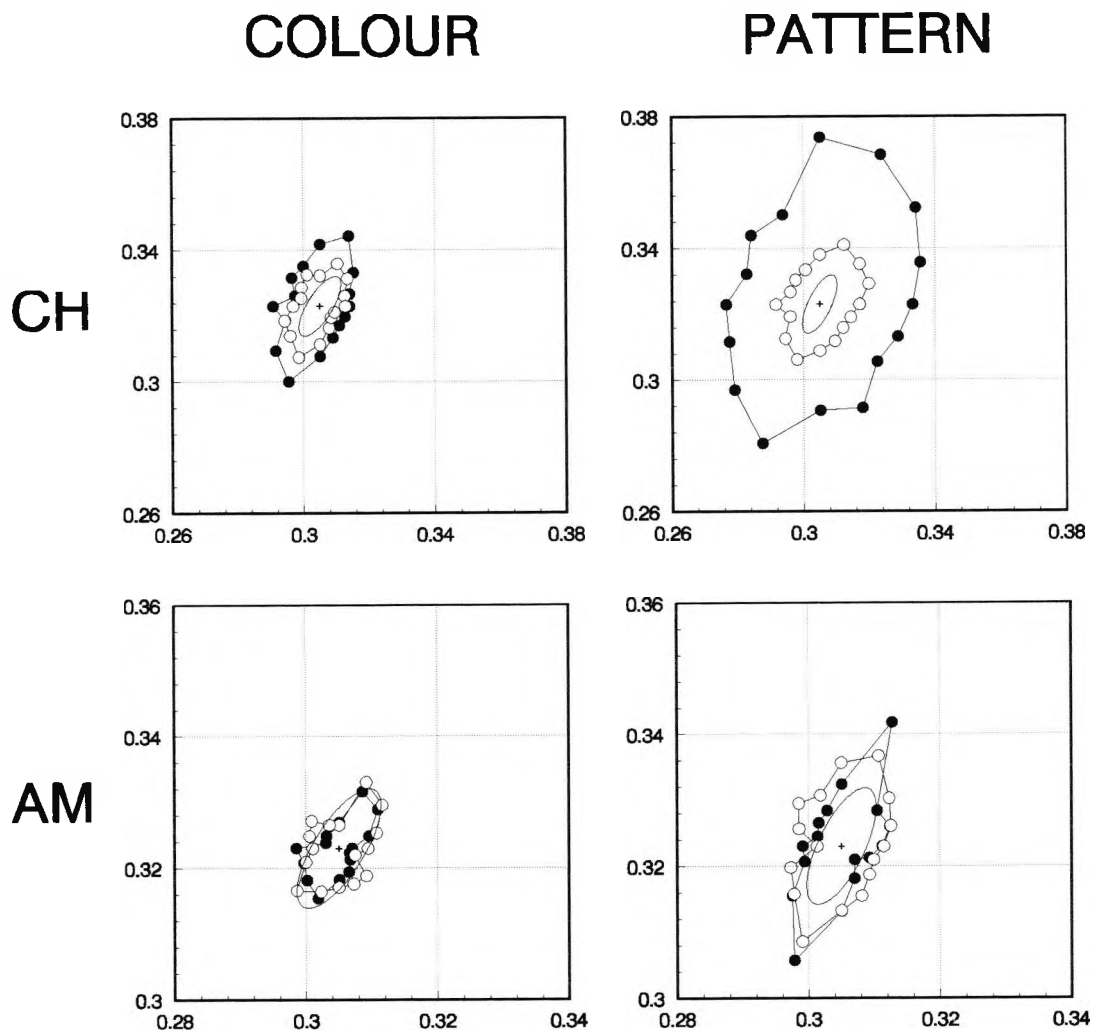


Figure 5.16 Chromatic discrimination ellipses for colour and pattern tests for CH and AM, optic neuritis patients (affected eye (left for CH) shown by filled circles, unaffected eye (right for CH) shown by open circles). The best fit ellipses for normal data (from Figures 5.3 and 5.4) are included for comparison. Stimulus configurations as shown in Figure 5.2. For subject AM (lower graphs), the filled circles indicate data for the unaffected eye, and open circles indicate data for the affected eye.

experiment a variety of findings was observed, but none of the six subjects repeated the pattern of results found with GW and DM. Both subject CH's eyes had been affected by optic neuritis and both performed worse at the pattern test than the colour test. For subject AM, the affected eye showed a poorer performance on the pattern test, but unlike the normal subjects, his unaffected eye also gave higher thresholds for the pattern than the colour test. RA performed worse at the pattern test with his *unaffected* eye, while his affected eye unexpectedly performed similarly to the normal subjects, with no significant difference found between the tests. RH's affected eye performed worse on the colour test, while the unaffected eye showed no difference, as in the normal subjects. POL performed worse at the colour test for both eyes. PL showed normal results in that there was no difference between the tests for either eye.

The dimensions of the ellipses obtained give an indication of chromatic discrimination ability. Best-fit ellipses were fitted to the results obtained for the six optic neuritis patients, and Figures 5.17 and 5.18 show the major and minor half-axes of the ellipses fitted to the data obtained for the affected eyes of these subjects. The values for normal subjects obtained in section 5.2 are included for comparison. This may be a more convenient index of performance for presenting and comparing results than the actual ellipses obtained.

## Conclusions

The aim of this experiment was to use psychophysical colour discrimination measurements to explore specific losses in the use of chromatic signals caused by optic neuritis. It is clear from the results obtained from the six subjects studied here that optic neuritis can cause various residual effects on colour vision as measured using the pattern and colour tests. No common pattern of impairment was observed in these subjects, and none of them showed the same pattern of results as was found for GW and DM. From these results there is no obvious connection between GW and DM, and the optic neuritis subjects, and it cannot therefore be concluded that there is a common underlying mechanism.

In section 5.3, two possible hypotheses were proposed to explain the results found for GW and DM. The first suggestion was that many Type I cells had been destroyed, and

that the reduced sampling frequency was sufficient to signal colour changes over a large area (good performance on the colour test) but not colour changes over small areas (poor performance on the pattern test). The second hypothesis was that there are different neural substrates at an early stage in the visual system for handling the coding and use of chromatic signals, and Type I and Type II cells were suggested as candidates for such parallel systems. If the results for eyes which have suffered optic neuritis are considered, three out of seven perform better on the colour test (both CH's eyes and AM's affected eye) while two out of seven perform better on the pattern test (RH and POL). A further two eyes having previously suffered with optic neuritis performed equally on the two tests (PL and RA). These results seem to rule out the first hypothesis, which would not allow better performance at the pattern test than at the colour test. The results obtained therefore support the idea of different neural substrates working in parallel at the level of the retina or optic nerve.

Even in such a small sample group, it is clear that the colour vision losses caused by optic neuritis vary greatly between subjects. Hess and Plant (1986) state that "one of the characteristic features of optic neuritis is the great variety of psychophysical loss that can be found amongst the clinical group" and colour vision appears to be no exception. It would be of interest to study greater numbers of these patients in order to examine more fully the variation between them. However, the purpose of this study was to investigate the possibility of similar losses in optic neuritis patients and the subjects described in section 5.3, and it has been shown that there do not appear to be any such similarities.

## 5.5 Summary

This chapter describes the use of the psychophysical colour vision tests developed by Barbur et al (1994a) in which chromatic signals are used either to define spatial structure or to limit any possible discrimination to the detection of a colour change. Data were initially collected for a group of normal subjects. Two subjects (GW and DM) were investigated using these tests after conventional testing had failed to account for their symptoms, and it was concluded that they were suffering from optic or retinal neuropathy of unknown origin. A small group of subjects who had suffered optic

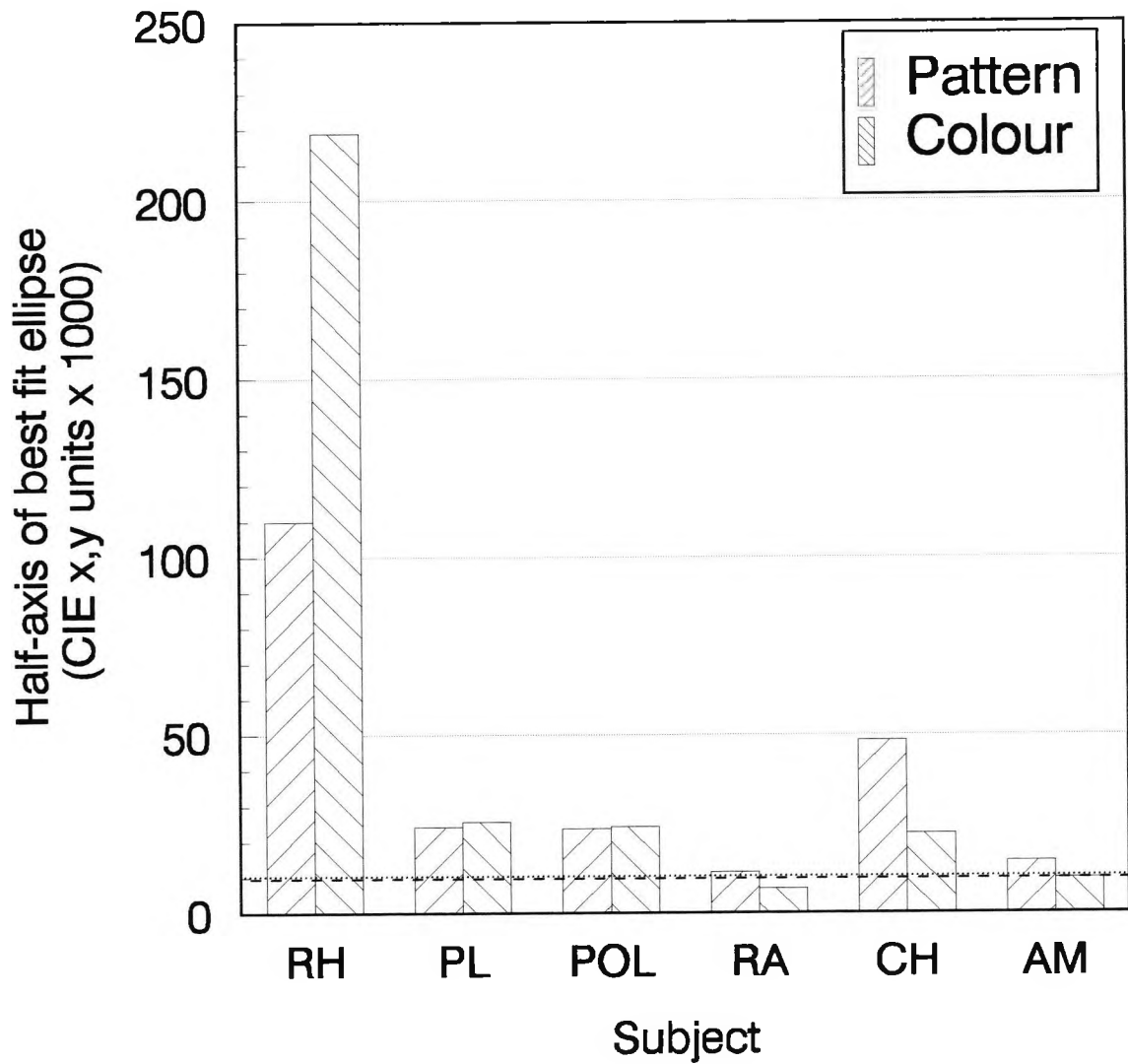


Figure 5.17 The major axis dimensions for the ellipses fitted to the data for the affected eyes of the optic neuritis subjects in Figures 5.14, 5.15 and 5.16 (left eye for CH). Each column indicates the half-axis length. The corresponding values for normal subjects from the mean data shown in Figures 5.3 and 5.4 are included for comparison (dashed line for pattern test, dotted line for colour test)

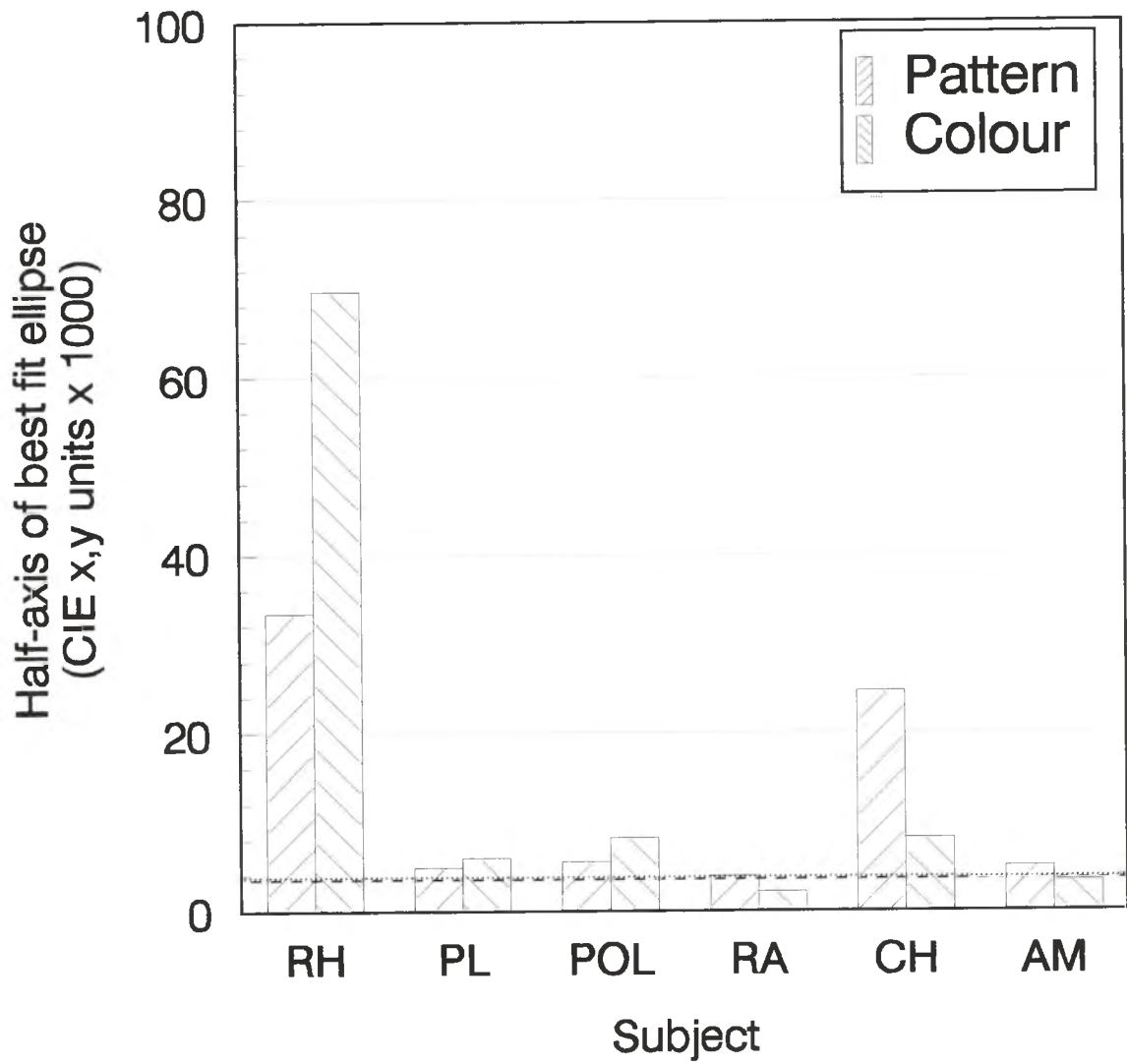


Figure 5.18 The minor axis dimensions for the ellipses fitted to the data for the affected eyes of the optic neuritis subjects in Figures 5.14, 5.15 and 5.16 (left eye for CH). Each column indicates the half-axis length. The corresponding values for normal subjects from the mean data shown in Figures 5.3 and 5.4 are included for comparison (dashed line for pattern test, dotted line for colour test)

neuritis were then examined, but these subjects had varying losses, none of which were similar to those found in GW and DM.

From the results obtained for GW and DM, two hypotheses were proposed to explain the different uses of chromatic signals for the pattern and colour tests. The first hypothesis suggests that all colour coding is mediated by colour-opponent, centre-surround cells, such as the Type I cells of Wiesel and Hubel (1966). The results obtained for GW and DM could reflect a considerable loss of Type I cells, with the reduced sampling frequency only able to signal colour changes over large areas. The second hypothesis suggests that there are different neural substrates which handle the coding and use of chromatic signals, with Type I and Type II cells as possible candidates. However, the results from the optic neuritis subjects show some dissociation between the two tests, with some eyes performing better at the colour test in the same way as GW and DM, and others performing better at the pattern test. These results therefore tend to support the second view, that is, that there are parallel pathways mediating the different uses of chromatic signals. These different neural mechanisms can be affected differently but not specifically in optic neuritis.

It is still not clear what the underlying pathogenesis of the problems suffered by GW and DM could be. If a group of patients with a known disease could be shown to have the same colour vision defects, a common aetiology could be indicated. No clear link was found between the results for GW and DM and for the optic neuritis subjects, but other conditions could be investigated. One criterion that would have to be met was that the visual acuity would have to be adequate to resolve the bars of the pattern test. Possible groups that could be considered are patients with glaucoma or dominant optic atrophy, both known to cause colour vision problems but usually associated with normal or near-normal visual acuity (Birch et al, 1979).

This chapter has raised many questions about selective colour vision impairments, and much remains to be understood about the coding and use of chromatic signals in human vision. This work and further studies of chromatic discrimination in subjects with retinal or optic nerve disorders may contribute to this understanding.

## CHAPTER 6 CONCLUDING REMARKS

The performance of the visual system arises as a result of the total activity of its receptors and post-receptor mechanisms. It is therefore of both clinical and scientific interest to develop an understanding of the mechanisms involved and their mode of action.

Psychophysical testing methods reflect the performance of the visual system as a whole, and must be carefully designed if specific mechanisms are to be demonstrated (see for example, Livingstone and Hubel, 1987). Psychophysical methods require a certain degree of co-operation and ability from the subjects, which limits the use of these methods, for example with infants, animals and patients with certain types of brain damage. In these cases, objective testing methods may be more appropriate.

Intracellular recordings can give detailed information about the responses of cells to specific visual stimuli, and such studies have revealed the 'building blocks' of the visual system, for example, Barlow (1953) and Kuffler (1953) demonstrated the receptive field arrangements of retinal ganglion cells, and Wiesel and Hubel (1966) were able to classify LGN cells according to their responses to achromatic and chromatic stimuli. Lesion studies can help to determine the significance of specific areas of the visual pathways by examining the effects of their removal or damage upon visual performance. Animal studies have the advantage that the lesions can be carefully controlled and verified later by post mortem if required. Examples of such studies include Pasik and Pasik (1982) who examined the visual functions of monkeys as different parts of the brain were removed and Schiller et al (1990) who made selective lesions of the magnocellular and parvocellular regions of the LGN to examine the functions of these groups of cells. In animal studies, however, results have to be obtained by objective methods or by using lengthy forced-choice testing methods with statistical analysis of the results. Human studies of patients with brain damage face the difficulty of knowing the exact extent of the damage and the health of the patients may not always permit lengthy experimental testing.

Measurement of pupil responses has long been used as an objective test of visual function. As the technology of recording devices has improved, it has proved possible to investigate in detail pupillary responses to coloured stimuli, gratings and checkerboards (see section 1.2.6). Pupil responses have also formed the basis of an objective perimetry technique (Kardon, 1992) showing that stimuli presented in abnormal areas of visual field generate reduced pupil responses. Abnormal pupil responses have been found in subjects with damaged primary visual cortex, for example, Barbur and Thomson (1987) failed to demonstrate pupil responses to gratings presented in the blind hemifield of GY, and Keenleyside (1989) measured no responses to small coloured stimuli presented in the blind visual field of hemianopes, although significant responses were seen for the same stimuli when presented in sighted field. This suggests that there is some cortical involvement in the generation of the pupil responses.

The work described in Chapter 3 supports the view that there is cortical input to the pupil light reflex response (PLR). It has been shown that by using dynamic spatial random luminance modulation (RLM<sub>s</sub>) it is possible to eliminate part of the PLR in normal subjects. The RLM<sub>s</sub> does not appear to have the same effect when measuring the PLR in GY's cortically blind hemifield. These results led to the hypothesis that the cortical input to the PLR may be a specific mechanism, driven largely by local increments of luminance contrast. The rest of the PLR appears to be concerned with large area summation of luminance increments and is probably mediated by a subcortical input to the olivary pretectal nucleus (Pierson and Carpenter, 1974; Gamlin et al, 1984; Clarke and Gamlin, 1995). Experiments to investigate the effect of stimulus area and contrast on these two parts of the pupil response are also described in Chapter 3. The proposed cortical component appears to have a high contrast gain, but this component saturates at contrast levels above 30%. The subcortical component has a low contrast gain, and can signal luminance increments over a large range. Both components show spatial summation but this is more pronounced for the subcortical component. It was proposed that the subcortical component may be associated with the control of steady state pupil size. A patient with optic nerve drusen causing a relative afferent pupillary defect was studied, whose PLR in the affected eye was almost entirely eliminated by the RLM<sub>s</sub>. These results suggest that the component

unaffected by the RLM, is reduced or absent in this subject. Such findings are consistent with the hypothesis that the missing component in this subject determines the steady state size of the pupil. The properties of the two proposed components are summarised in Table 3.5.

The work described has shown how objective measurements have led to the hypothesis of two separate mechanisms contributing to the PLR. Suggestions have been made for further experiments which could be carried out to investigate these two components more thoroughly, for example, to investigate their temporal properties more fully, or to establish whether the same components are present in primates so that comparisons may be made with the results obtained in human subjects with normal or damaged primary visual cortex.

Further use has been made of the pupil response as an objective measure of colour vision in experiments described in Chapter 4. The work described in this chapter builds on previous studies (Hedin and Glansholm, 1976; Young et al, 1987; Barbur et al, 1993a) which have suggested that dichromatic observers may be identified by using pupillary responses to coloured stimuli. Computer-generated coloured stimuli were used in conjunction with luminance masking, and it was shown that significant responses were obtained for all colours tested in normal trichromatic observers, albeit with some variation of amplitude between subjects. When pupil colour responses were measured for dichromats, no significant responses were seen when stimuli were presented whose chromaticities were on the same confusion line as the background chromaticity. This technique may be developed into an objective clinical test of colour vision. More work is needed to determine a choice of stimulus chromaticities which could simplify and shorten the test.

Past studies have not demonstrated PCRs in subjects with cortical damage when small coloured stimuli are used (Keenleyside, 1989). Studies using larger coloured stimuli (Sahraie, 1993; Stoerig et al, 1994) have shown pupil responses, but these may have been contaminated by rod-driven contributions (Gamlin et al, in press). Section 4.4 describes experiments to investigate PCRs to large stimuli in subjects with cortical damage. Care was taken to eliminate any contamination by luminance or rod-driven

responses by using RLM<sub>s</sub> and RLM<sub>t</sub>. Small but significant responses were found particularly for long-wavelength stimuli used for GY, who has damaged V1. A subject with incomplete cerebral achromatopsia, LR, was also tested, who was presumed to have a lesion in V4, but intact V1. Small but significant responses were also found in this subject particularly for the long-wavelength stimuli used. Possible neural pathways involved in the generation of these results are discussed in section 4.4. If V4 is the source of cortical input to the PCR, its influence is likely to be reduced in subjects with damaged V1, as information from the retina has to reach V4 via an alternative pathway (retina to LGN (via LGN interneurons or superior colliculus) to V4). If there is common mechanism underlying the PCRs measured in GY and LR (which is plausible, given the qualitative similarities between their results) it is unlikely to involve V4 as this is the presumed site of LR's damage. This mechanism could be subcortical, for example, via the superior colliculus cells responding preferentially to certain wavelengths (Kadoya et al, 1971; Marrocco and Li, 1977). GY's superior colliculus has been shown to be active when red stimuli are presented in his cortically blind hemifield (Barbur et al, in press). It is not possible to say with any certainty what the mechanisms are from this very small study using only one subject for each type of brain damage. Brain imaging studies and the use of more subjects may provide a clearer picture of the pathways involved.

The use of colour vision to explore visual mechanisms was continued in the work described in Chapter 5, this time using psychophysical experiments. Two patients were investigated with presumed optic nerve damage of unknown origin, which appeared to cause selective damage to the use of chromatic signals. They showed impaired performance at detection of coloured patterns formed by small checks, yet were able to detect a colour change when large, chromatically uniform targets were used. The performance of a small group of optic neuritis patients was examined using the same test procedure to see if similar results were obtained. It was hoped that a common pathogenesis could be proposed for both groups. In fact, the optic neuritis patients showed widely varying performances, which is consistent with previous reports of the variability of this condition. The hypothesis put forward to explain the results obtained with patients GW and DM is that there are two parallel mechanisms using chromatic signals which may be selectively damaged. Anatomically, the first mechanism is

consistent with a pathway involving Type I LGN cells (Wiesel and Hubel, 1966) and their retinal counterparts which show colour-opponent, centre-surround receptive field arrangements and would be ideal candidates to signal information about small chromatic targets. The second mechanism could involve Type II LGN cells, which would be able to signal information about large coloured targets (Rodieck, 1991). The retinal input is less clear, although Dacey et al (1996) have demonstrated horizontal cells with blue-yellow colour-opponent, spatially-coextensive receptive fields. This work shows how a comparison of psychophysical results in normal subjects and patients with nerve damage may give information about mechanisms playing a role in the overall performance of the visual system

This thesis describes work which attempts to reveal and isolate mechanisms contributing to the pupil light response, the pupil colour response and the different uses of chromatic signals in human vision. This has been achieved using both objective and subjective methods, and in particular by a comparison of results obtained for normal subjects and in patients with various forms of nerve damage. Further investigations are needed to build on these results, and to yield more specific information about the proposed mechanisms. Such studies will contribute to our understanding of the neural mechanisms involved in mediating vision.

## REFERENCES

- Ahnelt, P.K., Kolb, H., Pflug, R. (1987) Identification ~~to~~<sup>of</sup> a subtype of cone photoreceptor, likely to be blue sensitive, in the human retina. *Journal of Comparative Neurology* **255**, 18-34.
- Alexandridis, E. (1985) *The Pupil*. Springer-Verlag, New York.
- Alexandridis, E., Argyropoulos, T., Krastel, H. (1981) The latent period of the pupil light reflex in lesions of the optic nerve. *Ophthalmologica* **182**, 211-217
- Alexandridis, E., Leendertz, J.A., Barbur, J.L. (1991) Methods for studying the behaviour of the pupil. *Journal of Psychophysiology* **5**, 223-239.
- Alpern, M., Campbell, F.W. (1962) The spectral sensitivity of the consensual light reflex. *Journal of Physiology* **164**, 478-507.
- Alpern, M., Ohbe, N., Birndork, L. (1974) Can the response of the iris to light be used to break the code of the second cranial nerve in man? In: *Pupillary Dynamics and Behavior*. Edited by Janisse, M.P. Plenum Press, New York. pp.9-38
- Barbur, J.L. (1991) Pupillary responses to grating stimuli. *Journal of Psychophysiology* **5**, 259-263.
- Barbur, J.L. (1995) A study of pupil response components in human vision In: *Basic and Clinical Perspectives in Vision Research*. Edited by Robbins, J. Plenum Press, New York. pp. 3-18.
- Barbur, J.L., Forsyth, P.M. (1986) Can the pupil response be used as a measure of the visual input associated with the geniculo-striate pathway? *Clinical Vision Science* **1**, 107-111.
- Barbur, J.L., Thomson, W.D. (1987) Pupil response as an objective measure of visual acuity. *Ophthalmic and Physiological Optics* **7**, 425-429.
- Barbur, J.L., Birch, J., Harlow, A.J. (1992a) Threshold and suprathreshold responses to chromatic stimuli using psychophysical and pupillometric methods. *Noninvasive assessment of the visual system, technical digest*. *Journal of Optical Society of America* **2**, 51-54.
- Barbur, J.L., Birch, J., Harlow, A.J. (1993a) Colour vision testing using spatiotemporal luminance masking. Psychophysical and pupillometric methods. In: *Colour Vision Deficiencies*. Edited by Drum, B. Kluwer Academic Publishers, Dordrecht. pp. 417-426.
- Barbur, J.L., Cole, V.A., Plant, G.T. (1997) Chromatic discrimination in subjects with both congenital and acquired colour vision deficiencies. In: *Colour Vision Deficiencies XIII*. Edited by: Cavonius, C.R. Kluwer Academic Publishers, Dordrecht. pp. 211-223.

- Barbur, J.L., Harlow, A.J., Plant, G.T. (1994a) Insights into the different exploits of colour in the visual cortex. *Proceedings of the Royal Society of London B.* **258**, 327-334.
- Barbur, J.L., Harlow, A.J., Sahraie, A. (1992b) Pupillary responses to stimulus structure, colour and movement. *Ophthalmic and Physiological Optics* **12**, 137-141.
- Barbur, J.L., Harlow, A.J., Weiskrantz, L. (1994b) Spatial and temporal response properties of residual vision in a case of hemianopia. *Philosophical Transactions of Royal Society of London B.* **343**, 157-166.
- Barbur, J.L., Hess, R.F., Pinney, H.D. (1994c) Pupillary function in human amblyopia. *Ophthalmic and Physiological Optics* **14**, 139-149.
- Barbur, J.L., Keenleyside, M.S., Thomson, W.D. (1989) Investigation of central visual processing by means of pupillometry. In: "Seeing Contour and Colour", the proceedings of the 3rd International Symposium of the Northern Eye Institute, Manchester, UK. Edited by Kulikowski, J.J., Dickinson, C.M. and Murray, I.J. Pergamon Press. pp. 431-451.
- Barbur, J.L., Ruddock, K.H., Waterfield, V.A. (1980) Human visual responses in the absence of the geniculocalcarine projection. *Brain* **103**, 905-928.
- Barbur, J.L., Thomson, W.D., Forsyth, P.M. (1987) A new system for the simultaneous measurement of pupil size and two-dimensional eye movements. *Clinical Vision Science* **2**, 131-142.
- Barbur, J.L., Birch, J., Harlow, A.J., Plant, G. (1992c) The pupil colour response: Evidence for involvement of central neural mechanisms. *Perception* **21**, 74.
- Barbur, J.L., Cole, V.A., Harlow, J.A., Levy, I.S. (1996) Isolation of pupil light reflex response components: selective loss of function in a subject with optic nerve drusen. *Vision Science and its Applications* **1**, 50-53.
- Barbur, J.L., Watson, J.D.G., Frackowiak, R.S.J., Zeki, S. (1993b) Conscious visual perception without V1. *Brain* **116**, 1293-1302.
- Barbur, J.L., Harlow, J.A., Sahraie, A., Stoerig, P., Weiskrantz, L. (1994d) Responses to chromatic stimuli in the absence of V1: pupillometric and psychophysical studies. *Noninvasive assessment of the visual system, technical digest. Journal of Optical Society of America* **2**, 312-315.
- Barbur, J.L., Sahraie, A., Simmons, A., Weiskrantz, L., Williams, S.C.R. (in press) Residual processing of chromatic signals in the absence of a geniculostriate projection.
- Barlow, H. (1953) Summation and inhibition in the frog's retina. *Journal of Physiology* **119**, 69-88.

- Bender, D.B. (1988) Electrophysiological and behavioural experiments on the primate pulvinar. In: *Progress in Brain Research* Vol 75. Edited by Hicks, T.P., Benedek, G. Elsevier Science Publishers B.V. pp. 55-65.
- Benevento, L.A., Standage, G.P. (1983) The organization of projections of the retinorecipient and non retinorecipient nuclei of the pretectal complex and layers of the superior colliculus to the lateral pulvinar and medial pulvinar in the macaque monkey. *Journal of Comparative Neurology* **217**, 307-336.
- Bennett, A.G., Rabbetts, R.B. (1984) *Clinical Visual Optics*. Butterworths, London.
- Birch, J. (1974) Colour vision tests and colour vision advice. *British Journal of Physiological Optics* **29**, 1-29.
- Birch, J. (1991) Colour vision tests: general classification. In: *Vision and Visual Dysfunction*, Vol VIII, Inherited and acquired colour vision deficiencies. Edited by: Foster, D.H. Macmillan Press. pp. 215-234.
- Birch, J., Barbur, J.L., Harlow, A.J. (1992) New method based on random luminance masking for measuring isochromatic zones using high resolution colour displays. *Ophthalmic and Physiological Optics* **12**, 133-136.
- Birch, J., Chilsholm, I.A., Kinnear, P., Marre, M., Pinckers, A.J.L.G., Pokorny, J., Smith, V.C., Verriest, G. (1979) Acquired color vision defects. In: *Congenital and Acquired Color Vision Defects*. Edited by Pokorny, J., Smith, V.C., Verriest, G. and Pinckers, A.J.L.G. Grune and Stratton, New York.
- Blythe, I.M., Kennard, C., Ruddock, K.H. (1987) Residual vision in patients with retrogeniculate lesions of the visual pathways. *Brain* **110**, 887-905.
- Boycott, B.B., Wassle, H. (1974) The morphological types of ganglion cells of the domestic cat's retina. *Journal of Physiology* **240**, 397-419.
- Brent, P.J., Kennard, C., Ruddock, K.H. (1994) Residual colour vision in a human hemianope: spectral responses and colour discrimination. *Proceedings of the Royal Society London B* **256**, 219-225.
- Brindley, G.S., Gautier-Smith, P.C., Lewin, W. (1969) Cortical blindness and the functions of the non-geniculate fibres of the optic tracts. *Journal of Neurology Neurosurgery and Psychiatry* **32**, 259-264.
- Brodmann, K. (1909) *Vergleichende Lokalisationlehre der Grosshirnrinde*. Barth. Leipzig. p.131 and p.151.
- Bullier, J., Kennedy, H. (1983) Projection of the lateral geniculate nucleus onto cortical area V2 in the macaque monkey. *Experimental Brain Research* **53**, 168-172.
- Calkins, D.J., Schein, S.J., Tsukamoto, Y., Sterling, P. (1995) Ganglion cell circuits in primate fovea. In: *Colour Vision Deficiencies XII*. Edited by Drum, B. Kluwer Academic Publishers, Dordrecht. pp. 267-274.

Campbell, F.W., Robson, J.G. (1968) Application of Fourier analysis to the visibility of gratings. *Journal of Physiology* **197**, 551-566.

Campion, J., Latto, R., Smith, Y.M. (1983) Is blindsight an effect of scattered light, spared cortex, and near-threshold vision? *The Behavioral and Brain Sciences* **6**, 423-486.

Carpenter, M.B., Sutin, J. (1983) *Human Neuroanatomy*. Williams and Wilkins, Baltimore.

Casagrande, V.A. (1994) A third parallel visual pathway to primate area V1. *Trends in Neuroscience* **17**, 305-310.

Celesia, G.G., Bushnell, D., Cone Toleikis, S., Brigell, M.G. (1991) Cortical blindness and residual vision: is the "second" visual system in humans capable of more than rudimentary visual perception? *Neurology* **41**, 862-869.

Cibis, G.W., Campos, E.C., Aulhorn, E. (1975) Pupillary hemiakinesia in suprageniculate lesions. *Archives of Ophthalmology* **93**, 1322-1327.

Cicerone, C.M., Nerger, J.L. (1989) The relative numbers of long-wavelength-sensitive to middle-wavelength-sensitive cones in the human fovea centralis. *Vision Research* **29**, 115-128.

Clarke R.J., Ikeda, H. (1985a) Luminance and darkness detectors in the olivary and posterior pretectal nuclei and their relationship to the pupillary light reflex in the rat. I. Studies with steady luminance levels. *Experimental Brain Research* **57**, 224-232.

Clarke R.J., Ikeda, H. (1985b) Luminance detectors in the olivary pretectal nucleus and their relationship to the pupillary light reflex in the rat. II. Studies using sinusoidal light. *Experimental Brain Research* **59**, 83-90.

Clarke, R.J., Gamlin, P.D.R. (1995) Latency and dynamics of pupilloconstriction determined by microstimulation of the Edinger-Westphal nucleus and oculomotor nerve in the primate. *Society for Neuroscience Abstracts*, **21**, 1918.

Cleland, B.G., Dubin, M.W., Levick, W.R. (1971) Sustained and transient neurones in the cat's retina and lateral geniculate nucleus. *Journal of Physiology* **217**, 473-496.

Cocker, K.D., Moseley, M.J. (1992) Visual acuity and the pupil grating response. *Clinical Vision Science* **7**, 143-146.

Cole, V.A. (1995) Different uses of chromatic signals in patients with congenital and acquired colour vision deficiencies. *Ophthalmic and Physiological Optics* **15**, 399-402.

Cowey, A., Stoerig, P. (1991a) Reflections on blindsight. In: *The neuropsychology of consciousness*. Academic Press Ltd. pp. 11-37.

- Cowey, A., Stoerig, P. (1991b) The neurobiology of blindsight. *Trends in Neuroscience* **14**, 140-145.
- Cowey, A., Stoerig, P. (1995) Blindsight in monkeys. *Nature* **373**, 247-249.
- Cox, T.A. (1992) Pupillary escape. *Neurology* **42**, 1271-1273.
- Dacey, D.M., Lee, B.B., Stafford, D.K., Pokorny, J., Smith, V.C. (1996) Horizontal cells of the primate retina: cone specificity without spectral opponency. *Science* **271**, 656-659.
- De Monasterio, F.M., Gouras, P. (1975) Functional properties of ganglion cells in the rhesus monkey retina. *Journal of Physiology* **251**, 167-195.
- De Monasterio, F.M., Schein, S.J., McCrane, E.P. (1981) Staining of blue-sensitive cones of the macaque retina by a fluorescent dye. *Science* **213**, 1278-1281.
- Derrington A.M., Lennie, P. (1984) Spatial and temporal contrast sensitivities of neurones in lateral geniculate nucleus of macaque. *Journal of Physiology* **357**, 219-240.
- Derrington A.M., Krauskopf, J., Lennie, P. (1984) Chromatic mechanisms in lateral geniculate nucleus of macaque. *Journal of Physiology* **357**, 241-265.
- De Valois, R.L., De Valois, K.K. (1993) A multi-stage color model. *Vision Research* **33**, 1053-1065.
- Dineen, J., Keating, E.G. (1981) The primate visual system after bilateral removal of striate cortex. *Experimental Brain Research* **41**, 338-345.
- Dowling, J.E. (1987) The retina: an approachable part of the brain. Belknap Press of Harvard University Press.
- Dowling, J.E. (1990) Functional and pharmacological organization of the retina: dopamine, interplexiform cells, and neuromodulation. In: *Vision and the brain*. Edited by Cohen, B., Bodis-Wollner, I. Raven Press Ltd, New York. pp. 1-18.
- Ellis, C.J.K. (1981) The pupillary light reflex in normal subjects. *British Journal of Ophthalmology* **65**, 754-759.
- Enroth-Cugell, C., Robson, J.G. (1966) The contrast sensitivity of retinal ganglion cells of the cat. *Journal of Physiology* **187**, 517-552.
- van Essen, D.C. (1985) Functional organisation of primate visual cortex. In: *Cerebral Cortex, Vol III, Visual cortex*. Edited by: Peters, A., Jones, E.G. Plenum Press, New York. pp. 259-330.

Falk, G. (1991) Retinal physiology. In: Principles of Retinal Cell Biology. Principles and Practice of Clinical Electrophysiology of Vision. Edited by Heckenlively, J., Arden, G.B. Mosby, Chicago. pp 69-84.

Fallowfield, L., Krauskopf, J. (1984) Selective loss of chromatic sensitivity in demyelinating disease. *Investigative Ophthalmology and Visual Science* **25**, 771-773.

Felleman, D.J., van Essen, D.C. (1991) Distributed hierarchical processing in the primate cerebral cortex. *Cerebral Cortex* **1**, 1-47.

Felsten, G., Benevento, L.A., Burman, D. (1983) Opponent-color responses in macaque extrageniculate visual pathways: the lateral pulvinar. *Brain Research* **288**, 363-367.

Fendrich, R., Wessinger, C.M., Gazzaniga, M.S. (1992) Residual vision in a scotoma: implications for blindsight. *Science* **258**, 1489-1491.

Foster, D.H. (1986) Psychophysical loss in optic neuritis: luminance and colour aspects. In: Optic Neuritis, edited by Hess, R.H. and Plant, G.T. Cambridge University Press. pp. 152-191.

Foster, D.H., Snelgar, R.S., Heron, J.R. (1985) Nonselective losses in foveal chromatic and luminance sensitivity in Multiple Sclerosis. *Investigative Ophthalmology and Visual Science* **26**, 1431-1441.

Gamlin, P.D.R., Clarke, R.J. (1995) The pupillary light reflex pathway of the primate. *Journal of the American Optometric Association* **66**, 415-418.

Gamlin, P.D.R., Zhang, H., Clarke, R.J. (1995) Luminance neurons in the pretectal olivary nucleus mediate the pupillary light reflex in the rhesus monkey. *Experimental Brain Research* **106**, 177-180.

Gamlin, P.D.R., Zhang, H., Harlow, J.A., Barbur, J.L. (in press) Pupil responses to stimulus color, structure and light flux increments in the rhesus monkey.

Gamlin, P.D.R., Reiner, A., Erichsen, J.T., Karten, H.J., Cohen, D.H. (1984) The neural substrate for the pupillary light reflex in the pigeon (*Columba livia*). *Journal of Comparative Neurology*, **226**, 523-543.

Garey, L.J., Dreher, B., Robinson, S.R. (1991) The organisation of the visual thalamus. In: Vision and Visual Dysfunction, Vol III, Neuroanatomy of the visual pathways and their development. Edited by Dreher, B., Robinson, S.R. Macmillan Press. pp. 176-234.

Goldberg, M.E., Wurtz, R.H. (1972) Activity of superior colliculus in behaving monkey. I. Visual receptive fields of single neurons. *Journal of Neurophysiology* **35**, 542-559.

Gouras, P. (1969) Antidromic responses of orthodromically identified ganglion cells in monkey retina. *Journal of Physiology* **204**, 407-419.

- Grutzner, P. (1972) Acquired color vision defects. In: Handbook of Sensory Physiology, Vol VII/4: Visual Psychophysics. Edited by Jameson, D., Hurvich, L. Springer-Verlag New York. pp. 643-659.
- Hedin, A., Glansholm, A. (1976) Pupillary spectral sensitivity in normals and colour defectives. *Modern Problems in Ophthalmology* **17**, 231-236.
- Hess, E.H. (1965) Attitude and pupil size. *Scientific American* **227** 46-54.
- Hess, R.F., Plant, G.T. (1986) The psychophysical loss in optic neuritis: spatial and temporal aspects. In: Optic Neuritis, edited by Hess, R.H. and Plant, G.T. Cambridge University Press. pp. 109-151.
- Hess, R.F., Pointer, J.S. (1989) Spatial and temporal contrast sensitivity in hemianopia. A comparative study of the sighted and blind hemifields. *Brain* **112**, 871-894.
- Holmes, G. (1918) Disturbances of vision by cerebral lesions. *British Journal of Ophthalmology* **2**, 353-384.
- Hubel, D.H. (1988) Eye, Brain and Vision. Scientific American Library, USA.
- Hubel, D.H., Livingstone, M.S. (1987) Segregation of form, color, and stereopsis in primate area 18. *Journal of Neuroscience* **7**, 3378-3415.
- Hubel, D.H., Livingstone, M.S. (1989) Segregation of form, colour, movement and depth processing: anatomy and physiology. In: "Seeing Contour and Colour", the proceedings of the 3rd International Symposium of the Northern Eye Institute, Manchester, UK. Edited by Kulikowski, J.J., Dickinson, C.M. and Murray, I.J. Pergamon Press. pp. 116-119.
- Humphrey, N.K. (1974) Vision in a monkey without striate cortex: a case study. *Perception* **3**, 241-255.
- Hunt, R.G.W. (1991) Measuring Colour. Ellis Horward Ltd, Chichester.
- Kadoya, S., Wolin, L.R., Massopust, L.C. (1971) Collicular unit responses to monochromatic stimulation in squirrel monkey. *Brain Research* **32**, 251-254.
- Kaiser, P., Lee, B.B., Martin, P.R., Valberg, A. (1990) The physiological basis of the minimally distinct border demonstrated in the ganglion cells of the macaque retina. *Journal of Physiology* **422**, 153-183.
- Kaplan, E., Shapley, R.M. (1982) X and Y cells in the lateral geniculate nucleus of macaque monkeys. *Journal of Physiology* **330**, 125-143.
- Kaplan, E., Shapley, R.M. (1986) The primate retina contains two types of ganglion cells, with high and low contrast sensitivity. *Proceedings of National Academy of Science USA* **83**, 2755-2757.

- Kardon, R.H. (1992) Pupil perimetry. *Current Opinion in Ophthalmology* **3**, 565-570.
- Keating, E.G. (1979) Rudimentary color vision in the monkey after removal of striate and preoccipital cortex. *Brain Research* **179**, 379-384.
- Keating, E.G. (1980) Residual spatial vision in the monkey after removal of striate and preoccipital cortex. *Brain Research* **187**, 271-290.
- Keenleyside, M.S. (1989) Pupillometry and assessment of visual function. DPhil thesis: University of Oxford.
- Keenleyside, M.S., Barbur, J.L., Pinney, H.D. (1988) Stimulus-specific pupillary responses in normal and hemianopic subjects. *Perception* **17**, 347.
- King, S.M., Azzopardi, P., Cowey, A., Oxbury, J., Oxbury, S. (1996) The role of light scatter in the residual visual sensitivity of patients with complete cerebral hemispherectomy. *Visual Neuroscience* **13**, 1-13.
- Kingdom, F.A.A., Mullen, K.T. (1995) Separating colour and luminance information in the visual system. *Spatial Vision* **9**, 191-219.
- Kisvarday, Z.F., Cowey, A., Stoerig, P., Somogyi, P. (1991) Direct and indirect retinal input into degenerated dorsal lateral geniculate nucleus after striate cortical removal in monkey: implications for residual vision. *Experimental Brain Research* **86**, 271-292.
- Kluver, H. (1942) Functional significance of the geniculostriate. *Biological Symposium* **7**, 254-299.
- Kolb, H. (1991) The neural organization of the human retina. In: Principles of Retinal Cell Biology. Principles and Practice of Clinical Electrophysiology of Vision. Edited by Heckenlively, J., Arden, G.B. Mosby, Chicago. pp. 25-52.
- Kohn, M., Clynes, M. (1969) Color dynamics of the pupil. *Annals of New York Academy of Sciences* **156**, 931-950.
- Krastel, H. Moreland, J.D. (1991) Colour vision deficiencies in ophthalmic diseases. In: Vision and Visual Dysfunction, Vol VIII, Inherited and acquired colour vision deficiencies. Edited by: Foster, D.H. Macmillan Press. pp.115-172.
- Krastel, H., Alexandridis, E., Gertz, J. (1985) Pupil increment thresholds are influenced by colour opponent mechanisms. *Ophthalmologica* **191**, 35-38.
- Krieger, H.P. (1953) Effect of retrochiasmal lesion upon variability of the absolute visual threshold. *A M A Archives of Neurology and Psychiatry* **70**, 70-76.
- Krieger, H.P., Bender, M.B. (1951) Dark adaptation in perimetrically blind fields. *A M A Archives of Ophthalmology* **46**, 625-636.

- Kuffler, S.W. (1953) Discharge patterns and functional organization of mammalian retina. *Journal of Neurophysiology* **16**, 37-68.
- Laurens, H. (1923) The relative physiological value of spectral lights. III. The pupillomotor effects of wavelengths of equal energy content. *American Journal of Physiology* **64**, 97-119.
- Lee, B.B., Martin, P.R., Valberg, A. (1988) The physiological basis of heterochromatic flicker photometry demonstrated in the ganglion cells of the macaque retina. *Journal of Physiology* **404**, 323-347.
- Lee, B.B., Pokorny, J., Smith, V., Martin, P.R., Valberg, A. (1990) Luminance and chromatic modulation sensitivity of macaque ganglion cells and human observers. *Journal of Optical Society of America A* **7**, 2223-2236.
- Lennie, P., D'Zmura, M. (1988) Mechanisms of colour vision. *Critical Reviews in Neurobiology* **3**, 333-400.
- Lepore, F., Cardu, B., Rasmussen, T., Malmø, R.B. (1975) Rod and cone sensitivity in destriate monkeys. *Brain Research* **93**, 203-221.
- Levatin, P. (1959) Pupillary escape in disease of the retina or optic nerve. *A M A Archives of Ophthalmology* **62**, 768-779.
- Livingstone, M., Hubel, D. (1984a) Anatomy and physiology of a color system in the primate visual cortex. *Journal of Neuroscience* **4**, 309-356.
- Livingstone, M., Hubel, D. (1984b) Specificity of intrinsic connections in primate primary visual cortex. *Journal of Neuroscience* **4**, 2830-2835.
- Livingstone, M., Hubel, D. (1987) Psychophysical evidence for separate channels for the perception of form, color, movement, and depth. *Journal of Neuroscience* **7**, 3416-3468.
- Loewenfeld, I.E. (1966) Pupillary movements associated with light and near vision. An experimental review of the literature. *National Academy of Sciences NRC Publication* **1272**, 17-105.
- Loewenfeld, I.E. (1993) *The Pupil*. Wayne State University Press, Detroit.
- Lowenstein, O., Loewenfeld, I.E. (1958) Electronic pupillography. A new instrument and some clinical observations. *Archives of Ophthalmology* **59**, 352-363.
- Lowenstein, O., Loewenfeld, I.E. (1969) The pupil. In: *The Eye*, Vol 3, ed. by Davson H. Academic Press, New York and London. pp. 255-337.
- Lowenstein, O., Kawabata, H., Loewenfeld, I. (1968) The pupil as indicator of retinal activity. *American Journal of Ophthalmology* **57**, 569-595.

- MacAdam, D.L. (1942) Visual sensitivities to color differences in daylight. *Journal of Optical Society of America* **32**, 247-274.
- Marc, R.E., Sperling, H.G. (1977) Chromatic organisation of primate cones. *Science* **196**, 454-456.
- Marcel, A.J. (1983) Conscious and unconscious perception: experiments on visual masking and word recognition. *Cognitive Psychology* **15**, 197-237.
- Mariani, A.P. (1984) The neuronal organisation of the outer plexiform layer of the primate retina. *International Review of Cytology* **86**, 285-320.
- Marrocco, R.T., Li, R.H. (1977) Monkey superior colliculus: properties of single cells and their afferent inputs. *Journal of Neurophysiology* **40**, 844-860.
- Maunsell, J.H.R., Newsome, W.T. (1987) Visual processing in monkey extrastriate cortex. *Annual Review of Neuroscience* **10**, 363-401.
- McDonald, W.I. (1986) The pathogenesis of optic neuritis. In: *Optic Neuritis*, edited by Hess, R.H. and Plant, G.T. Cambridge University Press. pp. 42-50.
- Merigan, W.H. (1991) P and M pathway specialization in the macaque. In: *From pigments to perception*. Edited by Valberg, A., Lee, B.B. Plenum Press, New York. pp. 117-125.
- Merigan, W.H., Maunsell, J.H.R. (1993) How parallel are the primate visual pathways? *Annual Review of Neuroscience* **16**, 369-402.
- Michael, C.R. (1989) The origin of double opponency in the monkey striate cortex. In: "Seeing Contour and Colour", the proceedings of the 3rd International Symposium of the Northern Eye Institute, Manchester, UK. Edited by Kulikowski, J.J., Dickinson, C.M. and Murray, I.J. Pergamon Press. pp. 59-65.
- Mohler, C.W., Wurtz, R.H. (1977) Role of striate cortex and superior colliculus in visual guidance of saccadic eye movements in monkeys. *Journal of Neurophysiology* **40**, 74-94.
- Mollon, J.D., Baker, M.R. (1995) The use of CRT displays in research on colour vision. In: *Colour Vision Deficiencies XII*. Edited by Drum, B. Kluwer Academic Publishers, Dordrecht. pp. 423-444.
- Mollon, J.D., Reffin, J.P. (1989) A computer-controlled colour vision test that combines the principles of Chibret and of Stilling. *Journal of Physiology (London)* **414**, 5P.
- Moore, T., Rodman, H.R., Repp, A.B., Gross, C.G. (1995) Localisation of visual stimuli after striate cortex damage in monkeys: parallels with human blindsight. *Proceedings of the National Academy of Science USA* **92**, 8215-8218.

- Mullen, K.T. (1985) The contrast-sensitivity of human colour vision to red-green and blue-yellow chromatic gratings. *Journal of Physiology* **359**, 381-400.
- Mullen, K.T., Plant, G.T. (1986) Colour and luminance vision in human optic neuritis. *Brain* **109**, 1-13.
- Osterberg, G. (1935) Topography of the layer of rods and cones in the human retina. *Acta Ophthalmologica Supplement* **6**, 1-103.
- Padgham, C.A., Saunders, J.E. (1975) *The Perception of Light and Colour*. G. Bell & Sons, London.
- Pasik, P., Pasik, T. (1982) Visual functions in monkeys after total removal of visual cerebral cortex. *Contributions to Sensory Physiology* **7**, 147-200.
- Pasik, T., Pasik, P. (1971) The visual world of monkeys deprived of striate cortex: effective stimulus parameters and the importance of the accessory optic system. *Vision Research Supplement* **No 3**, 419-435.
- Payne, B.R., Lomber, S.G., MacNeil, M.A., Cornwell, P. (1996) Evidence for greater sight in blindsight following damage of primary visual cortex early in life: a review. *Neuropsychologia* **34**, 741-774.
- Perenin, M.T. (1978) Visual function within the hemianopic field following early cerebral hemidecortication in man. II. Pattern discrimination. *Neuropsychologia* **16**, 697-708.
- Perenin, M.T., Jeannerod, M. (1978) Visual function within the hemianopic field following early cerebral hemidecortication in man. I. Spatial localisation. *Neuropsychologia* **16**, 1-13.
- Perenin, M.T., Ruel, J., Hecaen, H. (1980) Residual visual capacities in a case of cortical blindness. *Cortex* **16**, 605-612.
- Perrett, D.I., Harries, M.H., Mistlin, A.J., Chitty, A.J. (1990) Recognition of objects and actions: frameworks for neuronal computation and perceptual experience. In: Higher order sensory processing. Edited by Guthrie. Manchester University Press. pp. 155-173.
- Perry, V.H., Cowey, A. (1984) Retinal ganglion cells that project to the superior colliculus and pretectum in the macaque monkey. *Neuroscience* **12**, 1125-1137.
- Perry, V.H., Oehler, R., Cowey, A. (1984) Retinal ganglion cells that project to the dorsal lateral geniculate nucleus in the macaque monkey. *Neuroscience* **12**, 1101-1123.
- Petersen, S.E., Robinson, D.L., Keys, W. (1985) Pulvinar nuclei of the behaving rhesus monkey: visual responses and their modulation. *Journal of Neurophysiology* **54**, 867-886.

- Piantanida, T. (1991) Genetics of inherited colour vision deficiencies. In: Vision and Visual Dysfunction, Vol VIII, Inherited and acquired colour vision deficiencies. Edited by: Foster, D.H. Macmillan Press. pp. 88-114.
- Pierson, R.J., Carpenter, M.B. (1974) Anatomical analysis of pupillary reflex pathways in the rhesus monkey. *Journal of Comparative Neurology* **158**, 121-144.
- Plant, G.T. (1991) Disorders of colour vision in diseases of the nervous system. In: Vision and Visual Dysfunction, Vol VIII, Inherited and acquired colour vision deficiencies. Edited by: Foster, D.H. Macmillan Press. pp. 173-198.
- Poppel, E., Held, R., Frost, D. (1973) Residual visual function after brain wounds involving the central visual pathways in man. *Nature* **243**, 295-296.
- Ptito, A., Lassonde, M., Lepore, F., Ptito, M. (1987) Visual discrimination in hemispherectomised patients. *Neuropsychologia* **25**, 869-879.
- Purpura, K., Kaplan, E., Shapley, R.M. (1988) Background light and the contrast gain of primate P and M retinal ganglion cells. *Proceedings of National Academy of Science USA* **85**, 4534-4537.
- Rodieck, R.W. (1988) The primate retina. *Comparative Primate Biology* **4**, 203-278.
- Rodieck, R.W. (1991) Which cells code for colour? In: From pigments to perception. Edited by Valberg, A., Lee, B.B. Plenum Press, New York. pp. 83-93.
- Rodieck, R.W., Watanabe, M. (1993) Survey of the morphology of macaque retinal ganglion cells that project to the pretectum, superior colliculus, and parvicellular laminae of the lateral geniculate nucleus. *Journal of Comparative Neurology* **338**, 289-303.
- Rowe, M.H. (1991) Functional organization of the retina. In: Vision and Visual Dysfunction, Vol III, Neuroanatomy of the visual pathways and their development. Edited by Dreher, B., Robinson, S.R. Macmillan Press. pp. 1-68.
- Rowe, M.H., Cox, J.F. (1993) Spatial receptive field structure of cat retinal W cells. *Visual Neuroscience* **10**, 765-779.
- Rowe, M.H., Palmer, L.A. (1995) Spatio-temporal receptive-field structure of phasic W cells in cats. *Visual Neuroscience* **12**, 117-39.
- Ruddock, K.H. (1991a) Psychophysics of inherited colour vision deficiencies. In: Vision and Visual Dysfunction, Vol VIII, Inherited and acquired colour vision deficiencies. Edited by: Foster, D.H. Macmillan Press. pp. 4-37.
- Ruddock, K.H. (1991b) Spatial vision after cortical lesions. In: Vision and visual dysfunction Vol 10: Spatial Vision. Edited by Regan, D. Macmillan Press. pp. 261-289.

- Ruskell, G. (1988) Neurology of visual perception. In: Optometry. Edited by Edwards, K., Llewellyn, R. Butterworths. pp 3-24.
- Sahraie, A. (1993) Some aspects of the pupil response in relation to stimulus movement and colour. PhD thesis: City University.
- Saini, V.D., Cohen, G.H. (1979) Using color substitution pupil mechanisms to expose chromatic mechanisms. *Journal of Optical Society of America* **69**, 1029-1035.
- Schilder, P., Pasik, P., Pasik T. (1972) Extrageniculostriate vision in the monkey. III. Circle vs. triangle and "red vs. green" discrimination. *Experimental Brain Research* **14**, 436-448.
- Schiller, P.H., Koerner, F. (1971) Discharge characteristics of single units in superior colliculus of the alert rhesus monkey. *Journal of Neurophysiology* **34**, 920-936.
- Schiller, P.H., Malpeli, J.G. (1978) Functional specificity of lateral geniculate nucleus laminae of the rhesus monkey. *Journal of Neurophysiology* **41**, 788-797.
- Schiller, P.H., Finlay, B.L., Volman, S.F. (1976) Quantitative studies of single cell properties in monkey striate cortex. I. Spatiotemporal organization of receptive fields. *Journal of Neurophysiology* **39**, 1288-1319.
- Schiller, P.H., Logothetis, N.K., Charles, E.R. (1990) Functions of the colour-opponent and broad-band channels of the visual system. *Nature* **343**, 68-70.
- Schiller, P.H., Malpeli, J.G., Schein, S.J. (1979) Composition of geniculostriate input to superior colliculus of the rhesus monkey. *Journal of Neurophysiology* **42**, 1124-1133.
- Schweitzer, N.M.J. (1956) Threshold measurements on the light reflex of the pupil in the dark-adapted eye. *Documenta Ophthalmologica* **10**, 1-78.
- Shapley, R., Kaplan, E., Soodak, R. (1981) Spatial summation and contrast sensitivity of X and Y cells in the lateral geniculate nucleus of the macaque. *Nature* **292**, 543-545.
- Shipp, S. (1995) The odd couple. *Current Biology* **5**, 116-119.
- Simpson, J.I. (1984) The accessory optic system. *Annual Review in Neuroscience* **7**, 13-41.
- Slooter, J. (1981) Clinical use of visual acuity measured with pupil responses. *Documenta Ophthalmologica* **50**, 389-399.
- Slooter, J. (1985) The pupil, mirror of visual activity. PhD thesis/monograph. Catholic University of Nijmegen.

Slooter, J., van Norren, D. (1980) Visual acuity measured with pupil responses to checkerboard stimuli. *Investigative Ophthalmology and Visual Science* **19**, 105-108.

Smith, V.C., Pokorny, J. (1975) Spectral sensitivity of the foveal cone photopigments between 400 and 500 nm. *Vision Research* **15**, 161-171.

Stewart, B.E., Young, R.S.L. (1989) Pupillary response: an index of visual threshold. *Applied Optics* **28**, 1122-1127.

Stoerig, P. (1987) Chromaticity and achromaticity. Evidence for a functional differentiation in visual field defects. *Brain* **110**, 869-886.

Stoerig, P. (1993) Sources of blindsight. *Science* **261**, 493.

Stoerig, P., Cowey, A. (1989a) Residual target detection as a function of stimulus size. *Brain* **112**, 1123-1139.

Stoerig, P., Cowey, A. (1989b) Wavelength sensitivity in blindsight. *Nature* **342**, 916-917.

Stoerig, P., Cowey, A. (1991) Increment-threshold spectral sensitivity in blindsight. *Brain* **114**, 1487-1512.

Stoerig, P., Cowey, A. (1992) Wavelength discrimination in blindsight. *Brain* **115**, 425-444.

Stoerig, P., Hubner, M., Poppel, E. (1985) Signal detection analysis of residual vision in a field defect due to a post-geniculate lesion. *Neuropsychologia* **23**, 589-599.

Stoerig, P., Barbur, J.L., Sahraie, A., Weiskrantz, L. (1994) Discrimination of chromatic stimuli in blindsight: pupillometry and psychophysics. *Investigative Ophthalmology and Visual Science* **35**, 1813.

Stone, J. (1983) Parallel processing in the visual system. Plenum Press, New York.

Thompson, H.S., Montague, P., Cox, T.A., Corbett, J.J. (1982) The relationship between visual acuity, pupillary defect and visual field loss. *American Journal of Ophthalmology* **93**, 681-688.

Torjussen, T. (1976) Residual function in cortically blind hemifields. *Scandinavian Journal of Psychology* **17**, 320-322.

Troelstra, A. (1968) Detection of time-varying light signals as measured by the pupillary response. *Journal of Optical Society of America* **58**, 685-690.

Ts'o, D.Y., Gilbert, C.D. (1988) The organisation of chromatic and spatial interactions in the primate striate cortex. *Journal of Neuroscience* **8**, 1712-1727.

- Ukai, K. (1985) Spatial pattern as a stimulus to the pupillary system. *Journal of Optical Society of America A* **2**, 1094-1099.
- Valverde, F. (1985) The organizing principles of the primary visual cortex in the monkey. In: *Cerebral Cortex Volume 3: Visual Cortex*. Edited by Peters, A., Jones, E.G. Plenum Press, New York. pp. 207-257.
- Valverde, F. (1991) The organisation of the striate cortex. In: *Vision and Visual Dysfunction Volume 3: Neuroanatomy of the visual pathways and their development*. Edited by Dreher, B., Robinson, S.R. Macmillan Press. pp. 235-277.
- Varju, D. (1969) Human pupil dynamics. In: *Processing of optical data by organisms and by machines*. Edited by Reichardt, W. Academic Press, New York. pp. 442-464.
- Wall, M. (1995) The retrogeniculate sensory visual system and higher cortical function, 1993. *Journal of Neuro-Ophthalmology* **15**, 48-55.
- Warwick, R. (1953) Representation of the extraocular muscles in the oculomotor nuclei in the monkey. *Journal of Comparative Neurology* **98**, 449-504.
- Wassle, H., Boycott, B.B. (1991) Functional architecture of the mammalian retina. *Physiological Reviews* **71**, 447-480.
- Webster, J.G., Cohen, G.H., Boynton, R.M. (1968) Optimising the use of the criterion response for the pupil light reflex. *Journal of Optical Society of America* **58**, 419-424.
- Weiskrantz, L. (1980) Varieties of residual experience. *Quarterly Journal of Experimental Psychology* **32**, 365-386.
- Weiskrantz, L. (1986) *Blindsight: a case study and implications*. Clarendon Press, Oxford.
- Weiskrantz, L. (1987) Residual vision in a scotoma. A follow-up study of 'form' discrimination. *Brain* **110**, 77-92.
- Weiskrantz, L. (1995) Blindsight - not an island unto itself. *Current Directions in Psychological Science* **4**, 146-151.
- Weiskrantz, L., Barbur, J.L., Sahraie, A. (1995) Parameters affecting conscious versus unconscious visual discrimination with damage to the visual cortex (V1) *Proceedings of the National Academy of Science USA* **92**, 6122-6126.
- Weiskrantz, L., Harlow, A., Barbur, J.L. (1991) Factors affecting visual sensitivity in a hemianopic subject. *Brain* **114**, 2269-2282.
- Weiskrantz, L., Warrington, E.K., Sanders, M.D., Marshall, J. (1974) Visual capacity in the hemianopic field following a restricted occipital ablation. *Brain* **97**, 709-728.

- Weller, R.E., Kaas, J.H. (1989) Parameters affecting the loss of ganglion cells of the retina following ablations of striate cortex in primates. *Visual Neuroscience* **3**, 327-349.
- Wiesel, T.N., Hubel, D.H. (1966) Spatial and chromatic interactions in the lateral geniculate body of the rhesus monkey. *Journal of Neurophysiology* **29**, 1115-1156.
- Wilhelm, H. (1994) Pupil examination and evaluation of pupillary disorders. *Neuro-ophthalmology* **14**, 283-295.
- Williams, C.B. (1995) Colour constancy: human mechanisms and machine algorithms. PhD thesis: City University.
- Winn, B., Whitaker, D., Elliott, D.B., Phillips, N.J. (1994) Factors affecting light-adapted pupil size in normal human subjects. *Investigative Ophthalmology and Visual Science* **35**, 1132-1137.
- Wright, W.D. (1946) Researches on normal and defective colour vision. Kimpton, London.
- Wysecki, G., Stiles, W.S. (1982) Color science. John Wiley & Sons, New York.
- Young, R.S., Alpern, M. (1980) Pupil responses to foveal exchange of monochromatic lights. *Journal of Optical Society of America* **70**, 697-706.
- Young, R.S., Kennish, J. (1993) Transient and sustained components of the pupil response evoked by achromatic spatial patterns. *Vision Research* **33**, 2239-2252.
- Young, R.S., Clavadetscher, J.E., Teller, D.Y. (1987) Screening of red-green color deficient observers using the chromatic pupillary response. *Clinical Vision Science* **2**, 117-122.
- Young, R.S., Han, B-C., Wu, P-Y. (1993) Transient and sustained components of the pupillary responses evoked by luminance and color. *Vision Research* **33**, 437-446.
- Young, R.S., Kimura, E., Delucia, P.R. (1995) A pupillometric correlate of scotopic visual acuity. *Vision Research* **35**, 2235-2241.
- Yukie, M., Iwai, E. (1981) Direct projection from the dorsal lateral geniculate nucleus to the prestriate cortex in macaque monkeys. *Journal of Comparative Neurology* **201**, 81-97.
- Zeitner, R.M., Weight, D.G. (1979) The pupillometric response as a parameter of self-esteem. *Journal of Clinical Psychology* **35**, 176-183.
- Zeki, S. (1980) The representation of colours in the cerebral cortex. *Nature* **284**, 412-418.
- Zeki, S. (1993) A vision of the brain. Blackwell Scientific Publications, Oxford.

- Zihl, J., von Cramon, D., Mai, N. (1983) Selective disturbance of movement vision after bilateral brain damage. *Brain* **106**, 313-340.
- Zinn, K.M. (1972) *The Pupil*. Charles C Thomas, Springfield, Illinois.